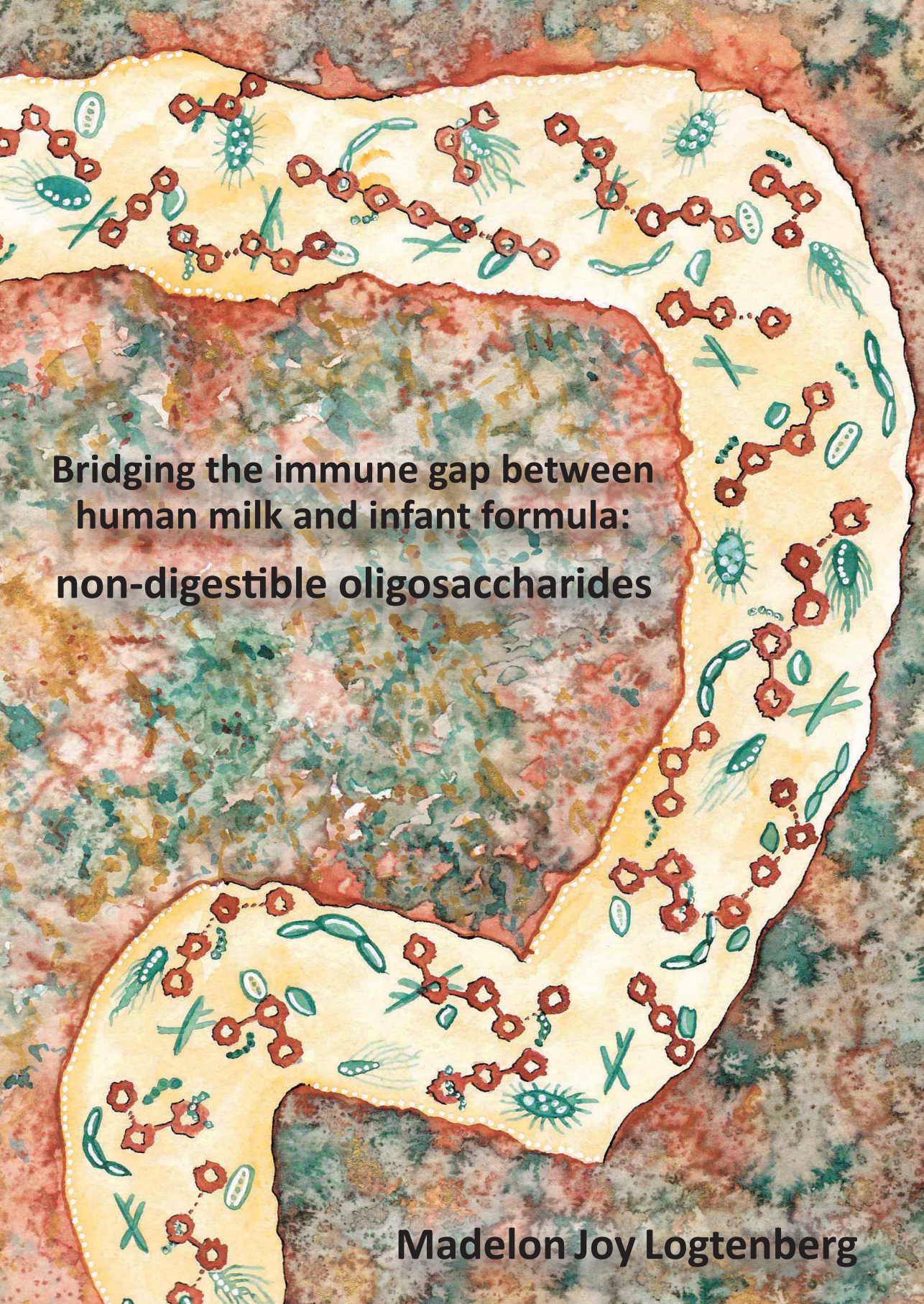

Bridging the immune gap between human milk and infant formula:

non-digestible oligosaccharides

Madelon Joy Logtenberg

Propositions

1. Establishing health effects of non-digestible carbohydrates without detailed structural information is of limited value.
   (this thesis)

2. Supplementation of infant formula with a combination of pre- and postbiotics could be of high value in the future.
   (this thesis)

3. Diet, mind and lifestyle together should get a more prominent role in medicine.

4. A compulsory weekly work-from-home day will contribute to a liveable society.

5. The individualistic nature of a PhD research should be reconsidered.

6. Worldwide economic equality is a main requirement to tackle global warming.

Propositions belonging to the thesis, entitled:
Bridging the immune gap between human milk and infant formula: non-digestible carbohydrates

Madelon Joy Logtenberg,
Wageningen, 18 September 2020

Bridging the immune gap between human milk and infant formula: non-digestible oligosaccharides

Madelon Joy Logtenberg

Thesis committee

Promotor

Prof. Dr H. A. Schols
Personal chair at the Laboratory of Food Chemistry
Wageningen University & Research

Other members

Prof. Dr M. Kleerebezem, Wageningen University & Research
Prof. Dr L. Dijkhuizen, University of Groningen
Dr F. Javier Moreno, CSIC, Madrid, Spain
Dr B. Stahl, Utrecht University

This research was conducted under the auspices of the Graduate School VLAG (Advanced studies in Food Technology, Agrobiotechnology, Nutrition and Health Sciences).

Bridging the immune gap between human milk and infant formula: non-digestible oligosaccharides

Madelon Joy Logtenberg

Thesis

submitted in fulfilment of the requirements for the degree of doctor
at Wageningen University
by the authority of Rector Magnificus,
Prof. Dr A.P.J. Mol,
in the presence of the
Thesis Committee appointed by the Academic Board
to be defended in public
on Friday 18 September 2020
at 1:30 p.m. in the Aula.

Madelon Joy Logtenberg
Bridging the immune gap between human milk and infant formula:
non-digestible oligosaccharides
168 pages

PhD thesis, Wageningen University, Wageningen, NL (2020)
With references, with summary in English and Dutch

ISBN 978-94-6395-432-7
DOI https://doi.org/10.18174/524463

Abstract

Cow-milk based infant formulas are commonly supplemented with non-digestible carbohydrates (NDCs) to resemble the functional properties of oligosaccharides present in human milk. NDCs support the development of a balanced immune system through their direct interaction with immune cells, but also through their fermentation by the gut microbiota. In this thesis, it was investigated how the structure of the NDCs affects the fermentability and the microbiota-dependent immune effects of the NDCs.

First, the use of pooled infant faecal inoculum in *in vitro* fermentation experiments was validated. This fermentation set-up enabled us to efficiently judge the fermentability of 7 structurally different NDCs by faecal microbiota of 2- and 8-week-old infants; galacto-oligosaccharides (GOS), fructo-oligosaccharides, native inulin, enzyme-treated and native oat β-glucan, isomaltose-oligosaccharides (IMO) and isomalto/malto-polysaccharides. The fermentability was dependent on the age of the infants and was negatively correlated with the size of the NDCs. In addition, a characterization method was developed based on ultra-high performance liquid chromatography-mass spectrometry (UHPLC-MS) with a stationary phase of porous graphitic carbon (PGC) to study the fate of individual isomers in the infant gut. The application of this method to digesta of GOS and IMO fermentation indicated that e.g. the type of glycosidic linkage, anomeric configuration, monomer composition and substitution of the terminal reducing residue all affect the fermentability of these complex NDCs by infant faecal microbiota. Finally, the incubation of the fermentation digesta with dendritic cells derived from the umbilical vein demonstrated the immune-attenuating effects of the NDCs, which could be linked to the bacteria-derived components and metabolites. The extent of attenuation by the NDCs depended on the age and consequent microbiota composition of the infants as well as the structure of the NDCs. These findings support the use of tailored NDC mixtures for substitution of infant formula to meet the needs of infants of different age.

Table of contents

Chapter 1

General introduction

Project outline

Early life nutrition is of utmost importance for health later in life. Human milk oligosaccharides (HMOs) are claimed to play an important role in the health benefits of human milk. These components are considered as prebiotics and guide the bacterial colonization of the infant gut. The bacteria and the metabolites formed upon fermentation of the HMOs support the development of a balanced immune system and also support maturation of the gut-barrier. HMOs can also directly influence immune function. For those infants where human milk is not a feasible option, cow-milk based infant formulas supplemented with e.g. non-digestible carbohydrates (NDC) are used to replace HMOs and to resemble their functional properties.
The prebiotic and immune effects of NDCs are not straightforward and vary depending on the structure, based on monomer composition, size and anomeric configuration as well as position of the glycosidic linkages. The research presented in this PhD thesis focuses on the relation between the chemical structure of NDCs, their fermentability by infant microbiota and their immune effects. An enhanced understanding of NDC structure-specific immune effects will enable the tailoring of NDC mixtures for substitution of infant formulas to meet the needs of infants of different ages and state of inflammation.

The immune system

Innate and adaptive immunity

The immune system protects us against the growth of pathogens, the growth of tumour cells and other harmful insults. Two types of immune responses that can be distinguished are the innate and the adaptive immune responses. Innate immune responses protect us immediately against pathogens in an unspecific way. Previous exposure is not required as pattern recognition receptors (PRRs) on immune cells such as macrophages or dendritic cells, recognize conserved biological patterns displayed by pathogens as well as damage-associated molecular patterns (DAMPs) induced by tissue stress or injury (Figure 1) [1,2]. Subsequently, the production of pro-inflammatory cytokines and non-transcriptional responses as phagocytosis are induced to initiate immune responses and fight the threatening situation [3].

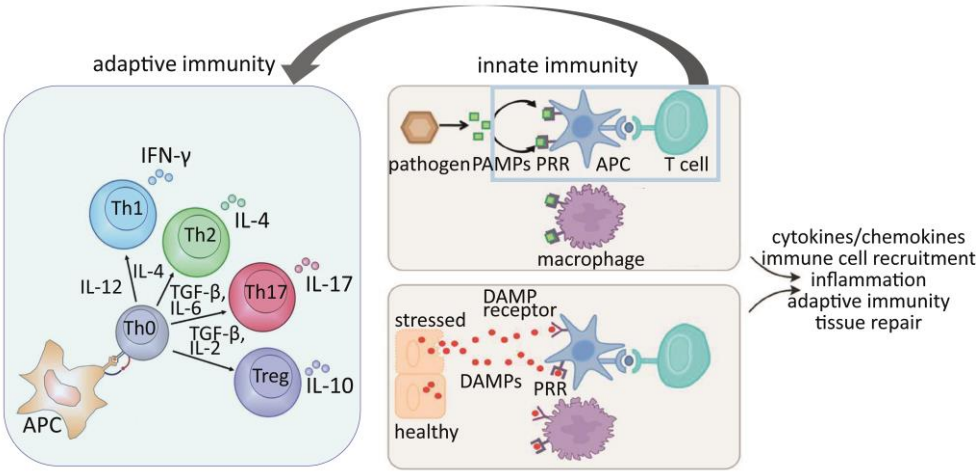

Figure 1 Schematic overview of adaptive and innate immunity with Th, T-helper cells; Treg, regulatory T-cells; IFN-γ, interferon-gamma; IL, interleukin; TGF-β, transforming growth factor beta; PAMPs, pathogen-associated molecular patterns; DAMPs, danger-associated molecular patterns; PRR, pattern recognition receptors and APC, antigen-presenting cells. Adapted from [13,14].

In contrast to innate immune responses, adaptive immune responses are highly specific, need more time for initiation and provide immunologic memory. Dendritic cells mature into antigen-presenting cells upon recognition of antigens and activate specific T-lymphocytes [4]. Activated T-cells proliferate and differentiate to either T helper type I (Th1), Th2, Th17 or regulatory T (Treg) cells, which process is largely affected by the presence of specific cytokines (Figure 1) [5].

Humoral and cellular immunity

Adaptive immune responses are classified as humoral or cellular immunity depending on the type of T helper cells activated upon antigen recognition. Of the different T-cells, differentiated Th17 and Th2 cells can direct the immune response into a humoral immune response, whereas Th1 cells can direct the immune response into a cellular response [5]. The humoral adaptive immunity includes the initiation of a specific antibody response upon the interaction of Th2 cells with B cells by the secretion of interleukin 4 (IL-4) (Figure 1). Response to a next encounter will be performed faster due to the persistence of some B cells, so called memory cells [6]. Immunoglobulin E (IgE) is the main antibody produced, which has important implications for the control of host-parasite interactions but is also responsible for triggering allergic reactions [7].

Cellular immunity includes the activity of e.g. macrophages, natural killer cells or neutrophils, which are capable of killing pathogens. These processes are stimulated upon the secretion of cytokines as interferon gamma (IFN-γ) and IL-17 by respectively Th1 and Th17 cells (Figure 1) [8]. Main difference between IFN-γ and IL-17 is the target of the

immune response. IFN-γ generates immune responses against intracellular pathogens, whereas IL-17 generates them against extracellular pathogens [9].
Excessive humoral or cellular immune responses are prevented by Treg cells which can suppress other T cells via a feedback loop [10]. The type of response induced by T-cells can also be altered upon changing the micro-environment, which shows the potential of immunomodulation in case of immune disease caused by inappropriate immune responses [11,12].

Intestinal immune system

The majority of immune cells (70-80%) present in the human body are located in the intestine, which represents the largest interface between the host and the external environment (Figure 2) [15]. Several lines of defence are present in both small intestine and colon to protect against invading pathogens. The first line of defence is constituted by a layer of mucus covering the epithelial layer. The mucus is build-up of mucins, which are secreted by goblet cells residing in the epithelial layer. Paneth cells and enterocytes secrete antimicrobial peptides (AMPs) into the mucus, which further prevents the translocation of pathogens from the lumen into the systemic circulation [16]. Secretory IgA also has important implications in the clearance of pathogens from the intestinal lumen [17].
The second line of defence is the intestinal epithelium, which forms a physical barrier with epithelial cells connected by tight junctions [18]. Despite the barrier function, important cross-talk exists between pathogens as well as commensal bacteria with immune cells on both sides of the intestinal epithelium. Some bacteria can affect host immunity by attaching to intestinal epithelial cells, which consequently secrete humoral factors or cytokines [19]. T-cell immune responses can also be directly altered by bacteria-derived molecules such as adenosine triphosphate (ATP) [20]. Furthermore, antigens can be transported via microfold (M) cells in the follicle-associated epithelium (FAE) [21], but they can also be sampled directly through the epithelium by specialized dendritic cells [22]. Through these pathways, pathogens and commensal bacteria can initiate a cascade of adaptive and innate immune responses. The type and extent of such responses are highly dependent on the region of the intestine as the immune landscape varies throughout the small and large intestine [23]. However, health implications of the regional immune specialization still largely remain to be discovered.

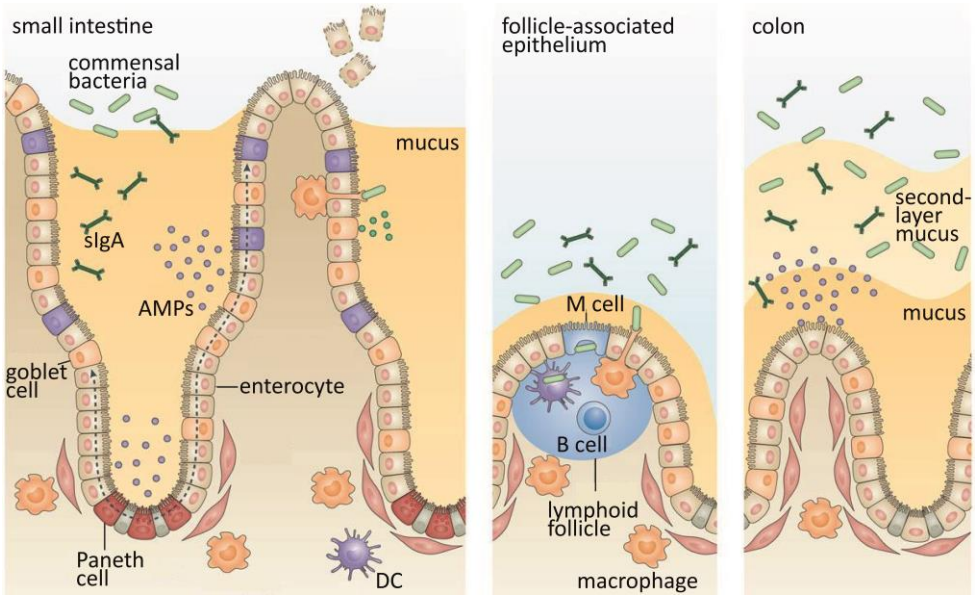

Figure 2 Schematic overview of the intestinal immune system as present in the small intestine, colon and the follicle-associated epithelium which is specialized for the uptake and processing of antigens and microorganisms; sIgA, secretory immunoglobulin A; M cell, microfold cell; DC, dendritic cell; AMPs, antimicrobial peptides [18].

Development of intestinal immunity in infants

The intestinal immune system is anatomically in place after about 28 weeks of gestation. Nonetheless, the first weeks postpartum are crucial for the maturation and actual protection of the infant as the intestinal epithelium is still permeable upon birth [24]. The main cause of the 'leaky' infant gut are immature tight junctions, which are supposed to attach adjacent epithelial cells and form a paracellular barrier. Tight junctions are composed of a protein complex (e.g. occludin, claudin) and proteins which link the complex to the actin cytoskeleton [25].

Next to the epithelial barrier integrity, the immune environment of the infant also changes drastically upon birth. In utero the immune responses mainly show an anti-inflammatory (Th-2) phenotype to protect the foetus from rejection. However, once the infant is born, a shift towards a balanced pro- and anti-inflammatory phenotype is needed to fight pathogens in a controlled way whilst at the same time protecting the infant against the development of allergies later in life [26]. A proper microbial colonization of the infant gut contributes to the development and maturation of the infant intestinal immune system [27].

Microbial colonization of the infant gut

The gut microbiota plays an essential role in both health and disease [28]. Bacteria make up the largest part of this complex ecosystem, which is also composed of archaea and fungi [29]. More than 1000 different bacterial species are present in the adult gut, with the large intestine representing highest bacterial density (10^{12} per gram of gut content) [28]. The relatively stable adult microbiota is preceded by a period with marked changes and high diversity in microbiota composition in the first years of life [30].

Establishment of gut microbiota in early life

When exactly the first bacteria establish in the gut is currently highly debated. For years it has been considered that the infant gut is sterile upon birth [31]. However, several studies have shown the presence of bacteria in the placenta, amniotic fluid and umbilical cord, which suggests the colonization of the foetal gut in utero [32-34]. Whether sterile or not, during birth the infant gut is introduced to a large diversity of maternal vaginal and intestinal bacteria as the infant passes though the birth canal [35]. The first colonizers are principally facultative anaerobes such as *Enterococcus* and *Escherichia*, which consume last traces of oxygen present in the gut. Over a period of days an anaerobic environment is created, which enables the growth of strict anaerobic bacteria (Bacteroidetes, Firmicutes and in particular Actinobacteria with high levels of *Bifidobacterium* [36]. Upon aging the bacterial diversity increases until, at an age of 2-5 years, a more adult-like microbiota composition has been reached [37]. Several factors influence the colonization process in these crucial first years, having implications for lifelong health.

Determinants in microbial colonization

Colonization of the infant gut in the first years of life is influenced by several factors, such as mode of delivery and gestational age (Figure 3). The mode of delivery is an important driver of the colonization as the birth canal harbours many bacteria. Infants born via caesarean section are reported to have lower gut microbial diversity and delayed colonization of Bacteroidetes as compared to infants born vaginally [38]. Next to delivery mode, the gestational age turned out to be of high importance. Preterm infants show a delayed gut colonization with strict anaerobic bacteria such as *Bifidobacterium* and *Bacteroides*, which could possibly be explained by antibiotic use, parenteral nutrition and the hospital environment [39]. Next to the environment and host genetics [40,41], the feeding mode has also been suggested to play a role in the infant gut colonization. Human milk is recently recognized to act as bacterial source to the infant gut with *Staphylococcus, Streptococcus, Bifidobacterium* and *Lactobacillus* being most abundant [42]. HMOs present in human milk have been associated with high levels of *Bifidobacterium* in the gut [43,44]. Hence, the feeding mode which is relatively easy to control, forms a potential pathway via which the colonization of the infant gut can be influenced.

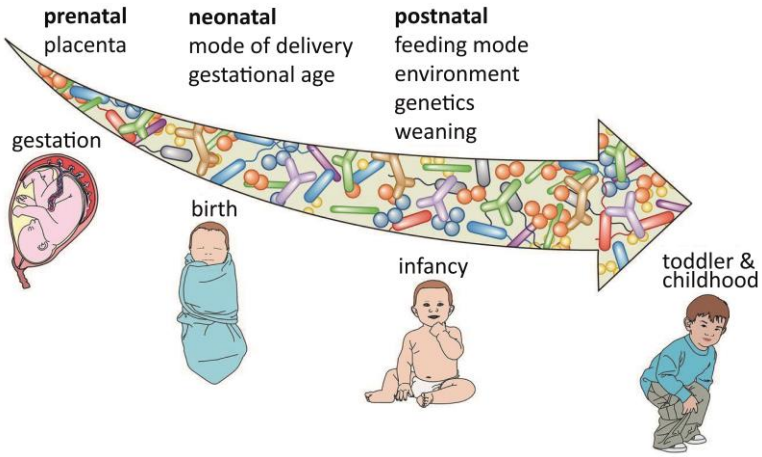

Figure 3 Main determinants of colonization of the infant intestine upon aging [45].

Human milk oligosaccharides

The World Health Organization recommends exclusive breastfeeding for infants up to 6 months as it provides several health benefits in early infancy but also later in life [46]. HMOs are the third most abundant component in human milk, after lactose and lipids. The concentration ranges between 5-25 g/L depending on the lactation stage. Highest concentrations are found in the colostrum, which is produced the first days after birth [47].

Chemical structure of HMOs

The term HMO comprises a whole array of oligosaccharide structures differing in size, type of linkage and decoration of the backbone (Figure 4). The backbone of HMOs is composed of lactose at the reducing end, which is elongated via β(1-3)-linkage by lacto-N-biose (Gal-(β1,3)-GlcNAc) or lactosamine (Gal-(β1,4)-GlcNAc) units, resulting in linear Type I or Type II HMOs respectively. Substitution of lacto-N-biose or lactosamine to the backbone via a β(1-6)-linkage introduces branching, so called *iso*-HMO [47]. The linear and branched chains can be further decorated by fucose or sialyl moieties resulting in either neutral or acidic HMOs [48]. These structural features led to the discovery of more than 200 different oligosaccharides in human milk, with the neutral oligosaccharides being most abundant [49,50]. The exact composition of the HMOs in human milk depends partly on the presence of Lewis and Secretor genes in the mammary gland. The Lewis gene is responsible for the fucosylation of the HMO backbone via an α(1-3)- or α(1-4)-linkage, whereas the activity of the Secretor gene results in fucosylation via an α(1-2)-linkage [48]. The four most predominant HMOs in the human milk of mothers with the prevalent secretor Lewis positive genotype: 2'FL (Fuc(α1-2)Gal(β1-4Glc), LNFP I (Fuc(α1-2)Gal(β1-3)GlcNAc(β1-3)Gal(β1-4)Glc), LNDFH I (Fuc(α1-2)Gal(β1-3)[Fuc(α1-4)]GlcNAc(β1-3)Gal(β1-4)Glc) and LNT (Gal(β1-3)GlcNAc (β1-3)Gal(β1-4)Glc), account for 25-33% of all HMOs [51].

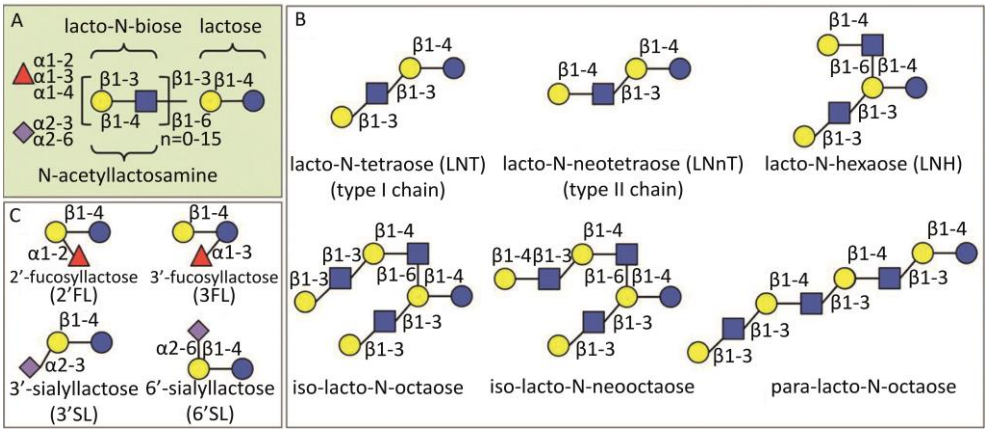

Figure 4 Structural composition of HMOs with A: structural blueprint, B: Elongations of lactose by lacto-N-biose (Type I) or lactosamine (Type II) resulting in linear (para) or branched chains (iso), C: Examples of fucosylated (neutral) and sialylated (acidic) HMOs [47].

Immune effects of HMOs

Breastfeeding has been associated with a decreased risk of the development of allergies and asthma, but also of infectious diseases such as diarrhoea and respiratory tract infections [52]. It is now well established from a variety of studies that HMOs play a significant role in the immune benefit of breastfeeding.

Several lines of evidence for an enhanced immunity are linked to the prebiotic effect of HMOs. HMOs are resistant to digestion in the small intestine, which makes them available as substrate for bacteria in the large intestine [53]. Mainly *Bifidobacterium* and *Bacteroides* species are stimulated by HMOs as these bacteria are equipped with enzymes to efficiently utilize HMOs [54]. Depending on the type of bacteria and its role in the microbial community, specific short chain fatty acids (SCFAs) such as butyrate, propionate and acetate, are produced upon fermentation. Principally, butyrate forms the major energy source for colonocytes [55]. The SCFAs also have shown to improve gut integrity by affecting tight junction proteins in the epithelial layer [56] and mucin production by goblet cells [57]. Furthermore, several studies have demonstrated that SCFAs regulate immune cell function both locally and systemically [58-60]. In addition to the bacterial metabolites, beneficial bacteria themselves can also affect immune cells as exemplified in previous research for *Bifidobacterium breve* [61]. *B. breve* affected the production of cytokines by epithelial cells, thereby modulating the local immune environment in the gut.

Next to the microbiota-dependent effects, HMOs can directly affect gut integrity and local immune landscape by interaction with epithelial and immune cells [62,63]. These effects could even be exerted systemically, as minor amounts of HMOs have shown to access the bloodstream [64,65]. HMOs also support the closure of the 'leaky' infant gut during the first weeks postpartum by stimulation of the maturation of the intestinal epithelium [66].

Additionally, HMOs can bind to pathogenic bacteria and in this way prevent their adhesion to the intestinal surface [67].
Interestingly, most of the observed microbiota-dependent and direct immune effects exerted by HMOs are structure-specific, as reviewed by Bode et al [68]. Fucosylated HMOs ((α1-2)-linked) could for example protect against infections with *Campylobacter jejuni* [67], while this specific structural feature was least effective in the prevention of *Entamoeba histolytica* infections by HMOs [69]. On the other hand, HMOs decorated with two sialic acids seem to play a crucial role in the protective effect of HMOs against necrotizing enterocolitis, a severe intestinal disorder commonly occurring in preterm infants [70].

Non-digestible carbohydrates

Commercial NDCs added to infant formula
Nowadays several NDCs are added to infant formula to take over the health effects of HMOs in infant formula. Most commonly used NDCs are described in more detail in this section. In addition, this section introduces some plant-based NDCs which could potentially be added to infant formula.

Galacto-oligosaccharides (GOS)
GOS are produced commercially by fungal, yeast or bacterial β-galactosidases, which catalyse the hydrolysis and transgalactosylation of lactose [71]. This process results in the production of a highly complex mixture of galactose chains with a terminal reducing glucose or galactose unit, varying in type of glycosidic linkage; β(1-3), β(1-4), β(1-6), β(1-2) and degree of polymerization (DP) (Figure 5A) [71]. The chains can be either linear or branched with a disubstituted terminal reducing glucose or galactose unit [72]. Also non-reducing GOS containing a β(1-1)-linkage between acceptor's terminal glucose residue and the enzymatically attached galactose residue have been reported (Figure 5B) [72,73]. The composition of GOS is highly dependent on the source of β-galactosidase, since the enzyme's origin influences the size of the produced oligosaccharides and the regioselectivity of the enzyme [74]. As the applied enzymes vary in industry, several structurally distinct GOS mixtures are commercially available [75].

Inulin-type fructans
Inulin-type fructans are commonly isolated from chicory root for commercial use [76]. The term inulin comprises a heterogenous group of oligomers and polymers consisting of linear chains of β(2-1)-linked fructose monomers. The chains vary in DP and can have either a glucose (GF series) (Figure 5C) or fructose (F series) (Figure 5D) moiety at the reducing end [76]. Inulin-type fructans are extracted and marketed as native inulin containing predominantly the inulin-type GF series DP 2-60. Native inulin can also be further hydrolysed using enzymes or acid to obtain fructo-oligosaccharides (FOS) with DP 2-10, also designated as oligofructose [77]. Long-chain inulin (DP 10-60) (lcFOS) is obtained from native

inulin with physical separation techniques and are commonly applied in infant formula in combination with GOS or FOS [78].

Polydextrose

Polydextrose is produced by a polycondensation reaction of glucose in the presence of citric acid and sorbitol. This process results in a mixture of highly branched glucan chains with a DP ranging between 2-110 (average DP12) (Figure 5E). The variation of glycosidic linkages contributes to the high complexity of polydextrose as α- and β(1-2)-, (1-3)-, (1-4)- and (1-6)-linkages occur [79].

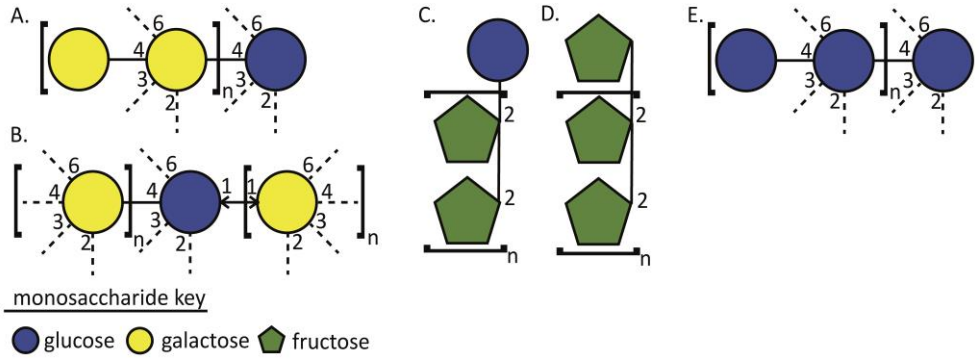

Figure 5 Structural blueprint of NDCs with A: Reducing GOS with n= DP3-8 and β-linkages, B: non-reducing GOS with n = DP 3-8 and β-linkages, C: FOS and inulin GF series with n = DP 2-10 and DP 2-60 respectively with α-linked glucose and β-linked fructose, D: FOS and inulin F series with n = DP 2-10 and DP 2-60 respectively, solely β-linkages and E: polydextrose with both α- and β-linkages.

Potential plant-based NDCs for supplementation of infant formula

Pectin oligosaccharides (POS) have received considerable attention for their promising prebiotic effects [80-82]. POS can be obtained by hydrolysis of pectin, which is present in plant cell wall material. For industrial use pectin is commonly extracted from by-products such as sugar beet pulp and citrus peels. Pectin is characterised by a high structural complexity, which leads to the formation of a broad range of oligosaccharides upon hydrolysis; arabinogalacto-oligosaccharides, galacto-oligosaccharides and arabino-oligosaccharides. In addition, acidic oligosaccharides are present such as oligo-galacturonides and rhamnogalacturonan-oligosaccharides, which both can be decorated with methyl- or acetyl ester groups. The exact composition of POS is highly dependent on the process and the source of pectin [85]. The immunomodulatory properties of so-called pAOS representing pectin oligogalacturonides have been recognized in several studies [83,84].

Next to pectin, also hemicellulose is present in the plant cell wall. This is a class of polysaccharides including xyloglucans, glucomannans, glucuronoxylan, arabinoxylan and xylan [86,87]. Upon hydrolysis of xylan, xylo-oligosaccharides (XOS) are produced which have shown to exhibit prebiotic activity [88,89]. XOS are composed of linear chains of β(1-4)-

linked xylose units ranging from DP 2-10. Agricultural by-products such as straw and corn stalks are potential sustainable sources with high xylan concentrations [90]. Also, arabinoxylo-oligosaccharides (AXOS) show increased interest due to their prebiotic potential as reviewed by Broekaert et al [91]. AXOS are produced by the degradation of arabinoxylan resulting in linear chains of β(1-4)-linked xylan units substituted with α-L-arabinofuranose units via a α(1-2) and/or α(1-3)-linkage [92]. Arabinoxylan is highly abundant in cell walls of cereal bran, which is a by-product of the milling process [93].
The cell walls of cereal bran also contain β-glucans, which prebiotic activity is widely studied [94]. Cereal β-glucans are linear β(1-3)- and β(1-4)-linked glucose polysaccharides. Other plant-based NDCs which have received considerable interest are isomalto/malto-polysaccharides (IMMP) and isomalto-oligosaccharide (IMO) preparations, which are enzymatically produced from potato starch [95,96]. IMMPs are polysaccharides composed of mainly α(1-4)- and α(1-6)-linked glucose moieties [97], whereas an IMO preparation is a highly complex mixture of α-gluco-oligosaccharides varying in the type of glycosidic linkages and size [98].
Prebiotic effects of the potential plant-based NDCs for supplementation of infant formula seem to be highly dependent on the chemical structure of the oligosaccharides [99-101]. Further studies need to be carried out to establish the structure-specific prebiotic and immune effects. Knowledge on the utilization pathways of currently applied and alternative NDCs by infant gut bacteria and consequent immune effects will pave the way for the design of novel NDCs (mixtures).

Fate of NDCs in the infant gut

To learn more about the structure-specific prebiotic and immune effects of NDCs in infants it would be most ideal to have direct access to the digesta in different segments of the infant gut. However, due to practical and ethical issues this is basically impossible. Both *in vivo* animal models and *in vitro* fermentation models can be used to overcome this limitation.

In vivo animal models

In vivo animal models allow us to study the interaction between the host and microbiota. Rodents are often used as animal model as they have a short life cycle, are easy to keep and have high reproductive rates [102]. Nonetheless, the microbiota composition is significantly different between rodents and humans, in particular with respect to the abundance of *Bifidobacterium* [103]. This could be solved by infant faecal transplantation to germ-free rodents [104]. However, it remains challenging to translate results to the infant situation as the anatomy of the intestinal tract and intestinal transit time differ between infants and rodents [105]. Due to these differences, the fermentation of NDCs takes place in different segments of the intestine; in the colon and cecum for respectively humans and rodents.

Additionally, rodents practice coprophagy, which highly affects the microbiota composition in the first segment of the colon [104].
Piglets are also commonly used as animal model for human intestinal studies as they show more physiological and anatomical similarities with humans. For example, digesta transit times and mechanisms of digestion and absorption in the gut are comparable between pigs and humans [106]. Nevertheless, drawbacks of piglets as animal model are longer reproductive cycles and increased costs of husbandry and maintenance compared to rodents [107]. In addition, animal models require large amounts of NDCs thereby hindering the study of highly tailored novel NDCs, which are only produced at small scale.

***In vitro* fermentation models**

In vitro fermentation models form a reasonable alternative to study the fate of NDCs in the infant gut as they are more cost-efficient, high-throughput and do not require ethical approval. In contrast to *in vivo* animal models, commonly used *in vitro* fermentation models do not consider the interaction between microbiota and host. Therefore, separate immune assays with intact NDCs and fermentation digesta are necessary to study the immune effects of NDCs. A benefit of this approach is the ability to differentiate between direct and microbiota-dependent immune effects, which is highly challenging in *in vivo* models [108].
In vitro fermentation models can be divided into continuous and static models. Continuous models are highly dynamic and the physiological conditions are closely related to the human intestine. Long-term effects of NDCs in different segments of the intestine can also be studied [108]. The models are classified as multistage or single-stage continuous fermentation models. The multistage fermentation models typically consist of multiple pH-controlled vessels, which are aligned in series and mimic the different segments of the intestine. Continuous replenishment of nutrients is ensured by peristaltic pumps connecting the neighbouring vessels. The SHIME model is an example of a commonly applied multistage continuous fermentation model [109].
Single-stage fermentation models generally simulate the conditions and metabolic activity of the proximal colon. A well-known example is the TIM-2 model, which even mimics the peristaltic movements in the colon via a flexible membrane. An additional benefit is the presence of a dialysis system which prevents the accumulation of microbial metabolites in the compartment. This extensively prolongs the maximum experiment duration as the microbiota remain active up to 3 weeks [110].
Recently, significant progress has been made in the development of continuous fermentation models which also take into account host-gut microbiota interactions. The multistage SHIME model has for example been connected to the Host-Microbiota Interaction (HMI) module, which is composed of a luminal and host compartment containing gut bacteria and enterocytes respectively. The two compartments are separated by a semi-permeable membrane and an artificial mucus layer, which enables studying the effect of NDCs on luminal and mucosa-associated microbiota and consequent effects on

enterocytes [111]. However, the method extensions further increase the complexity of the continuous fermentation models, which makes them even less suitable for screening purposes. In addition, continuous fermentation models are generally highly labour intensive as exemplified by an extensive stabilization period of two weeks required prior to the actual fermentation experiment in the SHIME model [112]. Furthermore, due to their high volume continuous models require substantial amounts of substrate [112].

Static fermentation models are less complex and labour intensive than continuous fermentation models. They are composed of one compartment, typically represented by a controlled reactor or sealed bottle. The compartment is operated under anoxic conditions and contains faecal inoculum, medium with nutrients and the NDC to be studied. Due to substrate depletion and accumulation of end-products in the compartment, the model is only applicable for short-term fermentations. Nevertheless, easy handling and low costs make it a highly suitable model for screening purposes related to fermentability of NDCs and the production of microbial metabolites formed upon fermentation [113].

Inoculation of in vitro fermentation models

Typically, *in vitro* fermentation models are inoculated with liquid faecal suspensions from single donors [114]. Due to high inter- and intra-individual variability in microbiota composition [115], separate *in vitro* experiments with faecal inoculum of multiple donors have to be performed to ensure biological replication [114]. To avoid high costs and workload, faecal material of multiple donors can be pooled and used as inoculum. It should be taken into account that intermicrobial interactions could occur which would not have taken place in case of *in vitro* fermentations with single faecal material of the individual donors [114]. Nonetheless, previous research showed that for an *in vitro* adult fermentation model, pooled faecal inoculum resulted in a comparable bacterial activity as found for the individual faecal inocula [116]. An alternative solution for reproducibility *of in vitro* fermentation experiments is the inoculation with prevalent bacterial isolates or defined populations of gut bacteria [117,118]. However, such approaches may ignore the importance of cross-feeding networks [119-121].

Characterization of NDCs and their fermentation degradation products

Structural elucidation of the NDCs and their degradation products is of utmost importance to determine structure-specific immune effects of NDCs. NDCs are commonly characterized by highly complex mixtures consisting of many oligosaccharides varying in degree of polymerization, type of linkage and monomer composition. The large number of isomers makes the characterization of NDCs rather challenging. Several techniques have been reported to tackle this challenge.

Chromatographic techniques

Liquid chromatography (LC) is commonly used for the separation and characterization of oligosaccharides. This technique is based on the difference in affinity of the analyte between the stationary and mobile phase [122]. High-performance anion-exchange chromatography (HPAEC) coupled to a pulsed amperometric detector (PAD) is often applied for the characterisation of GOS and FOS [123,124]. The oligosaccharides are separated based on charge and size by the anion-exchange stationary phase which is operated under alkaline conditions. A drawback of HPAEC-PAD is the fact that reference components are necessary for structural elucidation, as PAD does not provide structural information [123].

LC techniques can be coupled to mass spectrometric (MS) techniques to provide good separation as well as structural information. Some studies have reported on the use of HPAEC-MS for the characterization of oligosaccharides [125,126]. However, the alkaline eluents used in HPAEC are not easily compatible with MS and give rise to some challenges in set-up of the equipment including in-line desalting [125].

Ultra-high performance liquid chromatography (UHPLC) is more compatible with MS and has been commonly applied in oligosaccharide analysis with stationary phases based on hydrophilic interaction (HILIC) [75,127] and porous graphitic carbon (PGC) chromatography [49,128]. PGC chromatography showed to provide a more adequate separation of HMOs compared to HILIC [49,50,127]. This can be explained by the retention mechanism of PGC, which is based on the size, type of linkage and resulting 3D-structure of the oligosaccharides [129]. The chromatographic resolution of PGC even results in the partial separation of α- and β- anomers. The occurrence of such split- or double peaks can be avoided by reduction of the reducing end group of the oligomers prior to analysis [130].

Mass spectrometric techniques

Mass spectrometric techniques allow the determination of the molecular weight, as well as structural elucidation depending on the technique used. In short, oligosaccharides are ionized after which they are separated and detected based on their mass-to-charge (*m/z*). Most frequently used ionization techniques are matrix assisted laser desorption/ionization (MALDI) [131] and electrospray ionization (ESI) [132]. MALDI does not provide structural elucidation of oligosaccharides as spectra interpretation becomes quite complex due to the presence of different isomers [133]. UHPLC-ESI-MS overcomes this limitation as the ionization is preceded by the chromatographic separation of the different isomers present. This technique has been applied in several studies to touch upon the complexity of NDCs [75,134,135].

To enable the structural elucidation of the oligosaccharides, the ions are fragmented to generate structurally informative product ions [136]. For collision induced dissociation (CID) of negative ions specific pathways have been reported that define structural features of oligosaccharides. These pathways for example enable the determination of (1-4)- and (1-6)-linkages present in oligosaccharides [137,138]. However, complete characterization of

oligosaccharides by MS^2 fragmentation is still highly challenging due to the presence of many isomers differing in type of linkage, monomer composition or anomeric configuration [136]. The symmetric nature of many NDCs hinders the distinction between product ions containing a reducing and non-reducing end. Reduction of the reducing end prior to analysis overcomes this issue [139].

Other techniques for the characterization of NDCs

Nuclear magnetic resonance (NMR) analysis proves valuable for the conclusive characterization of oligosaccharides [140]. Nonetheless, this technique favours extensive preparative techniques to obtain rather pure compounds prior to structural analysis [141]. Another analytical tool with high sensitivity for oligosaccharides is capillary electrophoresis with laser induced fluorescent detection (CE-LIF), preceded by the labelling of oligosaccharides with the fluorescent dye 9-aminopyrene-1,4,6-trisulfonate (APTS). The retention mechanism of CE-LIF is based on the charge-to-mass ratio of the oligosaccharides [142,143]. Non-reducing oligosaccharides are not labelled and consequently not analysed. Additionally, this method requires the use of reference components for structural elucidation [142]. Coupling of CE with MS could overcome part of these limitations, but poses some technological challenges [144].

Fermentability and microbiota-dependent immune effects of NDCs

From a variety of studies it is now well established that NDCs can exert immune effects through their direct interaction with receptors on immune cells in the gut [145-147]. Next to the immune cells, the NDCs face the microbiota while travelling through the gut. The fermentation of the NDCs by the gut bacteria results in fermentation products which also could impact the immune environment as stated before for HMOs [56-60]. *In vitro* fermentation studies can provide mechanistic insights into these process as they allow dynamic sampling over time. So far, however, no study has investigated both the fermentation of the NDCs and the subsequent immune effects in infants. Instead, most studies only focus on the impact of the fermentation of NDCs on the microbiota composition and SCFAs production. In addition, the *in vitro* fermentations are commonly performed with adult faecal microbiota [80,148-150], which hinders the translation of the results to the infant situation due to large differences in microbiota composition between adults and infants [151].

Some studies used individual bacterial strains isolated from infant faeces to ferment NDCs (Table 1). Overall, FOS and GOS induced the growth of all individual *Bifidobacterium* species included in these studies, whereas inulin and long-chain inulin only induced minor growth of *Bifidobacterium* or resulted in no growth at all [152, 158, 159]. The study of Rada et al [152] also showed an increase in growth of *Clostridium* species by inulin, FOS and GOS. However, it is difficult to translate these results to complex communities present in the gut as

interspecies competition and cooperation is ignored in studies using individual bacterial strains [153].

The use of infant faeces as inoculum in *in vitro studies* provides a more relevant representation of the infant gut microbiota and has only been applied in a limited number of studies (Table 2). These studies reinforce part of the findings obtained with individual bacterial strains as fermentation of oligosaccharides such as GOS and FOS resulted in a higher abundance of *Bifidobacterium* than polysaccharides such as inulin [154-156]. However, these studies also showed that individual bacterial strains do not allow the prediction of the fermentation behaviour of that strain in a complex bacterial community. For example, *Clostridium* was not at all or less stimulated by the NDCs in the presence of other bacterial species compared to its single culture [157], presumably caused by interspecies competition.

Surprisingly, none of the studies provided in-depth structural information of the NDCs. In most studies the structural information was limited to a class and brand name, without almost any information on oligosaccharide structure and composition. None of the studies considered the actual utilization of the (individual) NDCs to determine if specific components were preferentially chosen by the faecal bacteria. As a result, it is not possible to draw any conclusions on structure-specific fermentability of NDCs by infant faecal microbiota.

Table 1 Overview of *in vitro* studies on fermentation of NDCs using individual bacterial strains isolated from infant faeces in static models. Data on the structure of the NDCs, the degradation kinetics, changes in microbiota composition and production of SCFAs are indicated as available in the corresponding reference.

study characteristics			outcomes					
NDC	brand	structural information	degradation kinetics	Bif.	other bacteria	SCFAs	immune effects	ref.
Inulin	Frutafit	-	-	↑	*Clostridium* ↑↑↑	-	-	[152]
FOS	Raftilose P85	-	-	↑↑↑	*Clostridium* ↑↑↑	-	-	[152]
FOS	Raftilose P95	-	-	↑↑	*Clostridium* ↑↑	-	-	[152]
GOS	Vivinal	-	-	↑↑↑	*Clostridium* ↑	-	-	[152]
FOS	Actilight 950P	DP 2-3	-	↑↑	n/a	-	-	[158]
lcFOS	Raftiline HP	DP 10-60	-	↑	n/a	-	-	[158]
FOS	Raftilose P95	DP 2-10	-	↑↑	n/a	-	-	[158]
FOS	Orafti P95	DP 2-10, average DP 4	-	↑	n/a	-	-	[159]
lcFOS	Orafti HP	DP 11-60, average DP 25	-	x	n/a	-	-	[159]
GOS	TOS-100	DP 3-7	-	↑↑	n/a	-	-	[159]

x: no growth ↑↓ : increase or decrease, compared to NDCs tested in same study
-: not determined Bif.: *Bifidobacterium*
n/a: not applicable

Table 2 Overview of in vitro studies on fermentation of NDCs using infant faecal inoculum. Data on the structure of the NDCs, the degradation kinetics, changes in microbiota composition and production of SCFAs are indicated as available in the corresponding reference.

study characteristics						outcomes					
NDC	brand	structural information	age	diet	model	degradation kinetics	Bif.	other bacteria	SCFAs	immune effects	ref.
GOS	GOS 95	-	2-4 mths	human milk	static	-	↑	*E. coli / C. perfringens*↓	↑↑↑	-	[154]
GOS	GOS 95	-	2-4 mths	infant formula	static	-	↑↑	*E. coli / C. perfringens*↓	↑↑↑↑	-	[154]
lcFOS	Orafti HP	-	2-4 mths	human milk	static	-	↑	*E. coli / C. perfringens*↓	↑	-	[154]
lcFOS	Orafti HP	-	2-4 mths	infant formula	static	-	↑↑	*E. coli / C. perfringens*↓	↑↑	-	[154]
GOS	Vivinal 15	28% GOS / 45% DP>10	4 wks	-	static	-	↑↑	*E. coli*↓	↑↑		[155]
lcFOS	Beneo HP	DP≥6	4 wks	-	static	-	x	x	x		[155]
inulin	Beneo Synergy 1	-	4 wks	-	static	-	↑	x	↑		[155]
FOS:GOS	Raftilose / Vivinal (1:1)	-	7 mths	weaning	static	-	↑	*Clostridium cluster XIVa*↑	↑	-	[157]
FOS	Nutraflora P-95	95% FOS: average DP 3.6	6 mths	-	continuous	-	↑	*Lactobacillus*↑ *Clostridium / Bacteroides*↓	↑	-	[160]
FOS	Orafti P95	95% FOS: DP 2-9	4 mths	infant formula	continuous	-	↑↑	*Bacteroides - prevotella*↓	↑	-	[156]
inulin	Orafti Synergy 1	30% FOS / 70% DP>10	4 mths	infant formula	continuous	-	↑	*C. coccoides - E. rectale*↓	↑	-	[156]
inulin	Oraft HSI	60% FOS / 28% DP>10	4 mths	infant formula	continuous	-	↑	*Bacteroides - prevotella*↓	↑	-	[156]
FOS	Raftilose	-	7 wks	infant formula	static	-	-	-	↑	-	[161]
FOS	Raftilose	-	12 wks	liquid food	static	-	-	-	↑	-	[161]
FOS	Raftilose	-	9 mths	solid food	static	-	-	-	↑	-	[161]
FOS	Raftilose	-	5 wks	human milk	static	-	-	-	↑	-	[162]
FOS	Raftilose	-	6 wks	infant formula	static	-	-	-	↑↑	-	[162]

x: no growth
-: not determined
n/a: not applicable
↑↓ : increase or decrease, compared to NDCs tested in same study
Bif.: *Bifidobacterium*

Thesis outline

To date minor knowledge is available on structure-specific fermentability and consequent immune effects of NDCs in infants. Hence, the aim of this thesis was firstly, to get more understanding of the structural complexity of several NDCs. Secondly, by applying this knowledge we aimed to determine the structure-specific fermentability of NDCs by infant microbiota. Finally, it was intended to determine if and how the fermentation of the NDCs influences their immunomodulating properties. **Chapter 2** describes and validates the use of pooled infant faecal inoculum in *in vitro* fermentation experiments for high-throughput screening purposes of the fermentability of novel NDCs. The validated *in vitro* fermentation set-up was used to study the fermentation of several NDCs by faecal microbiota of 2- and 8-week-old infants, which is discussed in following chapters. **Chapter 3** focuses on the fermentability of two types of fructans differing in size, as well as the impact of the fermentation on the microbiota composition and the organic acid production. In addition, the effects of the fermentation digesta on the cytokine production by dendritic cells are discussed. The same applies to native and endo-1,3(4)-β-glucanase-treated oat β-glucan, for which the fermentation characteristics and immunomodulating properties are presented and discussed in **Chapter 4**. The same chapter describes the effect of the fermentation digesta on the activation of Dectin-1 receptors, important β-glucan binding receptors present on dendritic cells. **Chapter 5** demonstrates the developed characterisation method of GOS being based on UHPLC-PGC-MS, which enables us to study the fate of individual oligomers present in complex NDC mixtures during fermentation by infant faecal microbiota. **In Chapter 6**, the results obtained in this research are discussed and compared alongside some first results concerning the fermentability and immune effects of GOS, the IMO preparation and isomalto/malto-polysaccharides. In the same chapter, the implications of our results for future research on the humanization of infant formula are discussed.

References

1. Schaefer, L. Complexity of danger: the diverse nature of damage-associated molecular patterns. *J. Biol. Chem.* **2014**, *289*, 35237-35245.
2. Ygberg, S.; Nilsson, A. The developing immune system – from foetus to toddler. *Acta Paediatr.* **2012**, *101*, 120-127.
3. Brubaker, S.W.; Bonham, K.S.; Zanoni, I.; Kagan, J.C. Innate immune pattern recognition: a cell biological perspective. *Annu. Rev. Immunol.* **2015**, *33*, 257-290.
4. Janeway, C.A.; Travers, P.; Walport, M. The production of armed effector T cells. In *Immunobiology: the immune system in health and disease*, 5th edition; Garland Sciences: New York, **2001**, Chapter 8.
5. Zhu, J.; Yamane, H.; Paul, W.E. Differentiation of effector CD4 T cell populations. *Annu. Rev. Immunol.* **2010**, *28*, 445-489.
6. Bonilla, F.A.; Oettgen, H.C. Adaptive immunity. *J. Allergy Clin. Immunol.* **2010**, *125*, S33-S40.
7. Janeway, C.A.; Travers, P.; Walport, M. The production of IgE. In *Immunobiology: the immune system in health and disease*; 5th edition; Garland Science: New York, **2001**, Chapter 12.
8. Silva, M.T. Neutrophils and macrophages work in concert as inducers and effectors of adaptive immunity against extracellular and intracellular microbial pathogens. *J. Leukocyte Biol.* **2010**, *87*, 805-813.
9. Commins, S.P.; Borish, L.; Steinke, J.W. Immunologic messenger molecules: cytokines, interferons, and chemokines. *J. Allergy Clin. Immunol.* **2010**, *125*, S53-72.
10. Sakaguchi, S.; Yamaguchi, T.; Nomura, T.; Ono, M. Regulatory T Cells and immune tolerance. *Cell* **2008**, *133*, 775-787.
11. Geginat, J.; Paroni, M.; Maglie, S.; Alfen, J.S.; Kastirr, I.; Gruarin, P.; De Simone, M.; Pagani, M.; Abrignani, S. Plasticity of human CD4 T cell subsets. *Front. Immunol.* **2014**, *5*.
12. Cosmi, L.; Maggi, L.; Santarlasci, V.; Liotta, F.; Annunziato, F. T helper cells plasticity in inflammation. *Cytometry, Part A* **2014**, *85*, 36-42.
13. Russ, B.; Prier, J.; Rao, S.; Turner, S. T cell immunity as a tool for studying epigenetic regulation of cellular differentiation. *Front. Gen.* **2013**, *4*.
14. Valles, P.G.; Lorenzo, A.G.; Bocanegra, V.; Valles, R. Acute kidney injury: what part do toll-like receptors play? *Int. J. Nephrol. Renovasc. Dis.* **2014**, *7*, 241-251.
15. Furness, J.B.; Kunze, W.A.A.; Clerc, N. II. The intestine as a sensory organ: neural, endocrine, and immune responses. *Am. J. Physiol.: Gastrointest. Liver Physiol.* **1999**, *277*, G922-G928.
16. Dupont, A.; Heinbockel, L.; Brandenburg, K.; Hornef, M.W. Antimicrobial peptides and the enteric mucus layer act in concert to protect the intestinal mucosa. *Gut Microbes* **2014**, *5*, 761-765.
17. Mantis, N.J.; Rol, N.; Corthésy, B. Secretory IgA's complex roles in immunity and mucosal homeostasis in the gut. *Mucosal Immunol.* **2011**, *4*, 603-611.
18. Peterson, L.W.; Artis, D. Intestinal epithelial cells: regulators of barrier function and immune homeostasis. *Nat. Rev. Immunol.* **2014**, *14*, 141.
19. Ivanov, I.I.; Atarashi, K.; Manel, N.; Brodie, E.L.; Shima, T.; Karaoz, U.; Wei, D.; Goldfarb, K.C.; Santee, C.A.; Lynch, S.V.; Tanoue, T.; Imaoka, A.; Itoh, K.; Takeda, K.; Umesaki, Y.; Honda, K.; Littman, D.R. Induction of intestinal Th17 cells by segmented filamentous bacteria. *Cell* **2009**, *139*, 485-498.
20. Chewning, J.H.; Weaver, C.T. Development and survival of Th17 cells within the intestines: the influence of microbiome- and diet-derived signals. *J. Immunol.* **2014**, *193*, 4769-4777.
21. Mabbott, N.A.; Donaldson, D.S.; Ohno, H.; Williams, I.R.; Mahajan, A. Microfold (M) cells: important immunosurveillance posts in the intestinal epithelium. *Mucosal Immunol.* **2013**, *6*, 666.
22. Niess, J.H.; Brand, S.; Gu, X.; Landsman, L.; Jung, S.; McCormick, B.A.; Vyas, J.M.; Boes, M.; Ploegh, H.L.; Fox, J.G.; Littman, D.R., Reinecker, H.C. CX3CR1-mediated dendritic cell access to the intestinal lumen and bacterial clearance. *Science* **2005**, *307*, 254-258.
23. Mowat, A.M.; Agace, W.W. Regional specialization within the intestinal immune system. *Nat. Rev. Immunol.* **2014**, *14*, 667.
24. van Elburg, R.M.; Fetter, W.P.F.; Bunkers, C.M.; Heymans, H.S.A. Intestinal permeability in relation to birth weight and gestational and postnatal age. *Arch. Dis. Child. - Fetal Neonatal Ed.* **2003**, *88*, F52-F55.
25. Günzel, D.; Yu, A.S.L. Claudins and the modulation of tight junction permeability. *Physiol. Rev.* **2013**, *93*, 525-569.
26. Walker, W.A.; Iyengar, R.S. Breast milk, microbiota, and intestinal immune homeostasis. *Pediatr. Res.* **2015**, *77*, 220-228.
27. Sommer, F.; Backhed, F. The gut microbiota--masters of host development and physiology. *Nat. Rev. Microbiol.* **2013**, *11*, 227-238.
28. Ohland, C.L.; Jobin, C. Microbial Activities and Intestinal Homeostasis: A Delicate Balance Between Health and Disease. *Cell. Mol. Gastroenterol. Hepatol.* **2015**, *1*, 28-40.
29. Hoffmann, C.; Dollive, S.; Grunberg, S.; Chen, J.; Li, H.; Wu, G.D.; Lewis, J.D.; Bushman, F.D. Archaea and fungi of the human gut microbiome: correlations with diet and bacterial residents. *PloS one* **2013**, *8*, e66019.

30. Lozupone, C.A.; Stombaugh, J.I.; Gordon, J.I.; Jansson, J.K.; Knight, R. Diversity, stability and resilience of the human gut microbiota. *Nature* **2012**, *489*, 220-230.
31. Escherich, T. The intestinal bacteria of the neonate and breast-fed infant. *Rev. Infect. Dis.* **1989**, *11*, 352-356.
32. Jiménez, E.; Fernández, L.; Marín, M.L.; Martín, R.; Odriozola, J.M.; Nueno-Palop, C.; Narbad, A.; Olivares, M.; Xaus, J.; Rodríguez, J.M. Isolation of commensal bacteria from umbilical cord blood of healthy neonates born by cesarean section. *Curr. Microbiol.* **2005**, *51*, 270-274.
33. DiGiulio, D.B.; Romero, R.; Amogan, H.P.; Kusanovic, J.P.; Bik, E.M.; Gotsch, F.; Kim, C.J.; Erez, O.; Edwin, S.; Relman, D.A. Microbial prevalence, diversity and abundance in amniotic fluid during preterm labor: a molecular and culture-based investigation. *PloS one* **2008**, *3*, e3056.
34. Aagaard, K.; Ma, J.; Antony, K.M.; Ganu, R.; Petrosino, J.; Versalovic, J. The placenta harbors a unique microbiome. *Sci. Transl. Med.* **2014**, *6*, 237ra265-237ra265.
35. Houghteling, P.D.; Walker, W.A. Why is initial bacterial colonization of the intestine important to infants' and children's health? *J. Pediatr. Gastroenterol. Nutr.* **2015**, *60*, 294-307.
36. Jost, T.; Lacroix, C.; Braegger, C.P.; Chassard, C. New insights in gut microbiota establishment in healthy breast fed neonates. *PloS one* **2012**, *7*, e44595.
37. Rodriguez, J.M.; Murphy, K.; Stanton, C.; Ross, R.P.; Kober, O.I.; Juge, N.; Avershina, E.; Rudi, K.; Narbad, A.; Jenmalm, M.C.; Marchesi, J.R.; Collado, M.C. The composition of the gut microbiota throughout life, with an emphasis on early life. *Microb. Ecol. Health Dis.* **2015**, *26*, 26050.
38. Jakobsson, H.E.; Abrahamsson, T.R.; Jenmalm, M.C.; Harris, K.; Quince, C.; Jernberg, C.; Bjorksten, B.; Engstrand, L.; Andersson, A.F. Decreased gut microbiota diversity, delayed Bacteroidetes colonisation and reduced Th1 responses in infants delivered by caesarean section. *Gut* **2014**, *63*, 559-566.
39. Arboleya, S.; Binetti, A.; Salazar, N.; Fernández, N.; Solís, G.; Hernández-Barranco, A.; Margolles, A.; de los Reyes-Gavilán, C.G.; Gueimonde, M. Establishment and development of intestinal microbiota in preterm neonates. *FEMS Microbiol. Ecol.* **2012**, *79*, 763-772.
40. Leamy, L.J.; Kelly, S.A.; Nietfeldt, J.; Legge, R.M.; Ma, F.; Hua, K.; Sinha, R.; Peterson, D.A.; Walter, J.; Benson, A.K.; Pomp, D. Host genetics and diet, but not immunoglobulin A expression, converge to shape compositional features of the gut microbiome in an advanced intercross population of mice. *Genome Biol.* **2014**, *15*, 552.
41. Grzeskowiak, L.; Collado, M.C.; Mangani, C.; Maleta, K.; Laitinen, K.; Ashorn, P.; Isolauri, E.; Salminen, S. Distinct gut microbiota in southeastern African and northern European infants. *J. Pediatr. Gastroenterol. Nutr.* **2012**, *54*, 812-816.
42. Collado, M.C.; Delgado, S.; Maldonado, A.; Rodríguez, J.M. Assessment of the bacterial diversity of breast milk of healthy women by quantitative real-time PCR. *Lett. Appl. Microbiol.* **2009**, *48*, 523-528.
43. Roger, L.C.; Costabile, A.; Holland, D.T.; Hoyles, L.; McCartney, A.L. Examination of faecal *Bifidobacterium* populations in breast- and formula-fed infants during the first 18 months of life. *Microbiology* **2010**, *156*, 3329-3341.
44. German, J.B.; Freeman, S.L.; Lebrilla, C.B.; Mills, D.A. Human milk oligosaccharides: evolution, structures and bioselectivity as substrates for intestinal bacteria. *Nestle. Nutr. Workshop Ser., Pediatr. Program* **2008**, *62*, 205-218; discussion 218-222.
45. Milani, C.; Duranti, S.; Bottacini, F.; Casey, E.; Turroni, F.; Mahony, J.; Belzer, C.; Delgado Palacio, S.; Arboleya Montes, S.; Mancabelli, L.; Lugli, G.A.; Rodriguez, J.M.; Bode, L.; de Vos, W.; Gueimonde, M.; Margolles, A.; van Sinderen, D.; Ventura, M. The first microbial colonizers of the human gut: composition, activities, and health implications of the infant gut microbiota. *Microbiol. Mol. Biol. Rev.* **2017**, *81*, e00036-00017.
46. World Health Organization, UNICEF. *Global strategy for infant and young child feeding* **2003**.
47. Bode, L. Human milk oligosaccharides: every baby needs a sugar mama. *Glycobiology* **2012**, *22*, 1147-1162.
48. Thurl, S.; Munzert, M.; Henker, J.; Boehm, G.; Muller-Werner, B.; Jelinek, J.; Stahl, B. Variation of human milk oligosaccharides in relation to milk groups and lactational periods. *Br. J. Nutr.* **2010**, *104*, 1261-1271.
49. Wu, S.; Tao, N.; German, J.B.; Grimm, R.; Lebrilla, C.B. Development of an annotated library of neutral human milk oligosaccharides. *J. Proteome Res.* **2010**, *9*, 4138-4151.
50. Wu, S.; Grimm, R.; German, J.B.; Lebrilla, C.B. Annotation and structural analysis of sialylated human milk oligosaccharides. *J. Proteome Res.* **2011**, *10*, 856-868.
51. Urashima, T.; Asakuma, S.; Leo, F.; Fukuda, K.; Messer, M.; Oftedal, O.T. The predominance of type I oligosaccharides is a feature specific to human breast milk. *Adv. Nutr.* **2012**, *3*, 473s-482s.
52. Breastfeeding and the use of human milk. *Pediatrics* **2012**, *129*, e827-841.
53. Engfer, M.B.; Stahl, B.; Finke, B.; Sawatzki, G.; Daniel, H. Human milk oligosaccharides are resistant to enzymatic hydrolysis in the upper gastrointestinal tract. *Am. J. Clin. Nutr.* **2000**, *71*, 1589-1596.
54. Marcobal, A.; Sonnenburg, J.L. Human milk oligosaccharide consumption by intestinal microbiota. *Clin. Microbiol. Infect.* **2012**, *18*, 12-15.
55. Suzuki, T.; Yoshida, S.; Hara, H. Physiological concentrations of short-chain fatty acids immediately suppress colonic epithelial permeability. *Br. J. Nutr.* **2008**, *100*, 297-305.

56. Peng, L.; Li, Z.-R.; Green, R.S.; Holzman, I.R.; Lin, J. Butyrate enhances the intestinal barrier by facilitating tight junction assembly via activation of AMP-activated protein kinase in Caco-2 cell monolayers. *J. Nutr.* **2009**, *139*, 1619-1625.
57. Burger-van Paassen, N.; Vincent, A.; Puiman, Patrycja J.; van der Sluis, M.; Bouma, J.; Boehm, G.; van Goudoever, Johannes B.; van Seuningen, I.; Renes, Ingrid B. The regulation of intestinal mucin MUC2 expression by short-chain fatty acids: implications for epithelial protection. *Biochem. J.* **2009**, *420*, 211-219.
58. Maslowski, K.M.; Vieira, A.T.; Ng, A.; Kranich, J.; Sierro, F.; Yu, D.; Schilter, H.C.; Rolph, M.S.; Mackay, F.; Artis, D. Regulation of inflammatory responses by gut microbiota and chemoattractant receptor GPR43. *Nature* **2009**, *461*, 1282.
59. Usami, M.; Kishimoto, K.; Ohata, A.; Miyoshi, M.; Aoyama, M.; Fueda, Y.; Kotani, J. Butyrate and trichostatin A attenuate nuclear factor κB activation and tumor necrosis factor α secretion and increase prostaglandin E2 secretion in human peripheral blood mononuclear cells. *Nutr. Res.* **2008**, *28*, 321-328.
60. Vinolo, M.A.; Rodrigues, H.G.; Hatanaka, E.; Sato, F.T.; Sampaio, S.C.; Curi, R. Suppressive effect of short chain fatty acids on production of proinflammatory mediators by neutrophils. *J. Nutr. Biochem.* **2011**, *22*, 849-855.
61. Sánchez, B.; González-Rodríguez, I.; Arboleya, S.; López, P.; Suárez, A.; Ruas-Madiedo, P.; Margolles, A.; Gueimonde, M. The effects of *Bifidobacterium breve* on immune mediators and proteome of HT29 cells monolayers. *Biomed. Res. Int.* **2015**, *2015*, 479140-479140.
62. Comstock, S.S.; Wang, M.; Hester, S.N.; Li, M.; Donovan, S.M. Select human milk oligosaccharides directly modulate peripheral blood mononuclear cells isolated from 10-d-old pigs. *Br. J. Nutr.* **2014**, *111*, 819-828.
63. Lane, J.A.; O'Callaghan, J.; Carrington, S.D.; Hickey, R.M. Transcriptional response of HT-29 intestinal epithelial cells to human and bovine milk oligosaccharides. *Br. J. Nutr.* **2013**, *110*, 2127-2137.
64. Goehring, K.C.; Kennedy, A.D.; Prieto, P.A.; Buck, R.H. Direct evidence for the presence of human milk oligosaccharides in the circulation of breastfed infants. *PloS one* **2014**, *9*, e101692.
65. Bode, L.; Rudloff, S.; Kunz, C.; Strobel, S.; Klein, N. Human milk oligosaccharides reduce platelet neutrophil complex formation leading to a decrease in neutrophil β 2 integrin expression. *J. Leukocyte Biol.* **2004**, *76*, 820-826.
66. Holscher, H.D.; Davis, S.R.; Tappenden, K.A. Human milk oligosaccharides influence maturation of human intestinal Caco-2Bbe and HT-29 cell lines. *J. Nutr.* **2014**, *144*, 586-591.
67. Ruiz-Palacios, G.M.; Cervantes, L.E.; Ramos, P.; Chavez-Munguia, B.; Newburg, D.S. *Campylobacter jejuni* binds intestinal H(O) antigen (Fuc alpha 1, 2Gal beta 1, 4GlcNAc), and fucosyloligosaccharides of human milk inhibit its binding and infection. *J. Biol. Chem.* **2003**, *278*, 14112-14120.
68. Bode, L.; Jantscher-Krenn, E. Structure-function relationships of human milk oligosaccharides. *Adv. Nutr.* **2012**, *3*, 383s-391s.
69. Jantscher-Krenn, E.; Lauwaet, T.; Bliss, L.A.; Reed, S.L.; Gillin, F.D.; Bode, L. Human milk oligosaccharides reduce *Entamoeba histolytica* attachment and cytotoxicity *in vitro*. *Br. J. Nutr.* **2012**, *108*, 1839-1846.
70. Jantscher-Krenn, E.; Zherebtsov, M.; Nissan, C.; Goth, K.; Guner, Y.S.; Naidu, N.; Choudhury, B.; Grishin, A.V.; Ford, H.R.; Bode, L. The human milk oligosaccharide disialyllacto-N-tetraose prevents necrotising enterocolitis in neonatal rats. *Gut* **2012**, *61*, 1417-1425.
71. Torres, D.P.M.; Gonçalves, M.d.P.F.; Teixeira, J.A.; Rodrigues, L.R. Galacto-Oligosaccharides: production, properties, applications, and significance as prebiotics. *Compr. Rev. Food Sci. Food Saf.* **2010**, *9*, 438-454.
72. Coulier, L.; Timmermans, J.; Bas, R.; Van Den Dool, R.; Haaksman, I.; Klarenbeek, B.; Slaghek, T.; Van Dongen, W. In-depth characterization of prebiotic galacto-oligosaccharides by a combination of analytical techniques. *J. Agric. Food Chem.* **2009**, *57*, 8488-8495.
73. Fransen, C.T.; Van Laere, K.M.; van Wijk, A.A.; Brull, L.P.; Dignum, M.; Thomas-Oates, J.E.; Haverkamp, J.; Schols, H.A.; Voragen, A.G.; Kamerling, J.P.; Vliegenthart, J.F. alpha-D-Glcp-(1-1)-beta-D-Galp-containing oligosaccharides, novel products from lactose by the action of beta-galactosidase. *Carbohydr. Res.* **1998**, *314*, 101-114.
74. Iqbal, S.; Nguyen, T.-H.; Nguyen, T.T.; Maischberger, T.; Haltrich, D. β-Galactosidase from *Lactobacillus plantarum* WCFS1: biochemical characterization and formation of prebiotic galacto-oligosaccharides. *Carbohydr. Res.* **2010**, *345*, 1408-1416.
75. Hernández-Hernández, O.; Calvillo, I.; Lebrón-Aguilar, R.; Moreno, F.J.; Sanz, M.L. Hydrophilic interaction liquid chromatography coupled to mass spectrometry for the characterization of prebiotic galactooligosaccharides. *J. Chromatogr. A* **2012**, *1220*, 57-67.
76. Kelly, G. Inulin-type prebiotics--a review: part 1. *Altern. Med. Rev.* **2008**, *13*, 315-329.
77. Singh, R.; Nagra, R. Production of fructooligosaccharides from inulin by endoinulinases and their prebiotic potential. *Food Technol. Biotechnol.* **2010**, *48*, 435-450.
78. Roberfroid, M.B. Introducing inulin-type fructans. *Br. J. Nutr.* **2005**, *93 Suppl 1*, S13-25.
79. Radosta, S.; Boczek, P.; Grossklaus, R. Composition of Polydextrose® before and after intestinal degradation in rats. *Starch* **1992**, *44*, 150-153.

80. Gomez, B.; Gullon, B.; Remoroza, C.; Schols, H.A.; Parajo, J.C.; Alonso, J.L. Purification, characterization, and prebiotic properties of pectic oligosaccharides from orange peel wastes. *J. Agric. Food Chem.* **2014**, *62*, 9769-9782.
81. Gullón, B.; Gómez, B.; Martínez-Sabajanes, M.; Yáñez, R.; Parajó, J.C.; Alonso, J.L. Pectic oligosaccharides: Manufacture and functional properties. *Trends Food Sci. Technol.* **2013**, *30*, 153-161.
82. Onumpai, C.; Kolida, S.; Bonnin, E.; Rastall, R.A. Microbial utilization and selectivity of pectin fractions with various structures. *Appl. Environ. Microbiol.* **2011**, *77*, 5747-5754.
83. Vos, A. P.; Haarman, M.; van Ginkel, J. W.; Knol, J.; Garssen, J.; Stahl, B.; Boehm, G.; M'Rabet, L. Dietary supplementation of neutral and acidic oligosaccharides enhances Th1-dependent vaccination responses in mice. *Pediatr. Allergy Immunol.* **2007**, *18*, 304-12.
84. Vos, A. P.; van Esch, B. C.; Stahl, B.; M'Rabet, L.; Folkerts, G.; Nijkamp, F. P.; Garssen, J. Dietary supplementation with specific oligosaccharide mixtures decreases parameters of allergic asthma in mice. *Int. Immunopharmacol.* **2007**, *7*, 1582-1587.
85. Babbar, N.; Dejonghe, W.; Gatti, M.; Sforza, S.; Elst, K. Pectic oligosaccharides from agricultural by products: production, characterization and health benefits. *Crit. Rev. Biotechnol.* **2016**, *36*, 594-606.
86. Scheller, H.V.; Ulvskov, P. Hemicelluloses. *Annu. Rev. Plant Biol.* **2010**, *61*, 263-289.
87. O' Neill, M.; York, W.S. The composition and structure of plant primary cell walls. In *The plant cell wall: annual plant review;* Rose, J.K.C., Ed.; CRC Press: Boca Raton, United States, **2003**, pp 1-54.
88. Chapla, D.; Pandit, P.; Shah, A. Production of xylooligosaccharides from corncob xylan by fungal xylanase and their utilization by probiotics. *Bioresour. Technol.* **2012**, *115*, 215-221.
89. Lecerf, J.M.; Depeint, F.; Clerc, E.; Dugenet, Y.; Niamba, C.N.; Rhazi, L.; Cayzeele, A.; Abdelnour, G.; Jaruga, A.; Younes, H.; Jacobs, H.; Lambrey, G.; Abdelnour, A.M.; Pouillart, P.R. Xylo-oligosaccharide (XOS) in combination with inulin modulates both the intestinal environment and immune status in healthy subjects, while XOS alone only shows prebiotic properties. *Br. J. Nutr.* **2012**, *108*, 1847-1858.
90. Carvalho, A.F.A.; Neto, P.d.O.; da Silva, D.F.; Pastore, G.M. Xylo-oligosaccharides from lignocellulosic materials: Chemical structure, health benefits and production by chemical and enzymatic hydrolysis. *Food Res. Int.* **2013**, *51*, 75-85.
91. Broekaert, W.F.; Courtin, C.M.; Verbeke, K.; Van de Wiele, T.; Verstraete, W.; Delcour, J.A. Prebiotic and other health-related effects of cereal-derived arabinoxylans, arabinoxylan-oligosaccharides, and xylooligosaccharides. *Crit. Rev. Food Sci. Nutr.* **2011**, *51*, 178-194.
92. Hughes, S.; Rastall, R.A. Health-functional carbohydrates: properties and enzymatic manufacture. In *Novel enzyme technology for food applications*; Rastall, R., Ed.; Woodhead Publishing: Cambridge, England, **2007**; pp 215-242.
93. Zhang, Z.; Smith, C.; Li, W. Extraction and modification technology of arabinoxylans from cereal by products: A critical review. *Food Res. Int.* **2014**, *65*, 423-436.
94. Lam, K.-L.; Chi-Keung Cheung, P. Non-digestible long chain beta-glucans as novel prebiotics. *Bioact. Carbohydr. Diet. Fibre* **2013**, *2*, 45-64.
95. Leemhuis, H.; Dobruchowska, J.M.; Ebbelaar, M.; Faber, F.; Buwalda, P.L.; van der Maarel, M.J.E.C.; Kamerling, J.P.; Dijkhuizen, L. Isomalto/malto-polysaccharide, a novel soluble dietary fiber made via enzymatic conversion of starch. *J. Agric. Food Chem.* **2014**, *62*, 12034-12044.
96. Hu, Y.; Ketabi, A.; Buchko, A.; Gänzle, M.G. Metabolism of isomalto-oligosaccharides by *Lactobacillus reuteri* and bifidobacteria. *Lett. Appl. Microbiol.* **2013**, *57*, 108-114.
97. van der Zaal, P.H.; Schols, H.A.; Bitter, J.H.; Buwalda, P.L. Isomalto/malto-polysaccharide structure in relation to the structural properties of starch substrates. *Carbohydr. Polym.* **2018**, *185*, 179-186.
98. Sorndech, W.; Nakorn, K.N.; Tongta, S.; Blennow, A. Isomalto-oligosaccharides: Recent insights in production technology and their use for food and medical applications. *LWT* **2018**, *95*, 135-142.
99. Van Craeyveld, V.; Swennen, K.; Dornez, E.; Van de Wiele, T.; Marzorati, M.; Verstraete, W.; Delaedt, Y.; Onagbesan, O.; Decuypere, E.; Buyse, J.; De Ketelaere, B.; Broekaert, W.F.; Delcour, J.A.; Courtin, C.M. Structurally different wheat-derived arabinoxylooligosaccharides have different prebiotic and fermentation properties in rats. *J. Nutr.* **2008**, *138*, 2348-2355.
100. Kabel, M.A.; Kortenoeven, L.; Schols, H.A.; Voragen, A.G. *In vitro* fermentability of differently substituted xylo-oligosaccharides. *J. Agric. Food Chem.* **2002**, *50*, 6205-6210.
101. Al-Tamimi, M.A.H.M.; Palframan, R.J.; Cooper, J.M.; Gibson, G.R.; Rastall, R.A. *In vitro* fermentation of sugar beet arabinan and arabino-oligosaccharides by the human gut microflora. *J. Appl. Microbiol.* **2006**, *100*, 407-414.
102. Bryda, E.C. The Mighty Mouse: the impact of rodents on advances in biomedical research. *Mo. Med.* **2013**, *110*, 207-211.
103. Tomas, J.; Langella, P.; Cherbuy, C. The intestinal microbiota in the rat model: major breakthroughs from new technologies. *Anim. Health Res. Rev.* **2012**, *13*, 54-63.
104. Nguyen, T.L.A.; Vieira-Silva, S.; Liston, A.; Raes, J. How informative is the mouse for human gut microbiota research? *Dis. Models Mech.* **2015**, *8*, 1-16.

105. Schwarz, R.; Kaspar, A.; Seelig, J.; Künnecke, B. Gastrointestinal transit times in mice and humans measured with 27Al and 19F nuclear magnetic resonance. *Magn. Reson. Med.* **2002**, *48*, 255-261.
106. Gonzalez, L.M.; Moeser, A.J.; Blikslager, A.T. Porcine models of digestive disease: the future of large animal translational research. *Transl. Res.* **2015**, *166*, 12-27.
107. Ziegler, A.; Gonzalez, L.; Blikslager, A. Large animal models: the key to translational discovery in digestive disease research. *Cell. Mol. Gastroenterol. Hepatol.* **2016**, *2*, 716-724.
108. Venema, K.; van den Abbeele, P. Experimental models of the gut microbiome. *Best Pract. Res., Clin. Gastroenterol.* **2013**, *27*, 115-126.
109. Van de Wiele, T.; Van den Abbeele, P.; Ossieur, W.; Possemiers, S.; Marzorati, M. The Simulator of the Human Intestinal Microbial Ecosystem (SHIME®). In *The impact of food bioactives on health: in vitro and ex vivo models*; Verhoeckx, K., Cotter, P., López-Expósito, I., Kleiveland, C., Lea, T., Mackie, A., Requena, T., Swiatecka, D., Wichers, H., Eds.; Springer International Publishing: Cham, Switzerland, **2015**; pp 305-317.
110. Venema, K. The TNO *in vitro* model of the colon (TIM-2). In *The impact of food bioactives on health: in vitro and ex vivo models*; Verhoeckx, K., Cotter, P., López-Expósito, I., Kleiveland, C., Lea, T., Mackie, A., Requena, T., Swiatecka, D., Wichers, H., Eds.; Springer International Publishing: Cham, Switzerland, **2015**; pp 293-304.
111. Marzorati, M.; Vanhoecke, B.; De Ryck, T.; Sadaghian Sadabad, M.; Pinheiro, I.; Possemiers, S.; Van den Abbeele, P.; Derycke, L.; Bracke, M.; Pieters, J.; Hennebel, T.; Harmsen, H.J.; Verstraete, W.; Van de Wiele, T. The HMI module: a new tool to study the Host Microbiota Interaction in the human gastrointestinal tract *in vitro*. *BMC Microbiol.* **2014**, *14*, 133.
112. Williams, C.F.; Walton, G.E.; Jiang, L.; Plummer, S.; Garaiova, I.; Gibson, G.R. Comparative Analysis of Intestinal Tract Models. *Annu. Rev. Food Sci. Technol.* **2015**, *6*, 329-350.
113. Aura, A.-M.; Maukonen, J. One compartment fermentation model. In *The impact of food bioactives on health: in vitro and ex vivo models*; Verhoeckx, K., Cotter, P., López-Expósito, I., Kleiveland, C., Lea, T., Mackie, A., Requena, T., Swiatecka, D., Wichers, H., Eds.; Springer International Publishing: Cham, Switzerland, **2015**; pp 281-292.
114. Payne, A.N.; Zihler, A.; Chassard, C.; Lacroix, C. Advances and perspectives in *in vitro* human gut fermentation modeling. *Trends Biotechnol.* **2012**, *30*, 17-25.
115. Rajilic-Stojanovic, M.; Heilig, H.G.; Tims, S.; Zoetendal, E.G.; de Vos, W.M. Long-term monitoring of the human intestinal microbiota composition. *Environ. Microbiol.* **2012**, 10.1111/1462-2920.12023.
116. Aguirre, M.; Ramiro-Garcia, J.; Koenen, M.E.; Venema, K. To pool or not to pool? Impact of the use of individual and pooled fecal samples for *in vitro* fermentation studies. *J. Microbiol. Methods* **2014**, *107*, 1-7.
117. Newton, D.F.; Macfarlane, S.; Macfarlane, G.T. Effects of antibiotics on bacterial species composition and metabolic activities in chemostats containing defined populations of human gut microorganisms. *Antimicrob. Agents Chemother.* **2013**, *57*, 2016-2025.
118. Ruiz-Moyano, S.; Totten, S.M.; Garrido, D.A.; Smilowitz, J.T.; German, J.B.; Lebrilla, C.B.; Mills, D.A. Variation in consumption of human milk oligosaccharides by infant gut-associated strains of *Bifidobacterium breve*. *Appl. Environ. Microbiol.* **2013**, *79*, 6040-6049.
119. Belenguer, A.; Duncan, S.H.; Calder, A.G.; Holtrop, G.; Louis, P.; Lobley, G.E.; Flint, H.J. Two routes of metabolic cross-feeding between *Bifidobacterium adolescentis* and butyrate-producing anaerobes from the human gut. *Appl. Environ. Microbiol.* **2006**, *72*, 3593-3599.
120. Duncan, S.H.; Holtrop, G.; Lobley, G.E.; Calder, A.G.; Stewart, C.S.; Flint, H.J. Contribution of acetate to butyrate formation by human faecal bacteria. *Br. J. Nutr.* **2004**, *91*, 915-923.
121. Mahowald, M.A.; Rey, F.E.; Seedorf, H.; Turnbaugh, P.J.; Fulton, R.S.; Wollam, A.; Shah, N.; Wang, C.; Magrini, V.; Wilson, R.K.; Cantarel, B.L.; Coutinho, P.M.; Henrissat, B.; Crock, L.W.; Russell, A.; Verberkmoes, N.C.; Hettich, R.L.; Gordon, J.I. Characterizing a model human gut microbiota composed of members of its two dominant bacterial phyla. *Proc. Natl. Acad. Sci.* **2009**, *106*, 5859-5864.
122. Smith, R.M. Column liquid chromatography. In *Chromatography 6th edition: Fundamentals and applications of chromatography and related differential migration methods*; Heftmann, E., Ed.; Elsevier: Amsterdam, The Netherlands, **2004**; pp 95-138.
123. Corradini, C.; Bianchi, F.; Matteuzzi, D.; Amoretti, A.; Rossi, M.; Zanoni, S. High-performance anion exchange chromatography coupled with pulsed amperometric detection and capillary zone electrophoresis with indirect ultra violet detection as powerful tools to evaluate prebiotic properties of fructooligosaccharides and inulin. *J. Chromatogr. A.* **2004**, *1054*, 165-173.
124. Watson, D.; O'Connell Motherway, M.; Schoterman, M.H.; van Neerven, R.J.; Nauta, A.; van Sinderen, D. Selective carbohydrate utilization by lactobacilli and bifidobacteria. *J. Appl. Microbiol.* **2013**, *114*, 1132-1146.
125. Poinsot, V.; Carpéné, M.A.C.; Couderc, F. Coupled mass spectrometric strategies for the determination of carbohydrates at very low concentrations: the case of polysaccharides involved in the molecular dialogue between plants and rhizobia. In *The complex world of polysaccharides*; Karunaratne, D.N., Ed.; InTech: Rijeka, Croatia, **2012**.

126. Coulier, L.; Zha, Y.; Bas, R.; Punt, P.J. Analysis of oligosaccharides in lignocellulosic biomass hydrolysates by high-performance anion-exchange chromatography coupled with mass spectrometry (HPAEC-MS). *Bioresour. Technol.* **2013**, *133*, 221-231.
127. Marino, K.; Lane, J.A.; Abrahams, J.L.; Struwe, W.B.; Harvey, D.J.; Marotta, M.; Hickey, R.M.; Rudd, P.M. Method for milk oligosaccharide profiling by 2-aminobenzamide labeling and hydrophilic interaction chromatography. *Glycobiology* **2011**, *21*, 1317-1330.
128. Jensen, P.H.; Karlsson, N.G.; Kolarich, D.; Packer, N.H. Structural analysis of N-and O-glycans released from glycoproteins. *Nat. Protoc.* **2012**, *7*, 1299.
129. Ruhaak, L.R.; Deelder, A.M.; Wuhrer, M. Oligosaccharide analysis by graphitized carbon liquid chromatography–mass spectrometry. *Anal. Bioanal. Chem.* **2009**, *394*, 163-174.
130. Bao, Y.; Chen, C.; Newburg, D.S. Quantification of neutral human milk oligosaccharides by graphitic carbon high-performance liquid chromatography with tandem mass spectrometry. *Anal. Biochem.* **2013**, *433*, 28-35.
131. Mechref, Y.; Novotny, M.V.; Krishnan, C. Structural characterization of oligosaccharides using Maldi-TOF/TOF tandem mass spectrometry. *Anal. Chem.* **2003**, *75*, 4895-4903.
132. Zhang, Z.; Linhardt, R.J. Sequence Analysis of Native Oligosaccharides Using Negative ESI Tandem MS. *Curr. Anal. Chem.* **2009**, *5*, 225-237.
133. Lattova, E.; Perreault, H.; Krokhin, O. Matrix-assisted laser desorption/ionization tandem mass spectrometry and post-source decay fragmentation study of phenylhydrazones of N-linked oligosaccharides from ovalbumin. *J. Am. Soc. Mass Spectrom.* **2004**, *15*, 725-735.
134. Zauner, G.; Deelder, A.M.; Wuhrer, M. Recent advances in hydrophilic interaction liquid chromatography (HILIC) for structural glycomics. *Electrophoresis* **2011**, *32*, 3456-3466.
135. Westphal, Y.; Schols, H.A.; Voragen, A.G.J.; Gruppen, H. Introducing porous graphitized carbon liquid chromatography with evaporative light scattering and mass spectrometry detection into cell wall oligosaccharide analysis. *J. Chromatogr. A* **2010**, *1217*, 689-695.
136. Kailemia, M.J.; Ruhaak, L.R.; Lebrilla, C.B.; Amster, I.J. Oligosaccharide analysis by mass spectrometry: a review of recent developments. *Anal. Chem.* **2014**, *86*, 196-212.
137. Black, B.A.; Lee, V.S.; Zhao, Y.Y.; Hu, Y.; Curtis, J.M.; Gänzle, M.G. Structural identification of novel oligosaccharides produced by *Lactobacillus bulgaricus* and *Lactobacillus plantarum*. *J. Agric. Food Chem.* **2012**, *60*, 4886-4894.
138. Wang, Y.; Black, B.A.; Curtis, J.M.; Gänzle, M.G. Characterization of α-galacto-oligosaccharides formed via heterologous expression of α-galactosidases from *Lactobacillus reuteri* in *Lactococcus lactis*. *Appl. Microbiol. Biotechnol.* **2014**, *98*, 2507-2517.
139. Reis, A.; Coimbra, M.A.; Domingues, P.; Ferrer-Correia, A.J.; Domingues, M.R.M. Fragmentation pattern of underivatised xylo-oligosaccharides and their alditol derivatives by electrospray tandem mass spectrometry. *Carbohydr. Polym.* **2004**, *55*, 401-409.
140. Duus, J.; Gotfredsen, C.H.; Bock, K. Carbohydrate structural determination by NMR spectroscopy: modern methods and limitations. *Chem. Rev.* **2000**, *100*, 4589-4614.
141. van Leeuwen, S.S.; Kuipers, B.J.; Dijkhuizen, L.; Kamerling, J.P. 1 H NMR analysis of the lactose/β-galactosidase-derived galacto-oligosaccharide components of Vivinal® GOS up to DP5. *Carbohydr. Res.* **2014**, *400*, 59-73.
142. Albrecht, S.; van Muiswinkel, G.C.; Schols, H.A.; Voragen, A.G.; Gruppen, H. Introducing capillary electrophoresis with laser-induced fluorescence detection (CE-LIF) for the characterization of konjac glucomannan oligosaccharides and their *in vitro* fermentation behavior. *J. Agric. Food Chem.* **2009**, *57*, 3867-3876.
143. Difilippo, E.; Pan, F.; Logtenberg, M.; Willems, R.H.; Braber, S.; Fink-Gremmels, J.; Schols, H.A.; Gruppen, H. Milk Oligosaccharide Variation in sow milk and milk oligosaccharide fermentation in piglet intestine. *J. Agric. Food Chem.* **2016**, *64*, 2087-2093.
144. Albrecht, S.; Schols, H.A.; van den Heuvel, E.G.; Voragen, A.G.; Gruppen, H. CE-LIF-MSn profiling of oligosaccharides in human milk and feces of breast-fed babies. *Electrophoresis* **2010**, *31*, 1264-1273.
145. Vogt, L.M.; Meyer, D.; Pullens, G.; Faas, M.M.; Venema, K.; Ramasamy, U.; Schols, H.A.; de Vos, P. Toll-like receptor 2 activation by beta2-->1-fructans protects barrier function of T84 human intestinal epithelial cells in a chain length-dependent manner. *J. Nutr.* **2014**, *144*, 1002-1008
146. Ortega-Gonzalez, M.; Ocon, B.; Romero-Calvo, I.; Anzola, A.; Guadix, E.; Zarzuelo, A.; Suarez, M.D.; Sanchez de Medina, F.; Martinez-Augustin, O. Nondigestible oligosaccharides exert nonprebiotic effects on intestinal epithelial cells enhancing the immune response via activation of TLR4-NFkappaB. *Mol. Nutr. Food Res.* **2014**, *58*, 384-393.
147. Capitán-Cañadas, F.; Ortega-González, M.; Guadix, E.; Zarzuelo, A.; Suárez, M.D.; de Medina, F.S.; Martínez-Augustin, O. Prebiotic oligosaccharides directly modulate proinflammatory cytokine production in monocytes via activation of TLR4. *Mol. Nutr. Food Res.* **2014**, *58*, 1098-1110
148. Sivieri, K.; Morales, M.L.V.; Saad, S.M.I.; Adorno, M.A.T.; Sakamoto, I.K.; Rossi, E.A. Prebiotic effect of fructooligosaccharide in the Simulator of the Human Intestinal Microbial Ecosystem (SHIME® Model). *J. Med. Food* **2014**, *17*, 894-901.
149. Koecher, K.J.; Noack, J.A.; Timm, D.A.; Klosterbuer, A.S.; Thomas, W.; Slavin, J.L. Estimation and interpretation of fermentation in the gut: coupling results from a 24 h batch *in vitro* system with

fecal measurements from a human intervention feeding study using fructo-oligosaccharides, inulin, gum acacia, and pea fiber. *J. Agric. Food Chem.* **2014**, *62*, 1332-1337.
150. Reis, S.F.; Gullon, B.; Gullon, P.; Ferreira, S.; Maia, C.J.; Alonso, J.L.; Domingues, F.C.; Abu-Ghannam, N. Evaluation of the prebiotic potential of arabinoxylans from brewer's spent grain. *Appl. Microbiol. Biotechnol.* **2014**, *98*, 9365-9373.
151. Wall, R.; Ross, R.P.; Ryan, C.A.; Hussey, S.; Murphy, B.; Fitzgerald, G.F.; Stanton, C. Role of gut microbiota in early infant development. *Clin. Med. Pediatr.* **2009**, *3*, 45-54.
152. Rada, V.; Nevoral, J.; Trojanova, I.; Tomankova, E.; Smehilova, M.; Killer, J. Growth of infant faecal bifidobacteria and clostridia on prebiotic oligosaccharides in *in vitro* conditions. *Anaerobe* **2008**, *14*, 205-208.
153. Flint, H.J.; Duncan, S.H.; Scott, K.P.; Louis, P. Interactions and competition within the microbial community of the human colon: links between diet and health. *Environ. Microbiol.* **2007**, *9*, 1101-1111.
154. Vester Boler, B.M.; Rossoni Serao, M.C.; Faber, T.A.; Bauer, L.L.; Chow, J.; Murphy, M.R.; Fahey, G.C. *In vitro* fermentation characteristics of select nondigestible oligosaccharides by infant fecal inocula. *J. Agric. Food Chem.* **2013**, *61*, 2109-2119.
155. Stiverson, J.; Williams, T.; Chen, J.; Adams, S.; Hustead, D.; Price, P.; Guerrieri, J.; Deacon, J.; Yu, Z. Prebiotic oligosaccharides: comparative evaluation using *in vitro* cultures of infants' fecal microbiomes. *Appl. Environ. Microbiol.* **2014**, *80*, 7388-7397.
156. Le Blay, G.; Chassard, C.; Baltzer, S.; Lacroix, C. Set up of a new *in vitro* model to study dietary fructans fermentation in formula-fed babies. *Br. J. Nutr.* **2010**, *103*, 403-411.
157. Shen, Q.; Tuohy, K.M.; Gibson, G.R.; Ward, R.E. *In vitro* measurement of the impact of human milk oligosaccharides on the faecal microbiota of weaned formula-fed infants compared to a mixture of prebiotic fructooligosaccharides and galactooligosaccharides. *Lett. Appl. Microbiol.* **2011**, *52*, 337-343.
158. Pérez-Conesa, D.; López, G.; Rosau, G. Fermentation capabilities of bifidobacteria using nondigestible oligosaccharides, and their viability as probiotics in commercial powder infant formula. *J. Food Sci.* **2005**, *70*, m279-m285.
159. Thum, C.; Roy, N.C.; McNabb, W.C.; Otter, D.E.; Cookson, A.L. *In vitro* fermentation of caprine milk oligosaccharides by bifidobacteria isolated from breast-fed infants. *Gut Microbes* **2015**, *6*, 352-363.
160. Cinquin, C.; Le Blay, G.; Fliss, I.; Lacroix, C. Comparative effects of exopolysaccharides from lactic acid bacteria and fructo-oligosaccharides on infant gut microbiota tested in an *in vitro* colonic model with immobilized cells. *FEMS Microbiol. Ecol.* **2006**, *57*, 226-238.
161. Parrett, A.M.; Lokerse, E.; Edwards, C.A. Colonic fermentation capacity *in vitro*: development during weaning in formula-fed infants. *Microb. Ecol. Health Dis.* **2003**, *15*, 10-14.
162. Parrett, A.M.; Edwards, C.A. *In vitro* fermentation of carbohydrate by breast fed and formula fed infants. *Arch. Dis. Child.* **1997**, *76*, 249-25.

Chapter 2

Pooled faecal inoculum can predict infant fibre fermentability despite high inter-individual variability of microbiota composition

Abstract

Infants are known for their high inter-individual variability in gut microbiota composition in the first months of life. This poses difficulties when predicting the fate of non-digestible carbohydrates (NDCs) in the infant gut using *in vitro* models, since numerous experiments with individual faecal inocula of different infants are required. In this study an *in vitro* fermentation experiment was performed with galacto-oligosaccharides (GOS) using both individual and pooled faecal inocula of five two-week-old infants. It was shown that pooled faecal inoculum can be used to judge the fermentability of GOS, as a similar trend in total organic acid production and relative increase in *Bifidobacterium* was observed for the pooled faecal inoculum and four out of five individual faecal inocula. An additional fermentation using pooled faecal inoculum of five other infants of the same age confirmed these findings. Additionally, we provided evidence for both size- and isomer-specific fermentation of GOS by infant microbiota, which reveals the potential for the production of tailored NDC mixtures to meet the needs of specific subgroups of infants. Hence, the use of pooled faecal inocula contributes to increasing our knowledge on structure-specific effects of NDCs in infants efficiently.

Logtenberg, M.J.; Vink, J.C.M.; Serierse, R.M.; An, R.; Hermes, G.D.A.; Smidt, H.; Schols, H.A., **2020**, In press: *Bioactive Carbohydrates and Dietary Fibre*.

Introduction

There is a growing body of literature that recognizes the link between early life gut microbial dynamics and infant's health [1]. Recent research suggests various associations between the likelihood of developing metabolic or inflammatory diseases in later life and the abundance of specific bacteria [2] [3].

In general clear evidence was found for the colonization upon birth by facultative anaerobic bacteria, which reduce the oxygen levels and in this way promote further colonization by strictly anaerobic microorganisms [4]. Principally, during the first days after birth, members of the Proteobacteria predominate, after which members of the Clostridia and bifidobacteria become more prominent [4]. Additionally, in the first months of life large inter-individual variation in microbiota composition and dynamics between infants has been observed. These differences are to a large extent caused by the mode of delivery, gestational age at birth, the infant feeding mode, maternal diet, environment and host genetics [5]. Furthermore also large intra-individual differences exist during the first weeks after birth, as the infant microbiota is highly dynamic with more stable periods alternated with complete shifts in composition caused by e.g. fever, antibiotic therapy or changes in diet [5].

Diet shapes the infant microbiota and can prevent future health complaints. Previous research comparing the microbiota composition of formula- and breast-fed infants revealed profound differences caused by the presence of a complex mixture of human milk oligosaccharides (HMOs) in breast milk [6]. HMOs are resistant to digestion in the small intestine and serve as a prebiotic in the large intestine [7]. Furthermore, HMOs have been shown to support the maturation of the gut barrier by promoting the differentiation of enterocytes [8]. To mimic the effects of HMOs, non-digestible carbohydrates (NDCs) can be added to cow's milk-based infant formulas. However, very little is known about the relation between specific HMOs and NDCs and the effect on the infant gut microbiota. Studies up to now have mainly focused on *in vitro* fermentation experiments with prevalent bacterial isolates. Such approaches ignore the importance of cross-feeding networks [9-11]. However, the high inter-individual variability in microbiota composition requires *in vitro* experiments with individual faecal inocula of around ten infants, which makes the study of several structurally different NDCs laborious and costly [12]. An alternative approach could be the use of pooled infant faecal inoculum, which consists of the faecal material of multiple infants. In previous research the use of pooled faecal inoculum has already been validated for adults who generally show a more stable faecal microbiota composition than infants. The pooled adult faecal inoculum resulted in a comparable bacterial activity as the individual faecal inocula [13].

The objective of this study was to determine whether pooled infant faecal inoculum can be used as an alternative for individual infant faecal inoculum leading to a more efficient

screening of the fermentability of NDCs. *In vitro* fermentations were performed with galacto-oligosaccharides (GOS) as carbohydrate source using both individual and pooled faecal inocula of two-week-old infants. The microbiota composition and production of organic acids were followed in time, as well as the fate of individual GOS compounds using LC-MS, which showed us that pooled faecal inoculum can be used to judge the fermentability of GOS and potentially also other NDCs.

Materials and Methods

Materials

Purified Vivinal GOS (degree of polymerization (DP) 1 and 2 partly removed) was kindly provided by Friesland Campina DOMO (Borculo, The Netherlands). An overview of the complexity of the Vivinal GOS mixture with the isomers present per DP is shown in Figure 1. Relative abundance of different DPs in purified Vivinal GOS was as follows: DP1, 2.5%; DP2, 10.9%, DP3, 46.2%, DP4, 25.4%, DP5, 9.6%, DP6, 3.7%, DP>7, 1.7%. GOS DP3 standards β-3-Galactosyl-lactose, β-4-Galactosyl-lactose and β-6-Galactosyl-lactose were purchased from Carbosynth (Berkshire, UK).

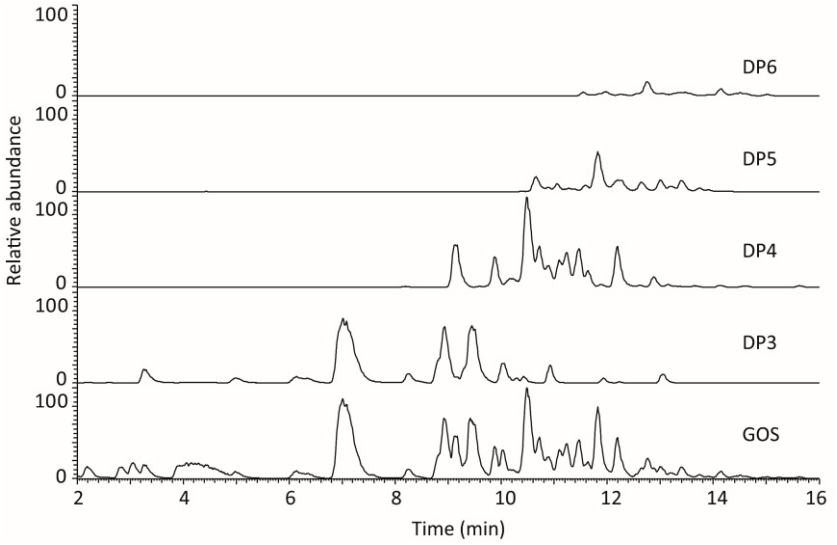

Figure 1 UHPLC-PGC-MS profile of total reduced GOS and of DP 3-6 after selection of the appropriate m/z for that DP. Elution profiles were normalized to the real contribution of each DP to the total mixture.

Fermentation of GOS by infant faecal inoculum

Culture medium

Standard ileal efflux medium (SIEM; Tritium Microbiology, Veldhoven, The Netherlands) was prepared as described elsewhere with minor modifications [14]. Low amount of carbohydrates was added to mimic the infant ileal environment while minimizing

background fermentation. The carbohydrate medium component contained (g/L): pectin, 12; xylan, 12; arabinogalactan, 12; amylopectin, 12; and starch, 12 with a final concentration of only 0.24 g/L).The pH was adjusted to 5.8 using MES buffer.

2.2.2 Infants and infant faecal inoculum

Ten two-week-old infants were included in the current study. The solely breast-fed infants were born vaginally and did not show any health complaints. These infants did not receive antibiotic treatment in the first 2 weeks of life. Faecal inoculum was prepared as reported elsewhere with some minor modifications [15]. Parents collected faecal material from the diaper of two-week-old infants directly after defecation. Faecal material was immediately transferred to tubes and stored at -20 degrees. Afterwards tubes were stored at -80 degrees.

After thawing, faecal material (± 100 mg) was diluted with 6 mL sterilized 0.9% (w/v) NaCl solution in a laminar flow cabinet. In case of pooled faecal inocula, faecal material of five infants (5x ±100 mg) was combined and diluted to obtain a similar final concentration. An additional pool containing faecal material of five other infants was included in this study to determine reproducibility. The ten infants were randomly divided over the 2 pools. Homogenization was performed by the addition of sterile glass beads prior to shaking using a vortex.

The following steps were performed in an anaerobic chamber (gas phase: 81% N_2, 15% CO_2 and 4% H_2). Faecal solutions were combined with SIEM medium in a ratio of 5:82 (v/v) in a sterile 20 mL serum bottle. The bottle was closed with a rubber stopper and secured with a metal crimp cap. The final faecal inoculum adapted to the new environment by overnight incubation in an incubator shaker (Innova 40, New Brunswick Scientific, Nijmegen, The Netherlands) (37 °C, 100 rpm) [16].

In vitro fermentation

The *in vitro* fermentation was performed in an anaerobic chamber**.** Activated faecal inoculum was combined with SIEM medium containing GOS (11.1 mg/ml) in sterile serum bottles in a ratio of 1:10 (v/v). Serum bottles were closed with a rubber stopper and secured with a metal crimp cap. Afterwards they were placed in an incubator shaker (Innova 40)(37 °C, 100 rpm). At the start and after 6, 12, 24, 34 and 48 h, three aliquots of each 70 µl were taken from the serum bottle with a syringe and put into separate tubes. One series of samples was immediately frozen in liquid nitrogen and stored at -80 °C to preserve the samples for later microbial analysis. The remaining two series were heated for 5 min in a boiling water bath to inactivate the enzymes. Subsequently they were stored at -20 °C until further analysis.

In vitro fermentations were performed in duplicate and blanks without faecal inoculum or substrate were included to monitor possible contamination of the substrate or background fermentation over time. Data on the fermentation of infant 5 after 12 h is missing due to a broken serum bottle.

Fate of GOS upon fermentation

GOS pre-treatment before analysis

Prior to analysis fermentation samples were reduced to avoid anomerisation of oligosaccharides. Freshly prepared 0.5 M sodium borohydride ($NaBH_4$) in water was added to 10 times diluted fermentation samples in a ratio of 1:1 (v/v) with a final volume of 400 µl. Samples were incubated overnight at room temperature.

Solid phase extraction (SPE) was applied to remove salts in order to purify the reduced fermentation samples. First cartridges (Carbograph, Supelclean ENVI carb, bed weight: 250 mg; Sigma Aldrich) were activated with 1.5 ml of 80:20 (v/v) ACN/H_2O containing 0.1% (v/v) TFA, followed by 1.5 ml H_2O (Milli-Q). The reduced sample was loaded on the column, after which the column was washed 4 times with 1.5 mL H_2O (Milli-Q). Subsequently reduced GOS were eluted with 1.5 mL of 40:60 (v/v) ACN/H_2O containing 0.05% (v/v) TFA. Eluted reduced GOS were dried under nitrogen gas, solubilized in 400 µl of H_2O (ULC-MS grade) and centrifuged (5 min, 15 000g).

Characterization of GOS by UHPLC-PGC-MS

Reduced GOS were analysed on an Accela Ultra High Liquid Chromatography (UHPLC) system (Thermo Scientific, San Jose, CA, USA). The system was equipped with pump and autosampler. Samples (5 µl) were injected on a porous graphitic carbon (PGC) column (3 µm particle size, 2.1 mm x 100 mm; Hypercarb, Thermo Scientific) in combination with a guard column (3 µm particle size, 2 mm x 10 mm; Hypercarb, Thermo Scientific).

As mobile phase A: ULC-MS water + 0.1% (v/v) formic acid + 1% (v/v) ACN was used. Mobile phase B consisted of ACN + 0.1% (v/v) formic acid. The flow rate was 300 µL/min. The solvents were eluted according to the following profile: 0-3.3 min, 3% B; 3.3-8 min, 3-10% B; 8-20 min, 10-20% B; 20-26.7 min, 20-40% B; 26.7-27.5 min, 40-100% B; 27.5-37.5 min, 100% B; 37.5-38.5 min, 100-3% B; 38.5-43.5 min, 3% B. The temperature of the autosampler and column oven was controlled at 10 and 45 °C, respectively. Needle wash solvent containing 3% ACN was used to wash the autosampler.

To obtain mass spectrometric (MS) data, the flow of the UHPLC was directed to a Thermo Scientific LTQ-Velos Pro equipped with an electrospray ionisation (ESI) probe. Helium and nitrogen were used as sheath and auxiliary gas, respectively. The MS settings were set to a source voltage of 3.5 kV, a source heater temperature of 225 °C, a capillary temperature of 350˚C, a sheath gas flow of 38 and an auxiliary gas flow of 11.

MS data in negative mode were collected over an m/z range of 300-2000. Data dependent MS^2 analysis was performed with a normalized collision energy of 30%, activation Q of 0.25, activation time of 30 ms and isolation width of m/z 2. MS^2 fragmentation was performed on the 1st and 2nd most abundant ion in the MS chromatogram from a parent list containing *m/z* of both unreduced and reduced GOS.

DP3 standards β-3-Galactosyl-lactose, β-4-Galactosyl-lactose and β-6-Galactosyl-lactose were used for the identification of GOS isomers. Vivinal GOS was used in a concentration of

0.005-1 mg/ml to create calibration curves per DP. GOS DPs were quantified by selection of the specific mass range followed by integration of the peaks. Data acquisition and processing were performed using Xcalibur (version 2.2, Thermo Scientific).

Production of SCFAs and other organic acids

In order to quantify the production of volatile SCFAs fermentation samples were analysed using gas chromatography (GC). Fermentation samples were 10x diluted with water (ULC-MS grade). Standards containing acetic acid, butyric acid and propionic acid in concentration range 0.01-3 mg/mL were also included in the analysis. Standards and diluted fermentation samples were mixed in a ratio of 2:1 (v/v) with a solution containing HCl (0.3M), oxalic acid (0.09M) and the internal standard 2-ethyl butyric acid (0.45 mg/mL). The mixture was kept for 30 min at room temperature and afterwards centrifuged (5 min, 15 000g).

Samples (1 µl) were injected in a CP-FFAP CB column (25m x 0.53 mm x 1.00 µm) (Agilent Technologies, Santa Clara, CA, USA). The temperature profile during GC analysis was as follows: 100 °C, maintained for 0.5 min; raised to 180 °C at 8 °C/min, maintained for 1 min; raised to 200 °C at 20 °C/min, maintained for 5 min. Glass wool was inserted in the glass liner of the split injection port to protect the column from contamination [17]. Obtained data were integrated using Xcalibur software (Thermo Scientific).

Organic acids were analysed using high-performance liquid chromatography (HPLC) on an Organic Acid column as described elsewhere [18]. Besides 10x diluted fermentation samples, standards of lactic and succinic acid in a concentration range of 0.01-1 mg/mL were included in the analysis. Obtained data were integrated using Chromeleon 7.0 (Thermo Scientific).

Microbial composition analysis

DNA extraction

DNA was extracted from fermentation samples using repeated bead beating. Briefly each fermentation sample (70 µl) was added to a sterilized screwed cap tube containing 0.25 grams of zirconia beads and 3 glass beads (2.5 mm). After the addition of 300 µl Stool Transport and Recovery Buffer (STAR; Roche Diagnostics Corporation, Indianapolis, IN), the samples were treated with a bead beater (room temperature, 5.5 m/s for 3x 1 min) (Precellys 24, Bertin Technologies) and heated for 15 min (95 °C, 100 rpm). Subsequently the samples were centrifuged for 5 min (4 °C, 14000g) and supernatants were collected. Another cycle was performed with the pellet using 200 µl of STAR buffer. Supernatants of both cycles were combined, and 250 µl was purified using Maxwell 16 Tissue LEV Total RNA Purification Kit Cartridge (AS1220). DNA was eluted with 50 µl of Nuclease-Free water (Promega, Wisconsin, USA). Finally, DNA concentrations were determined using a NanoDrop ND-1000 spectrophotometer (NanoDrop Technologies, Wilmington, DE, USA) and if needed diluted to a concentration of 20 ng/µl with Nuclease-Free water.

PCR amplification

Microbiota profiling was performed as described previously with some modifications [19]. The V5-V6 region of 16S ribosomal RNA (rRNA) genes was amplified in triplicate PCR reactions with an uniquely barcoded primer pair F784 (RGGATTAGATACCC) and 1064R (CGACRRCCATGCANACCT). For samples containing 4.8-7.4, 7.8-12 and 15-20 ng/µl DNA template respectively 5, 3 or 0.7 µl DNA template was used in each reaction. The samples were amplified with 0.7 µl of 10 µM stock solutions of the primer pair, 7 µl of 5x HF buffer (Finnzymes, Vantaa, Finland), 0.7 µl of 10 mM dNTPs (Roche, Diagnostics GmbH, Mannheim, Germany) and 0.35 µl of 2U/µl Phusion® Hot Start II High Fidelity DNA Polymerase (Finnzymes, Vantaa, Finland). Nuclease-free water was added to reach a total reaction volume of 35 µl. The amplification program included a 30 s initial denaturation step at 98 °C, followed by 25 cycles of denaturation at 98 °C for 10 s, annealing at 42 °C for 10 s, elongation at 72 °C for 10 s, and a final extension at 72 °C for 7 min. The PCR product presence and size (≈290 bp) was confirmed with gel electrophoresis using the Lonza FlashGel System (Lonza, Cologne, Germany). Synthetic Mock communities of known composition were included as positive control [19].

Library preparation and sequencing

PCR products were purified using HighPrep PCR kit (MagBio Genomics, Alphen aan den Rijn, The Netherlands). Purified amplicons were quantified using Qubit dsDNA BR assay kit (Life Technologies, Leusden, The Netherlands). Seventy unique barcode tags were used in each library [19]. An amplicon pool was formed by combining 150 ng of each barcoded sample and afterwards concentrated to 40 µl volume using the HighPrep PCR kit. The resulting library was sent for adapter ligation and sequencing on an Illumina Hiseq2500 instrument (GATC-Biotech, Konstanz, Germany).

Data analysis

Processing and analysis of the 16S rRNA gene sequence data was carried out using the NG-Tax pipeline and R version 3.5.0 [19].

Beta-diversity was calculated using weighted UniFrac distances based on relative abundance of bacteria at genus level present in the fermentation digesta using the functions *tax_glom* and *ordinate* in the *phyloseq* R package. The output was visualized using Principal Coordinate Analysis (PCoA) using the function *plot_ordination* in the *phyloseq* R package.

The contribution of taxa to the principle coordinates was determined from a PCoA plot of the taxa based on the same distances using the function *plot_ordination (type: taxa)* in the *phyloseq* R package. Taxa vectors with the extracted x- and y- coordinates were plotted on the first PCoA plot using the function *geom_segment* in the *ggplot2* R package.

A higher resolution analysis of *Bifidobacterium* at the level of individual sequences (Amplicon Sequencing Variants (ASVs)) was performed using the function *subset_taxa* in the *phyloseq* R package. Bifidobacterial ASVs with a relative abundance of less than 0.5% in

each sample were removed using the functions *filterfun* and *filter_taxa* in the *genefilter* and *phyloseq R* package.

Results and discussion

Relative increase in *Bifidobacterium* upon fermentation of GOS using both individual and pooled infant faecal inoculum

The responsiveness of the microbiota to NDCs is dependent on the microbiota composition [20]. As such, it is important to determine the effect of pooling of infant faecal inocula on the changes in microbiota composition upon fermentation of GOS. Fermentation samples were analysed with 16S rRNA gene amplicon sequencing followed by Principal Coordinates Analysis (PCoA) using weighted UniFrac distances (Figure 2). The contribution of most abundant taxa to PC1 and PC2 is visualized by taxa vectors. Together these taxa comprise more than 70% of each fermentation sample. Relative abundances of all bacterial taxa present in the fermentation samples are shown in Figure S1.

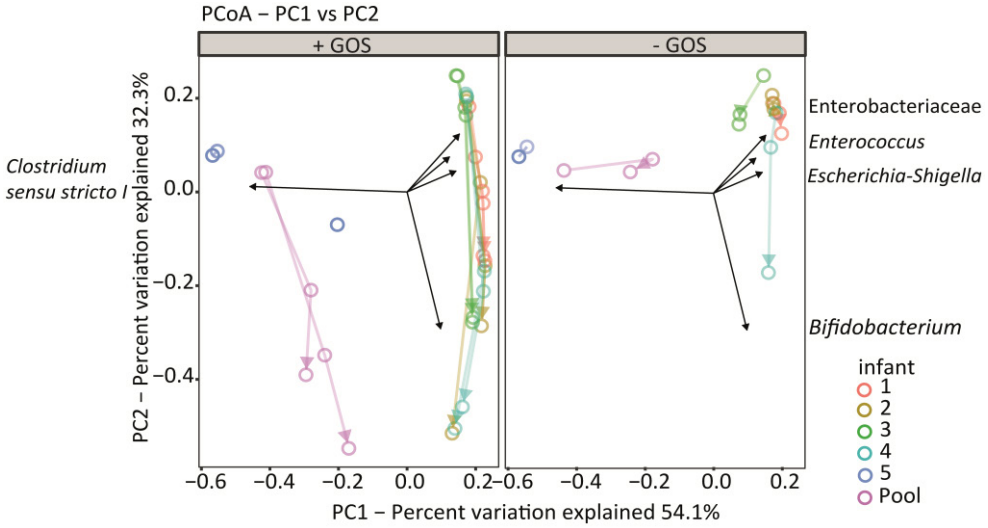

Figure 2 PCoA using weighted UniFrac distances of microbiota composition in digesta collected at the start and after 12 and 24 h of *in vitro* fermentation with (left) and without (right) GOS using inoculum of two-week-old infants. Direction of changes in time is presented by arrows in the same colour. Direction and length of the taxa arrows (black) presents the contribution of selected taxa to PC1 and PC2.

First of all, it must be stated that initial microbiota composition of the faecal inocula does not relate to faecal microbiota of two-week-old infants previously reported in literature, where *Bifidobacterium* and *Bacteroides* are present at high levels [21]. Instead, bacteria belonging to the genera *Clostridium, Enterococcus, Shigella* and *Escherichia* and the family Enterobacteriaceae were found to be present at high relative abundance at the start of the

fermentation of GOS using the individual and pooled faecal inocula as well as the background fermentation (Figure 2). Growth of these facultative anaerobic bacteria could be explained by traces of oxygen still present during the overnight activation of the faecal inoculum. However, these bacteria were also reported to grow well on peptides and amino acids, which are present in high abundance in the SIEM medium: bactopeptone (24 g/L), casein (24 g/L), ox-bile (0.4 g/L) and cysteine (0.16 g/L) [22]. Prior to fermentation faecal bacteria were activated overnight in SIEM medium, and the microbiota composition measured suggests the adaptation of the bacteria to the medium constituents [23]. This also explains why the initial composition of the pooled faecal inoculum does not represent the average composition of the individual faecal inocula.

However, despite the aberrant initial microbiota composition still a clear compositional shift was observed upon fermentation of GOS for faecal inocula of infant 1-4 (Figure 2). The shift was mainly characterized by a relative increase in *Bifidobacterium*, which is consistent with data obtained in previous *in vitro* [24] and *in vivo* studies [25]. For infant 1 the initial relative abundance of *Bifidobacterium* was 2-11% and increased up to 24-29% in 24 h of fermentation. For faecal inocula of infant 2-4 this was lower than 1.3% at the start of the fermentation but increased up to 43-68% in 24 h of fermentation of GOS. Differences in relative increase of *Bifidobacterium* between individual infant faecal inocula could possibly be ascribed to differences at the species level, since it has been reported that bifidobacterial species show different levels of cell reproduction upon fermentation of GOS [26]. Classification of bacteria at species level is hindered by sequence similarity of the 16S rRNA gene between different species within the same genus [27]. However, a higher resolution analysis at the level of individual sequences (Amplicon Sequencing Variants (ASVs)) showed a high variability in bifidobacterial ASVs between the individual faecal inocula suggesting the presence of multiple bifidobacterial species (Figure S2). No significant changes in the less abundant bacteria were observed upon fermentation of GOS using individual faecal inocula of infant 1-4.

In contrast, faecal inoculum of infant 5 did not contain *Bifidobacterium* and was dominated by bacteria belonging to the genus *Clostridium sensu stricto* (Figure 2). After 12 h of fermentation faecal inoculum of infant 5 even consisted exclusively of bacteria belonging to this genus. Additionally, the fermentation showed aberrant behaviour after 12 h as organic acids were not detected and GOS concentrations seemed to increase (Figure 3 and 4). Unfortunately, a missing duplicate fermentation of infant 5 prohibited confirmation of this outlier.

Clostridium sensu stricto was also present in the initial pooled faecal inoculum at high relative abundance (79-80%) (Figure 2). Despite the presence of the aberrant faecal inoculum of infant 5, a clear increase in *Bifidobacterium* relative abundance was observed during the fermentation of GOS using pooled faecal inoculum (39-63%). Background fermentations without the addition of GOS did not show such shift in *Bifidobacterium*

relative abundance. These findings indicate the potential of using pooled faecal inoculum to screen for bifidogenic potential of NDCs, although the microbiota composition of the pooled infant faecal inoculum does not mimic the microbiota composition of the individual infant faecal inocula.

Production of SCFAs and other organic acids

Upon the fermentation of GOS, SCFAs and the intermediate fermentation products lactic and succinic acid were produced by the bacteria, which were analysed by GC and HPLC (Figure 3). The total amount of organic acids increased to 10.9-14.6 µmol/mg GOS after 48 h of fermentation using individual infant faecal inocula 1-4. Composition of the organic acids produced during the fermentation differed for the individual infant faecal inocula. Nevertheless, in all fermentations, acetate was produced at highest abundance followed by lactate.

Reproducibility was confirmed by duplicate fermentations (Table S1). In addition, both background fermentations without GOS or inoculum showed hardly any production of organic acids (Table S2). Taking into account both the organic acid production and the changes in microbiota composition, it could thus be suggested that the high abundance of acetate upon fermentation of GOS could be ascribed to a large extent to the growth of *Bifidobacterium*, members of which are known as acetate- and lactate- producing bacteria [28].

Fermentation of GOS using pooled infant faecal inoculum resulted in similar amounts of organic acids after 48 h as the individual infant faecal inoculum that produced most organic acids (infant 4), respectively 14.5 and 14.6 µmol/mg GOS. Both faecal inoculum of infant 4 and the pool were dominated by *Bifidobacterium* after 24 h of fermentation, respectively 69% and 63%, while fermentation using faecal inoculum of infant 1 and 3 individually resulted in a relative abundance of only 27 and 44% respectively. These findings suggest the overruling effect of *Bifidobacterium* species of faecal inoculum of infant 4 over other bacteria within the pool.

In contrast to faecal inoculum of infant 4, pooled faecal inoculum resulted in the production of minor amounts of butyrate (0.6 µmol/mg) after 24 h of fermentation. *Clostridium sensu stricto* is the 2nd most abundant genus-level group in the pool, but is not detected in the faecal inoculum of infant 4 (Figure 2). Cross-feeding between *Bifidobacterium* and *Clostridium sensu stricto* could have resulted in the minor production of butyrate during fermentation of GOS using pooled infant faecal inoculum [29].

Notwithstanding the aberrant microbiota and organic acid composition, it can be concluded that the fermentability of GOS is reflected by the total organic acid production upon fermentation using pooled infant faecal inoculum.

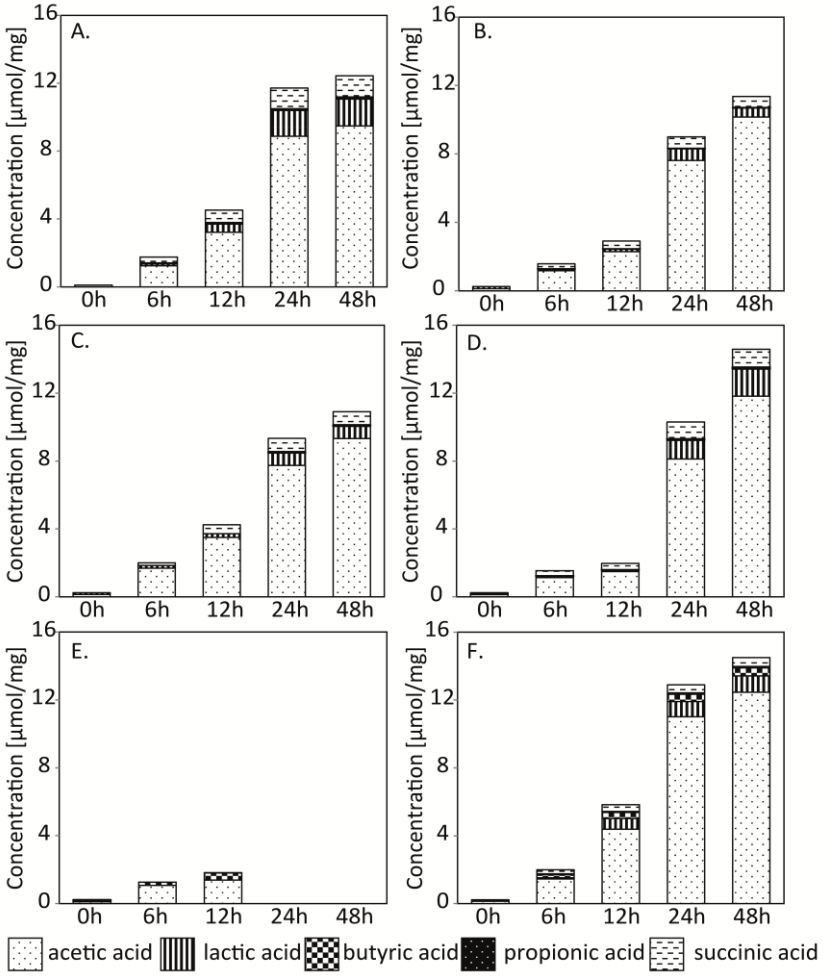

Figure 3 Production of organic acids upon *in vitro* fermentation of GOS using faecal inoculum of individual infants 1: A, 2: B, 3: C, 4: D, 5: E, and the pool of inocula infant 1-5: F.

Degradation kinetics of GOS

Degradation of GOS was monitored by UHPLC-PGC-MS to determine the effect of pooling faecal inocula on the degradation capability of individual GOS structures. To visualize the degradation kinetics of GOS by individual and pooled faecal inocula, both the proportion of the remaining total GOS mixture and oligomers with different DPs present in the mixture are shown in Figure 4. Individual inocula showed different speed of degradation of total GOS, with a slower degradation for individual inocula of infant 2 and 4 (>40% remaining) and faster degradation for infant 1 and 3 (<25% remaining) after 24 h of fermentation. As expected, a lower amount of GOS remaining coincided with a higher amount of organic acids produced (Figure 3 and 4).

Zooming in on the degradation kinetics at DP level showed a high variability in preference for specific DPs of GOS between individual infant inocula. For the fermentation using faecal inocula of infant 2, 3 and 4, oligomers DP≤3 were fermented faster than DP4 and DP5 oligomers. Contrarily, DP≥6 oligomers were the first to be degraded during the fermentation using faecal inoculum of infant 1. These differences could be explained by the DP-specific oligomer utilization of GOS by different species, as exemplified for *Bifidobacterium* [26]. Degradation of total GOS was observed to be somewhat faster and more complete during fermentation using pooled faecal inocula compared to the individual faecal inocula, i.e. 7% of oligosaccharides were remaining after 48h of fermentation using pooled inocula, compared to 8-17% for individual inocula 1-4. This finding could be explained again by the overruling of specific *Bifidobacterium* species which were able to utilize GOS most efficiently [26].

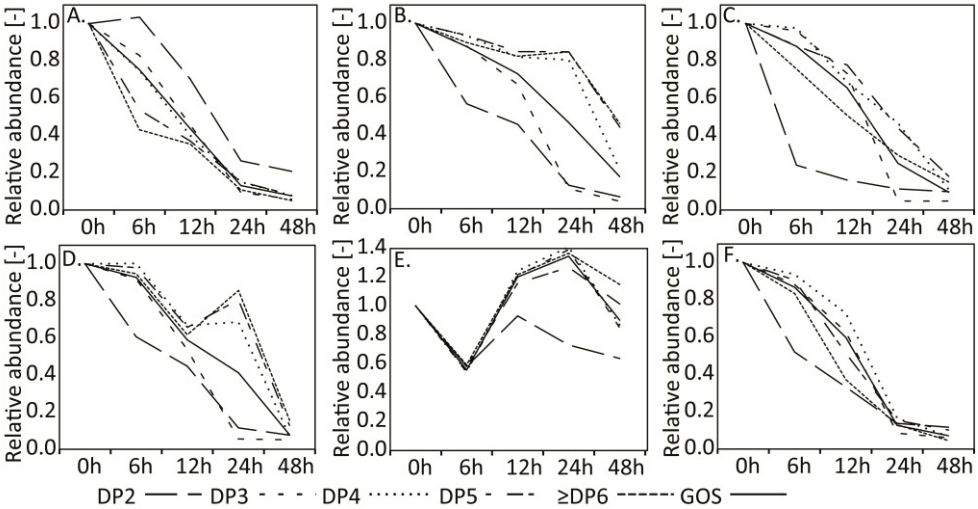

Figure 4 Relative proportion of remaining oligosaccharides from GOS and individual DPs of GOS during *in vitro* fermentation using faecal inoculum of individual infants 1: A, 2: B, 3: C, 4: D, 5: E and the pool: F. Analysis was performed by RP-UHPLC-PGC-MS. Concentrations per DP in the original GOS mixture were set to 1.0.

Comparison of the degradation kinetics of the individual and pooled faecal inocula reflected again the dominance of the *Bifidobacterium* species of the inoculum of infant 4 in the pooled faecal inoculum. DP3 isomer 2, 11, 12 and 13 were degraded almost completely in the first 12 h of fermentation by both inocula, whereas these isomers were still present upon the fermentation of GOS using inocula of infant 1, 2 and 3. Nevertheless, the degradation of GOS using pooled faecal inoculum was not solely caused by the bacteria originating from infant 4. The complete degradation of isomer 16 in the first 12 h of

fermentation using pooled faecal inoculum could for example be ascribed to bacteria originating from infant 2 (Figure 5).

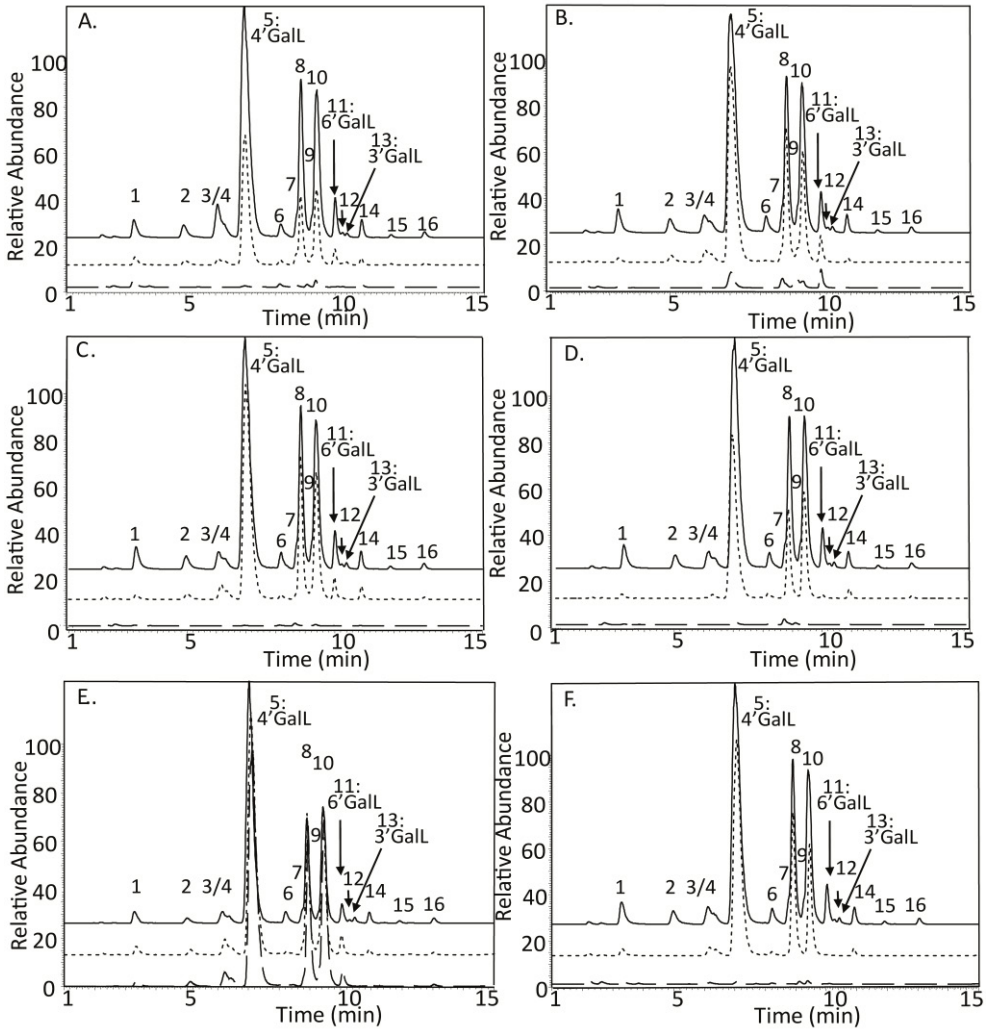

Figure 5 UHPLC-PGC-MS profile of reduced GOS with selection of DP3 at the start (solid), after 12 (dotted) and 24 (dashed) h of fermentation using faecal inoculum of individual infants 1: A, 2: B, 3: C, 4: D, 5:E and the pool: F. All elution profiles were normalized to similar intensity.

The results on the degradation kinetics thus highlight again that a pooled faecal inoculum cannot predict the exact utilization of specific NDC structures by particular species present in the microbiota of a specific individual. However, fermentation using a pooled faecal inoculum clearly demonstrates the ability of infant microbiota in general to utilize specific oligosaccharides and facilitates the efficient screening of the potentially prebiotic NDC mixtures.

Validation of pooled infant faecal inoculum

An additional fermentation using faecal material of 5 other infants of the same age (2 weeks) was performed to validate the use of pooled infant faecal inoculum. Faecal microbiota of these infants fermented GOS significantly faster than the primary pooled faecal inoculum described above. After 12 h of fermentation of the validation trial, only 7% of the total GOS mixture was remaining (Figure S3), while still 60% was remaining for the primary pooled faecal inoculum. However, similar preference on DP level was observed as DP2 and DP≥6 were fermented first for both pooled faecal inocula (Figure S3). GOS DP 3 was degraded completely between 6 and 12 h of fermentation. As a consequence, no information on preferential degradation of specific isomers could be obtained from the digesta taken at the given time points (Figure S4).

Despite the differences in fermentation speed between the two pooled faecal inocula, a similar increase in *Bifidobacterium* was observed upon fermentation of GOS (Figure 6). After 24 h 68-74% of the bacteria belonged to the genus *Bifidobacterium*. The fermentation coincided with a slightly higher total production of organic acids compared to the primary pool in this study, respectively 15.0 and 14.5 µmol/mg after 24 h of fermentation (Figure S5). This validation experiment with the pooled inoculum containing faecal material of 5 other infants of the same age thus reinforced that the use of pooled infant faecal inoculum allows judgement of the fermentability of GOS efficiently.

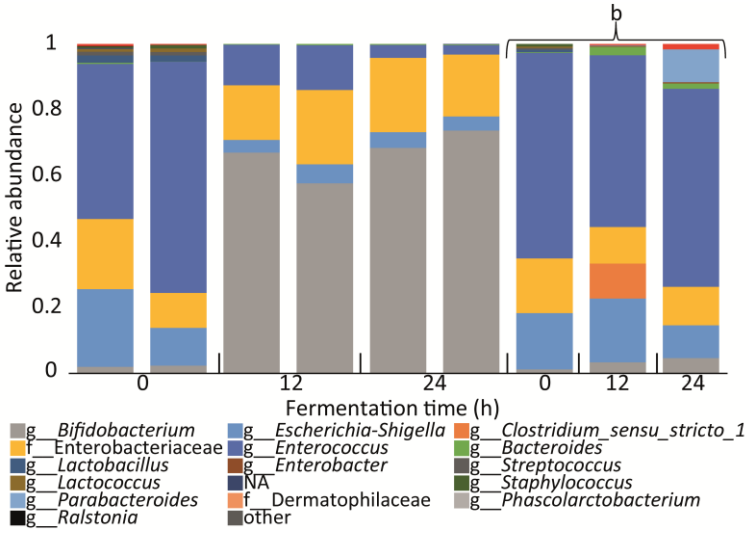

Figure 6 Relative abundance of bacteria with highest known taxonomy in duplicate fermentation digesta collected at the start and after 12 and 24 h of an additional fermentation of GOS using pooled faecal inoculum of 5 other infants at the same age (2 weeks) for validation with b: background fermentation (only SIEM medium and inoculum).

Conclusions

During the last decade several studies have been published on the *in vitro* fermentation of GOS by individual bacterial strains, which neglect important cross-feeding relations between different bacteria. The use of infant faecal inoculum results in a better view on the actual fate of GOS in the infant gut. However, it introduces some challenges due to high inter-individual variability of the infant microbiota requiring numerous *in vitro* experiments using individual faecal inocula of different infants. In this study it has been shown that pooled infant faecal inoculum can function as an alternative approach. Our data reinforced that, despite the divergent microbiota composition, the bacterial functionality of the pooled faecal inoculum was largely equivalent to that of the individual faecal inocula, as a similar trend in organic acid production and relative increase in *Bifidobacterium* was observed between the pooled faecal inoculum and 4 out of 5 individual faecal inocula. These findings were confirmed by an additional fermentation using pooled faecal inoculum of 5 other infants of the same age. The functionality of the pooled faecal inoculum was thus largely representative of the faecal inocula of the infant population in general and thus suitable for high throughput screening purposes of the fermentability of novel NDCs.
Additionally, the use of UHPLC-PGC-MS with their excellent separation of oligosaccharide isomers showed us some first insights on DP and isomer-specific fermentation of GOS by infant microbiota. Knowledge on the structure-specific effects of GOS and other NDCs could give potential for the production of tailored NDC mixtures to meet the needs of specific subgroups of infants. With this perspective in mind the use of pooled faecal inoculum will help us to move forward in future studies as it will make room for the incorporation of multiple NDCs in one study. Highly promising NDCs can be selected by *in vitro* fermentations using pooled inocula prior to further *in vitro* and *in vivo* experiments targeting responses of individuals. In this way our understanding of structure-specific effects of NDCs on infant microbiota will be increased efficiently.

Acknowledgements

This research was performed in the public-private partnership 'CarboKinetics' coordinated by the Carbohydrate Competence Center (CCC, www.cccresearch.nl). CarboKinetics is financed by participating industrial partners Agrifirm Innovation Center B.V., Cooperatie Avebe U.A., DSM Food Specialties B.V., FrieslandCampina Nederland B.V., Nutrition Sciences N.V., VanDrie Holding N.V. and Sensus B.V., and allowances of The Netherlands Organisation for Scientific Research (NWO).

References

1. Wang, M.; Monaco, M.H.; Donovan, S.M. Impact of early gut microbiota on immune and metabolic development and function. *Semin. Fetal Neonatal Med.* **2016**, *21*, 380-387.
2. de Goffau, M.C.; Fuentes, S.; van den Bogert, B.; Honkanen, H.; de Vos, W.M.; Welling, G.W.; Hyöty, H.; Harmsen, H.J.M. Aberrant gut microbiota composition at the onset of type 1 diabetes in young children. *Diabetologia* **2014**, *57*, 1569-1577.
3. Li, M.; Wang, M.; Donovan, S.M. Early development of the gut microbiome and immune-mediated childhood disorders. *Semin. Reprod. Med.* **2014**, *32*, 074-086.
4. Korpela, K.; de Vos, W.M. Early life colonization of the human gut: microbes matter everywhere. *Curr. Opin. Microbiol.* **2018**, *44*, 70-78.
5. Milani, C.; Duranti, S.; Bottacini, F.; Casey, E.; Turroni, F.; Mahony, J.; Belzer, C.; Delgado Palacio, S.; Arboleya Montes, S.; Mancabelli, L.; Lugli, G.A.; Rodriguez, J.M.; Bode, L.; de Vos, W.; Gueimonde, M.; Margolles, A.; van Sinderen, D.; Ventura, M. The first microbial colonizers of the human gut: Composition, activities, and health implications of the infant gut microbiota. *Microbiol. Mol. Biol. Rev.* **2017**, *81*, e00036-00017.
6. Bezirtzoglou, E.; Tsiotsias, A.; Welling, G.W. Microbiota profile in feces of breast- and formula-fed newborns by using fluorescence in situ hybridization (FISH). *Anaerobe* **2011**, *17*, 478-482.
7. Engfer, M.B.; Stahl, B.; Finke, B.; Sawatzki, G.; Daniel, H. Human milk oligosaccharides are resistant to enzymatic hydrolysis in the upper gastrointestinal tract. *Am. J. Clin. Nutr.* **2000**, *71*, 1589-1596.
8. Holscher, H.D.; Bode, L.; Tappenden, K.A. Human milk oligosaccharides influence intestinal epithelial cell maturation *in vitro*. *J. Pediatr. Gastroenterol. Nutr.* **2017**, *64*, 296-301.
9. Valdés-Varela, L.; Ruas-Madiedo, P.; Gueimonde, M. *In vitro* fermentation of different fructo-oligosaccharides by *Bifidobacterium* strains for the selection of synbiotic combinations. *Int. J. Food Microbiol.* **2017**, *242*, 19-23.
10. Ruiz-Moyano, S.; Totten, S.M.; Garrido, D.A.; Smilowitz, J.T.; German, J.B.; Lebrilla, C.B.; Mills, D.A. Variation in consumption of human milk oligosaccharides by infant gut-associated strains of *Bifidobacterium breve*. *Appl. Environ. Microbiol.* **2013**, *79*, 6040-6049.
11. Cockburn, D.W.; Koropatkin, N.M. Polysaccharide degradation by the intestinal microbiota and its influence on human health and disease. *J. Mol. Biol.* **2016**, *428*, 3230-3252.
12. Dogra, S.; Sakwinska, O.; Soh, S.-E.; Ngom-Bru, C.; Brück, W.M.; Berger, B.; Brüssow, H.; Lee, Y.S.; Yap, F.; Chong, Y.-S.; Godfrey, K.M.; Holbrook, J.D. Dynamics of infant gut microbiota are influenced by delivery mode and gestational duration and are associated with subsequent adiposity. *mBio* **2015**, *6*.
13. Aguirre, M.; Ramiro-Garcia, J.; Koenen, M.E.; Venema, K. To pool or not to pool? Impact of the use of individual and pooled fecal samples for *in vitro* fermentation studies. *J. Microbiol. Methods* **2014**, *107*, 1-7.
14. Gu, F.; Borewicz, K.; Richter, B.; van der Zaal, P.H.; Smidt, H.; Buwalda, P.L.; Schols, H.A. *In vitro* fermentation behavior of isomalto/malto-polysaccharides using human fecal inoculum indicates prebiotic potential. *Mol. Nutr. Food Res.* **2018**, *62*, e1800232.
15. Leijdekkers, A.G.M.; Aguirre, M.; Venema, K.; Bosch, G.; Gruppen, H.; Schols, H.A. *In vitro* fermentability of sugar beet pulp derived oligosaccharides using human and pig fecal inocula. *J. Agric. Food Chem.* **2014**, *62*, 1079-1087.
16. Venema, K. The TNO *In Vitro* Model of the Colon (TIM-2). In *The Impact of Food Bioactives on Health: in vitro and ex vivo models*, Verhoeckx, K.; Cotter, P.; López-Expósito, I.; Kleiveland, C.; Lea, T.; Mackie, A.; Requena, T.; Swiatecka, D.; Wichers, H., Eds.; Springer International Publishing: Cham, Switzerland, **2015**, pp. 293-304.
17. Zhao, G.; Nyman, M.; Jonsson, J.A. Rapid determination of short-chain fatty acids in colonic contents and faeces of humans and rats by acidified water-extraction and direct-injection gas chromatography. *Biomed. Chromatogr.* **2006**, *20*, 674-682.
18. Ladirat, S.E.; Schuren, F.H.; Schoterman, M.H.; Nauta, A.; Gruppen, H.; Schols, H.A. Impact of galacto-oligosaccharides on the gut microbiota composition and metabolic activity upon antibiotic treatment during *in vitro* fermentation. *FEMS Microbiol. Ecol.* **2014**, *87*, 41-51.
19. Ramiro-Garcia, J.; Hermes, G.D.A.; Giatsis, C.; Sipkema, D.; Zoetendal, E.G.; Schaap, P.J.; Smidt, H. NG-Tax, a highly accurate and validated pipeline for analysis of 16S rRNA amplicons from complex biomes. *F1000Research* **2016**, *5*, 1791-1791.
20. Walker, A.W.; Ince, J.; Duncan, S.H.; Webster, L.M.; Holtrop, G.; Ze, X.; Brown, D.; Stares, M.D.; Scott, P.; Bergerat, A.; Louis, P.; McIntosh, F.; Johnstone, A.M.; Lobley, G.E.; Parkhill, J.; Flint, H.J. Dominant and diet-responsive groups of bacteria within the human colonic microbiota. *ISME J.* **2011**, *5*, 220-230.
21. Hill, C.J.; Lynch, D.B.; Murphy, K.; Ulaszewska, M.; Jeffery, I.B.; O'Shea, C.A.; Watkins, C.; Dempsey, E.; Mattivi, F.; Tuohy, K.; Ross, R.P.; Ryan, C.A.; O' Toole, P.W.; Stanton, C. Evolution of gut microbiota composition from birth to 24 weeks in the INFANTMET Cohort. *Microbiome* **2017**, *5*, 4.
22. Richardson, A.J.; McKain, N.; Wallace, R.J. Ammonia production by human faecal bacteria, and the enumeration, isolation and characterization of bacteria capable of growth on peptides and amino acids. *BMC Microbiol.* **2013**, *13*, 6-6.

23. Maathuis, A.; Hoffman, A.; Evans, A.; Sanders, L.; Venema, K. The effect of the undigested fraction of maize products on the activity and composition of the microbiota determined in a dynamic *in vitro* model of the human proximal large intestine. *J. Am. Coll. Nutr.* **2009**, *28*, 657-666.
24. Watson, D.; O'Connell Motherway, M.; Schoterman, M.H.; van Neerven, R.J.; Nauta, A.; van Sinderen, D. Selective carbohydrate utilization by lactobacilli and bifidobacteria. *J. Appl. Microbiol.* **2013**, *114*, 1132-1146.
25. Matsuki, T.; Tajima, S.; Hara, T.; Yahagi, K.; Ogawa, E.; Kodama, H. Infant formula with galacto-oligosaccharides (OM55N) stimulates the growth of indigenous bifidobacteria in healthy term infants. *Benefic. Microbes* **2016**, *7*, 453-461.
26. Barboza, M.; Sela, D.A.; Pirim, C.; LoCascio, R.G.; Freeman, S.L.; German, J.B.; Mills, D.A.; Lebrilla, C.B. Glycoprofiling bifidobacterial consumption of galacto-oligosaccharides by mass spectrometry reveals strain-specific, preferential consumption of glycans. *Appl. Environ. Microbiol.* **2009**, *75*, 7319-7325.
27. Janda, J.M.; Abbott, S.L. 16S rRNA gene sequencing for bacterial identification in the diagnostic laboratory: pluses, perils, and pitfalls. *J. Clin. Microbiol.* **2007**, *45*, 2761-2764.
28. Palframan, R.J.; Gibson, G.R.; Rastall, R.A. Carbohydrate preferences of *Bifidobacterium* species isolated from the human gut. *Curr. Issues Intest. Microbiol.* **2003**, *4*, 71-75.
29. Rivière, A.; Selak, M.; Lantin, D.; Leroy, F.; De Vuyst, L. Bifidobacteria and butyrate-producing colon bacteria: Importance and strategies for their stimulation in the human gut. *Front. Microbiol.* **2016**, *7*, 979.
30. Cardelle-Cobas, A.; Corzo, N.; Olano, A.; Pelaez, C.; Requena, T.; Avila, M. Galactooligosaccharides derived from lactose and lactulose: influence of structure on *Lactobacillus*, *Streptococcus* and *Bifidobacterium* growth. *Int. J. Food Microbiol.* **2011**, *149*, 81-87.

Supporting information

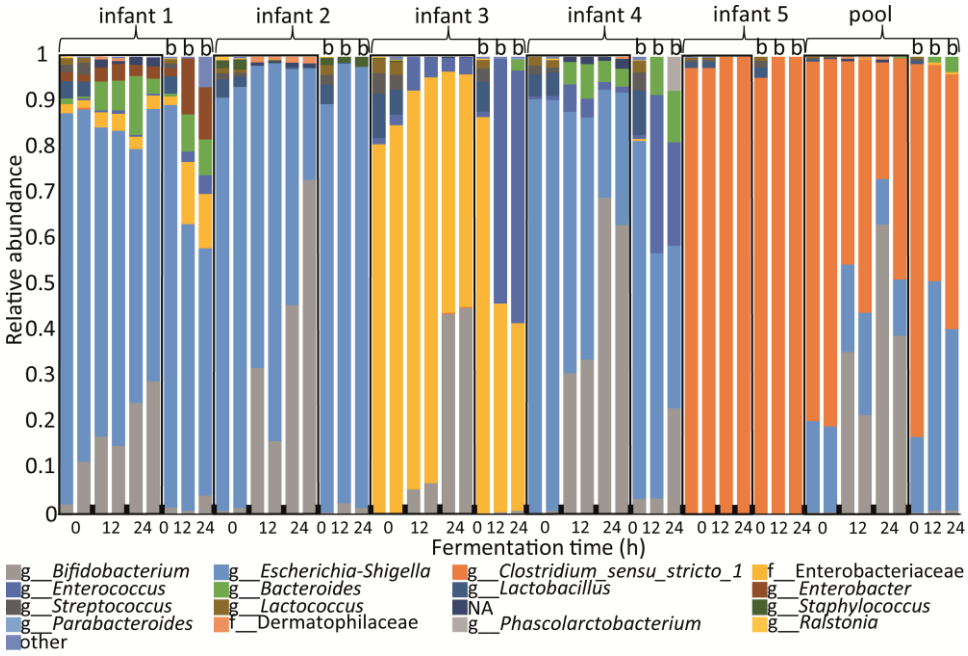

Figure S1 Relative abundance of bacteria with highest known taxonomy in duplicate fermentation digesta collected at the start and after 12 and 24 h from *in vitro* fermentation of GOS using faecal inoculum of 2-week-old infants with b: background fermentation (only SIEM medium and inoculum).

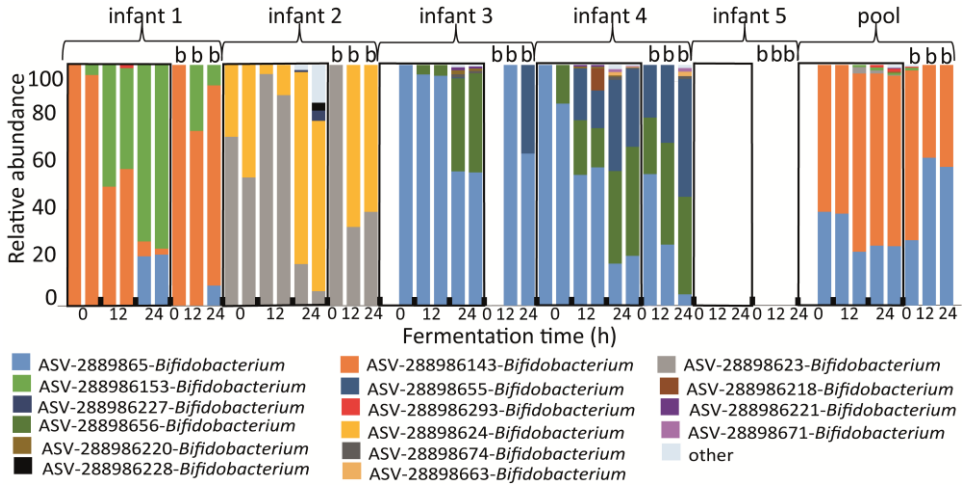

Figure S2 Composition of bifidobacterial Amplicon Sequencing Variants (ASVs) in fermentation digesta collected at the start and after 12 and 24 h from *in vitro* fermentation using individual and pooled infant faecal inocula with b: background fermentation (only SIEM medium and inoculum).

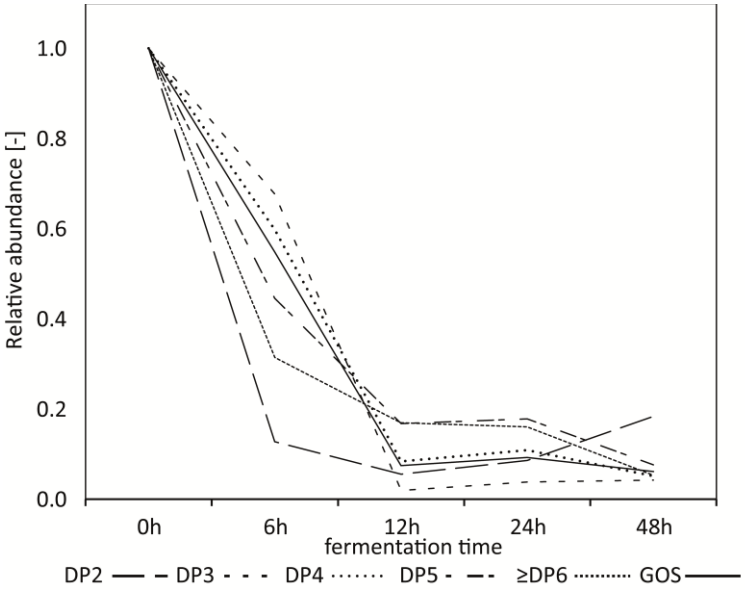

Figure S3 Relative proportion of remaining oligosaccharides from GOS and individual DPs of GOS during an additional *in vitro* fermentation using pooled faecal inoculum of 5 other infants at the same age (2 weeks) for validation. Analysis was performed by RP-UHPLC-PGC-MS. Concentrations per DP in the GOS mixture were set to 1.0.

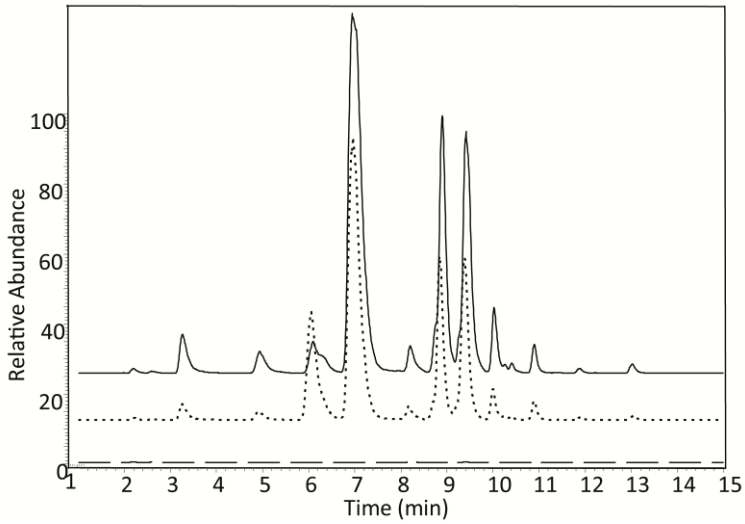

Figure S4 UHPLC-PGC-MS profile of reduced GOS with selection of DP3 at the start (solid), after 6 (dotted) and after 12 (dashed) hours of an additional fermentation using pooled faecal inoculum of 5 other infants at the same age (2 weeks) for validation. All elution profiles were normalised to similar intensity.

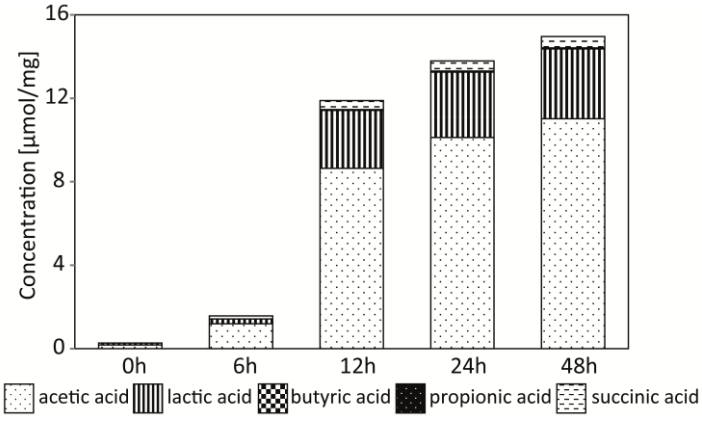

Figure S5 Production of organic acids upon an additional *in vitro* fermentation of GOS using pooled faecal inoculum of 5 infants at the same age (2 weeks) for validation.

Table S1 Production of organic acids upon *in vitro* fermentation of GOS using individual and pooled faecal inoculum of infant 1-5, as well as pooled faecal inoculum of 5 other infants at the same age for validation, with b: biological replicate and -: not found.

infant	timepoint (h)	acetate	butyrate	propionate	lactacte	succinate
1	0	0.10	0.03	-	-	-
	0[b]	0.15	-	-	-	-
	6	1.24	-	0.03	0.11	0.34
	12	3.21	-	0.05	0.48	0.73
	12[b]	2.36	-	0.04	-	-
	24	8.88	-	0.06	1.51	1.21
	48	9.48	-	0.06	1.59	1.25
	48[b]	9.10	-	0.08	1.66	1.14
2	0	0.12	-	-	0.12	-
	0[b]	0.10	0.04	0.03	0.10	0.04
	6	1.17	-	0.03	0.09	0.29
	12	2.28	-	0.02	0.16	0.44
	12[b]	2.24	-	0.03	0.21	0.45
	24	7.61	-	0.03	0.70	0.67
	48	10.15	-	0.03	0.54	0.64
	48[b]	11.30	-	0.06	0.40	0.35
3	0	0.13	-	-	0.10	-
	0[b]	0.17	-	-	-	-
	6	1.69	-	-	0.16	0.15
	12	3.50	-	-	0.22	0.53
	12[b]	3.55	-	-	0.22	0.47
	24	7.74	0.04	0.03	0.75	0.78
	48	9.33	0.05	0.03	0.73	0.76
	48[b]	8.43	-	0.03	0.94	1.06
4	0	0.13	-	-	0.07	0.04
	0[b]	0.14	-	-	0.12	0.06
	6	1.13	-	0.02	0.09	0.30
	12	1.49	-	0.02	0.09	0.37
	12[b]	2.09	-	0.03	0.19	0.74
	24	8.12	-	0.09	1.11	0.98
	48	11.82	-	0.11	1.61	1.04
	48[b]	11.36	-	0.20	1.90	1.11
5	0	0.19	-	-	-	-
	0[b]	0.12	-	-	0.09	-
	6	1.07	0.19	-	-	-
	12	1.38	0.42	0.03	-	-
	12[b]			sample missing		
	24	-	-	-	-	-
	48	-	-	-	-	-
	48[b]			sample missing		
Pool: 1-5	0	0.14	-	0.01	0.07	-
	0[b]	0.17	-	-	0.08	-
	6	1.45	0.18	0.05	0.07	0.24
	12	4.38	0.35	0.06	0.64	0.40
	12[b]	3.36	0.35	0.06	0.62	0.48
	24	11.01	0.43	0.08	0.90	0.47
	48	12.45	0.47	0.09	0.97	0.52
	48[b]	10.68	0.54	0.09	1.91	0.67
Pool: other 5	0	0.18	-	-	0.10	-
	0[b]	0.17	-	-	0.10	0.05
	6	1.19	-	-	0.23	0.15
	12	8.64	-	0.05	2.78	0.43
	12[b]	8.95	-	0.04	3.34	0.45
	24	10.13	-	0.05	3.13	0.49
	48	11.02	-	0.05	3.35	0.54
	48[b]	10.57	-	0.06	3.37	0.48

Table S2 Production of organic acids upon background fermentations including only SIEM medium and individual or pooled faecal inoculum of infant 1-5, as well as pooled faecal inoculum of 5 other infants at the same age for validation. *: background fermentation of GOS without inoculum and -: not found.

infant	timepoint (h)	acetate	butyrate	propionate	lactate	succinate
1	0	0.33	0.37	0.19	0.08	0.05
	12	0.83	-	0.11	0.05	0.35
	48	0.98	-	0.37	-	0.43
2	0	0.10	-	-	0.04	-
	12	0.58	-	0.05	-	0.28
	48	0.83	-	0.05	-	0.37
3	0	0.11	-	-	0.08	-
	12	0.49	-	-	0.08	0.16
	48	1.65	-	-	-	0.24
4	0	0.10	-		0.05	-
	12	0.71	-	0.06	-	0.39
	48	1.41	-	0.88	-	-
5	0	0.12	-	-	0.07	-
	12			sample missing		
	48	0.94	0.19	0.08	0.10	-
Pool: 1-5	0	0.14	-	-	0.08	0.03
	12	0.89	0.06	0.10	0.06	0.20
	48	1.20	0.08	0.62	-	-
Pool: other 5	0	0.12	-	0.02	0.11	0.05
	12	0.79	-	0.09	0.07	0.21
	48	1.43	-	0.28	-	0.38
*	0	0.07	-	-	0.13	-
	12	0.05	-	-	0.08	-
	48	0.28	-	-	0.14	-

Chapter 3

Fermentation of chicory fructo-oligosaccharides and native inulin by infant faecal microbiota attenuates pro-inflammatory responses in immature dendritic cells in an infant-age dependent and fructan-specific way

Abstract

Inulin-type fructans are commonly applied in infant formula to support development of gut microbiota and immunity. These inulin-type fructans are considered to be fermented by gut microbiota, but it is unknown how fermentation impacts immune modulating capacity and whether the process of fermentation is dependent on the infant's age. We investigated the *in vitro* fermentation of chicory fructo-oligosaccharides (FOS) and native inulin using pooled faecal inocula of 2- and 8-week-old infants. Both inocula primarily utilized the trisaccharides in FOS, while they almost completely utilized native inulin with degree of polymerization (DP) 3-8. Faecal microbiota of 8-week-old infants degraded longer chains of native inulin up to DP 16. This correlated with a higher abundance of *Bifidobacterium* and higher production of acetate and lactate after 26 h of fermentation. Fermented FOS and native inulin attenuated pro-inflammatory cytokines (MCP-1/CCL2, IL-1β, TNFα) produced by immature dendritic cells (DCs) but profiles and magnitude of attenuation were stronger with native inulin than with FOS. Our findings demonstrate that fermentation of FOS and native inulin is dependent on the infant's age and fructan structure. Fermentation enhances attenuating effects of pro-inflammatory responses in DCs, which depend mainly on microbial metabolites formed during fermentation.

Logtenberg, M.J.*; Akkerman, R.*; An, R.; Hermes, G.D.A.; de Haan, B.J.; Faas, M.M.; Zoetendal, E.G.; Schols, H.A.; de Vos, P. *Molecular Nutrition and Food Research*; **2020**; 64: 2000068.

* authors contributed equally

Introduction

The quality of postnatal nutrition is crucial for health later in life as it is closely intertwined with the microbial colonization of the intestine and the development of the gastrointestinal (GI) tract and immune system [1,2]. Exclusive breastfeeding is the gold standard for infants up to 6 months as recommended by the World Health Organization [3]. Human milk oligosaccharides (HMOs) are an important component of mother milk, which function as prebiotics and boost immune development for example by supporting the development of the gut immune barrier [4,5]. In Europe only approximately 25% of the infants receive exclusive breastfeeding up to an age of 6 months [6]. There is infant formula available for infants for which breast milk is not an option. These formula are supplemented with non-digestible carbohydrates (NDCs) such as galacto-oligosaccharides and inulin to mimic the health effects offered by HMOs [7,8].

A class of NDCs, commonly used in infant formulas are inulin-type fructans. Inulin-type fructans are generally isolated from chicory roots and composed of linear chains of β(2-1)-linked fructose monomers with varying degree of polymerization (DP) [9]. The chains can have either a glucose (GF series) or fructose (F series) moiety at the reducing end, which contributes to structural diversity of the inulin-type fructans [9]. Native inulin predominantly contains the inulin-type GF series DP2-60, while the partial hydrolysis product of inulin contains a DP2-10 GF and F series and is referred to as fructo-oligosaccharides (FOS - synonym oligofructose).

In recent years evidence has accumulated for the essence of chain length in immune modulation by inulin-type fructans [10,11]. Previous *in vitro* studies demonstrated direct interaction of inulin-type fructans with immune cells via pattern recognition receptors (PRRs) [11]. Inulin-type fructans with shorter chains resulted in a more anti-inflammatory cytokine production than inulin-type fructans with longer chains due to differences in stimulation of PRRs [11]. Besides the direct interaction, inulin-type fructans can also affect immune responses via their fermentation by specific bacteria resulting in the production of e.g. SCFAs [12,13]. However, it is unknown how the fermentation of inulin-type fructans by infant microbiota impacts their immune modulating capacity and whether specific structures of the inulin-type fructans influence the fermentability and immune effects.

As fermentation capacity is dependent on the age of infants [14], also the impact on immunity might be dependent on the age of the infants. The microbial colonization of the infant gut starts upon birth, when exposure occurs to maternal vaginal and environmental bacteria [15]. Initially, due to the high concentration of oxygen present in the gut of the newborn, aerobic and facultative anaerobic bacteria will colonize [15]. These bacteria will consume oxygen and thereby create a more anaerobic environment in the infant gut allowing colonization of strict anaerobic bacteria such as clostridia and bifidobacteria [15]. This maturation process most likely influences the utilization of NDCs in the first months of

life as different sets of enzymes will become available for the degradation of NDCs depending on the bacteria present in the infant gut [14]. In previous studies a clear difference in utilization of HMOs was shown between 2- and 8-week-old infants [14]. Hence, both age groups were included in this study to be able to study the effects of NDCs in this crucial timeframe of infant microbiota development.

In the present study we investigated the fermentation of chicory FOS and native inulin in an in vitro fermentation set-up using pooled faecal inoculum of 2- and 8-week-old infants, whose bacterial functionality was proven to be largely representative of the faecal inocula of the infant population in general (unpublished data). The ability of the infant faecal microbiota to degrade FOS and native inulin was studied as well as the production of SCFAs and the microbiota composition in time. Fermentation digesta at different time points were incubated with immature dendritic cells derived from the umbilical vein to determine the effect of the fermentation products on cytokine production by immature dendritic cells.

Material and methods

Materials

Frutalose® OFP (FOS, DP2-10) and Frutafit® IQ (native inulin, DP2-60) were provided by Sensus (Roosendaal, The Netherlands).

Fermentation of FOS and native inulin by infant faecal inoculum

Culture medium

Standard ileal efflux medium (SIEM; Tritium Microbiology, Veldhoven, The Netherlands) was prepared as described elsewhere with minor modifications [16]. Low amount of carbohydrates was added to mimic the infant ileal environment while minimizing background fermentation. The carbohydrate medium component contained (g/L): pectin, 12; xylan, 12; arabinogalactan, 12; amylopectin, 12; and starch, 12 with a final concentration of only 0.24 g/L). The pH was adjusted to 5.8 using MES buffer.

Infant faecal inoculum

Faecal samples were collected from 4 exclusively breast-fed and vaginally born infants. The infants did not receive antibiotic treatment and did not have health issues. At an age of 2 and 8 weeks faecal material was collected from the diaper directly after defecation, transferred to tubes and stored at -20 °C. After the second collection time point, all samples were stored at -80 °C.

The inoculum was prepared as reported elsewhere with some minor modifications [17]. After thawing, faecal material of 4 infants were combined (4x 0.1 gram) and diluted in 24 ml sterilized NaCl solution (0.9% (w/v)) in an anaerobic chamber (gas phase: 81% N_2, 15% CO_2 and 4% H_2) (Bactron 300, Sheldon Manufacturing, Cornelius, USA). Homogenization was performed by the addition of sterile glass beads prior to thorough mixing (2000 rpm). The faecal solution was combined with SIEM medium in a ratio of 5:82 (v/v) and used as pooled

faecal inoculum, whose bacterial functionality was proven to be largely equivalent to that of the individual faecal inocula (unpublished data).

In vitro fermentation

Fermentations were performed in duplicate in an anaerobic chamber. Faecal inoculum was combined with SIEM medium containing FOS or native inulin in sterile fermentation flasks in a ratio of 1:10 (v/v) with a total volume of 54 ml. The final concentration of FOS and native inulin in the fermentation liquid was 10 mg/ml. The final concentration of SIEM medium carbohydrates only reached 0.24 mg/ml. Fermentation flasks were closed with a rubber stopper that is secured with a metal lid to ensure anoxic conditions. Afterwards flasks were put in an incubator shaker (Innova 40) (37 °C, 100 rpm). At the start and after 14, 20 and 26 h, digesta were collected in triplicate with a syringe. One sample was immediately frozen in liquid nitrogen and stored at -80 °C to preserve the bacteria for later microbial analysis. Both other samples were heated for 5 min in a boiling water bath to inactivate enzymes present. Subsequently they were stored at -20 °C until further analysis.

The following control fermentations were included: (1) inoculum without added FOS and native inulin to monitor background fermentation, (2) FOS and native inulin without inoculum to monitor contamination of the substrate. From these latter controls, only native inulin with SIEM showed some unexpected fermentation after 26 h including inulin utilization and production of substantial amounts of organic acids. Since a later control fermentation using the same set-up and substrate did not show any sign of fermentation/contamination, it was concluded that the contamination of only the inulin control did not originate from the substrate neither from SIEM. As such, it did not pose any limitations for this study.

Fate of FOS and native inulin upon fermentation

Degradation of FOS and native inulin during fermentation was analysed by High Performance Anion Exchange Chromatography (HPAEC). Fermentation samples were diluted until a concentration of 50 µg/ml and centrifuged (5 min, 15 000g). Ten µl of sample was injected to an ISC5000 HPLC system (Dionex, Sunnyvale, CA, USA) with a CarboPac PA-1 column (250 mm x 2 mm ID), a CarboPac PA guard column (25 mm x 2 mm ID) and a ISC5000 ED detector (Dionex) in the pulsed amperometric detector (PAD) mode. Mobile phase A (0.1 M sodium hydroxide) and B (1 M sodium acetate in 0.1 M sodium hydroxide) were used with the following elution profile: 0-25 min, 0-40% B; 25-30 min, 40-100% B; 30-35 min, washing step with 100% B; 35-35.1 min, 100-0% B; 35.1-50 min, equilibration with 100% A. Flow rate was set at 0.3 ml/min. The data were analysed using Chromeleon 7.0 (Thermo Scientific).

Production of SCFAs and other organic acids upon fermentation

In order to quantify the production of SCFAs and organic acids, fermentation samples were subjected to GC and HPLC analysis as described elsewhere [18] with minor modifications.

For GC, fermentation samples (1 mg/ml) were mixed in a 2:1 ratio with a solution containing HCl (0.3M), oxalic acid (0.09M) and internal standard 2-ethyl butyric acid (0.45 mg/ml). The mixture was allowed to stand at room temperature for 30 min.
The temperature profile during GC analysis was as follows: 100°C, maintained for 0.5 min; raised to 180°C at 8°C/min, maintained for 1 min; raised to 200°C at 20°C/min, maintained for 5 min. Glass wool was inserted in the glass liner of the split injection port to protect the column from contamination [19].

Microbial composition analysis

DNA extraction

DNA was extracted from fermentation samples using the repeated beat beating method [20] and afterwards purified using the Maxwell 16 Tissue LEV Total RNA Purification Kit Cartridge (AS1220).

PCR amplification

Microbiota profiling was performed as described previously with some modifications [21]. The V5V6 region of 16S ribosomal RNA (rRNA) genes was amplified in triplicate PCR reactions with a unique barcoded primer pair BSF784 (RGGATTAGATACCC) and R1064 (CGACRRCCATGCANACCT). For the t0 samples which contained 1.4-4.6 ng/µl DNA, 10 µl of DNA template was used in each reaction. For samples with higher DNA concentrations, 0.7 µl of DNA template was used. Two synthetic communities with known composition were included to evaluate the sequencing performance for reflection of the theoretical composition [22]. The communities consisted of 55 16S rRNA gene amplicons of phylotypes associated with the human gut with staggered concentrations typical for the human gut (1) and with relative abundances between 0.001 and 2.49% (2).

Library preparation and sequencing

PCR products were purified using HighPrep PCR kit (MagBio Genomics, Alphen aan den Rijn, The Netherlands). Purified amplicons were quantified using Qubit dsDNA BR assay kit (Life Technologies, Leusden, The Netherlands). Seventy unique barcode tags were used in each library [22]. Two amplicon pools were formed by combining 200 ng of each barcoded sample and afterwards concentrated to 50 µl volume using the HighPrep PCR kit. Libraries were sent for adapter ligation and sequencing on an Illumina Hiseq2500 instrument (GATC-Biotech, Konstanz, Germany).

Data analysis

Processing and analysis of the 16S rRNA gene amplicon sequencing data was carried out using the NG-Tax pipeline, with default settings [22] and R version 3.5.0. Amplicon sequencing variants (ASVs) with a relative abundance below 0.1% were removed. The threshold for taxonomic assignment was set at 80%.

Bifidobacteria were analysed at the level of individual sequences (Amplicon Sequencing Variants (ASVs)). Species information was obtained with NG-Tax 2.0 [23] and SILVA database release 132 [24]. Tax4Fun2 was used to predict the functional capability of the microbial communities based on 16S rRNA genes [25]. Output was visualized in a heatmap with relative abundance of KEGG functional orthologs in the fermentation samples scaled per row and hierarchical clustering using the Ward.D2 algorithm and Euclidean distances using the *pheatmap* R package [26].

UniProt Knowledgebase was used to extract all bacterial genes encoding for β-fructofuranosidase together with the corresponding taxonomic classification. Afterwards Bologna Unified Subcellular Component Annotator (BUSCA) was used to predict the subcellular localization of the enzyme [27].

Quantification of total bacterial 16 rRNA gene copy number

The total bacterial abundance was determined by quantitative PCR (qPCR) analysis of total 16S rRNA genes using the forward primer 5'-GTGSTGCAYGGYYGTCGTCA-3' and reverse primer 3'-ACGTCRTCCMCNCCTTCCTC-5' [28]. qPCR amplifications were performed in triplicate and *E. coli* was used as standard for quantification. The qPCR reaction mixture contained 6.25 µl iQ SYBR Green Supermix (Bio-Rad, Hercules, CA, USA), 200 nM forward and reverse primers, 3.25 µl of Nuclease free water and 2.5 µl of sample DNA (1ng/µl). qPCR cycling conditions and apparatus were used as described elsewhere with a minor modification as an annealing temperature of 52 °C was used instead of 56 °C [29].

Stimulation of DCs with FOS and native inulin fermentation samples

Cell culture and stimulation

DCs generated from umbilical cord blood $CD34^+$ progenitor cells (hematopoietic stem cells) were purchased from MatTek Corporation (Ashland, MA, USA). DCs were freshly thawed and seeded into 96-well plates at a density of $70x10^4$ cells/well and cultured under normal conditions (37 ^oC, 21% O_2 and 5% CO_2) for 24 h according to manufacturer's instructions. After 24 h of culturing, cells were attached and medium could be replaced. To stimulate DCs with fermentation products of the *in vitro* fermentation of FOS and native inulin using infant faecal inoculum, bacteria were removed from the fermentation samples by centrifugation (10 min, RT, 12000g). Subsequently supernatants were filtered through a 0.2 µm filter and diluted in DC-MM culture medium (MatTek Corporation, Ashland, MA, USA) containing Polymyxin-B (50 ng/ml) (Invivogen) at a ratio of 1:10. The pH was set at 7.4 by the addition of 2N NaOH. DCs were then incubated with 200 µl/well medium containing 20 µl of fermentation samples for 48 h. After incubation supernatants were collected and stored at -20 ^oC until further analysis. All experiments were repeated 6 times.

Assessment of cytokine expression

A magnetic Luminex® Assay (R&D systems, Bio-Techne, Minneapolis, USA) was used to measure the levels of MCP-1/CCL2, MIP-1α/CCL3, IL-1β, IL-6, IL-10 and TNFα in the DC supernatant. The assay was performed according to manufacturer's protocol. Briefly, cytokine standards were resuspended and serial dilutions were prepared. Antibody magnetic bead mix was added to a 96-well plate. Standards and samples were added and incubated overnight at 4 ^{o}C while shaking. After washing the plate 3 times, detection antibodies were added and the plate was incubated for 30 min at RT while shaking. After incubation, the plate was washed again and incubated with streptavidin-PE for 30 min at RT while shaking. Finally, the plate was washed again and 100 µl of wash buffer was added to each well. Subsequently, the plate was analysed using a Luminex 200 System. The data obtained was analysed using the Luminex xPONENT software.

Statistical analysis

All statistical tests were performed using Prism 8 software (GraphPad, San Diego, CA, USA). Outliers were removed after testing using a Grubbs outlier test (alpha = 0.05). Data are shown as averages and error bars represent standard error of the means. Data was distributed normally and analysed using a mixed-effects model (REML) to test for differences between the 2- and 8- weeks groups, followed by a Tukey's multiple comparisons test, to test if the fermentation samples of either 14h or 26h could induce significantly higher cytokine responses than their corresponding 0h sample. We also compared the induced cytokine responses by the FOS and native inulin samples at the different time points to their corresponding blank samples.

Results

DP and structure-specific utilization of FOS and native inulin by faecal microbiota of 2- and 8-week-old infants

As it has been shown that faecal microbiota of 2- and 8-week-old infants have a different composition and consequently a different expression of carbohydrate degrading enzymes [14], their ability to ferment FOS (DP2-10) and native inulin (DP2-60) were compared. During *in vitro* fermentation, samples were collected and analysed with HPAEC to follow the fate of the NDCs. A detailed overview of remaining DP after fermentation of FOS and native inulin is shown in Figure S1.

Faecal microbiota of both 2- and 8-week-old infants were able to ferment the trisaccharides with either a terminal fructose or glucose moiety (F and GF series) present in FOS, although 8-week-old infants did this at a higher rate (Figure 1). The fermentation was limited to these DP3 oligomers during the first 14 h of fermentation. Between 14 and 26 h of fermentation also only minor degradation of FOS DP>3 took place, but fermentation of DP3 oligomers was still most pronounced. After 26 h of fermentation, less than 3% of the DP3 oligomers

was remaining, while ≈77% of FOS DP>3 was still intact with faecal microbiota of 2- and 8-week-old infants.

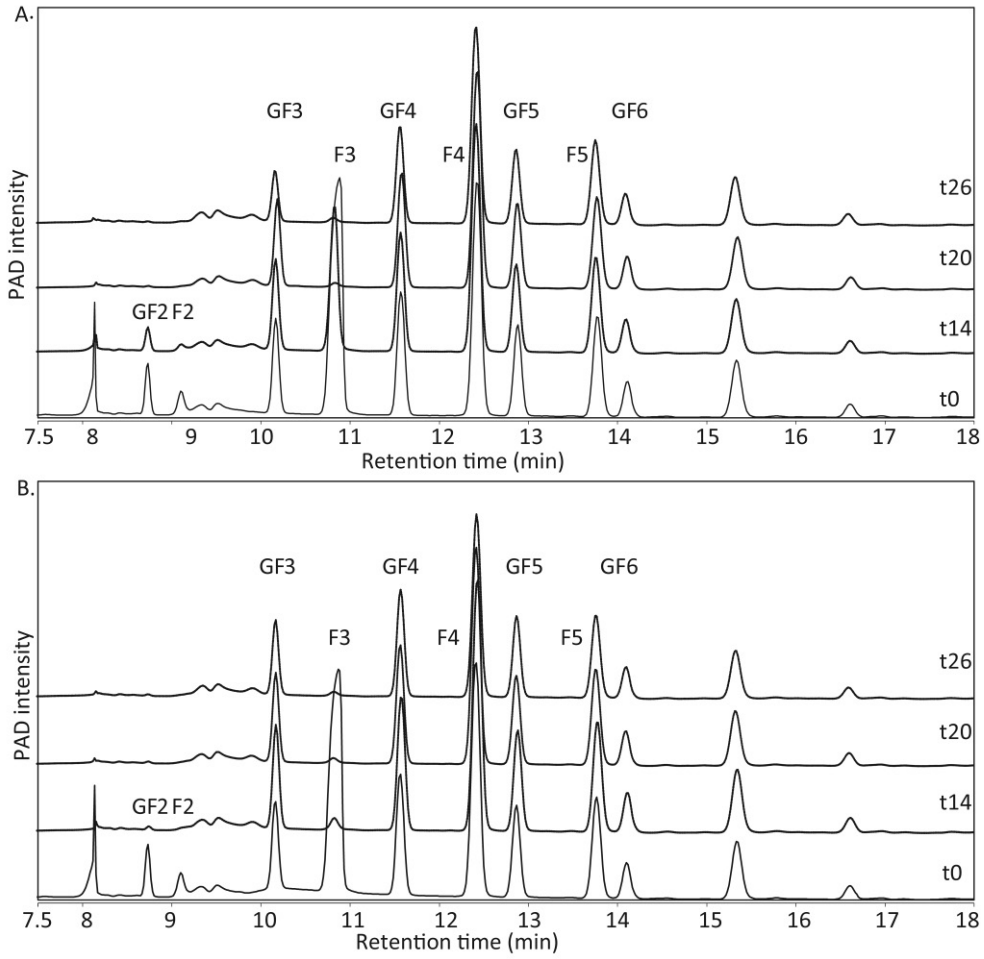

Figure 1 HPAEC profiles of FOS at the start and after 14, 20 and 26 h of fermentation using pooled faecal inoculum of 2- (A) and 8- (B) week-old infants. DP and F/GF series are annotated.

Faecal microbiota of 2-week-old infants were able to degrade oligomers of native inulin up to DP9 while higher DPs remained virtually intact (Figure 2). There was a relative high recovery of 62% and 99% for respectively DP 9-15 and DP ≥16 after 26 h of fermentation. Longer incubation times did not result in significant fermentation of higher DPs (Figure S2). The faecal microbiota of 2-week-old infants had a similar preference for the trisaccharides F3 and GF2 during the first 14 h of fermentation as was observed in the fermentation study with FOS, although the F-series was less abundant in native inulin compared to FOS.

Fermentation of native inulin using faecal microbiota of 8-week-old infants resulted in different degradation patterns compared to the 2-week-old infants, as they were able to degrade native inulin of higher DP values. The faecal microbiota of 8-week-old infants was able to completely degrade native inulin up to DP16 and higher DPs were degraded for 40% after 26 h of fermentation. Also, in this case a clear preference for the trisaccharides F3 and GF2 was observed during the first 14 h of fermentation.

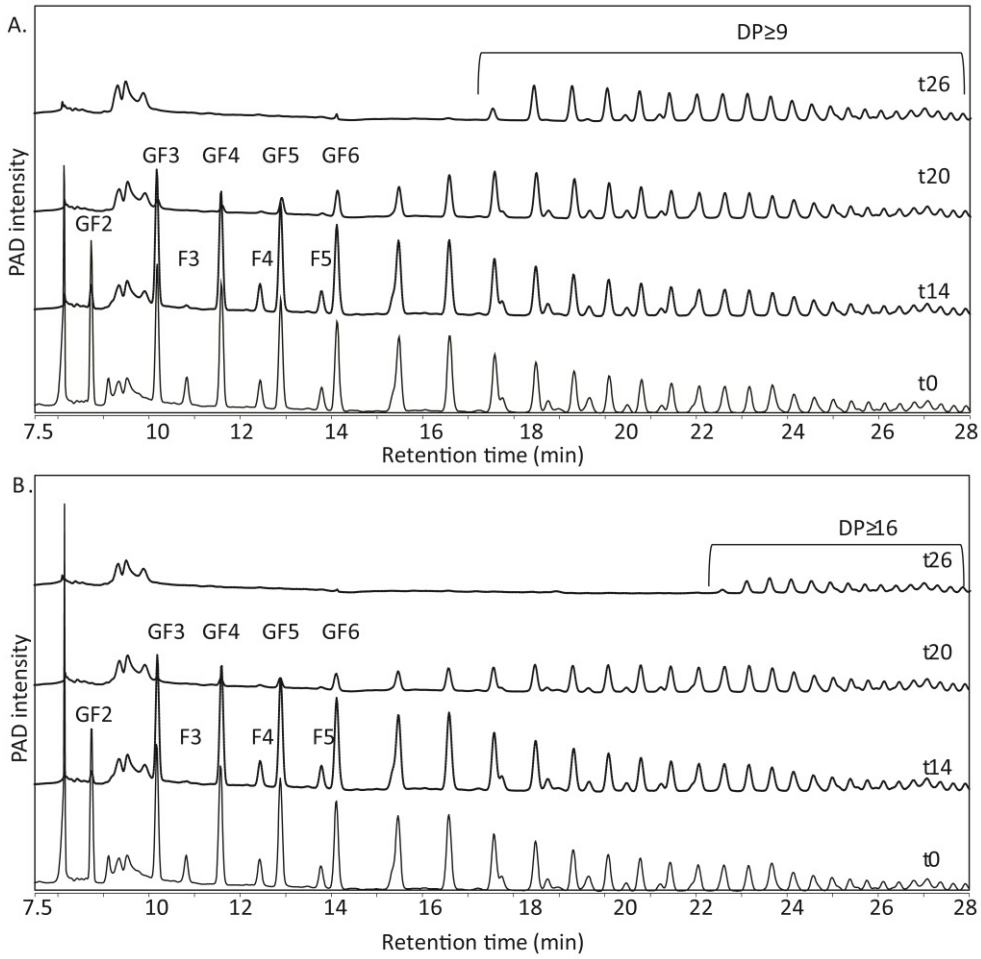

Figure 2 HPAEC profiles of native inulin at the start and after 14, 20 and 26 h of fermentation using pooled faecal inoculum of 2- (A) and 8- (B) week-old infants. DP and F/GF series are annotated.

Impact of native inulin on faecal microbiota composition is different between 2- and 8-week-old infants

To study the impact of FOS and native inulin on the faecal microbiota of 2- and 8-week-old infants, 16S rRNA gene amplicon sequencing and quantitative PCR (qPCR) of total bacteria was performed. With FOS fermentation, a decrease in relative abundance of *Bifidobacterium* was observed in the first 14 h with both faecal inocula of 2- and 8-week-old infants (Figure 3, Table S1) as well as in control fermentations without NDCs (Figure S3). However, taking into account quantitative PCR analysis of total bacteria demonstrating a 2000-fold increase in 16S rRNA gene copy numbers between 0 and 14 h of fermentation (Table S2), fermentation of FOS increased the absolute number of *Bifidobacterium* from $2.8x10^6$ to $1.1x10^9$ copies in the first 14 h for inocula of 2-week-old infants. After 26 h of fermentation 43-49% of the bacteria belonged to the genus *Bifidobacterium*. A control fermentation without NDCs did not result in an increase in *Bifidobacterium* (Figure S3).

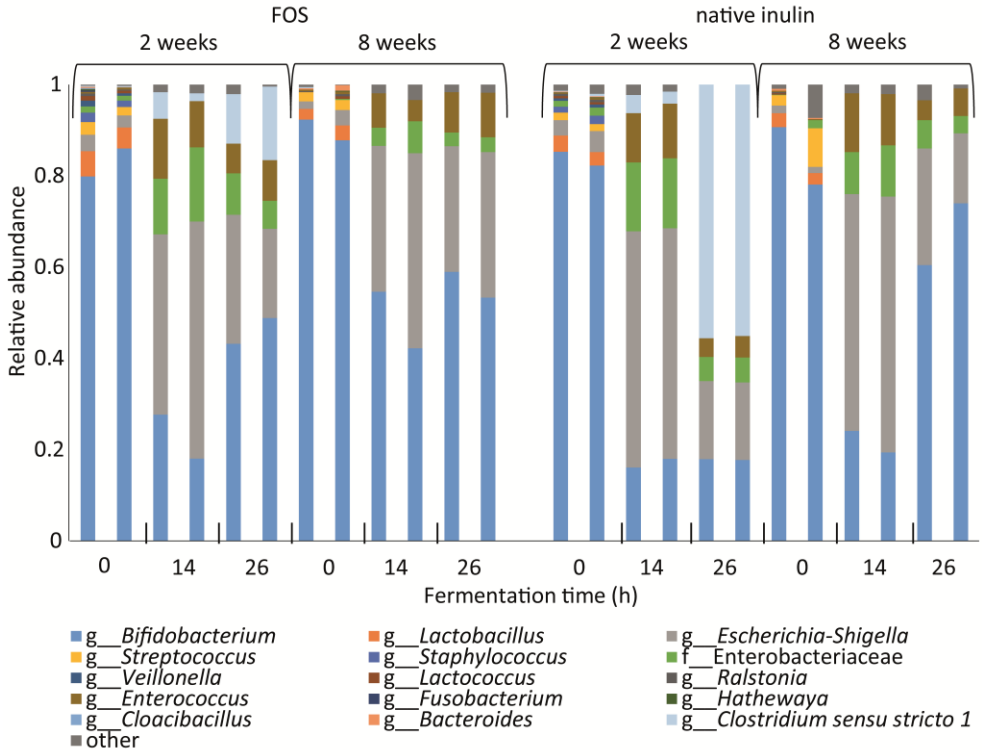

Figure 3 Relative abundance of bacteria at the highest classified taxonomy in duplicate fermentation digesta collected at the start and after 14 and 26 h from *in* vitro fermentation of FOS and native inulin using pooled faecal inoculum of 2- and 8-week-old infants with the 15 most abundant bacteria visualized individually and less abundant bacteria summarized as 'other'.

Fermentation of FOS using faecal inoculum of 2-week-old infants also resulted in an increase in *Clostridium sensu stricto* resulting in a 11-16% contribution to all bacteria after 26 h. In addition, an enrichment in bacteria belonging to the genera *Enterococcus*, *Escherichia-Shigella* and the family Enterobacteriaceae was observed. This enrichment was also observed for control fermentations without added NDCs.
FOS fermented by inoculum of 8-week-old infants also induced an increase in relative abundance of *Bifidobacterium* to 53-59% after 26 h of fermentation. Furthermore, a similar enrichment in bacteria belonging to the genera *Enterococcus* and *Escherichia-Shigella* and the family Enterobacteriaceae was observed. However, fermentation of FOS by faecal microbiota of 8-week-old infants did not result in an increase in the relative abundance of *Clostridium sensu stricto*.
Native inulin decreased the relative abundance of *Bifidobacterium* for inocula of 2- and 8-week-old infants in the first 14 h of fermentation. Again, the qPCR illustrated that this relative decrease did not represent a decrease in absolute numbers of *Bifidobacterium* (Table S2). After 26 h of fermentation the faecal microbiota of 2-week-old infants was for 18% composed of bacteria belonging to the genus *Bifidobacterium. Clostridium sensu stricto* was most abundant; 55% after 26 h of fermentation. Similar to the fermentation of FOS, background fermentation of SIEM medium components was observed.
Native inulin induced a higher increase in relative abundance of *Bifidobacterium* for inocula of 8-week-old infants than for 2-week-old infants, but no relative increase in *Clostridium sensu stricto* was observed. After 26 h of fermentation 60-74% of the bacteria belonged to the genus *Bifidobacterium.* Fermentation of native inulin thus showed an age-dependent stimulation of *Bifidobacterium*, which was not observed for FOS.

Differences in predicted functional capabilities of microbial communities from 2- and 8-week-old infants during native inulin fermentation

As the degradation kinetics of native inulin differed between the faecal microbiota of 2- and 8-week-old infants, we questioned whether this might be explained by differences in the predicted functional capability and more specifically in expression of the enzymes β-fructofuranosidase and fructan β-fructosidase which are necessary for degradation of native inulin. To this end, an additional analysis was performed to predict the functional capability of the microbial communities based on 16S rRNA genes using Tax4Fun2 (Figure 4). The heatmap shows a clear clustering based on fermentation time and infant age. With native inulin a higher relative abundance of β-fructofuranosidase and fructan β-fructosidase was observed for faecal microbiota of 8-week-old infants compared to 2-week-old infants.

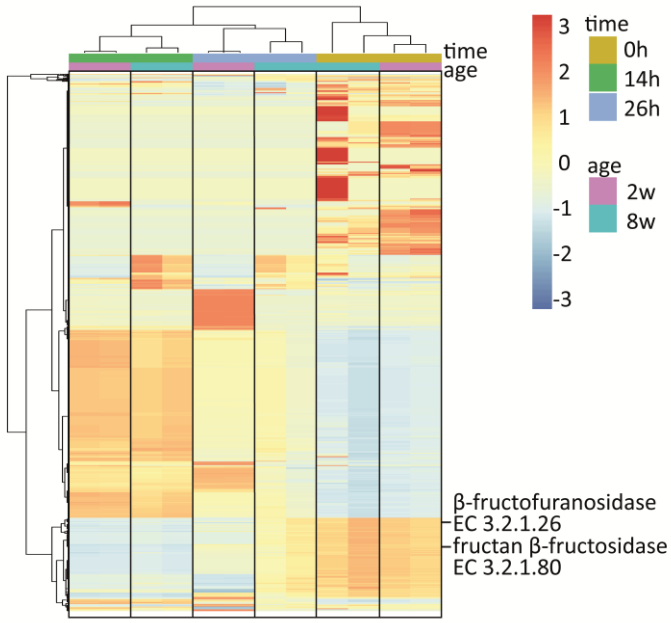

Figure 4 Heatmap of relative abundance of KEGG functional orthologs in fermentation digesta collected at the start and after 14 and 26 h from *in vitro* fermentation of native inulin using pooled faecal inoculum of 2- and 8-week-old infants. Colours given by taxa scaling per row with the mean relative abundance in yellow. Hierarchical clustering using Ward.D2 algorithm and Euclidean distances. KEGG functional orthologs necessary for degradation native inulin shown in figure. On top of the heatmap different colours as explained in the legend depict the infant age and fermentation time.

High relative abundance of one specific ASV in fermentations of both FOS and native inulin

Since mainly *Bifidobacterium* was increased by FOS and native inulin, we performed a higher resolution analysis at the level of their individual sequences (Amplicon Sequencing Variants (ASVs)), which can be considered as a proxy for *Bifidobacterium* species (Figure 5). ASV 2554220 was the most abundant ASV during fermentations of both FOS and native inulin using faecal inoculum of 2- and 8-week-old infants. Comparison of the sequence with the SILVA database release 132 showed that the sequence was an exact match with species such as *Bifidobacterium breve, Bifidobacterium longum* subspecies *infantis* and *Bifidobacterium longum* subspecies *longum* (Table 1).

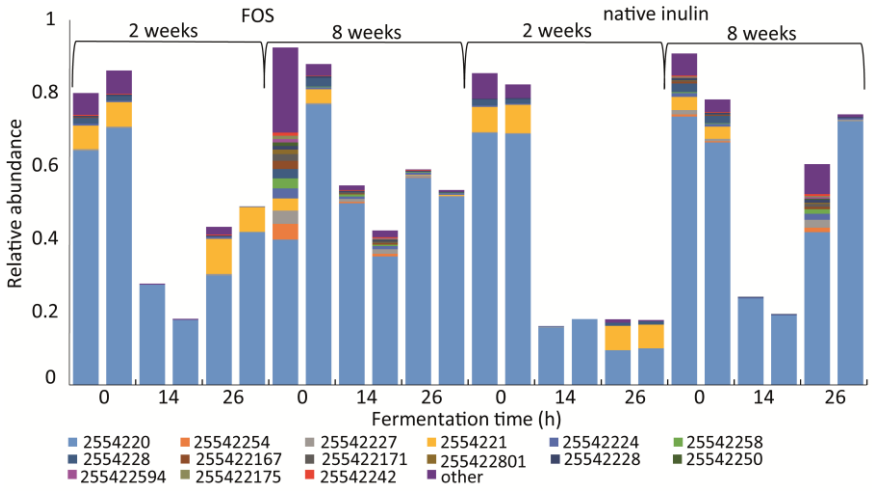

Figure 5 Relative abundance of *Bifidobacterium* Amplicon Sequencing Variants (ASVs) in duplicate fermentation digesta collected at the start and after 14 and 26 h from *in vitro* fermentation of FOS and native inulin using pooled faecal inoculum of 2- and 8-week-old infants.

Table 1 Taxa matching with ASV 2554220 according to SILVA database release 132

g_*Bifidobacterium* ASV 2554220
TGGTAGTCCACGCCGTAAACGGTGGATGCTGGATGTGGGGCCCGTTCCACGGGTTCCGTGTCGGAGCTAA
GTGAACCCGCCCCGAAGGGAAACCCCATCTCTGGGATCGTCGGGAACATGTCAAGCCCAGGTAAGGTTCT

taxa	database hits
breve	74
uncultured organism	45
human gut metagenome	38
longum subspecies infantis	34
longum subspecies longum	11
longum subspecies infantis_ATCC_15697_\u003d_JCM_1222_\u003d_DSM_20088	11
unidentified	9
uncultured bacterium	9
*breve*_DSM_20213_\u003d_JCM_1192	5
*breve*_S27	3
*breve*_ACS-071-V-Sch8b	3
*longum subspecies longum*_JDM301	3
*breve*_689b	2
*breve*_UCC2003	2
*breve*_12L	2
*breve*_JCM_7017	2

Extracellular β-fructofuranosidase not detected in *Bifidobacterium* species present in faecal microbiota of 8-week-old infants

As the expression of extracellular β-fructofuranosidase could be essential for the utilization of long-chain inulin, we questioned whether *Bifidobacterium* species present in the faecal microbiota of 8-week-old infants contain the gene that encodes for extracellular β-

fructofuranosidase. The distribution of this gene among bacterial genomes was investigated using UniProtKB and BUSCA (Figure 6). Only 3 out of 351 bacterial genes encoding for extracellular β-fructofuranosidase belong to *Bifidobacterium* species, namely to *Bifidobacterium adolescentis, mongoliense* and *psychraerophilum.* These *Bifidobacterium* species were not detected in native inulin exposed microbiota of 2- and 8-week-old infants, suggesting that *Bifidobacterium* was not responsible for the utilization of long-chain inulin.

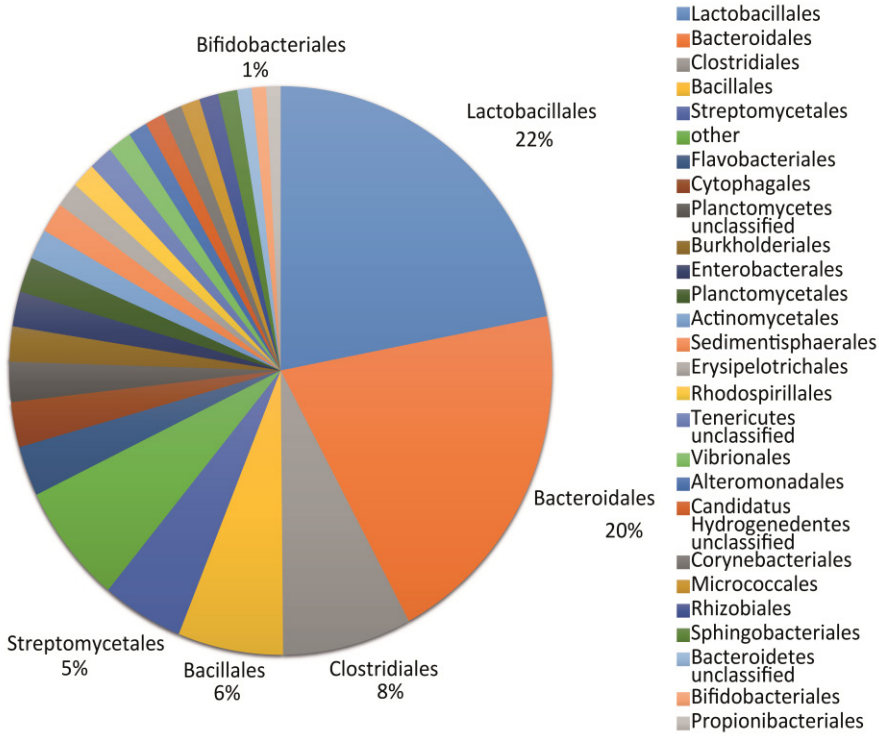

Figure 6 Distribution of extracellular β-fructofuranosidase genes within sequenced bacterial genomes on order level.

SCFAs and organic acids are produced in an age- and fructan-dependent fashion

Since SCFAs and other organic acids have shown to be primary fermentation metabolites with important immunomodulatory activity, SCFAs production during fermentation of FOS and native inulin was quantified (Figure 7). Reproducibility was confirmed with duplicate fermentations. A control fermentation without added NDCs showed only minor production of organic acids (Figure S4). Fermentation of FOS by faecal inoculum of 2-week-old infants resulted in a total organic acid production of 5.8 µmol/mg after 26 h in a ratio of 66:26:5:2:1 for respectively acetate, lactate, succinate, butyrate and propionate. Fermentation of FOS by faecal inoculum of 8-week-old infants resulted in a lower amount of total organic acids

produced (4.9 µmol/mg). Acetate, lactate, succinate, butyrate and propionate were produced in a ratio of 73:18:7:1:1.

Differences in both total production and composition of organic acids were observed for the fermentation of native inulin using both inocula. The fermentation using faecal inoculum of 2-week-old infants resulted in a total organic acid production after 26 h of 4.5 µmol/mg with a considerable amount of butyrate (0.9 µmol/mg). Acetate, lactate, succinate, butyrate and propionate were produced in a ratio of 53:19:6:20:2. Fermentation of native inulin by faecal inoculum of 8-week-old infants resulted in a two-fold higher amount of total organic acids produced, namely 8.9 µmol/mg. Acetate, lactate, succinate, butyrate and propionate were produced in a ratio of 72:22:4:1:1.

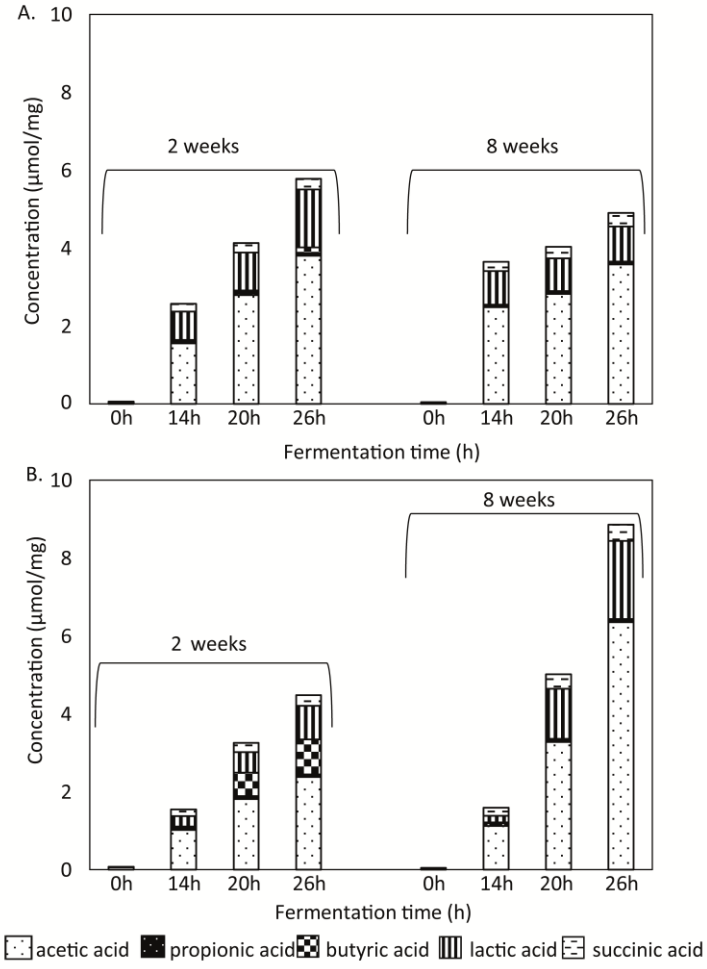

Figure 7 Production of SCFAs, lactate and succinate upon fermentation of FOS (A) and native inulin (B) using pooled faecal inoculum of 2- and 8-week-old infants.

Fermentation digesta of FOS and native inulin induce infant's age-dependent cytokine responses in dendritic cells

As *in vivo* the gastrointestinal tract is aligned with numerous dendritic cells, we studied the impact of digesta of FOS and native inulin fermentation on DC cytokine responses. We compared the impact of digesta of FOS and native inulin fermented by faecal inocula from 2- and 8-week-old infants. To this end, DCs were incubated with fermentation digesta for 48h and the pro-inflammatory chemokines and cytokines MCP-1/CLL2, MIP-1α/CCL3, IL-1β, IL-6 and TNFα as well as the anti-inflammatory cytokine IL-10 induced in DCs were measured.

Digesta from control fermentations without added NDCs were incubated with DCs (Figure 8). Both t=14 and t=26 digesta of 2- and 8-week inoculum significantly increased the secretion of most chemokines and cytokines, when compared to t=0. Incubation of DCs with t=14 digesta of the control fermentation with 2-week inoculum significantly increased the chemokines MCP-1/CCL2 and MIP-1α/CCL3, the pro-inflammatory cytokines IL-1β, IL-6 and TNFα but not the anti-inflammatory cytokine IL-10. The t=26 digesta induced a significant increase of all chemokines and cytokines measured. The total upregulation of all chemokines and cytokines was more pronounced with microbiota of 8-week-old infants.

Incubation of DCs with t=14 FOS digesta of 2-week-old infants inoculum significantly increased the levels of the chemokine MIP-1α/CCL3 and cytokines IL-1β and IL-6 when compared to digesta of t=0, but levels were significantly lower than the levels induced by t=14 digesta of control fermentations with inocula of 2-week-old infants. Incubation of DCs with t=26 FOS digesta fermented with 2-week-old infant inoculum increased the same cytokines as well as IL-10 and TNFα. Again, the levels of MIP-1α/CCL3, IL-1β and IL-6 were lower than levels of these cytokines induced by the t=26 digesta of control fermentations.

DC incubation with digesta of FOS fermented with 8-week-old infant inoculum resulted in different cytokine patterns. DCs incubated with t=14 FOS digesta significantly increased secretion of the chemokines and cytokines MCP-1/CCL2, MIP-1α/CCL3, IL-1β and TNFα when compared to t=0. However, levels of MIP-1α/CCL3, IL-1β and IL-6 as well as levels of TNFα were significantly lower when compared to cytokine levels induced by t=14 digesta of control fermentations with inocula of 8-week-old infants. With t=26 digesta, levels of MCP-1/CCL2, MIP-1α/CCL3, IL-1β, IL-10 and TNFα were significantly increased, but levels of MIP-1α/CCL3, IL-1β, IL-6 and TNFα were still significantly lower when compared to cytokine levels induced by t=26 digesta of control fermentations with inocula of 8-week-old infants.

When chemokine and cytokine secretion patterns between DC stimulations with digesta of FOS fermentations with inoculum of 2- and 8-week-old infants were compared, significant differences between age categories were found for secretion of IL-6 ($p < 0.001$).

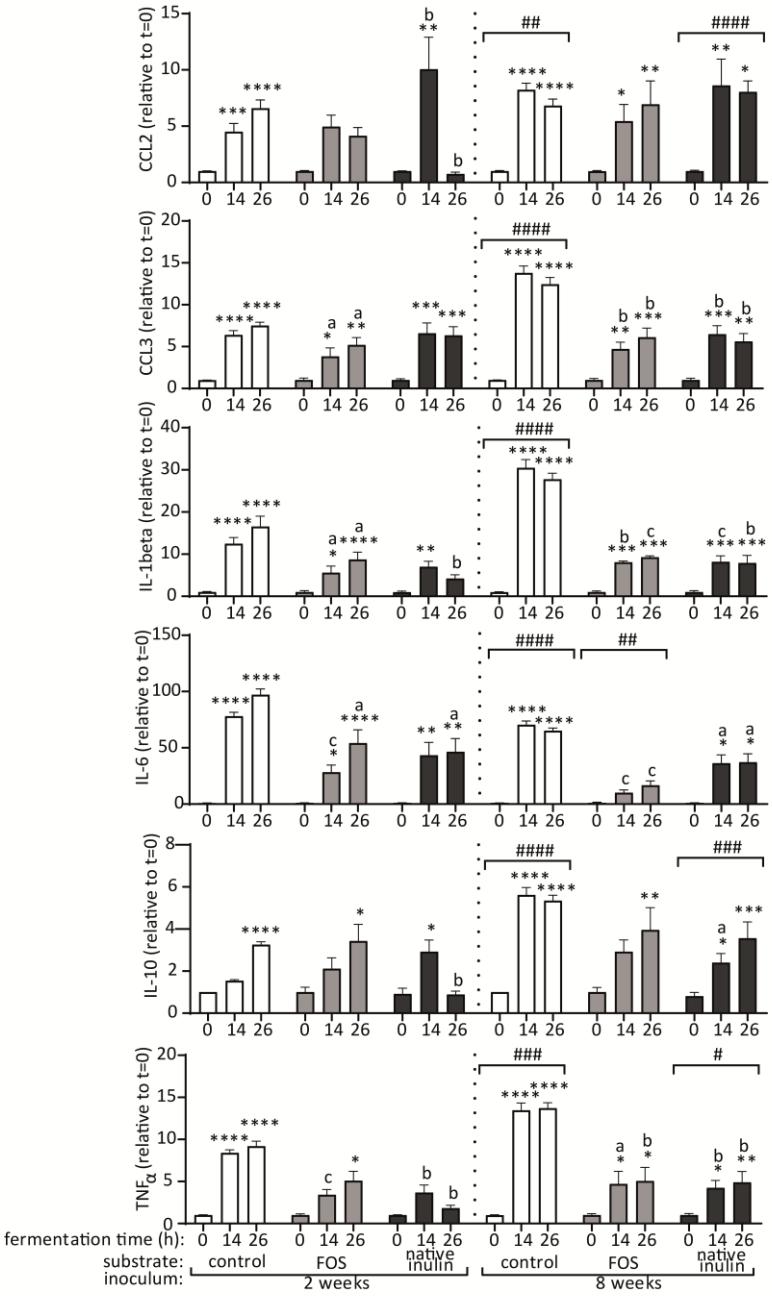

Figure 8 Induced cytokines (fold change of induction by 0h samples) by digesta of control fermentation, FOS and native inulin fermentation with pooled faecal inocula of 2- and 8-week-old infants with statistical different response compared to the 0h sample: *p<0.05, **p<0.01, ***p<0.001, ****p<0.0001, between 2 and 8 week groups: #p<0.05, ##p<0.01, ###p<0.001, ####p<0.0001 and between FOS and native inulin samples and their matched time sample of the control fermentation a p<0.05, b p<0.01, c p<0.001, d p<0.0001.

Fermentation of native inulin also demonstrates a clear age-dependent impact on DC cytokine responses. When DCs where incubated with t=14 native inulin digesta fermented with inoculum of 2-week-old infants, levels of the chemokines MCP-1/CCL2, MIP-1α/CCL3, IL-1β, IL-6 but also of IL-10 was significantly increased. Notably, the level of MIP-1α/CCL2 was significantly higher and the level of TNFα was significantly lower than that induced by t=14 digesta of control fermentations. Native inulin t=26 digesta only significantly increased secretion of chemokine MIP-1α/CCL3 and IL-6. The levels of the chemokine MIP-1α/CCL2 and the cytokines IL-1β, IL-6, IL-10 and TNFα were all significantly lower when compared to the t=26 digesta of the control fermentation.
Results were different with 8-week inoculum. DCs with native inulin t=14 digesta induced a significant increase in secretion of all chemokines and cytokines measured. However, the levels of MCP-1/CCL3, IL-1β, IL-6, IL-10 and TNFα were all still significantly lower than the levels of these cytokines induced by the t=14 digesta of the control fermentation. With native inulin t=26 digesta all cytokines significantly increased compared to t=0, but again MCP-1/CCL3, IL-1β, IL-6 and TNFα were still significantly lower than the levels of these cytokines induced by the t=26 digesta of the control fermentation with inoculum of 8-week-old infants.
When 2- and 8-week-old infants were compared, significant differences were found for secretion of chemokine MIP-1α/CCL3 ($p < 0.001$), the pro-inflammatory cytokine TNFα ($p < 0.05$) and the anti-inflammatory cytokine IL-10 ($p < 0.001$).

Discussion

Cow's milk-based infant formulas are often substituted with NDCs to mimic HMO functionalities. Chicory FOS and native inulin are supplemented to infant formula, but to date minor knowledge is available on structure-specific utilization of NDCs by infant gut microbiota, production of SCFAs and concomitant immune effects. Therefore, we investigated the degradation of FOS and native inulin by infant faecal microbiota and the effect of the fermentation digesta on dendritic cell responses.
Fermentation of FOS showed selective utilization of the trisaccharides F3 and GF2 in both 2- and 8-week-old infants, which coincided with an increase in *Bifidobacterium* and an increased production of mainly acetate and lactate. These organic acids are important end products of the bifid shunt, which is a unique hexose metabolism pathway, and consequently suggested to be mainly produced by *Bifidobacterium* [30]. The stimulation of *Bifidobacterium* by FOS corroborates findings of a previous in vivo study [31] in infants receiving FOS-supplemented infant formula. The utilization of FOS by *Bifidobacterium* is attributed to several properties such as expression of the gene that encodes for β-fructofuranosidase, which is responsible for the cleavage of the β(2-1) bonds between the fructose units in FOS [32].

Our data suggest that fermentation of FOS mostly benefit *Bifidobacterium breve*, which is commonly found in the infant gut [33]. In contrast to other *Bifidobacterium* species, *Bifidobacterium breve* showed to have a similar preference for FOS DP3 [34]. DP3 was also first fermented when native inulin was used as substrate, but here, in our study, DP 2-8 F and GF series were degraded more extensively. This can be explained by the presence of higher DPs and the relatively low abundance of DP3 (8% vs 32%) in native inulin, what could have stimulated a broader range of bacterial enzymes.

Native inulin was fermented differently by faecal microbiota of 2- and 8-week-old infants. The faecal microbiota of 8-week-old infants fermented up to a higher DP than the 2-week-old infants. This correlated with a higher relative increase in *Bifidobacterium* and higher production of acetate and lactate. Whereas most *Bifidobacterium* species utilize FOS by intracellular uptake and degradation, this uptake has been suggested to be lower for longer inulin oligosaccharides due to their larger size [35]. Previous studies have shown that the growth of *Bifidobacterium* on inulin is dependent on the transcription of extracellular β-fructofuranosidase [36].

Extracellular β-fructofuranosidase is predominantly present among bacterial orders such as Bacteroidales and Lactobacillales. *Bifidobacterium* species which contain the gene encoding for extracellular β-fructofuranosidase were not detected in faecal microbiota of both 2- and 8-week-old infants. Therefore, it is possible that cross-feeding between *Bifidobacterium* and other bacteria occurred during degradation of higher DPs by the faecal microbiota of 8-week-old infants. Similar cross-feeding is reported between *Lactobacillus salivarius* and *Lactobacillus paracasei*, where the latter uses an exo-inulinase to degrade long-chain inulin [37]. However, it cannot be excluded that certain *Bifidobacterium* species can internalize native inulin DP 9-16 by ABC transport systems, which was reported for *Roseburia inulinivorans* [32].

Along with *Bifidobacterium*, also a relative increase in *Clostridium sensu stricto I* was observed during fermentation of FOS and native inulin by 2-week-old infants, which corresponded with an increased production of butyrate. In contrast to *Bifidobacterium*, several *Clostridium* species ferment hexoses through the Embden-Meyerhof-Parnas or pentose phosphate pathway with butyrate being one of the important end products [38]. Although *Clostridium* can utilize FOS and inulin [39], the increase in *Clostridium sensu stricto* in the control fermentation without added NDCs indicate their increase is due to fermentation of SIEM medium components.

Notably, more bacteria were stimulated by SIEM medium. For all fermentations an enrichment in bacteria belonging to the genera *Enterococcus* and *Escherichia-Shigella* and the family Enterobacteriaceae was observed in the first 14 h of fermentation. These bacteria were reported to grow well on peptides and amino acids which are highly abundant in SIEM medium: bactopeptone (24 g/L), casein (24 g/L), ox-bile (0.4 g/L) and cysteine (0.16 g/L) [40].

As the enrichment was also observed for control fermentations without added NDCs, it can be concluded that their growth was stimulated by these medium components.

Fermentation as such had a strong impact on cytokine production by immature umbilical vein derived dendritic cells. The control fermentation digests without added NDCs with both 2- and 8-week-old infant inoculum induced high levels of the chemokines and cytokines MCP-1/CLL2, MIP-1α/CCL3, IL-1β, IL-6 and TNFα as well as the anti-inflammatory cytokine IL-10. T=0 digesta only induced minor cytokine production in DCs, indicating that products formed during fermentation are responsible for the observed effects. As production of SCFAs in the control fermentation is very low, we assume that specific bacterial products such as ATP, lipoteichoic acid, polysaccharide A, peptidoglycan, exopolysaccharide and RNA/DNA sequences produced by bacteria during fermentation are responsible for these immune stimulating effects [41]. These bacterial products interact with specialized immune receptors on immune cells such as Toll like receptors (TLRs) that are expressed on immune cells such as dendritic cells [41].

Fermentation of FOS and native inulin reduced the induced enhancement of cytokines by control fermentation. For FOS we found a clear attenuation of the production of multiple pro-inflammatory cytokines compared to the control fermentation. This phenomenon could possibly be explained by the production of SCFAs upon fermentation as shown here and by others [42]. A very pronounced effect was observed for IL-6 secretion by DCs, which was virtually gone with FOS digesta of faecal inoculum of 8-week-old infants and profoundly reduced with faecal inoculum of 2-week-old infants fermenting FOS. For other cytokines no significant differences were observed between FOS and the control fermentation, which correlated with the similarities in changes in microbiota composition and functionality between faecal microbiota of 2- and 8-week-old infants upon fermentation of FOS.

Native inulin also attenuated the production of pro-inflammatory cytokines, however the profiles and magnitude of attenuation were different than with FOS. Surprisingly, for the digesta of 2-week-old infants this attenuation was more pronounced after 26 h of fermentation for the cytokines MCP-1/CCL2, IL-1β, IL-10 and TNFα. This specific native inulin-26h fermentation sample was also found to have a high relative increase in *Clostridium sensu stricto I* and increased production of butyrate. Butyrate is known to be an immune attenuating SCFA that acts via GPR109a receptor present on dendritic cells [43]. Previous studies also found that butyrate altered the production of pro-inflammatory cytokines as well as the anti-inflammatory cytokine IL-10 [44]. In addition, it was found that butyrate delayed maturation of DCs and thereby influences T-cell polarization [45]. The generation of butyrate from fermented native inulin might therefore beneficially influence immune development as butyrate can guide immune polarization [45].

Concluding remarks

This study provides insight into the complex relation between the structure of fructans, the faecal microbiota composition, fermentation capacity, SCFAs production and immune effects in infants. Our data shows that differences in microbial functionality between 2- and 8-week-old infants impacts fermentation of fructans and therewith the extent to which it performs attenuation of pro-inflammatory responses in immature DCs. Our findings may contribute to design and tailoring of NDCs mixtures for substitution of infant formulas to meet the needs of infants of different ages and state of inflammation.

Acknowledgements

This research was performed in the public-private partnership 'CarboKinetics' coordinated by the Carbohydrate Competence Center (CCC, www.cccresearch.nl). CarboKinetics is financed by participating industrial partners Agrifirm Innovation Center B.V., Cooperatie Avebe U.A., DSM Food Specialties B.V., FrieslandCampina Nederland B.V., Nutrition Sciences N.V., VanDrie Holding N.V. and Sensus B.V., and allowances of The Netherlands Organisation for Scientific Research (NWO).

References

1. Matamoros, S.; Gras-Leguen, C.; Le Vacon, F.; Potel, G.; de La Cochetiere, M.F. Development of intestinal microbiota in infants and its impact on health. *Trends Microbiol.* **2013**, *21*, 167-173.
2. Marques, T.M.; Wall, R.; Ross, R.P.; Fitzgerald, G.F.; Ryan, C.A.; Stanton, C. Programming infant gut microbiota: influence of dietary and environmental factors. *Curr. Opin. Biotechnol.* **2010**, *21*, 149-156.
3. Organization, W.H.; UNICEF. *Global strategy for infant and young child feeding*; 9241562218; 2003.
4. Smilowitz, J.T.; Lebrilla, C.B.; Mills, D.A.; German, J.B.; Freeman, S.L. Breast milk oligosaccharides: structure-function relationships in the neonate. *Annu. Rev. Nutr.* **2014**, *34*, 143-169.
5. Holscher, H.D.; Bode, L.; Tappenden, K.A. Human milk oligosaccharides influence intestinal epithelial cell maturation *in vitro*. *J. Pediatr. Gastroenterol. Nutr.* **2017**, *64*, 296-301.
6. Theurich, M.A.; Davanzo, R.; Busck-Rasmussen, M.; Diaz-Gomez, N.M.; Brennan, C.; Kylberg, E.; Baerug, A.; McHugh, L.; Weikert, C.; Abraham, K.; Koletzko, B. Breastfeeding rates and programs in europe: A survey of 11 national breastfeeding committees and representatives. *J. Pediatr. Gastroenterol. Nutr.* **2019**, *68*, 400-407.
7. Bych, K.; Mikš, M.H.; Johanson, T.; Hederos, M.J.; Vigsnæs, L.K.; Becker, P. Production of HMOs using microbial hosts — from cell engineering to large scale production. *Curr. Opin. Biotechnol.* **2019**, *56*, 130-137.
8. Verkhnyatskaya, S.; Ferrari, M.; de Vos, P.; Walvoort, M.T.C. Shaping the infant microbiome with non-digestible carbohydrates. *Front. Microbiol.* **2019**, *10*, 343-343.
9. Kelly, G. Inulin-type prebiotics--a review: part 1. *Altern. Med. Rev.* **2008**, *13*, 315-329.
10. Ito, H.; Takemura, N.; Sonoyama, K.; Kawagishi, H.; Topping, D.L.; Conlon, M.A.; Morita, T. Degree of polymerization of inulin-type fructans differentially affects number of lactic acid bacteria, intestinal immune functions, and immunoglobulin A secretion in the rat cecum. *J. Agric. Food Chem.* **2011**, *59*, 5771-5778.
11. Vogt, L.; Ramasamy, U.; Meyer, D.; Pullens, G.; Venema, K.; Faas, M.M.; Schols, H.A.; de Vos, P. Immune modulation by different types of beta2->1-fructans is toll-like receptor dependent. *PLoS One* **2013**, *8*, e68367.
12. Baxter, N.T.; Schmidt, A.W.; Venkataraman, A.; Kim, K.S.; Waldron, C.; Schmidt, T.M. Dynamics of human gut microbiota and short-chain fatty acids in response to dietary interventions with three fermentable fibers. *mBio* **2019**, *10*, e02566-02518.
13. Smith, P.M.; Howitt, M.R.; Panikov, N.; Michaud, M.; Gallini, C.A.; Bohlooly-Y, M.; Glickman, J.N.; Garrett, W.S. The microbial metabolites, short-chain fatty acids, regulate colonic treg cell homeostasis. *Science* **2013**, *341*, 569-573.
14. Albrecht, S.; Schols, H.A.; van den Heuvel, E.G.; Voragen, A.G.; Gruppen, H. Occurrence of oligosaccharides in feces of breast-fed babies in their first six months of life and the corresponding breast milk. *Carbohydr. Res.* **2011**, *346*, 2540-2550.
15. Korpela, K.; de Vos, W.M. Early life colonization of the human gut: microbes matter everywhere. *Curr. Opin. Microbiol.* **2018**, *44*, 70-78.
16. Gu, F.; Borewicz, K.; Richter, B.; van der Zaal, P.H.; Smidt, H.; Buwalda, P.L.; Schols, H.A. *In vitro* fermentation behavior of isomalto/malto-polysaccharides using human fecal inoculum indicates prebiotic potential. *Mol. Nutr. Food Res.* **2018**, *62*, e1800232.
17. Leijdekkers, A.G.; Aguirre, M.; Venema, K.; Bosch, G.; Gruppen, H.; Schols, H.A. In vitro fermentability of sugar beet pulp derived oligosaccharides using human and pig fecal inocula. *Journal of agricultural and food chemistry* **2014**, *62*, 1079-1087.
18. Ladirat, S.E.; Schuren, F.H.; Schoterman, M.H.; Nauta, A.; Gruppen, H.; Schols, H.A. Impact of galacto-oligosaccharides on the gut microbiota composition and metabolic activity upon antibiotic treatment during *in vitro* fermentation. *FEMS Microbiol. Ecol.* **2014**, *87*, 41-51.
19. Zhao, G.; Nyman, M.; Jonsson, J.A. Rapid determination of short-chain fatty acids in colonic contents and faeces of humans and rats by acidified water-extraction and direct-injection gas chromatography. *Biomed. Chromatogr.* **2006**, *20*, 674-682.
20. Salonen, A.; Nikkilä, J.; Jalanka-Tuovinen, J.; Immonen, O.; Rajilić-Stojanović, M.; Kekkonen, R.A.; Palva, A.; de Vos, W.M. Comparative analysis of fecal DNA extraction methods with phylogenetic microarray: Effective recovery of bacterial and archaeal DNA using mechanical cell lysis. *J. Microbiol. Methods* **2010**, *81*, 127-134.
21. An, R.; Wilms, E.; Smolinska, A.; Hermes, G.D.A.; Masclee, A.A.M.; de Vos, P.; Schols, H.A.; van Schooten, F.J.; Smidt, H.; Jonkers, D.; Zoetendal, E.G.; Troost, F.J. Sugar beet pectin supplementation did not alter profiles of fecal microbiota and exhaled breath in healthy young adults and healthy elderly. *Nutrients* **2019**, *11*.
22. Ramiro-Garcia, J.; Hermes, G.D.A.; Giatsis, C.; Sipkema, D.; Zoetendal, E.G.; Schaap, P.J.; Smidt, H. NG-Tax, a highly accurate and validated pipeline for analysis of 16S rRNA amplicons from complex biomes. *F1000Research* **2016**, *5*, 1791-1791.
23. Poncheewin, W.; Hermes, G.D.A.; van Dam, J.C.J.; Koehorst, J.J.; Smidt, H.; Schaap, P.J. NG-Tax 2.0: A semantic framework for high-throughput amplicon analysis. *Front. Genet.* **2020**, *10*.

24. Quast, C.; Pruesse, E.; Yilmaz, P.; Gerken, J.; Schweer, T.; Yarza, P.; Peplies, J.; Glöckner, F.O. The SILVA ribosomal RNA gene database project: improved data processing and web-based tools. *Nucleic Acids Res.* **2012**, *41*, D590-D596.
25. Wemheuer, F.; Taylor, J.A.; Daniel, R.; Johnston, E.; Meinicke, P.; Thomas, T.; Wemheuer, B. Tax4Fun2: a R-based tool for the rapid prediction of habitat-specific functional profiles and functional redundancy based on 16S rRNA gene marker gene sequences. *Environ. Microbiome* **2020**, *15*.
26. Kolde, R. Package 'pheatmap'. *R Package* **2015**, *1*.
27. Savojardo, C.; Martelli, Pier L.; Fariselli, P.; Profiti, G.; Casadio, R. BUSCA: an integrative web server to predict subcellular localization of proteins. *Nucleic Acids Res.* **2018**, *46*, W459-W466.
28. Yu, K.; Mu, C.; Yang, Y.; Su, Y.; Zhu, W. Segment-specific responses of intestinal epithelium transcriptome to in-feed antibiotics in pigs. *Physiol. Genomics* **2017**, *49*, 582-591.
29. Stolaki, M.; Minekus, M.; Venema, K.; Lahti, L.; Smid, E.J.; Kleerebezem, M.; Zoetendal, E.G. Microbial communities in a dynamic *in vitro* model for the human ileum resemble the human ileal microbiota. *FEMS Microbiol. Ecol.* **2019**, *95*.
30. Palframan, R.J.; Gibson, G.R.; Rastall, R.A. Carbohydrate preferences of *Bifidobacterium* species isolated from the human gut. *Curr. Issues Intest. Microbiol.* **2003**, *4*, 71-75.
31. Paineau, D.; Respondek, F.; Menet, V.; Sauvage, R.; Bornet, F.; Wagner, A. Effects of short-chain fructooligosaccharides on faecal bifidobacteria and specific immune response in formula-fed term infants: a randomized, double-blind, placebo-controlled trial. *J. Nutr. Sci. Vitaminol. (Tokyo)* **2014**, *60*, 167-175.
32. Scott, K.P.; Martin, J.C.; Chassard, C.; Clerget, M.; Potrykus, J.; Campbell, G.; Mayer, C.-D.; Young, P.; Rucklidge, G.; Ramsay, A.G.; Flint, H.J. Substrate-driven gene expression in *Roseburia inulinivorans*: Importance of inducible enzymes in the utilization of inulin and starch. *Proc. Natl. Acad. Sci.* **2011**, *108*, 4672-4679.
33. Milani, C.; Duranti, S.; Bottacini, F.; Casey, E.; Turroni, F.; Mahony, J.; Belzer, C.; Delgado Palacio, S.; Arboleya Montes, S.; Mancabelli, L.; Lugli, G.A.; Rodriguez, J.M.; Bode, L.; de Vos, W.; Gueimonde, M.; Margolles, A.; van Sinderen, D.; Ventura, M. The first microbial colonizers of the human gut: Composition, activities, and health implications of the infant gut microbiota. *Microbiol. Mol. Biol. Rev.* **2017**, *81*, e00036-00017.
34. McLaughlin, H.P.; Motherway, M.O.C.; Lakshminarayanan, B.; Stanton, C.; Paul Ross, R.; Brulc, J.; Menon, R.; O'Toole, P.W.; van Sinderen, D. Carbohydrate catabolic diversity of bifidobacteria and lactobacilli of human origin. *Int. J. Food Microbiol.* **2015**, *203*, 109-121.
35. Falony, G.; Lazidou, K.; Verschaeren, A.; Weckx, S.; Maes, D.; De Vuyst, L. *In vitro* kinetic analysis of fermentation of prebiotic inulin-type fructans by *Bifidobacterium* species reveals four different phenotypes. *Appl. Environ. Microbiol.* **2009**, *75*, 454-461.
36. Rossi, M.; Corradini, C.; Amaretti, A.; Nicolini, M.; Pompei, A.; Zanoni, S.; Matteuzzi, D. Fermentation of fructooligosaccharides and inulin by bifidobacteria: a comparative study of pure and fecal cultures. *Appl. Environ. Microbiol.* **2005**, *71*, 6150-6158.
37. Boger, M.C.L.; Lammerts van Bueren, A.; Dijkhuizen, L. Cross-Feeding among probiotic bacterial strains on prebiotic inulin involves the extracellular exo-inulinase of *Lactobacillus paracasei* Strain W20. *Appl. Environ. Microbiol.* **2018**, *84*, e01539-01518.
38. Rivière, A.; Selak, M.; Lantin, D.; Leroy, F.; De Vuyst, L. Bifidobacteria and butyrate-producing colon bacteria: Importance and strategies for their stimulation in the human gut. *Front. Microbiol.* **2016**, *7*, 979.
39. Rada, V.; Nevoral, J.; Trojanová, I.; Tománková, E.; Šmehilová, M.; Killer, J. Growth of infant faecal bifidobacteria and clostridia on prebiotic oligosaccharides in *in vitro* conditions. *Anaerobe* **2008**, *14*, 205-208.
40. Richardson, A.J.; McKain, N.; Wallace, R.J. Ammonia production by human faecal bacteria, and the enumeration, isolation and characterization of bacteria capable of growth on peptides and amino acids. *BMC Microbiol.* **2013**, *13*, 6-6.
41. Yiu, J.H.; Dorweiler, B.; Woo, C.W. Interaction between gut microbiota and toll-like receptor: from immunity to metabolism. *J Mol Med (Berl)* **2017**, *95*, 13-20.
42. Nastasi, C.; Candela, M.; Bonefeld, C.M.; Geisler, C.; Hansen, M.; Krejsgaard, T.; Biagi, E.; Andersen, M.H.; Brigidi, P.; Ødum, N.; Litman, T.; Woetmann, A. The effect of short-chain fatty acids on human monocyte-derived dendritic cells. *Sci. Rep.* **2015**, *5*, 16148.
43. Corrêa-Oliveira, R.; Fachi, J.L.; Vieira, A.; Sato, F.T.; Vinolo, M.A.R. Regulation of immune cell function by short-chain fatty acids. *Clin. Transl. Immunol.* **2016**, *5*, e73-e73.
44. Millard, A.L.; Mertes, P.M.; Ittelet, D.; Villard, F.; Jeannesson, P.; Bernard, J. Butyrate affects differentiation, maturation and function of human monocyte-derived dendritic cells and macrophages. *Clin. Exp. Immunol.* **2002**, *130*, 245-255.
45. Berndt, B.E.; Zhang, M.; Owyang, S.Y.; Cole, T.S.; Wang, T.W.; Luther, J.; Veniaminova, N.A.; Merchant, J.L.; Chen, C.-C.; Huffnagle, G.B.; Kao, J.Y. Butyrate increases IL-23 production by stimulated dendritic cells. *Am. J. Physiol. Gastrointest. Liver Physiol.* **2012**, *303*, G1384-G1392.

Supporting information

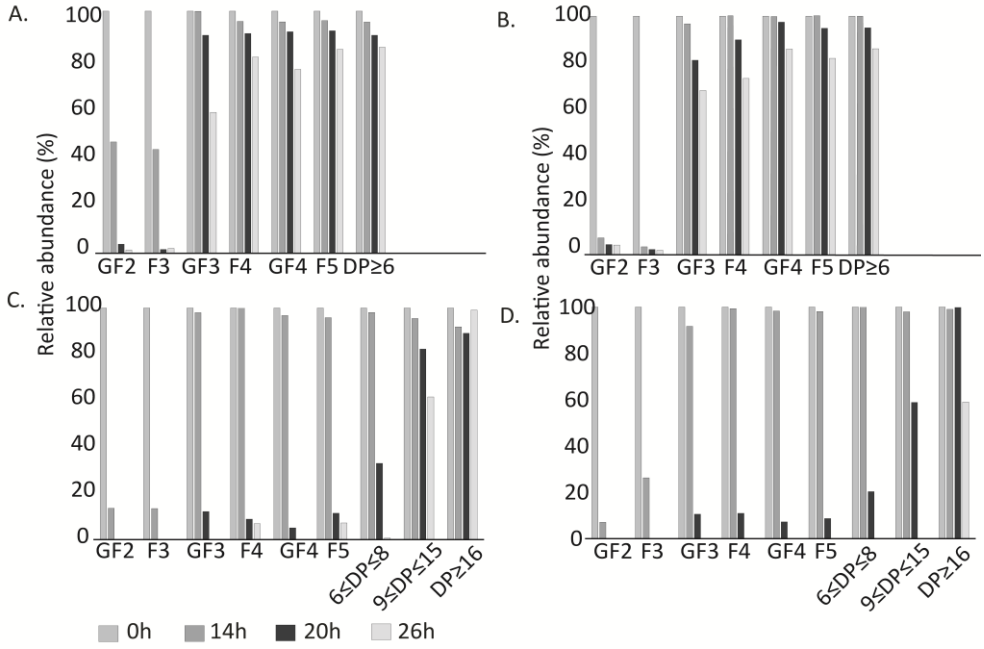

Figure S1 Percentages of remaining compounds with different DP present in FOS (A, B) and native inulin (C, D) during *in vitro* fermentation using pooled faecal inoculum of 2- (A, C) and 8- (B, D) week-old infants. Analysis was performed by HPAEC-PAD. Concentrations per compound/DP range in the original FOS and native inulin mixture were set to 100%.

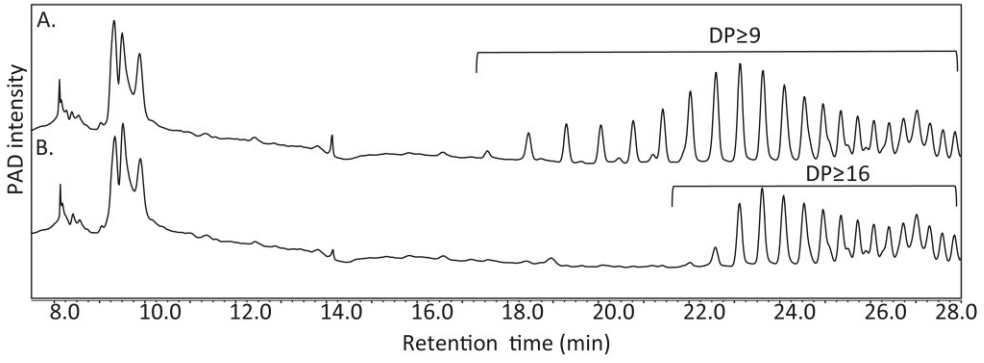

Figure S2 HPAEC profiles of native inulin after 36 hours of *in vitro* fermentation using pooled faecal inoculum of 2- (A) and 8- (B) week-old infants.

Table S1 Relative abundance of bacteria at the highest classified taxonomy in duplicate fermentation digesta (a,b) collected at the start and after 14 and 26 h from i*n vitro* fermentation of FOS and native inulin using pooled faecal inoculum of 2- and 8-week-old infants with the 15 most abundant bacteria individually and less abundant bacteria summarized as ' other' with control: control fermentation without added substrate.

taxonomic classification	FOS												native inulin												control					
	2 weeks						8 weeks						2 weeks						8 weeks						2 weeks			8 weeks		
	0^a	0^b	14^a	14^b	26^a	26^b	0^a	0^b	14^a	14^b	26^a	26^b	0^a	0^b	14^a	14^b	26^a	26^b	0^a	0^b	14^a	14^b	26^a	26^b	0	14	26	0	14	26
Bifidobacterium	79.9	86.0	27.7	18.1	43.2	48.9	92.3	87.8	54.6	42.3	58.9	53.4	85.3	82.3	16.1	18.0	17.9	17.8	90.7	78.1	24.1	19.4	60.4	74.0	40.5	4.2	2.6	86.2	10.4	4.7
Lactobacillus	5.5	4.5	0.0	0.0	0.0	0.0	2.4	3.3	0.0	0.0	0.0	0.0	3.5	3.0	0.0	0.0	0.0	0.0	3.1	2.5	0.0	0.0	0.0	0.0	3.6	0.0	0.0	2.8	0.0	0.0
Escherichia-Shigella	3.6	2.6	39.5	51.9	28.3	19.6	1.6	3.4	32.0	42.7	27.6	31.9	3.4	4.6	51.7	50.5	17.1	17.0	1.7	1.4	51.9	56.1	25.6	15.3	14.0	45.8	39.4	3.2	62.2	61.7
Streptococcus	2.8	1.8	0.0	0.0	0.0	0.0	2.1	2.2	0.0	0.0	0.0	0.0	1.6	1.6	0.0	0.0	0.0	0.0	2.3	8.5	0.0	0.0	0.0	0.0	2.4	0.0	0.0	2.3	0.0	0.0
Staphylococcus	2.1	1.4	0.0	0.0	0.0	0.0	0.0	0.0	0.0	0.0	0.0	0.0	1.3	1.8	0.0	0.0	0.0	0.0	0.0	0.0	0.0	0.0	0.0	0.0	1.5	0.0	0.0	0.0	0.0	0.0
Enterobacteriaceae	1.4	1.0	12.3	16.3	9.1	6.1	0.0	0.3	4.0	7.0	3.0	3.2	1.3	1.8	15.1	15.3	5.3	5.5	0.1	1.8	9.2	11.3	6.2	3.7	7.6	17.9	13.8	0.4	0.8	1.6
Veillonella	1.3	0.6	0.0	0.0	0.0	0.0	0.0	0.0	0.0	0.0	0.0	0.0	0.6	0.7	0.0	0.0	0.0	0.0	0.0	0.0	0.0	0.0	0.0	0.0	0.0	0.0	0.0	0.0	0.0	0.0
Lactococcus	1.0	0.5	0.0	0.0	0.0	0.0	0.0	0.5	0.0	0.0	0.0	0.0	0.4	0.5	0.0	0.0	0.0	0.0	0.3	0.0	0.0	0.0	0.0	0.0	1.0	0.0	0.0	0.4	0.0	0.0
Ralstonia	0.6	0.3	0.0	0.0	0.0	0.0	0.2	0.5	0.0	0.0	0.0	0.0	0.5	0.5	0.0	0.0	0.0	0.0	0.2	0.0	0.0	0.0	0.0	0.0	0.8	0.0	0.0	0.7	0.0	0.0
Enterococcus	0.3	0.3	13.1	10.2	6.5	8.9	0.3	0.5	7.6	4.7	8.8	9.8	0.2	0.4	10.8	12.0	4.1	4.7	0.3	0.2	12.9	11.2	4.4	6.0	2.7	27.2	25.9	2.2	25.8	29.7
Fusobacterium	0.3	0.0	0.0	0.0	0.0	0.0	0.0	0.0	0.0	0.0	0.0	0.0	0.0	0.0	0.0	0.0	0.0	0.0	0.0	0.0	0.0	0.0	0.0	0.0	0.0	0.0	0.0	0.0	0.0	0.0
Hathewaya	0.3	0.1	0.0	0.0	0.0	0.0	0.0	0.2	0.0	0.0	0.0	0.0	0.2	0.2	0.0	0.0	0.0	0.0	0.0	0.0	0.0	0.0	0.0	0.0	0.0	0.0	0.0	0.0	0.0	0.0
Cloacibacillus	0.3	0.0	0.0	0.0	0.0	0.0	0.0	0.0	0.0	0.0	0.0	0.0	0.0	0.0	0.0	0.0	0.0	0.0	0.0	0.0	0.0	0.0	0.0	0.0	0.0	0.0	0.0	0.0	0.0	0.0
Bacteroides	0.3	0.1	0.0	0.0	0.0	0.0	0.3	1.3	0.0	0.0	0.0	0.0	0.1	0.2	0.0	0.0	0.0	0.0	0.4	0.2	0.0	0.0	0.0	0.0	0.0	0.0	0.0	0.0	0.0	0.0
Clostridium sensu stricto 1	0.2	0.2	5.9	1.7	10.8	16.2	0.3	0.0	0.0	0.0	0.0	0.0	0.2	0.6	3.9	2.6	55.6	55.1	0.0	0.0	0.0	0.0	0.0	0.0	2.3	3.1	16.6	0.4	0.0	0.0
other	0.2	0.3	1.6	1.9	2.1	0.4	0.5	0.1	1.9	3.4	1.6	1.8	1.3	2.0	2.3	1.5	0.0	0.0	0.9	7.3	1.9	2.1	3.4	0.8	23.6	1.8	1.7	1.4	0.8	2.2

Table S2 Amount of DNA copies (log) in fermentation digesta collected at the start and after 14 and 26 hours from *in vitro* fermentation of FOS (A) and native inulin (B) using faecal inoculum of 2- and 8-week-old infants with a, b: biological replicate, *: control fermentation without inoculum. Control fermentations without added NDCs are displayed in C.

A. age	timepoint	DNA copies (log/ml fermentation digesta)
2	0	6.38[a]
2	0	6.64[b]
2	14	9.64[a]
2	14	9.75[b]
2	26	9.74[a]
2	26	9.93[b]
8	0	6.60[a]
8	0	6.66[b]
8	14	9.84[a]
8	14	9.93[b]
8	26	9.74[a]
8	26	9.68[b]
*	0	6.33
*	14	6.03
*	26	8.67

B. age	timepoint	DNA copies (log/ml fermentation digesta)
2	0	6.55[a]
2	0	6.62[b]
2	14	10.00[a]
2	14	9.89[b]
2	26	10.25[a]
2	26	10.16[b]
8	0	6.56[a]
8	0	7.02[b]
8	14	9.85[a]
8	14	9.84[b]
8	26	10.00[a]
8	26	9.91[b]
*	0	6.63
*	14	9.73
*	26	9.86

C. age	timepoint	DNA copies (log/ml fermentation digesta)
2	0	6.66
2	14	10.00
2	26	9.90
8	0	6.58
8	14	9.73
8	26	9.96

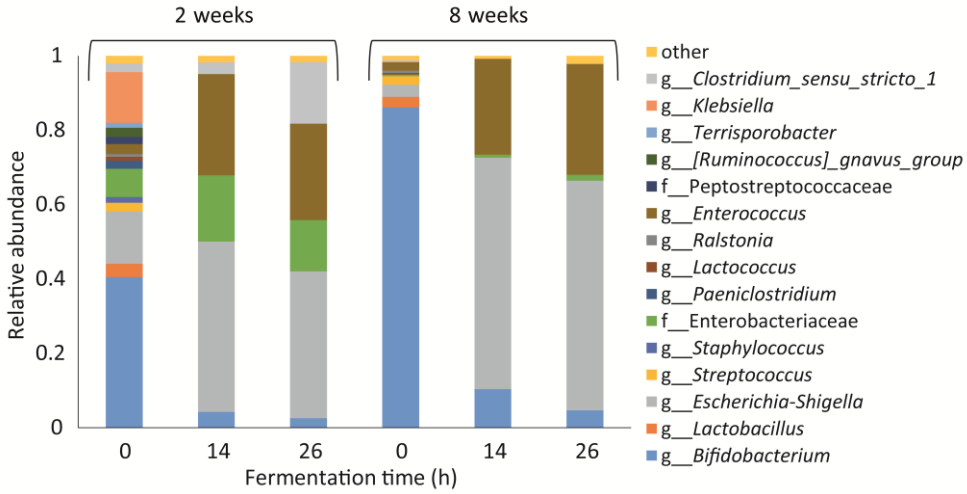

Figure S3 Relative abundance of bacteria at the highest classified taxonomy in fermentation digesta collected at the start and after 14 and 26 hours from *in vitro* fermentation containing solely SIEM medium and faecal inoculum of 2- and 8- week-old infants.

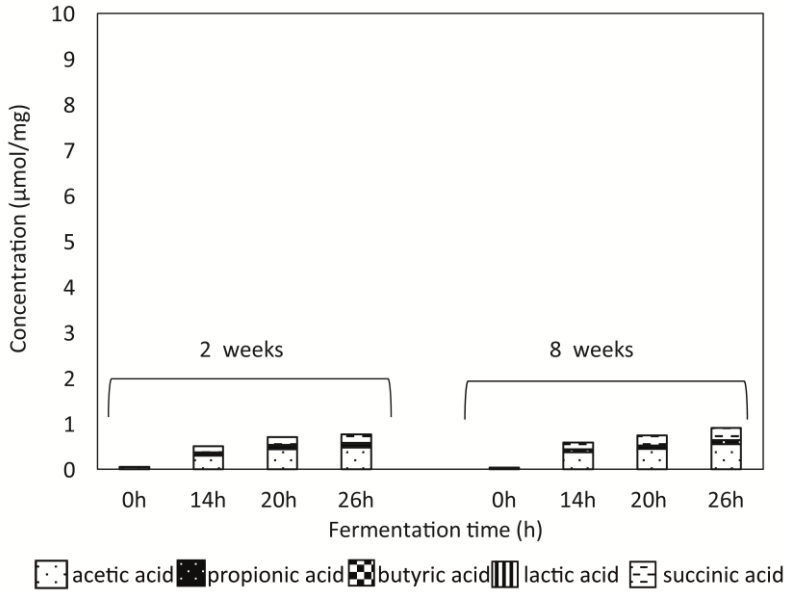

Figure S4 Production of SCFAs, lactic acid and succinic acid upon *in vitro* fermentation containing solely infant faecal inoculum and SIEM medium.

Chapter 4

Endo-1,3(4)-β-glucanase-treatment of oat β-glucan enhances fermentability by infant faecal microbiota, stimulates Dectin-1 activation and attenuates inflammatory responses in immature dendritic cells

Abstract

Non-digestible carbohydrates are added to infant formula to mimic human milk oligosaccharide effects by acting as prebiotics and stimulating the immune system. Although not yet used in infant formulas, β-glucans are known to have beneficial health effects and are therefore of potential interest for supplementation of infant formula.

We investigated the *in vitro* fermentation of native and endo-1,3(4)-β-glucanase-treated oat β-glucan using pooled faecal inocula of 2- and 8-week-old infants. While native oat β-glucan was not utilized, both inocula specifically utilized oat β-glucan oligomers containing β(1→4)-linkages formed upon enzyme treatment. The fermentation rate was highest for faecal microbiota of 2-week-old infants and correlated with a high lactate production. Fermentation of media supplemented with native and enzyme-treated oat β-glucans increased the relative abundance of *Enterococcus* and attenuated pro-inflammatory cytokine production (IL-1β, IL-6, TNFα) in immature dendritic cells. This attenuating effect was more pronounced after enzyme treatment. This attenuation might result from the enhanced capability of fermented oat β-glucan to stimulate Dectin-1 receptors.

Our findings demonstrate that endo-1,3(4)-β-glucanase treatment enhances the fermentability of oat β-glucan and attenuated pro-inflammatory responses. Hence, this study shows that especially enzyme-treated oat β-glucans have a high potential for supplementation of infant formula.

Akkerman. R.*; Logtenberg, M.J.*; An, R.; Van den Berg, M.A.; de Haan, B.J.; Faas, M.M.; Zoetendal, E.G.; de Vos, P.; Schols, H.A. *Nutrients*; **2020**; 12: 1660.

* authors contributed equally

Introduction

Early life nutrition is crucial for life-long health and is strongly influencing the development of the innate immune system and the composition of the intestinal microbiota [1,2]. The World Health Organization recommends exclusive breastfeeding for infants up to an age of 6 months [3]. An important component of mother milk are the human milk oligosaccharides (HMOs) which are considered as prebiotics and guide immune development and gut barrier maturation [4,5]. However, for many valid reasons, in Europe only approximately 25% of the infants receive exclusive breastfeeding up to an age of 6 months [6]. For infants for which breast milk is not an option, different types of infant formula are commercially available, which are often supplemented with non-digestible carbohydrates (NDCs) to mimic the effects of HMOs. Commonly used NDCs in infant formula include fructo-oligosaccharides (FOS) and galacto-oligosaccharides (GOS), which are added either individually or as combination [7,8]. The beneficial effects of FOS and GOS have been studied extensively [7-9]. However, there are many other NDCs with beneficial effects on microbiota compositions and the immune system that are of potential interest as supplement to infant formulas. An example of such NDC with demonstrated beneficial effects is β–glucan [10].

β–glucans are polymers of D-glucose building blocks linked by β(1→3), β(1→6) or β(1→4) linkages [11] and can be found in many food and feed components including cereals, yeast and mushrooms [12]. β-glucans from cereals, like oat and barley, are linear β(1→3) and β(1→4) linked glucose polysaccharides, whereas β–glucans from yeast and fungi consist of a β(1→3) linked glucan backbone with β(1→6) linked glucose residues as sidechains [11]. In recent years, multiple studies have shown immune modulating functions of β–glucans which are exerted via binding to different pattern recognition receptors (PRRs) including C-type lectin Dectin-1, complement receptor 3 and Toll-like receptors (TLRs) [13-15]. For oat β-glucans it has also been shown that microbiota derived enzymes may enhance their immune activity upon digestion, by increasing Dectin-1 stimulation. This was demonstrated by the ability of oat β-glucans to stimulate Dectin-1 receptors, which increased after enzyme treatment with endoglucanase [16].

Next to their direct effects, β–glucans might also influence immunity by changing the composition of the gut microbiota and the formation of short chain fatty acids (SCFAs) [17]. Previous studies demonstrated that the fermentability of β-glucans is dependent on their structure. Enzymatic pre-treatment of barley β-glucans enhanced their fermentability by adult faecal microbiota in an *in vitro* set-up [17]. Depolymerization of barley β-glucans by acid hydrolysis into fractions with MWs ranging from 6-104 kDa has also shown to increase glucan fermentability with inoculum of 9-15 month-old infants [18]. However, currently limited knowledge is available about the effects of fermentation of β-glucans on their immune-modulating properties and if an increase in fermentability, due to depolymerization, affects these processes.

In the present study, native oat β-glucan was treated with an enzyme preparation containing predominantly endo-1,3(4)-β-glucanase to decrease the molecular weight. Both native and enzyme-treated oat β-glucan were fermented in an *in vitro* set-up using infant faecal inoculum of 2- and 8-week old infants. We decided to use faecal inoculum of 2- and 8-week-old infants because microbiota compositions are rapidly developing in the first weeks of life [19] and different sets of enzymes for the degradation of NDCs will become available depending on the bacteria present in the infant gut. Therefore, it is likely that both age classes will have different fermentation capabilities. The glucan degradation kinetics, impact on microbiota composition and SCFA production during fermentation were studied. In addition, the effects of the fermentation digesta on Dectin-1 receptor binding and immature dendritic cells cytokine production were studied.

Materials and methods

Oat β-glucans and enzymatic modification

All Native oat β-glucan (OBG) and enzyme-treated oat β-glucan (eOBG) were kindly provided by DSM (Delft, The Netherlands). Native oat β-glucan (medium viscosity, Megazyme, Bray, Ireland) was treated with the commercial enzyme preparation Filtrase NL liquid (DSM batch 614308301), predominantly containing endo-1,3(4)-β-glucanase, to obtain enzyme-treated oat β-glucan. First native oat β-glucan (5 mg/mL) was dissolved in 10 mM sodium acetate buffer (pH 5.0), after which Filtrase NL liquid was added at 250 µl enzyme/g native oat β-glucan. The mixture was incubated at 37 °C for 5 h in a head-over-tail rotator. Subsequently, enzymes were inactivated by boiling the mixture for 10 min. The final solution was lyophilized for further use. OBG was treated similarly, but without addition of Filtrase NL liquid.

Fermentation of native and enzymatic treated oat β-glucans by infant faecal inoculum

Culture medium

Standard ileal efflux medium (SIEM; Tritium Microbiology, Veldhoven, The Netherlands) was prepared as described elsewhere with minor modifications [20]. A low amount of carbohydrates was added to mimic the infant ileal environment while minimizing background fermentation. The carbohydrate medium component contained the following carbohydrates in the same ratio: pectin, xylan, arabinogalactan, amylopectin and starch, with a concentration of only 0.24 g/L in the SIEM medium. The pH was adjusted to 5.8 using MES buffer.

Infant faecal inoculum

Faecal samples were collected from 4 exclusively breast-fed and vaginally born infants. The infants did not receive antibiotic treatment and did not have health issues. At the age of 2 and 8 weeks faecal material was collected from the diaper directly after defecation,

transferred to tubes and stored at -20 °C. After the second collection time point, all samples were stored at -80 °C.

The inoculum was prepared as reported elsewhere with some minor modifications [21]. After thawing, faecal material of 4 infants were combined (4x 0.1 gram) and diluted in 24 ml sterilized NaCl solution (0.9% (w/v)) in an anaerobic chamber (gas phase: 81% N2, 15% CO2 and 4% H2) (Bactron 300, Sheldon Manufacturing, Cornelius, USA). Homogenization was performed by the addition of sterile glass beads prior to thorough mixing (2000 rpm). After removal of the glass beads, the faecal solution was combined with SIEM medium in a ratio of 5:82 (v/v) and used as pooled faecal inoculum, whose bacterial functionality was found to be largely representative of the faecal inocula of the infant population in general [22].

In vitro fermentation

Fermentations were performed in duplicate in the anaerobic chamber. Pooled faecal inoculum was combined with SIEM medium containing native or enzyme-treated oat β-glucan (10 mg/ml) in sterile fermentation flasks in a ratio of 1:10 (v/v). Fermentation flasks were closed with a rubber stopper that is secured with a metal lid to ensure anoxic conditions. Afterwards flasks were put in an incubator shaker (Innova 40) (37 °C, 100 rpm). At the start and after 14, 20 and 26 h, digesta were collected in triplicate with a syringe. One sample was immediately frozen in liquid nitrogen and stored at -80 °C to preserve the bacteria for later microbial analysis. Both other samples were heated for 5 min in a water bath (100 °C) to inactivate enzymes present. Subsequently they were stored at -20 °C until further analysis.

The following control fermentations were included: (1) inoculum without glucan substrate to monitor background fermentation, (2) native oat β-glucan and enzyme-treated oat β-glucan without inoculum to monitor contamination.

Fate of OBG and eOBG upon fermentation

High performance size exclusion chromatography (HPSEC)

Degradation of OBG during fermentation was analysed by HPSEC on an Ultimate 3000 HPLC system (Dionex, Sunnyvale, CA, USA) equipped with a Shodex RI-101 refractive index detector (Showa Denko, Tokyo, Japan). Fermentation samples were diluted until a concentration of 2 mg/ml and centrifuged (5 min, 15 000g). Ten µl of sample was injected to three TSK-Gel columns connected in series (4000-3000-2500 SuperAW; 150 x 6 mm) preceded by a TSK Super AW-L guard column (35 x 4.6 mm) (Tosoh Bioscience, Tokyo, Japan). The columns covered a molecular mass range from 0-250 kDa. Samples were eluted with 0.2 M NaNO3, at 55°C with a flow rate of 0.6 ml/min. Pullulan standards (Polymer Laboratories, Palo Alto, Ca, USA) were used for calibration.

UHPLC-PGC-MS

To be able to study the fate of specific isomers with different degrees of polymerization (DP), enzyme-treated oat β-glucan was also analysed on a Vanquish Ultra High Performance Liquid Chromatography (UHPLC) system (Thermo Scientific, San Jose, CA, USA). Prior to analysis samples were reduced using sodium borohydride to avoid anomerisation of oligosaccharides, followed by a purification step using solid phase extraction [23].

Samples (0.5 µl, 0.5 mg/ml) were injected on a porous graphitic carbon (PGC) column (3 µm particle size, 2.1 mm x 150 mm; Hypercarb, Thermo Scientific) in combination with a guard column (3 µm particle size, 2 mm x 10 mm; Hypercarb, Thermo Scientific). As mobile phase A: ULC-MS water + 0.1% (v/v) formic acid was used. Mobile phase B consisted of ACN + 0.1% (v/v) formic acid. The flow rate was 300 µL/min. The gradient was as follows: 0-2 min, 3% B; 2-21 min, 3-33.6% B; 21-22.5 min, 33.6-100% B; 22.5-30.2 min, 100% B; 30.2-31.7 min, 100-3% B; 31.7-39.4 min, 3% B. The temperature of the autosampler and column oven was controlled at 10 and 25 °C, respectively. Needle wash solvent containing 3% ACN was used to wash the autosampler.

To obtain mass spectrometric (MS) data, the flow of the UHPLC was directed to a Thermo Scientific LTQ-Velos Pro equipped with an electrospray ionization (ESI) probe. Helium and nitrogen were used as sheath and auxiliary gas, respectively. The MS settings were set to a source voltage of 3.5 kV, a source heater temperature of 225°C, a capillary temperature of 350˚C, a sheath gas flow of 38 and an auxiliary gas flow of 11. MS data in negative mode were collected over a m/z range of 300-2000. Data dependent MS2 analysis was performed with a normalized collision energy of 35%, activation Q of 0.25, activation time of 10 ms and isolation width of *m/z* 1.5. MS2 fragmentation was performed on the 1st and 2nd most abundant ion in the MS chromatogram from a parent list containing m/z of reduced enzyme-treated oat β-glucan oligomers. MS3 fragmentation was performed on the product ions with m/z 505 (trimer) and 667 (tetramer). Cellobiose (Sigma-Aldrich, St. Louis, MO, USA), cellotriose (Megazyme, Bray, Ireland) and 1,3:1,4-β-glucotriose (Megazyme) were used as standards for the identification of oat β-glucan oligomers. Relative abundance of oligomers was determined by selection of the specific mass range followed by integration of the peaks. Data acquisition and processing were performed using Xcalibur (version 2.2, Thermo Scientific).

Production of SCFAs and other organic acids upon fermentation

In order to quantify the production of SCFAs and organic acids, fermentation samples were subjected to GC and HPLC analysis as described elsewhere [24], with minor modifications with respect to the GC analysis. For GC, fermentation samples (1 mg/ml) were mixed in a 2:1 ratio with a solution containing HCl (0.3M), oxalic acid (0.09M) and internal standard 2-ethyl butyric acid (0.45 mg/ml). The mixture was allowed to stand at room temperature for 30 min. The temperature profile during GC analysis was as follows: 100°C, maintained for 0.5 min; raised to 180°C at 8°C/min, maintained for 1 min; raised to 200°C at 20°C/min,

maintained for 5 min. Glass wool was inserted in the glass liner of the split injection port to protect the column from contamination [25].

Microbial composition analysis

DNA extraction was performed using the Repeated Bead Beating [26] followed by purification using the Maxwell 16 Tissue LEV Total RNA Purification Kit Cartridge (XAS1220) (Promega, Madison, WI, USA). PCR amplification of the V5-V6 region of 16S ribosomal RNA (rRNA) genes using the unique barcoded primer pair BSF784 (RGGATTAGATACCC) and R1064 (CGACRRCCATGCANACCT) was performed in triplicates as described elsewhere [27] with minor modification. Specifically, for t0 samples which contained 1.4-4.6 ng/µl DNA, 10 µl DNA template was used for the amplification, correspondingly decreasing the amount of nuclease free water to retain the same reaction volume. For samples with higher DNA concentrations, 0.7 µl of DNA template was used. Two synthetic microbial communities were included as positive controls [28].

After the amplification, PCR products were purified using HighPrep PCR kit (MagBio Genomics, Alphen aan den Rijn, The Netherlands). Purified amplicons were quantified using Qubit dsDNA BR assay kit (Life Technologies, Leusden, The Netherlands). Seventy unique barcode tags were used in each library [28]. Two amplicon pools were formed by combining 200 ng of each barcoded sample and afterwards concentrated to 50 µl using the HighPrep PCR kit. Libraries were sent for adapter ligation and sequencing with Illumina Hiseq2500 (GATC-Biotech, Konstanz, Germany).

Processing and analysis of the 16S rRNA gene amplicon sequencing data was carried out using the NG-Tax 2.0 pipeline, with default settings and R version 3.5.0 [29]. Amplicon sequencing variants (ASVs) with a relative abundance below 0.1% were removed. The threshold for taxonomic assignment was set at 80%.

Enterococci were analysed at the level of individual sequences (Amplicon Sequencing Variants (ASVs)). SILVA database release 132 [30] was used for taxonomic classification.

Stimulation of DCs with oat β-glucan fermentation samples

Cell culture and stimulation

Dendritic cells (DCs) generated from umbilical cord blood CD34+ progenitor cells were purchased from MatTek Corporation (Ashland, MA, USA). Cells were thawed and seeded at a density of 70x104 cells/well into 96-well plates and cultured (for 24 h 37^{o}C, 21% O2 and 5% CO2) according to manufacturer's instructions. After 24 h of culturing, cells were stimulated with fermentation products of the *in vitro* batch fermentation of medium supplemented with native oat β-glucan and enzyme-treated oat β-glucan using infant faecal inoculum. To this end, bacteria were removed from the fermentation samples by centrifugation (10 min, 12000g). Subsequently supernatants were filtered through a 0.2 µm filter and diluted in DC-MM culture medium (MatTek Corporation,) containing Polymyxin-B (50ng/ml) (Invivogen, Toulouse, France) at a ratio of 1:10. The pH was set to 7.4 by the

addition of 2M NaOH. DCs were then incubated with 200 µl/well medium containing the fermentation samples for 48 h After incubation supernatants were collected and stored at -20^{o}C until further analysis. All experiments were repeated 6 times.

Assessment of cytokine expression

The levels of MCP-1/CCL2, MIP-1α/CCL3, IL-1β, IL-6, IL-10 and TNFα in the DC supernatant were quantified using a magnetic Luminex® Assay (R&D systems, Biotechne, Minneapolis, USA) according to the manufacturers protocol. The plate was analysed using a Luminex 200 System. The data obtained was analysed using the Luminex xPONENT software.

HEK-Dectin1 reporter cell assays

HEK-Blue™ Null1 cells (Invivogen) were stably transfected with pUNO1- hDectin1a or pUNO1-hDectin1b plasmids (InvivoGen) to obtain HEK-Dectin1a and HEK-Dectin1b responsive reporter cells as previously described [31]. HEK-Dectin1 cell lines were cultured and maintained in DMEM culture medium (Lonza, Bornem, Belgium) containing 10% de-activated foetal calf serum (60^{o}C for 30 min), 50 U/ml Penicillin and 50µg/ml Streptomycin (Sigma-Aldrich), 100µg/ml Normocin (Invivogen) supplemented with 12µg/ml Blasticidin (for HEK-Dectin1a) and 100µg/ml zeocin (for HEK-Dectin1b) (Invivogen). Both cell lines express soluble embryonic alkaline phosphatase (SEAP) under control of a NF-κB AP-1 responsive promotor. Stimulation of the Dectin1a or Dectin1b receptor by a Dectin-1 agonist will activate the receptor, subsequently the NF-κB transcription factor will be transported to the nucleus, inducing transcription of the reporter gene, resulting in SEAP release into the medium. SEAP can be quantified using Quanti-Blue™ (Invivogen).

HEK-Dectin1a and HEK-Dectin1b cells were seeded into 96-well plates at a density of 10x104 cells/well in 200µl medium. After 24h cells were attached and medium was replaced by fresh medium containing the samples. Fermentation samples of medium supplemented with native oat β-glucan and enzyme-treated oat β-glucan were diluted at a ratio of 1:20 in culture medium and pH was neutralized by the addition of 2M NaOH. As a positive control, 200 µg/ml Zymosan depleted (Invivogen), a particulate β(1→3) glucan with a mean molecular weight of 240 kDa obtained from *Saccharomyces cerevisiae* was used. Medium was used as a negative control. All samples were incubated for 24h. Subsequently, the supernatant of activated reporter cells was mixed with Quanti-Blue™ at a ratio of 1:10 and quantified at 650nm using a Benchmark Plus Microplate Reader using Microplate Manager 5.2.1 version for data acquisition. Experiments were repeated 3 times in triplicate.

Statistical analysis

Data were analysed using Prism 8 software (GraphPad, San Diego, CA, USA). For the cytokine data, outliers were removed after testing using a Grubbs outlier test (alpha = 0.05). Cytokine data are shown as average with standard error of the mean (SEM). Data was distributed normally and analysed using a mixed-effects model (REML) to test for differences between the different samples, followed by a Tukey's multiple comparisons test to compare cytokine

responses between different groups. P-values < 0.05 were considered significant. Data from HEK-Dectin1 stimulation experiments were tested using a OneWay ANOVA test followed by a Tukey's multiple comparison test. P-values < 0.05 were considered significant.

Results

Formation of oligomers upon endo-1,3(4)-β-glucanase treatment of native oat β-glucan

To determine if a decrease in molecular weight would impact the fermentability and immune modulating capacity, native oat β-glucan (300 kDa) was treated with a commercial enzyme preparation which predominantly contains endo-1,3(4)-β-glucanase. The enzyme treatment of native oat β-glucan was monitored with UHPLC-PGC-MS and resulted in the formation of oligomers with a DP ranging from 2-5 (Table S1). The different oligomers were characterized based on MS2 and MS3 fragmentation and available references. Cellobiose (2a), cellotriose (3a), cellobiosyl-(1→3)-β-D-cellobiose (3b), glycosyl-(1→3)-β-D-cellotriose (4a) and a partially characterized DP5 oligomer (5a) were recognized to be present (Table S1), with glucosyl-(1→3)-β-D-cellotriose being most abundant (58%).

Size- and linkage-specific fermentation of oat β-glucan (oligomers) by infant faecal microbiota

Since the microbiota composition and functionality depend on the age of the infant [32], the degradation of native and enzyme-treated oat β-glucan was studied by using faecal microbiota of 2- and 8-week-old infants. Fermentation digesta were collected at 0, 14 and 26 h of *in vitro* batch fermentation followed by HPSEC and UHPLC-PGC-MS analysis to monitor the fermentability of respectively native and enzyme-treated oat β-glucan.

Faecal microbiota of both 2-and 8-week-old infants were unable to degrade native oat β-glucan as no significant shifts in molecular weight of native oat β-glucan were observed over 26 h of fermentation (Figure 1).

The treatment of native oat β-glucan with endo-1,3(4)-β-glucanase increased the fermentability to a large extent (Figure 2A, Figure S1). Faecal microbiota of 2-week-old infants were able to almost completely ferment oligomer 2a and 3a, while oligomer 3b and 4a with a β(1→3)-linked glucose at the non-reducing end remained virtually intact. The partially characterized DP5 oligomer (5a) was degraded for 50% after 26 h of fermentation. The increase of oligomer 3b and 4a during fermentation is assumed to be caused by the partial degradation of oligomer 5a. Since the most abundant oligomer 4a was highly resistant to fermentation, still 61% of the total mixture was remaining after 26 h of fermentation.

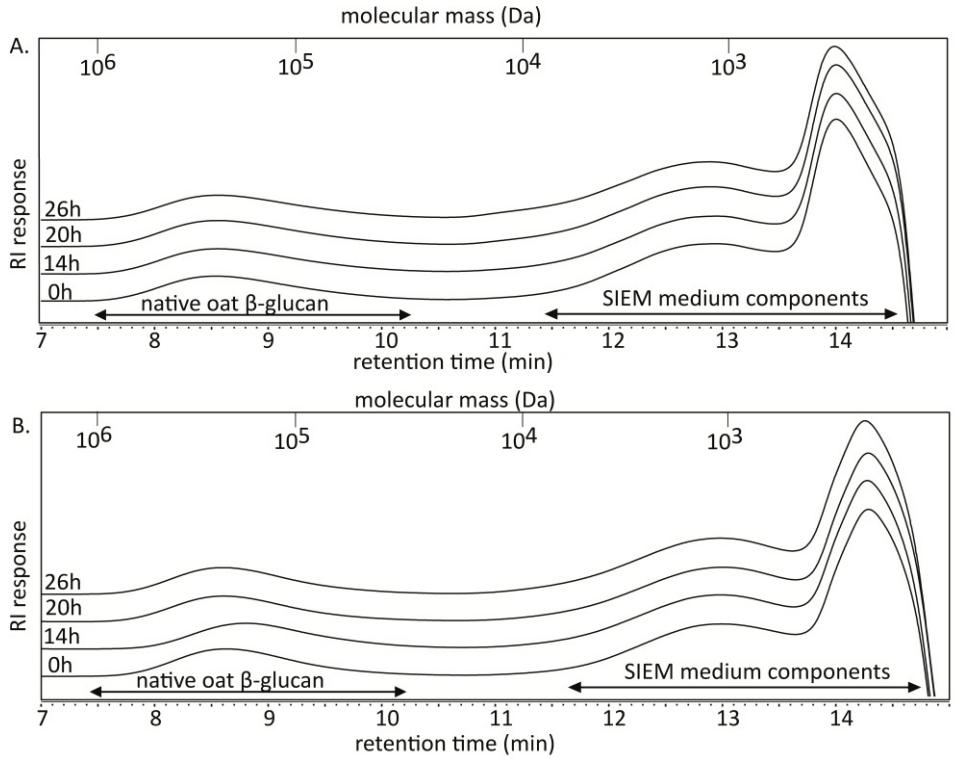

Figure 1 HPSEC profiles of native oat β-glucan at the start and after 14, 20 and 26 h of fermentation using pooled faecal inoculum of 2- (A) and 8- (B) week-old infants. Calibration of the system using pullulan standards is indicated.

Faecal microbiota of 8-week-old infants showed a similar preference for oligomers of enzyme-treated oat β-glucan which consist solely of β(1→4)-linked glucosyl residues (Figure 2B, Figure S1). However, the rate of fermentation was lower as compared to the faecal microbiota of 2-week-old infants as demonstrated by oligomer 3a and 5a remaining for 32% and 60% respectively after 26 h of fermentation. Nonetheless, in comparison to the non-fermentable native oat β-glucan, the enzyme treatment of native oat β-glucan increased the fermentability significantly for both 2- and 8-week-old infants.

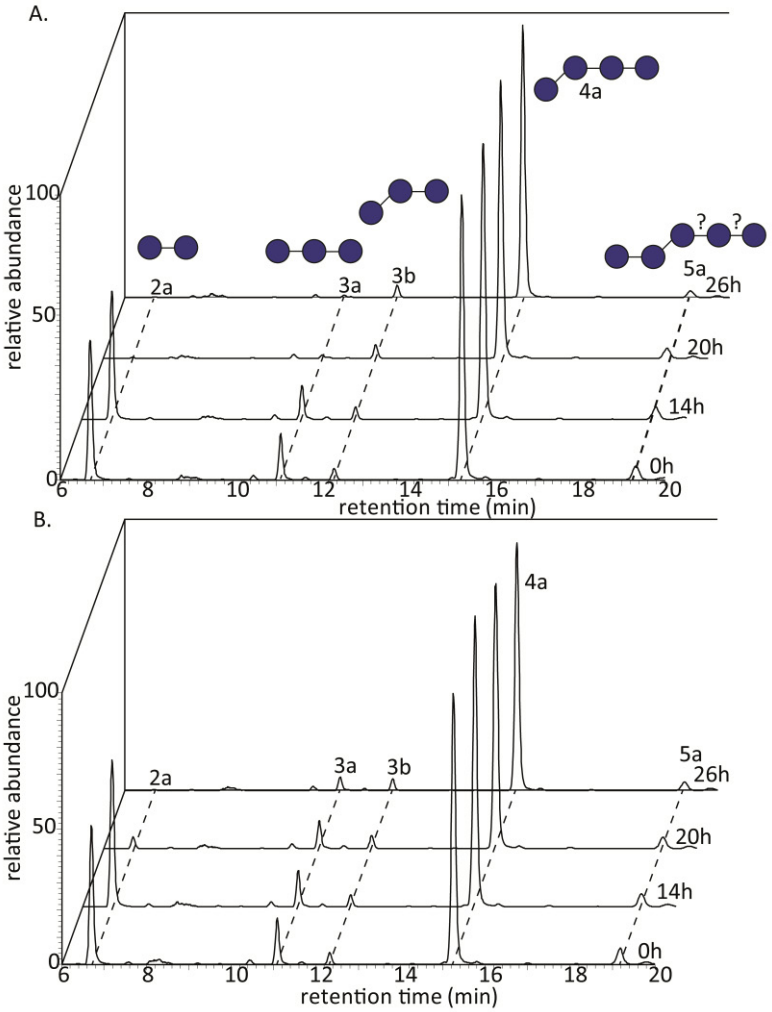

Figure 2 UHPLC-PGC-MS profiles of enzyme-treated oat β-glucan (eOBG) at the start and after 14, 20 and 26 h of fermentation using pooled faecal inoculum of 2- (A) and 8- (B) week-old infants. Peaks are labelled with 1a: 1= degree of polymerization, a= letter qualifier. Corresponding structures are placed above label with —: β(1-4)-linkage and /: β(1-3)-linkage.

Increase in *Enterococcus* during fermentation of media supplemented with native and enzyme-treated oat β-glucan

To study the impact of native and enzyme-treated oat β-glucan on infant microbiota composition, 16S rRNA gene amplicon sequencing was performed. Fermentation of media supplemented with native oat β-glucan increased the relative abundance of *Enterococcus* in faecal inoculum of 2-week-old infants (Figure 3). After 14 h of fermentation ≈72% of the bacteria belonged to the genus *Enterococcus*, which decreased slightly to ≈56% relative

abundance after 26 h of fermentation. Since the fermentation control without addition of native oat β-glucan showed a less pronounced increase in *Enterococcus* for faecal inoculum of 2-week-old infants (≈26% after 26 h) (Figure S2), it is suggested that the growth of *Enterococcus* is stimulated by the presence of the unfermentable native oat β-glucan. Next, an increase in *Bacillus* up to ≈18% was observed in the first 14 h of fermentation of media supplemented with native oat β-glucan, which decreased to ≈1% after 26 h of fermentation (Figure 3). In contrast, a clear increase in relative abundance was observed for both *Escherichia-Shigella* and *Clostridium Sensu Stricto I*, up to ≈17 and ≈18% respectively, after 26 h of fermentation. However, this increase was similar for *Clostridium Sensu Stricto I* and even more pronounced for *Escherichia-Shigella* in a control fermentation without native oat β-glucan (Figure S2). As these genera have been reported to grow well on peptides and amino acids which are highly abundant in SIEM medium [33], it cannot be excluded that their growth was stimulated by SIEM medium components.

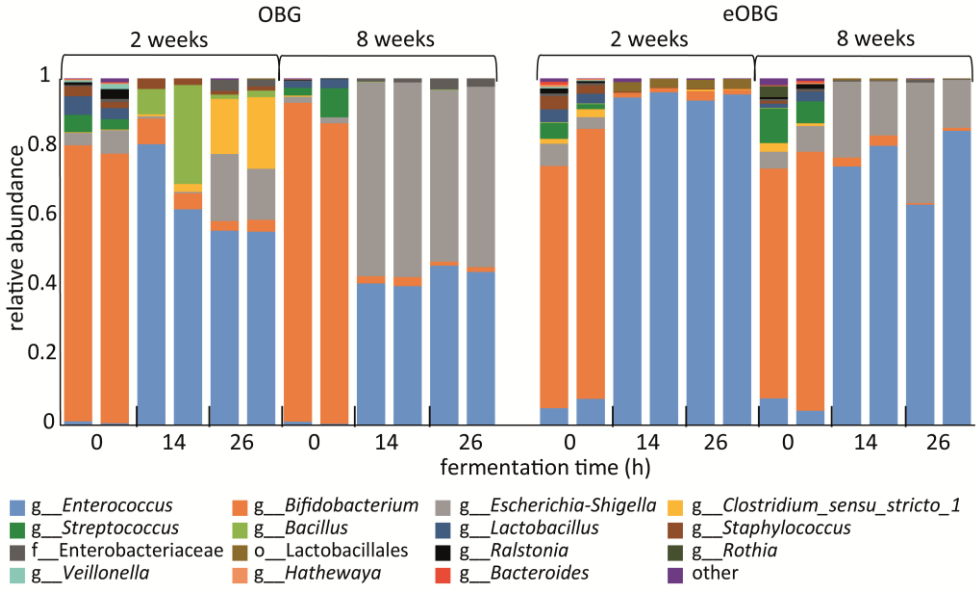

Figure 3 Relative abundance of bacteria at the highest classified taxonomy in duplicate fermentation digesta collected at the start and after 14 and 26 h from *in vitro* fermentation of media supplemented with native oat β-glucan (OBG) and enzyme-treated oat β-glucan (eOBG) using pooled faecal inoculum of 2- and 8-week-old infants.

Fermentation of media supplemented with native oat β-glucan by faecal microbiota of 8-week-old infants induced the relative abundance of *Enterococcus*, although to a lesser extent than with inocula of 2-week-old infants (Figure 3). After 14 h of fermentation, ≈40% of the bacteria belonged to the genus *Enterococcus*, which increased slightly up to ≈45% between 14 and 26 h of fermentation. In contrast to 2-week-old infants, no increase in relative abundance of *Bacillus* and *Clostridium sensu stricto I* was observed. However,

similar background fermentation of SIEM medium components by *Escherichia-Shigella* was observed, contributing to ≈50% of all bacteria after 26 h of fermentation.
Fermentation of enzyme-treated oat β-glucan resulted in a higher increase in relative abundance of *Enterococcus* as was observed for the fermentation of media supplemented with native oat β-glucan. After 14 and 26 h of fermentation by faecal microbiota of 2-week-old infants more than 94% of the bacteria belonged to the genus *Enterococcus*. The increase in *Enterococcus* was less pronounced with 8-week-old infants as the relative abundance increased to ≈75% after both 14 and 26 h of fermentation. Similar to the fermentation of media supplemented with native oat β-glucan, background fermentation of SIEM medium components by *Escherichia-Shigella* was observed for inoculum from 8-week-old-infants.

Increase of specific *Enterococcus* ASVs during fermentation of media supplemented with native and enzyme-treated oat β-glucan is dependent on the infant age

Since the relative abundance of *Enterococcus* after fermentation of media supplemented with native and enzyme-treated oat β-glucan was higher with faecal microbiota of 2-week-old infants than with 8-week-old infants, we questioned whether this might be explained by differences in *Enterococcus* species present. To this end, *Enterococcus* Amplicon Sequencing Variants (ASVs) were examined, which can be considered as a proxy for *Enterococcus* species. A difference in *Enterococcus* ASVs was observed between the fermentations using both inocula (Figure S3), which was most pronounced for enzyme-treated oat β-glucan. After 26 h of fermentation of enzyme-treated oat β-glucan ASV 39703838 was most abundant with faecal inoculum of 2-week-old infants, contributing to ≈81% of the enterococci. With faecal inoculum of 8-week-old infants ASV 39703836 was most abundant, contributing to ≈89% of the enterococci. Comparison of the sequences of ASV 39703838 and 39703836 (Table S2) with the SILVA database release 132 showed an exact match with respectively *Enterococcus faecium* and *Enterococcus faecalis*.

Lactate, a key metabolite formed during enzyme-treated oat β-glucan fermentation

The production of SCFAs and organic acids during fermentation of media supplemented with native oat β-glucan and enzyme-treated oat β-glucan was studied as these metabolites have shown to have important immunomodulatory activity [34,35]. The digesta collected during fermentation were analysed by GC and HPLC to quantify the SCFAs and other organic acids (Figure 4). The organic acids present at the start of the fermentation were originating from the sodium acetate buffer used in the preparation of the oat β-glucans, which was confirmed by the detection of a similar level of organic acids in the control fermentations without added inoculum (Figure S4). Reproducibility was confirmed with duplicate fermentations.
Fermentation of media supplemented with native oat β-glucan by both inocula resulted in a negligible total organic acid production of 1.2-1.3 µmol/mg after 26 h (Figure 4) compared to the control fermentations without added oat β-glucan ≈1 µmol/mg; Figure S4). The enzymatic treatment of native oat β-glucan increased the production of organic acids

(Figure 4). Fermentation by faecal microbiota of 2-week-old infants resulted in a total level of 2.5 µmol/mg after 14 h of fermentation, which increased up to 6 µmol/mg after 26 h of fermentation. Lactate, acetate, butyrate and propionate were present in a ratio of 79.4:20.4:0.1:0.1. Production of organic acids was slightly lower with faecal microbiota of 8-week-old infants (Figure 4). After 14 h of fermentation of enzyme-treated oat β-glucan a total level of 1.8 µmol/mg was reached, which increased up to 5.2 µmol/mg after 26 h of fermentation. Lactate, acetate, butyrate and propionate were present in a ratio of 72.4:27.3:0.2:0.1.

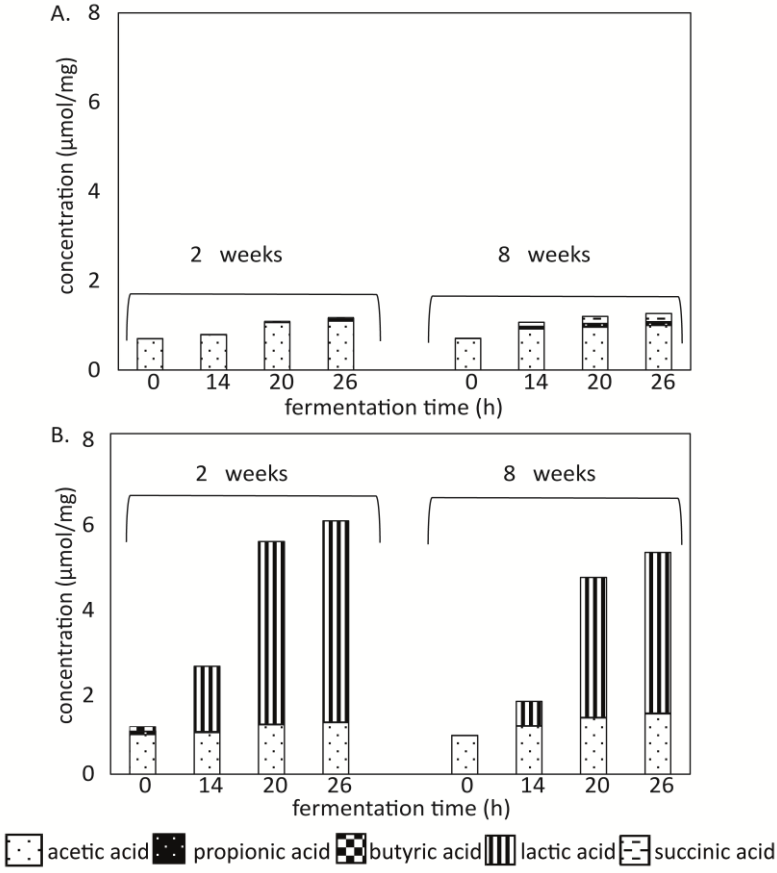

Figure 4 Production of SCFAs, lactic acid and succinic acid upon fermentation of media supplemented with native oat β-glucan (A) and enzyme-treated oat β-glucan (B) using pooled faecal inoculum of 2- and 8-week-old infants.

Cytokine production by dendritic cells (DC) differs between fermentation digesta of media supplemented with native oat β-glucan and enzyme treated oat β-glucan

DCs are present under the epithelial lining of the gastrointestinal tract and can therefore come in contact with dietary components such as oat β-glucan and its fermentation products. To test whether the digesta of media supplemented with native oat β-glucan and enzyme-treated oat β-glucan fermented with faecal inoculum of 2- and 8-week-old infants can impact intestinal immune responses, we incubated DCs from umbilical vein with fermentation samples taken at different time points. The pro-inflammatory chemokines and cytokines MCP-1/CLL2, MIP-1α/CCL3, IL-1β, IL-6 and TNFα as well as the anti-inflammatory cytokine IL-10 induced in the DC supernatant were studied.

Digesta from the control fermentation with only inoculum and SIEM medium were incubated with DCs (Figure 5). Digesta of both t=14 and t=26 from fermentations with either faecal inoculum of 2- or 8-week-old infants induced production of all chemokines and cytokines measured. Incubation of DCs with t=14 digesta of media supplemented with native oat β-glucan fermented with inoculum of 2-week-old infants attenuated DC activation and lowered production of MIP1α/CCL3, IL-1β, IL-6 and TNFα when compared to the t=14 digesta of the control fermentation (Figure 5). Incubation with t=26 digesta also induced lower levels of IL-6 and TNFα when compared to the control. The t=14 digesta of enzyme-treated oat β-glucan fermented with faecal inoculum of 2-week-old infants also resulted in lower levels of MIP1α/CCL3, IL-1β, IL-6 and TNFα in DCs when compared to the t=14 digesta of the control fermentation. Also, incubation with t=26 digesta resulted in lower levels of all chemokines and cytokines measured when compared to the control. When chemokine and cytokine patterns of DCs stimulated with native oat β-glucan and enzyme-treated oat β-glucan of fermentations with faecal inoculum of 2-week-old infants were compared, it was found that incubation with t=14 digesta of native oat β-glucan fermentation resulted in a significant lower level of MCP-1/CLL2 and a higher level of TNFα. In addition, the t=26 digest of native oat β-glucan induced a significant higher level of MCP-1/CLL2 and a lower level of IL-6 compared to the t=26 digesta of enzyme-treated oat β-glucan.

Incubation of DCs with t=14 digesta of native oat β-glucan fermented with faecal inoculum of 8-week-old infants induced a lower level of all chemokines and cytokines measured when compared to the control. The t=26 digesta reduced levels of IL-1β and TNFα when compared to the control. The t=14 digesta of enzyme treated oat β-glucan fermented with faecal inoculum of 8-week-old infant's induced significant lower levels of MIP1α/CCL3, IL-1β, IL-6, IL-10 and TNFα, while the t=26 digest of this fermentation only decreased the expression of IL-1β in DCs when compared to the control. When chemokine and cytokine patterns of DCs stimulated with native oat β-glucan or enzyme-treated oat β-glucan digesta of fermentations with 8-week inoculum were compared, the t=14 digesta of the native oat β-

glucan fermentation induced significant higher IL-6 levels compared to the t=14 digesta of the enzyme-treated oat β-glucan fermentation.

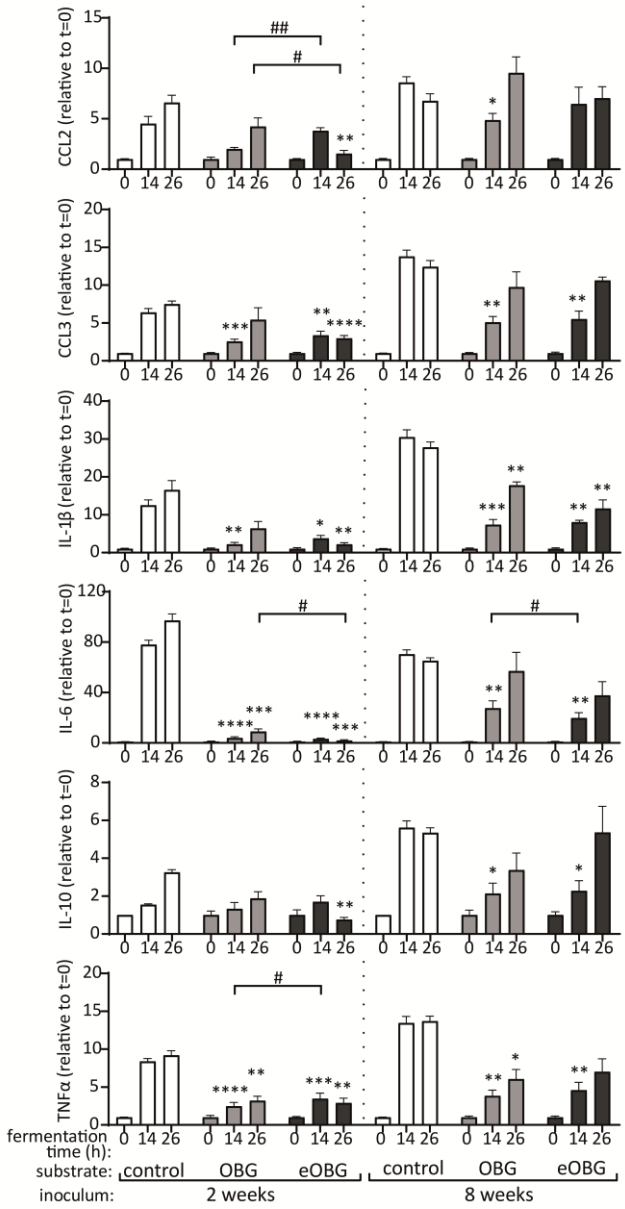

Figure 5 Induced cytokines (fold change of induction by 0h sample) by digesta of control fermentation, native (OBG) and enzyme-treated oat β-glucan (eOBG) fermentation with pooled faecal inocula of 2- and 8-week-old infants. Stars above bars represent statistical differences compared to the time-matched control samples (*p<0.05, **p<0.01, ***p<0.001, ****p<0.0001). Statistical differences between samples of OBG and eOBG fermentations are indicated above graphs (#p<0.05, ##p<0.01, ###p<0.001, ####p<0.0001) (n=6).

Fermentation of media supplemented with native oat β-glucan and enzyme-treated oat β-glucan by infant faecal inoculum enhances Dectin-1 activation

As Dectin-1 is the most important immune receptor for β-glucans and present on DCs [36], we also investigated whether enzyme treatment of native oat β-glucan and glucan fermentation by inoculum of 2- and 8-week-old infants impact activation of the Dectin-1 receptor. To this end, HEK-Dectin1a and HEK-Dectin1b reporter cell lines were incubated with digesta taken from the fermentation of native oat β-glucan and enzyme-treated oat β-glucan. Normal cell culture medium and Zymosan, a particulate β-glucan, which is known to have Dectin-1 stimulating activity, were used as the negative and positive control respectively.

First, samples of native oat β-glucan and enzyme-treated oat β-glucan fermented with either 2- or 8-week-old infant faecal inoculum were incubated with the HEK-Dectin1a reporter cells (full length variant) (Figure 6A). The t=0 digesta of enzyme-treated oat β-glucan fermented with inoculum of 2-week-old infants and the t=0 digesta of native oat β-glucan fermented with inoculum of 8-week-old infants resulted in slightly higher SEAP release in HEK-Dectin1a reporter cells when compared to the medium control. All t=14 and t=26 of native oat β-glucan and enzyme-treated oat β-glucan fermented with either 2- or 8-week inoculum could induce significant higher SEAP release in HEK-Dectin1a reporter cells when compared to the medium control and their own t=0 matched digesta. For native oat β-glucan and enzyme-treated oat β-glucan fermented with inoculum of 2-week-old infants, the Nf-κB release was also higher for t=26 digesta when compared to the t=14 digesta.

Fermentation digesta of native oat β-glucan and enzyme-treated oat β-glucan were also incubated with HEK-Dectin1b reporter cells (stalk-less variant) (Figure 6B). None of the t=0 digesta of native oat β-glucan and enzyme-treated oat β-glucan fermented with either 2- or 8-week inoculum were able to induce significant SEAP release when compared to the medium control. The t=14 and t=26 digesta of native oat β-glucan and enzyme-treated oat β-glucan fermented with either inoculum of 2- or 8-week-old infants could induce significant higher SEAP release in HEK-Dectin1b reporter cells when compared to the medium control. Again, the induction of SEAP release of all of these digesta was also higher when compared to their own t=0 matched digesta. For native oat β-glucan and enzyme-treated oat β-glucan fermented with inoculum of 2-week old infants, the SEAP release was also higher by t=26 digesta when compared to the t=14 digesta.

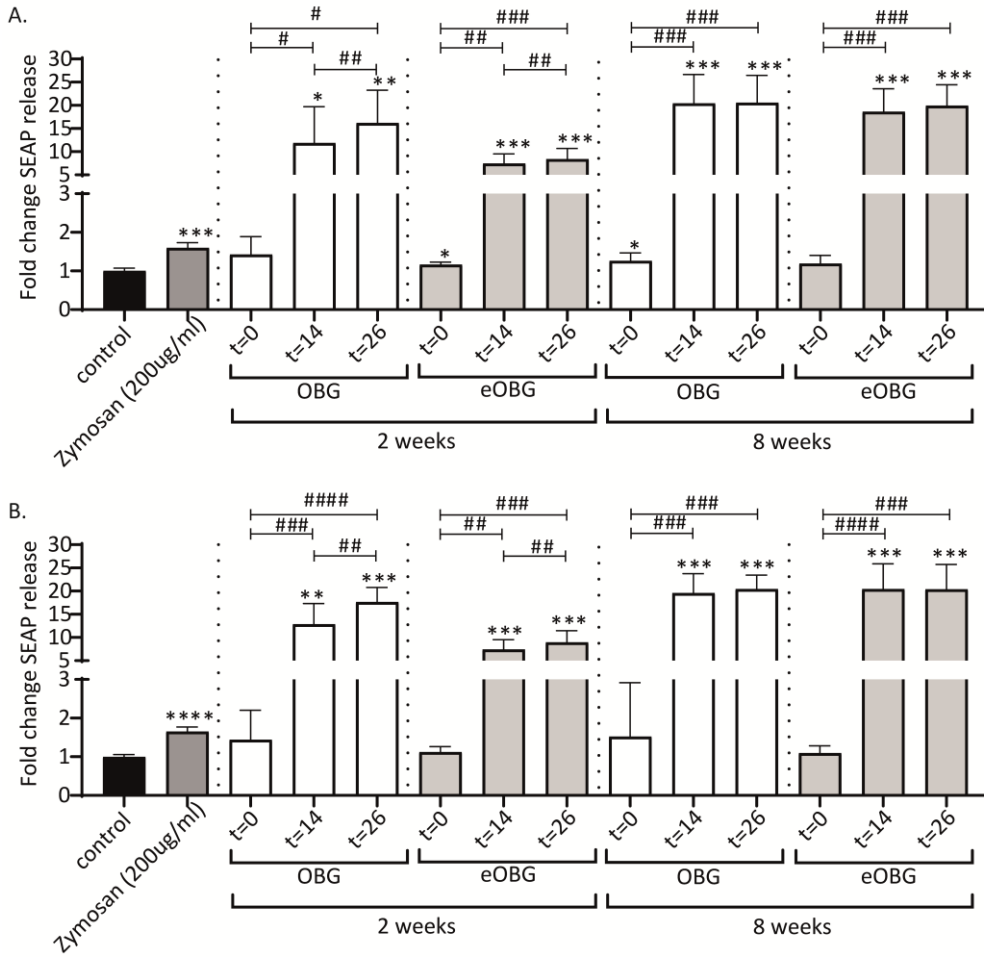

Figure 6 Relative NF-κB release by (A) HEK-Dectin1a and (B) HEK-Dectin1b reporter cell stimulation with (A) samples of native oat β-glucan (OBG) and enzyme-treated oat β-glucan (eOBG) fermented with 2-week old faecal inoculum and (B) OBG and eOBG fermented with 8-week old faecal inoculum. For all groups a medium control and Zymosan were included. Statistical differences were tested using a OneWay ANOVA test followed by a Tukey's multiple comparison test. Stars above bars represent statistical differences compared to the medium control (*p<0.05, **p<0.01, ***p<0.001, ****p<0.0001). Statistical differences between t=14 or t=26 and the matched t=0 are indicated above graphs (#p<0.05, ##p<0.01, ###p<0.001, ####p<0.0001). Experiments are repeated 3 times in triplicate.

Discussion

Non-digestible carbohydrates are often being added to cow milk-based infant formula to substitute HMO functions. Commonly used NDCs are FOS and GOS, however β-glucans might also have potential as possible addition to infant formula as these molecules also stimulate growth of beneficial microbes [17,18] and have immune modulating effects [14,15]. However, currently limited knowledge is available about the effects of fermentation of oat β-glucans on their immune-modulating properties. In this study, the degradation of native and enzyme-treated oat β-glucan by infant faecal microbiota was studied, as well as the effect of the fermentation digesta on cytokine production by dendritic cells and dectin-1 receptor activation, i.e. the receptor for β-glucans on immune cells [36].

Although it has been demonstrated *in vitro* that adult faecal microbiota can utilize native oat and barley β-glucans in the size range of 130-243 kDa [17], native oat β-glucan was not degraded by the faecal microbiota of both 2-and 8-week-old infants in current study. This finding, however, is in line with differences observed in GI microbial functionality in people of different age [37]. Bacterial species belonging to the *Clostridium histolyticum* group were mainly involved in the described utilization in adults, which was corroborated by the presence of genes encoding endo-β-glucanase for several members of this group, e.g. *C. longisporum* [38] and *C. acetobutylicum* [39]. The stimulation of *Clostridium* was also observed upon intake of barley β-glucans in an *in vivo* study with healthy adult volunteers [40]. In our study, using infant microbiota, bacteria belonging to the genus *Clostridium sensu stricto 1* comprising many different *Clostridium* species [30] were detected. Nevertheless, the absence of fermentation of native oat β-glucan by the infant faecal microbiota could possibly be ascribed to differences at species level, since the presence and abundance of specific *Clostridium* species gradually changes upon aging [41].

Instead, a clear increase in *Enterococcus* was observed upon fermentation of media supplemented with native oat β-glucan by faecal microbiota of 2- and 8-week-old infants, which was more pronounced than observed for control fermentations without added native oat β-glucan. As such, it is suggested that the presence of the unfermentable native oat β-glucan stimulated the growth of *Enterococcus* on SIEM medium components. As enterococci are known to be one of the first colonizers of the infant gut [42], the increase in enterococci might be relevant in infants for creating a new environment that allows colonization of the gut by strict anaerobes [2,19]. A similar stimulation of *Enterococcus* was shown in an *in vitro* fermentation study of barley β-glucans using faecal microbiota of 9-15 months old infants which received both human milk and solid foods [18]. With these age groups also substantial production of SCFAs was observed, which indicates that faecal microbiota of 9-15 months old infants are capable of degrading native oat β-glucan. It is therefore likely that differences in *Enterococcus* on species level upon aging [43,44] result in the availability of different sets of enzymes for the degradation of β-glucans for infants of different age groups. Our findings

suggest that the bacteria and their enzymes responsible for the degradation of β-glucans are not present yet the first weeks after birth, but are introduced upon aging.

In contrast to native oat β-glucan that was not fermented by infant faecal microbiota, endo-1,3(4)-β-glucanase-treated oat β-glucan was degraded by the faecal microbiota of both 2- and 8-week old infants. This result corroborates the findings of Lam et al [18], who observed an increase in SCFAs production when lowering the molecular weight of barley β-glucans in an *in vitro* fermentation study using infant faecal inocula. We also found that decreasing the size of the oat β-glucans upon enzyme treatment resulted in a stronger stimulation of *Enterococcus* and increased production of lactic acid, which were more pronounced with faecal inoculum of 2-week-old infants. Our data suggest that the fermentation of enzyme-treated oat β-glucan resulted in a selective increase of *E. faecium* and *E. faecalis* using faecal inoculum of respectively 2- and 8-week-old infants. Notably, for both inocula there was a clear preference for β(1→4)-linked oligomers present in the enzyme-treated oat β-glucan. Not much is known about specific carbohydrate-degrading enzymes and their structural preferences expressed by *Enterococcus* species. However, previous *in vitro* study using adult faecal inoculum also concluded that lower molecular weight barley β-glucans results in a stimulation of *Enterococcus* and *Lactobacillus* [17].

The fermentation digesta of both native and enzyme-treated oat β-glucan could attenuate multiple pro-inflammatory cytokine responses in immature dendritic cells. Digesta of the control fermentation with inoculum of either 2- or 8-week-old infants induced high levels of the chemokines and cytokines MCP-1/CLL2, MIP-1α/CCL3, IL-1β, IL-6 and TNFα as well as the anti-inflammatory cytokine IL-10. This effect was only observed for the t=14 and t=26 digesta and therefore it was likely caused by products formed during fermentation, like metabolic products of protein fermentation and other bacterial metabolites such as ATP, lipoteichoic acid, polysaccharide A, peptidoglycan, RNA/DNA sequences and exopolysaccharide [45]. The most pronounced attenuating effect by digesta of medium supplemented with native and enzyme-treated oat β-glucan was observed for IL-6 production. The strongest attenuation of IL-6 was observed for the digesta of fermentations with faecal inoculum of 2-week-old infants. Incubation with t=14 and t=26 digesta resulted in a significant lower induction of IL-6 compared to the controls. In addition, the t=26 digesta of enzyme-treated oat β-glucan resulted in a significant lower IL-6 production compared to the t=26 digesta of native oat β-glucan. The observed difference in DC stimulating capacity could possibly be explained by the formation of lactate which was only observed during the fermentation of enzyme-treated oat β-glucan. Lactate is the main end-product of the fermentation of carbohydrates by *Enterococcus* [46] and has been reported to modulate cytokine responses resulting predominantly in reduced inflammation in PBMCs and monocytes [47].

Despite the absence of glucan degradation and lactate formation, the digesta of medium supplemented with native oat β-glucan displayed significant immune attenuating effects.

As with fermentation of both medium supplemented with native and enzyme-treated oat β-glucan a clear increase in *Enterococcus* was observed, it is suggested that the microbiota composition plays an important role in the attenuation of the pro-inflammatory cytokine responses. The unfermentable native oat β-glucan resulted in a lower abundance of *Enterococcus* after 26 h of fermentation than the fermentable enzyme-treated oat β-glucan. Next to the SCFAs, the differences in relative abundance of *Enterococcus* could thus also possibly explain the difference in DC stimulation capacity between native and enzyme-treated oat β-glucan digesta. Although the bacterial content was removed from the digesta before incubation with DCs in our experiments, the presence of soluble immune-active bacterial fragments in the digesta might be possible, as exemplified for the supernatant of a *Lactobacillus casei* cell wall extract [48].

Enterococcus have been associated with immunomodulatory functions and gut health in several studies. For example, a cohort study by Bjorksten et al. found a negative correlation between the colonization of *Enterococcus* in the first year of life and the development of allergies [49]. Other *in vivo* studies observed a correlation between *E. faecium* and the reduction of infections in the gut, as reviewed by Franz et al [50]. There are also multiple studies demonstrating immunomodulatory properties of *E. faecalis* on different cell types. For example, *E. faecalis* could upregulate IL-10 through PPARγ1 activation in colonic cell lines [51]. A study by Wang et al. showed that several strains of *E. faecalis* isolated from new-born infants downregulated IL-8 secretion in Caco-2, HT-29 and HCT116 intestinal cell lines [52]. Interestingly, the immune attenuating effects were virtually gone when the carbohydrate moieties on the cell surface of *E. faecalis* were oxidized. This indicates the carbohydrates present on the cell surface of *E. faecalis* are the major effector molecules for regulating IL-8 secretion [52]. An additional study by Wang et al. demonstrated that IL-8 secretion in intestinal cell lines is attenuated by *E. faecalis* through inhibition of MAPK signalling pathways. This effect was suggested also to be caused by factors on the exterior cell wall of the bacteria [53]. As such, it can be hypothesized that the enzyme treatment induced the immune-attenuating effect of native oat ß-glucan due to the increased stimulation of *Enterococcus* and consequent production of lactate during the fermentation. As Dectin-1 receptors are important β-glucan binding receptors present on DCs [54], we tested the immune stimulating capacity of our digesta on Dectin-1 reporter cell lines. The t=0 digesta of medium supplemented with the native and enzyme-treated oat β-glucan did not stimulate the Dectin-1 receptors. This is in line with an earlier study showing that particulate β-glucans induce stronger immune responses than soluble β-glucan [14], as in our study we used soluble β-glucan while in addition any insoluble material was removed from the digesta by centrifugation and filtration prior to incubation with the receptors. The absence of any insoluble material could possibly also explain why we did not observe an increase in Dectin-1 stimulation after endoglucanase treatment as observed before [16].

Both the Dectin-1a and Dectin-1b receptors were strongly activated by the t=14 and t=26 digesta of both native and enzyme-treated oat β-glucan, fermented with either inoculum of 2- or 8-week-old infants. It is unlikely that conformational changes of oat β-glucan played a role in the receptor activation as reported elsewhere [55], as the stimulatory effects of the t=14 and t=26 digesta of the unfermentable native oat β-glucan and the fermented enzyme-treated oat β-glucan were very similar. This finding also indicates that the degradation of the enzyme-treated oat β-glucans and the consequent lactate production are not responsible for the observed effects. It is tempting to speculate that the observed Dectin-1 activation is an (in)direct consequence of the increase in *Enterococcus*. Although, fungal β-glucan with β(1→3) glycosidic bonds is the commonly accepted agonist of Dectin-1, there are reports of Dectin-1 activation by β(1↔1) trehalose [56], mannoprotein [56], lipopeptide [57] and bacterial cell walls [[48,58]]. As such, it could be hypothesized that the complex cell wall of *Enterococcus* containing amongst others lipoteichoic acid, surface proteins and capsular polysaccharides [59], plays a role in the activation of Dectin-1 receptors as observed in our study. The activation of Dectin-1 receptors has been reported to have immune effects. For example, in macrophages, Dectin-1 regulates IL-10 and induced regulatory macrophage markers [60]. The ability of the t=14 and t=26 digesta to stimulate Dectin-1 activation therefore might contribute to the immune attenuating effects we observed in DCs.

Conclusions

Our data shows that the fermentation capacity of oat β-glucans by faecal microbiota of 2- and 8-week-old infants increases after endo-1,3(4)-β-glucanase treatment. Both native and enzyme-treated oat β-glucans can attenuate pro-inflammatory responses, which was more pronounced for enzyme-treated oat β-glucans. The attenuation is suggested to be caused by the stimulation of *Enterococcus* upon fermentation and by the increase stimulation of Dectin-1 receptors by the fermentation digesta. Hence, this study shows that especially enzyme-treated oat β-glucans are highly relevant for infant formula as they exert beneficial effects on both microbiota composition and immunomodulation in infants.

Acknowledgements

This research was performed in the public-private partnership 'CarboKinetics' coordinated by the Carbohydrate Competence Center (CCC, www.cccresearch.nl). CarboKinetics is financed by participating industrial partners Agrifirm Innovation Center B.V., Cooperatie Avebe U.A., DSM Food Specialties B.V., FrieslandCampina Nederland B.V., Nutrition Sciences N.V., VanDrie Holding N.V. and Sensus B.V., and allowances of The Netherlands Organisation for Scientific Research (NWO).

References

1. Rautava, S.; Luoto, R.; Salminen, S.; Isolauri, E. Microbial contact during pregnancy, intestinal colonization and human disease. *Nat. Rev. Gastroenterol. Hepatol.* **2012**, *9*, 565-576.
2. Morelli, L. Postnatal development of intestinal microflora as influenced by infant nutrition. *J. Nutr.* **2008**, *138*, 1791s-1795s.
3. World Health Organization; UNICEF. *Global strategy for infant and young child feeding*; 9241562218; 2003.
4. Smilowitz, J.T.; Lebrilla, C.B.; Mills, D.A.; German, J.B.; Freeman, S.L. Breast milk oligosaccharides: structure-function relationships in the neonate. *Annu. Rev. Nutr.* **2014**, *34*, 143-169.
5. Bode, L. The functional biology of human milk oligosaccharides. *Early Hum. Dev.* **2015**, *91*, 619-622.
6. Theurich, M.A.; Davanzo, R.; Busck-Rasmussen, M.; Diaz-Gomez, N.M.; Brennan, C.; Kylberg, E.; Baerug, A.; McHugh, L.; Weikert, C.; Abraham, K.; Koletzko, B. Breastfeeding rates and programs in europe: A survey of 11 national breastfeeding committees and representatives. *J. Pediatr. Gastroenterol. Nutr.* **2019**, *68*, 400-407.
7. Vandenplas, Y.; Zakharova, I.; Dmitrieva, Y. Oligosaccharides in infant formula: more evidence to validate the role of prebiotics. *Br. J. Nutr.* **2015**, *113*, 1339-1344.
8. Akkerman, R.; Faas, M.M.; de Vos, P. Non-digestible carbohydrates in infant formula as substitution for human milk oligosaccharide functions: Effects on microbiota and gut maturation. *Crit. Rev. Food Sci. Nutr.* **2019**, *59*, 1486-1497.
9. Macfarlane, G.T.; Steed, H.; Macfarlane, S. Bacterial metabolism and health-related effects of galacto-oligosaccharides and other prebiotics. *J. Appl. Microbiol.* **2008**, *104*, 305-344.
10. Bermudez-Brito, M.; Sahasrabudhe, N.M.; Rosch, C.; Schols, H.A.; Faas, M.M.; de Vos, P. The impact of dietary fibers on dendritic cell responses *in vitro* is dependent on the differential effects of the fibers on intestinal epithelial cells. *Mol. Nutr. Food Res.* **2015**, *59*, 698-710.
11. Estrada, A.; Yun, C.H.; Van Kessel, A.; Li, B.; Hauta, S.; Laarveld, B. Immunomodulatory activities of oat beta-glucan *in vitro* and *in vivo*. *Microbiol. Immunol.* **1997**, *41*, 991-998.
12. Knudsen, K.E.B. Fiber and nonstarch polysaccharide content and variation in common crops used in broiler diets1. *Poult. Sci.* **2014**, *93*, 2380-2393.
13. Brown, G.D.; Gordon, S. Fungal beta-glucans and mammalian immunity. *Immunity* **2003**, *19*, 311-315.
14. Sahasrabudhe, N.M.; Dokter-Fokkens, J.; de Vos, P. Particulate β-glucans synergistically activate TLR4 and Dectin-1 in human dendritic cells. *Mol. Nutr. Food Res.* **2016**, *60*, 2514-2522.
15. Kanjan, P.; Sahasrabudhe, N.M.; de Haan, B.J.; de Vos, P. Immune effects of β-glucan are determined by combined effects on Dectin-1, TLR2, 4 and 5. *J. Funct. Foods* **2017**, *37*, 433-440.
16. Sahasrabudhe, N.M.; Tian, L.; van den Berg, M.; Bruggeman, G.; Bruininx, E.; Schols, H.A.; Faas, M.M.; de Vos, P. Endo-glucanase digestion of oat β-Glucan enhances Dectin-1 activation in human dendritic cells. *J. Funct. Foods* **2016**, *21*, 104-112.
17. Hughes, S.A.; Shewry, P.R.; Gibson, G.R.; McCleary, B.V.; Rastall, R.A. *In vitro* fermentation of oat and barley derived β-glucans by human faecal microbiota. *FEMS Microbiol. Ecol.* **2008**, *64*, 482-493.
18. Lam, K.L.; Ko, K.C.; Li, X.; Ke, X.; Cheng, W.Y.; Chen, T.; You, L.; Kwan, H.S.; Cheung, P.C. *In vitro* infant faecal fermentation of low viscosity barley beta-glucan and its acid hydrolyzed derivatives: Evaluation of their potential as novel prebiotics. *Molecules* **2019**, *24*.
19. Adlerberth, I.; Wold, A.E. Establishment of the gut microbiota in Western infants. *Acta Paediatr.* **2009**, *98*, 229-238.
20. Gu, F.; Borewicz, K.; Richter, B.; van der Zaal, P.H.; Smidt, H.; Buwalda, P.L.; Schols, H.A. *In vitro* fermentation behavior of isomalto/malto-polysaccharides using human fecal inoculum indicates prebiotic potential. *Mol. Nutr. Food Res.* **2018**, *62*, e1800232.
21. Leijdekkers, A.G.M.; Aguirre, M.; Venema, K.; Bosch, G.; Gruppen, H.; Schols, H.A. *In vitro* fermentability of sugar beet pulp derived oligosaccharides using human and pig fecal inocula. *J. Agric. Food Chem.* **2014**, *62*, 1079-1087.
22. Logtenberg, M.J.; Vink, J.C.M.; Serierse, R.M.; An, R.; Hermes, G.D.A.; Smidt, H.; Schols, H.A. Pooled faecal inoculum can predict infant prebiotic fermentability despite high inter-individual variability of microbiota composition. **2019**, *Submitted*.
23. Borewicz, K.; Gu, F.; Saccenti, E.; Arts, I.C.W.; Penders, J.; Thijs, C.; van Leeuwen, S.S.; Lindner, C.; Nauta, A.; van Leusen, E.; Schols, H.A.; Smidt, H. Correlating infant fecal microbiota composition and human milk oligosaccharide consumption by microbiota of 1-month-old breastfed infants. *Mol. Nutr. Food Res.* **2019**, *63*, 1801214.
24. Ladirat, S.E.; Schuren, F.H.; Schoterman, M.H.; Nauta, A.; Gruppen, H.; Schols, H.A. Impact of galacto-oligosaccharides on the gut microbiota composition and metabolic activity upon antibiotic treatment during *in vitro* fermentation. *FEMS Microbiol. Ecol.* **2014**, *87*, 41-51.
25. Zhao, G.; Nyman, M.; Jonsson, J.A. Rapid determination of short-chain fatty acids in colonic contents and faeces of humans and rats by acidified water-extraction and direct-injection gas chromatography. *Biomed. Chromatogr.* **2006**, *20*, 674-682.
26. Salonen, A.; Nikkilä, J.; Jalanka-Tuovinen, J.; Immonen, O.; Rajilić-Stojanović, M.; Kekkonen, R.A.; Palva, A.; de Vos, W.M. Comparative analysis of fecal DNA extraction methods with phylogenetic

microarray: Effective recovery of bacterial and archaeal DNA using mechanical cell lysis. *J. Microbiol. Methods* **2010**, *81*, 127-134.
27. An, R.; Wilms, E.; Smolinska, A.; Hermes, G.D.A.; Masclee, A.A.M.; de Vos, P.; Schols, H.A.; van Schooten, F.J.; Smidt, H.; Jonkers, D.; Zoetendal, E.G.; Troost, F.J. Sugar beet pectin supplementation did not alter profiles of fecal microbiota and exhaled breath in healthy young adults and healthy elderly. *Nutrients* **2019**, *11*.
28. Ramiro-Garcia, J.; Hermes, G.D.A.; Giatsis, C.; Sipkema, D.; Zoetendal, E.G.; Schaap, P.J.; Smidt, H. NG-Tax, a highly accurate and validated pipeline for analysis of 16S rRNA amplicons from complex biomes. *F1000Research* **2016**, *5*, 1791-1791.
29. Poncheewin, W.; Hermes, G.D.A.; van Dam, J.C.J.; Koehorst, J.J.; Smidt, H.; Schaap, P.J. NG-Tax 2.0: A semantic framework for high-throughput amplicon analysis. *Front. Genet.* **2020**, *10*.
30. Quast, C.; Pruesse, E.; Yilmaz, P.; Gerken, J.; Schweer, T.; Yarza, P.; Peplies, J.; Glöckner, F.O. The SILVA ribosomal RNA gene database project: improved data processing and web-based tools. *Nucleic Acids Res.* **2012**, *41*, D590-D596.
31. Sahasrabudhe, N.M.; Schols, H.A.; Faas, M.M.; de Vos, P. Arabinoxylan activates Dectin-1 and modulates particulate beta-glucan-induced Dectin-1 activation. *Mol. Nutr. Food Res.* **2016**, *60*, 458-467.
32. Albrecht, S.; Schols, H.A.; van den Heuvel, E.G.; Voragen, A.G.; Gruppen, H. Occurrence of oligosaccharides in feces of breast-fed babies in their first six months of life and the corresponding breast milk. *Carbohydr. Res.* **2011**, *346*, 2540-2550.
33. Richardson, A.J.; McKain, N.; Wallace, R.J. Ammonia production by human faecal bacteria, and the enumeration, isolation and characterization of bacteria capable of growth on peptides and amino acids. *BMC Microbiol.* **2013**, *13*, 6-6.
34. Smith, P.M.; Howitt, M.R.; Panikov, N.; Michaud, M.; Gallini, C.A.; Bohlooly-Y, M.; Glickman, J.N.; Garrett, W.S. The microbial metabolites, short-chain fatty acids, regulate colonic treg cell homeostasis. *Science* **2013**, *341*, 569-573.
35. Nastasi, C.; Candela, M.; Bonefeld, C.M.; Geisler, C.; Hansen, M.; Krejsgaard, T.; Biagi, E.; Andersen, M.H.; Brigidi, P.; Ødum, N.; Litman, T.; Woetmann, A. The effect of short-chain fatty acids on human monocyte-derived dendritic cells. *Sci. Rep.* **2015**, *5*, 16148.
36. Brown, G.D. Dectin-1: a signalling non-TLR pattern-recognition receptor. *Nat. Rev. Immunol.* **2006**, *6*, 33-43.
37. Bhattacharya, T.; Ghosh, T.S.; Mande, S.S. Global profiling of carbohydrate active enzymes in human gut microbiome. *PLoS One* **2015**, *10*, e0142038.
38. Mittendorf, V.; Thomson, J.A. Cloning of an endo-(1->4)-beta-glucanase gene, celA, from the rumen bacterium *Clostridium* sp. ('*C. longisporum*') and characterization of its product, CelA, in *Escherichia coli*. *J. Gen. Microbiol.* **1993**, *139*, 3233-3242.
39. Zappe, H.; Jones, W.A.; Jones, D.T.; Woods, D.R. Structure of an endo-beta-1,4-glucanase gene from *Clostridium acetobutylicum* P262 showing homology with endoglucanase genes from *Bacillus* spp. *Appl. Environ. Microbiol.* **1988**, *54*, 1289-1292.
40. Mitsou, E.K.; Panopoulou, N.; Turunen, K.; Spiliotis, V.; Kyriacou, A. Prebiotic potential of barley derived β-glucan at low intake levels: A randomised, double-blinded, placebo-controlled clinical study. *Food Res. Int.* **2010**, *43*, 1086-1092.
41. Ringel-Kulka, T.; Cheng, J.; Ringel, Y.; Salojärvi, J.; Carroll, I.; Palva, A.; de Vos, W.M.; Satokari, R. Intestinal microbiota in healthy U.S. young children and adults - a high throughput microarray analysis. *PLoS One* **2013**, *8*, e64315.
42. Fanaro, S.; Chierici, R.; Guerrini, P.; Vigi, V. Intestinal microflora in early infancy: composition and development. *Acta Paediatr. Suppl.* **2003**, *91*, 48-55.
43. Kirtzalidou, E.I.; Mitsou, E.K.; Pramateftaki, P.; Kyriacou, A. Screening Fecal Enterococci from Greek Healthy Infants for Susceptibility to Antimicrobial Agents. *Microb. Drug Resist.* **2012**, *18*, 578-585.
44. Obermajer, T.; Grabnar, I.; Benedik, E.; Tušar, T.; Robič Pikel, T.; Fidler Mis, N.; Bogovič Matijašić, B.; Rogelj, I. Microbes in infant gut development: Placing abundance within environmental, clinical and growth parameters. *Sci. Rep.* **2017**, *7*, 11230.
45. Yiu, J.H.C.; Dorweiler, B.; Woo, C.W. Interaction between gut microbiota and toll-like receptor: from immunity to metabolism. *J. Mol. Med. (Berl.)* **2017**, *95*, 13-20.
46. Ramsey, M.; Hartke, A.; Huycke, M. The physiology and metabolism of Enterococci. In *Enterococci: From Commensals to Leading Causes of Drug Resistant Infection;* Gilmore, M.S., Clewell, D.B., Ike Y., Eds.; Massachusetts Eye and Ear Infirmary: Boston, United states, **2014**.
47. Ratter, J.M.; Rooijackers, H.M.M.; Hooiveld, G.J.; Hijmans, A.G.M.; de Galan, B.E.; Tack, C.J.; Stienstra, R. *In vitro* and *in vivo* effects of lactate on metabolism and cytokine production of human primary PBMCs and monocytes. *Front. Immunol.* **2018**, *9*, 2564-2564.
48. Lin, I.C.; Suen, J.-L.; Huang, S.-K.; Huang, S.-C.; Huang, H.-C.; Kuo, H.-C.; Wei, C.-C.; Wang, F.-S.; Yu, H.-R.; Yang, K.D. Dectin-1/Syk signaling is involved in *Lactobacillus casei* cell wall extract-induced mouse model of Kawasaki disease. *Immunobiology* **2013**, *218*, 201-212.
49. Bjorksten, B. Evidence of probiotics in prevention of allergy and asthma. *Curr. Drug Targets Inflamm. Allergy* **2005**, *4*, 599-604.
50. Franz, C.M.; Huch, M.; Abriouel, H.; Holzapfel, W.; Galvez, A. Enterococci as probiotics and their implications in food safety. *Int. J. Food Microbiol.* **2011**, *151*, 125-140.

51. Are, A.; Aronsson, L.; Wang, S.; Greicius, G.; Lee, Y.K.; Gustafsson, J.-Å.; Pettersson, S.; Arulampalam, V. *Enterococcus faecalis* from newborn babies regulate endogenous PPARγ activity and IL-10 levels in colonic epithelial cells. *Proc. Natl. Acad. Sci.* **2008**, *105*, 1943-1948.
52. Wang, S.; Ng, L.H.M.; Chow, W.L.; Lee, Y.K. Infant intestinal *Enterococcus faecalis* down-regulates inflammatory responses in human intestinal cell lines. *World J. Gastroenterol.* **2008**, *14*, 1067-1076.
53. Wang, S.; Hibberd, M.L.; Pettersson, S.; Lee, Y.K. *Enterococcus faecalis* from healthy infants modulates inflammation through MAPK signaling pathways. *PLoS One* **2014**, *9*, e97523-e97523.
54. Taylor, P.R.; Brown, G.D.; Reid, D.M.; Willment, J.A.; Martinez-Pomares, L.; Gordon, S.; Wong, S.Y.C. The β-glucan receptor, Dectin-1, is predominantly expressed on the surface of cells of the monocyte/macrophage and neutrophil lineages. *J. Immunol.* **2002**, *169*, 3876-3882.
55. Elder, M.J.; Webster, S.J.; Chee, R.; Williams, D.L.; Hill Gaston, J.S.; Goodall, J.C. β-Glucan size controls Dectin-1-mediated immune responses in human dendritic cells by regulating IL-1β production. *Front. Immunol.* **2017**, *8*, 791-791.
56. Dzharullaeva, A.S.; Tukhvatulin, A.I.; Erokhova, A.S.; Bandelyuk, A.S.; Polyakov, N.B.; Solovyev, A.I.; Nikitenko, N.A.; Shcheblyakov, D.V.; Naroditsky, B.S.; Logunov, D.Y.; Gintsburg, A.L. Stimulation of Dectin-1 and Dectin-2 during parenteral immunization, but not mincle, induces Secretory IgA in intestinal mucosa. *J. Immunol. Res.* **2018**, *2018*, 3835720.
57. Mae, M.; Iyori, M.; Yasuda, M.; Shamsul, H.M.; Kataoka, H.; Kiura, K.; Hasebe, A.; Totsuka, Y.; Shibata, K. The diacylated lipopeptide FSL-1 enhances phagocytosis of bacteria by macrophages through a Toll-like receptor 2-mediated signalling pathway. *FEMS Immunol. Med. Microbiol.* **2007**, *49*, 398-409.
58. Rothfuchs, A.G.; Bafica, A.; Feng, C.G.; Egen, J.G.; Williams, D.L.; Brown, G.D.; Sher, A. Dectin-1 interaction with *Mycobacterium tuberculosis* leads to enhanced il-12p40 production by splenic dendritic cells. *J. Immunol.* **2007**, *179*, 3463-3471.
59. Hendrickx, A.P.; Schaik, W.v.; Willems, R.J. The cell wall architecture of *Enterococcus faecium*: from resistance to pathogenesis. *Future Microbiol.* **2013**, *8*, 993-1010.
60. Elcombe, S.E.; Naqvi, S.; Van Den Bosch, M.W.M.; MacKenzie, K.F.; Cianfanelli, F.; Brown, G.D.; Arthur, J.S.C. Dectin-1 regulates IL-10 production via a MSK1/2 and CREB dependent pathway and promotes the induction of regulatory macrophage markers. *PLoS One* **2013**, *8*, e60086.

Supporting information

Table S1 Overview of characterized oligomers formed upon enzymatic treatment of oat β-glucans with the relative abundance of the MS^2 and MS^3 fragments with *m/z* 263 with a: product ion with *m/z* 505, b: product ion with *m/z* 667 and T_R: retention time. Relative abundance of each component is determined by integration of peak areas in UHPLC-PGC-MS with sum of all as 100%.

peak no.	Tr (min)	$[M-H]^-$	relative abundance (%)	tentative / conclusive identification	MS^2 *m/z* 263 (%)	MS^3 *m/z* 263 (%)	confirmation by available reference
2a	6.7	343	27	β-D-Glc-(1→4)-D-Glc	n.d.		+
3a	11.1	505	8	β-D-Glc-(1→4)-βD-Glc-(1→4)-D-Glc	20.8		+
3b	12.4	505	2	β-D-Glc-(1→3)-βD-Glc-(1→4)-D-Glc	0.2		+
4a	15.3	667	58	β-D-Glc-(1→3)-β-D-Glc-(1→4)-β-D-Glc-(1→4)-D-Glc	0.7	8.3[a]	-
5a	19.3	829	5	β-D-Glc-(1→4)-β-D-Glc-(1→3)-β-D-Glc-(1→X)-β-D-Glc-(1→X)-D-Glc	2.7	0.4[b]	-

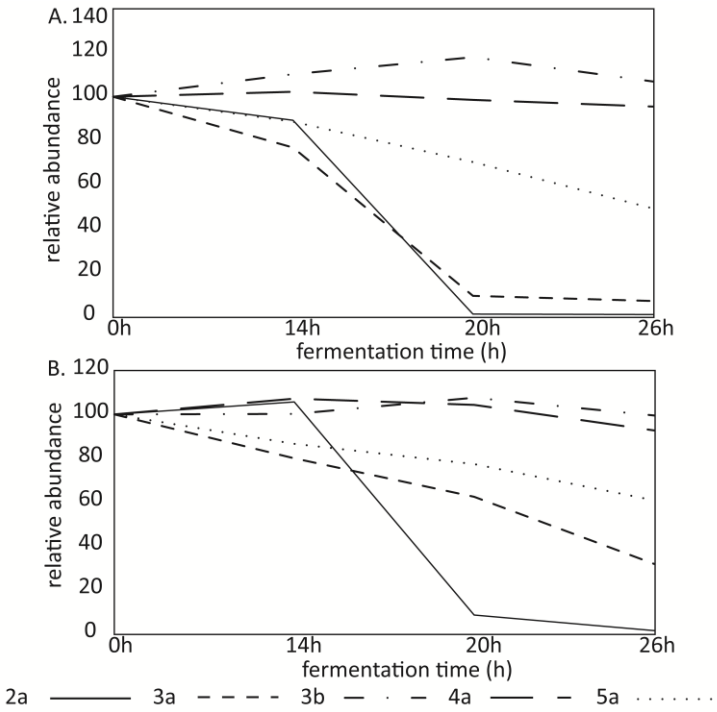

Figure S1 Percentages of remaining enzyme-treated oat β-glucan oligomers during *in vitro* fermentation using pooled faecal inoculum of 2- (A) and 8- (B) week-old infants. Concentrations per oligomer in the original enzyme-treated oat β-glucan were set at 100%. Chemical structures of oligomer 2a, 3a, 3b, 4a and 5a are summarized in Table S1.

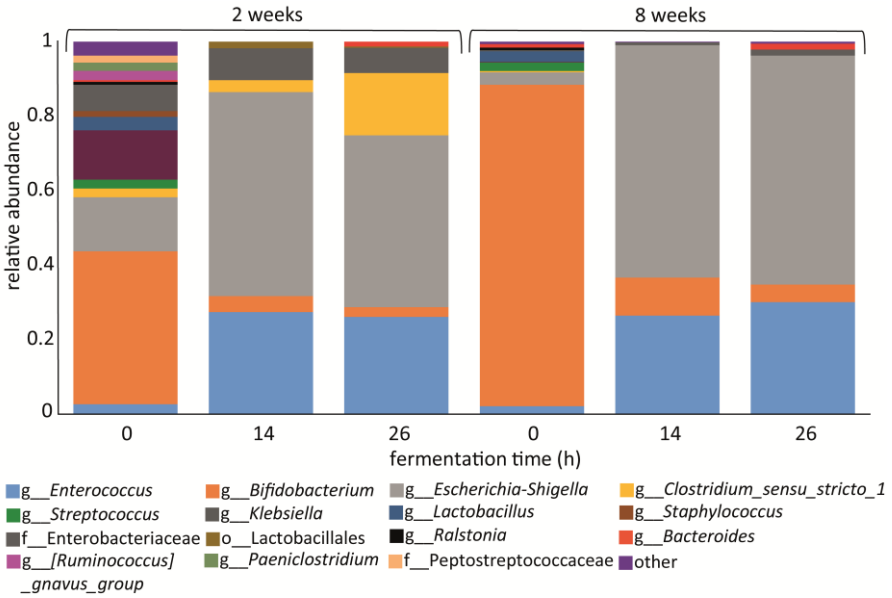

Figure S2 Relative abundance of bacteria at the highest classified taxonomy in fermentation digesta collected at the start and after 14 and 26 h from *in vitro* fermentation containing solely SIEM medium and faecal inoculum of 2- and 8-week-old infants.

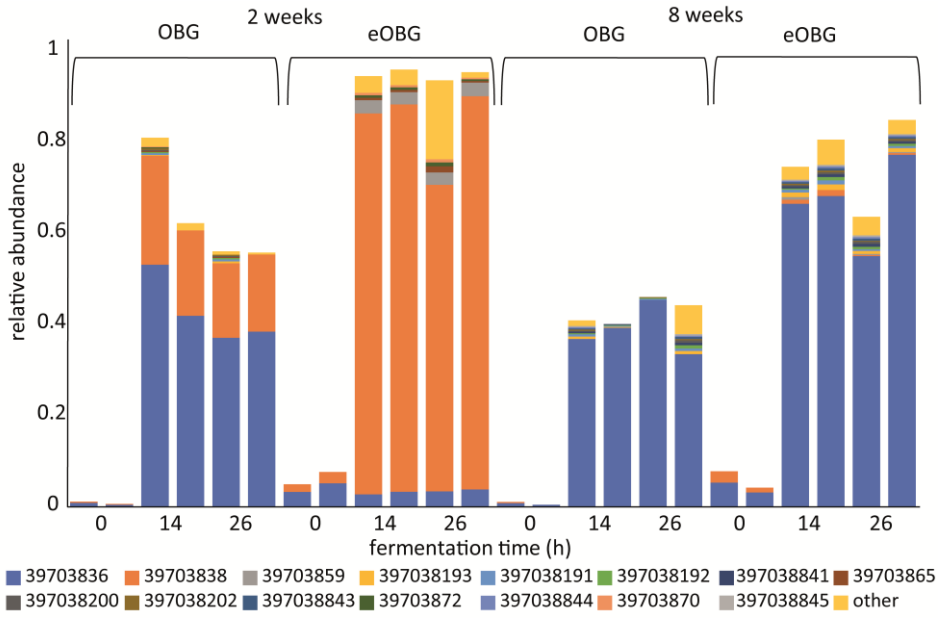

Figure S3 Relative abundance of *Enterococcus* Amplicon Sequencing Variants in duplicate fermentation digesta collected at the start and after 14 and 26 h from *in vitro* fermentation of media supplemented with native oat β-glucan (OBG) and enzyme-treated oat β-glucan (eOBG) using pooled faecal inoculum of 2- and 8-week-old infants.

Table S2 Sequences of *Enterococcus* ASVs 39703836 and 39703838.

ASV 39703836
TGGTAGTCCACGCCGTAAACGATGAGTGCTAAGTGTTGGAGGGTTTCCGCCCTTCAGTGCTGCAGCAAAC
GTCACTTTGTCCCCGAAGGGAAAGCTCTATCTCTAGAGTGGTCAAAGGATGTCAAGACCTGGTAAGGTTC

ASV 39703838
TGGTAGTCCACGCCGTAAACGATGAGTGCTAAGTGTTGGAGGGTTTCCGCCCTTCAGTGCTGCAGCTAAC
GTCACTTTGCCCCCGAAGGGGAAGCTCTATCTCTAGAGTGGTCAAAGGATGTCAAGACCTGGTAAGGTTC

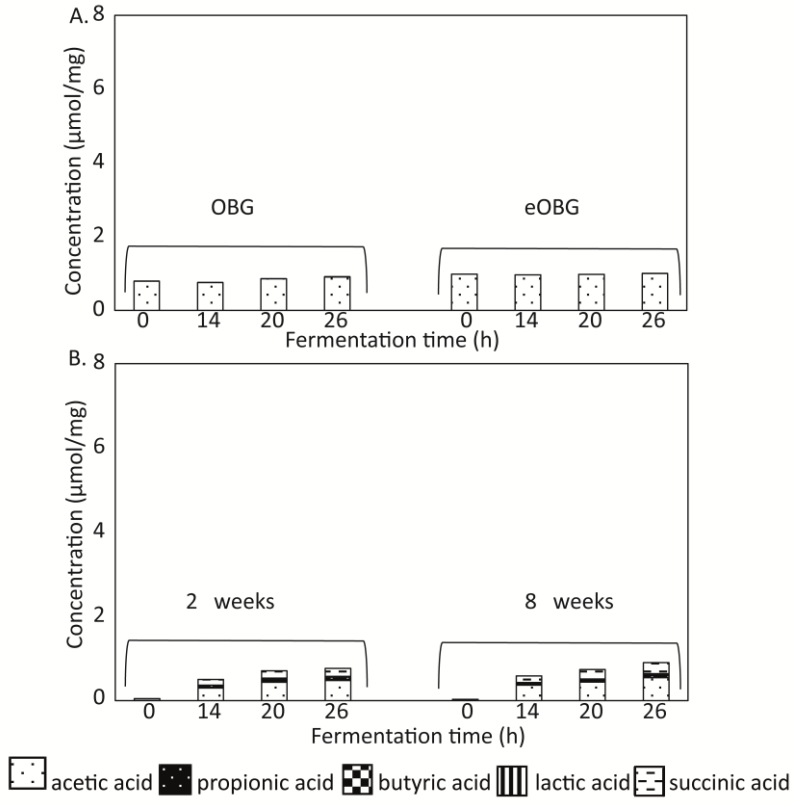

Figure S4 Production of SCFAs, lactic acid and succinic acid upon *in vitro* fermentation containing solely native oat β-glucan (OBG) / enzyme-treated oat β-glucan (eOBG) and SIEM medium (A) or infant faecal inoculum and SIEM medium (B). The acetate in the control fermentation without added inoculum is primarily originating from the sodium acetate buffer used in the OBG and eOBG preparation.

Chapter 5

Touching the high complexity of prebiotic Vivinal galacto-oligosaccharides using porous graphitic carbon ultra-high-performance liquid chromatography coupled to mass spectrometry.

Abstract

Galacto-oligosaccharides (GOS) are used in infant formula to replace the health effects of human milk oligosaccharides, which appear to be dependent on the structure of the individual oligosaccharides present. However, a comprehensive overview of the structure-specific effects is still limited due to the high structural complexity of GOS. In this study, porous graphitic carbon (PGC) was used as stationary phase during ultra-high performance liquid chromatography-mass-spectrometry (UHPLC-MS). This approach resulted in the recognition of more than 100 different GOS structures in one single run, including reducing and non-reducing GOS isomers. Using NMR-validated structures of GOS trisaccharides, we discovered MS fragmentation rules to distinguish reducing isomers with a mono- and di-substituted terminal glucose by UHPLC-PGC-MS. UHPLC-PGC-MS enabled effective recognition of structural features of individual GOS components in complex GOS preparations and during e.g. biological conversion reactions. Hence, this study lays the groundwork for future research into structure-specific health effects of GOS.

Logtenberg, M.J.; Donners, K.M.H.; Vink, J.C.M.; van Leeuwen, S.S.; de Waard, P.; de Vos, P.; Schols, H.A. *Journal of Agricultural and Food Chemistry*; **2020**; 68: 7800-7808.

Introduction

Postnatal nutrition has a lifelong impact on health and well-being as it guides the development of the complex interactions between the intestinal microbiota and the gastrointestinal immune system [1,2]. Although breast milk is still considered the gold standard, many types of infant formula are nowadays commercially available for those infants for which exclusive breastfeeding is not an option. Oligosaccharides present in human milk (HMOs) function as prebiotics and have a direct effect on immunity by supporting the development of the gut barrier [3,4]. Currently only a limited number of less complex HMOs such as 2'FL, 3'SL and LNT are commercially available and applied in infant formula [5]. Therefore, predominantly galacto-oligosaccharides (GOS) and the less complex fructo-oligosaccharides (FOS) are used as substitute to replace the health effects of HMOs in infant formula [6].

GOS are produced by hydrolysis and transgalactosylation of lactose, which process is catalysed by β-galactosidase [7]. This results in galactose chains with a terminal reducing glucose or galactose unit, varying in the degree of polymerization (DP) from 2-8 and in the type of glycosidic linkage; β(1-2), β(1-3), β(1-4) and β(1-6) [7]. Besides GOS with a free anomeric carbon at the terminal position (reducing GOS), also non-reducing GOS containing the structural motif α-D-Glc*p*-(1↔1)-β-D-Gal*p* or β-D-Glc*p*-(1↔1)-β-D-Gal*p* have been reported [8-10]. The source of the enzyme has a large influence on both the regioselectivity of the enzyme and the size of the produced oligosaccharides, resulting in mixtures enriched in either β(1-3)-, β(1-4)- or β(1-6)-linked galactose residues [11]. As the applied enzymes vary in industry, several structurally distinct GOS mixtures are commercially available [12,13].

The prebiotic effects of GOS vary depending on its monomer composition, type of glycosidic linkages and DP [14-17]. For example, previous *in vitro* studies with pig and human faecal microbiota showed the preference of microbiota for degradation of β(1-2)- and β(1-3)-linkages over β(1-4)- and β(1-6)-linkages [14,15]. In studies aiming on restoring *Bifidobacterium* levels in antibiotic-disrupted microbiota from adults, GOS DP≥4 was more efficient than GOS DP≤3 [14]. Also, immune effects are demonstrated to depend on the structure of GOS, as DP2 and DP3 showed to have a higher protective effect on the intestinal barrier integrity than higher DPs [18]. However, to date, there is little evidence of the exact relationship between the structure of individual GOS components and their prebiotic and immune effects [14-18], which could be partly explained by the lack of high-throughput characterisation methods which enable the recognition of individual GOS components in complex GOS preparations and during e.g. biological conversion reactions.

Over the past decade several studies described the characterization of GOS using techniques such as hydrophilic interaction chromatography (HILIC) coupled to mass spectrometry (MS) [13] and preparative HILIC of DP fractions prior to ^{1}H and ^{13}C nuclear magnetic resonance (NMR) analysis [8]. The study by van Leeuwen et al [10] offers probably

the most comprehensive overview so far of the different components present in Vivinal GOS, a commercial GOS mixture produced by a *Bacillus circulans* β-galactosidase [19]. Preparative high performance anion exchange chromatography combined with pulsed amperometric detection (HPAEC-PAD) of DP fractions prior to ^{1}H and ^{13}C NMR analysis revealed more than 40 different components [10]. The employed *Bacillus circulans* β-galactosidase introduced β(1-2), β(1-3), β(1-4) and β(1-6) elongations on the reducing glucose residue. However, longer oligosaccharides (DP≥4) were reported to be mainly β(1-4)-elongations of acceptor disaccharides and trisaccharides by β-D-Galp [10,11].

Nonetheless, HPAEC-based characterization methods alone might not be suitable for structure-function studies in which the complex relation between the structure of GOS and a specific bioactivity is monitored. Co-elution of isomers and GOS structures having a different DP hinders the annotation of individual GOS [10]. Labour-intensive size-exclusion chromatographic (SEC) fractionation of GOS into its constituent DPs prior to analysis will help, but is not suitable for structure-function studies. Porous graphitic carbon (PGC) chromatography could potentially overcome this limitation. The retention mechanism of this stationary phase is based on size, type of linkage and resulting 3D-structure of oligosaccharides [20]. As such, PGC chromatography provides adequate separation of GOS and HMOs and has a high sensitivity [21,22]. The excellent chromatographic resolution even resulted in the partial separation of α- and β- anomers [23], although complicating the already complex elution pattern. Reduction of the oligosaccharides prior to analysis avoids the occurrence of such double peaks, while maintaining a good separation of the different oligosaccharides [22].

PGC with ultra-high performance liquid chromatography (UHPLC) is highly compatible with MS, which enables the characterization of galacto-oligosaccharides based on *m/z* and MS^2 fragmentation spectra. Nonetheless, MS fragmentation pathways of derivatized galacto-oligosaccharides are highly complex and partly unknown [13] [24]. Hence, NMR generally proves to be highly valuable for the conclusive characterization of oligosaccharides [25].

In this study a high-throughput characterization method was developed for GOS based on UHPLC-PGC-MS. Both SEC and preparative UHPLC-PGC-MS were applied to obtain pure isomers representing different isomer classes. These isomers were analysed with NMR to be able to connect the structure to the observed MS^2 fragmentation. The developed characterization method will provide novel insight in the complexity of GOS mixtures currently applied in infant formula and ultimately will contribute to a better understanding of structure-specific health effects of GOS.

Material and methods

Materials

Purified Vivinal® GOS was kindly provided by Friesland Campina DOMO (Beilen, The Netherlands). Vivinal® GOS was fractionated to obtain the purified Vivinal® with <3% (w/w dry matter) monomers and lactose. In short, the lactose present in Vivinal® GOS was hydrolysed, followed by removal of the monosaccharides by nanofiltration.
GOS DP3 standards β-3'-Galactosyl-lactose, β-4'-Galactosyl-lactose and β-6'-Galactosyl-lactose were purchased from Carbosynth (Berkshire, UK).

Fractionation of Vivinal GOS

Fractionation on DP using Size Exclusion Chromatography

Vivinal GOS was fractionated on DP by size exclusion chromatography (SEC) using an AKTA purifier system (GE Healthcare, Chicago, United States). GOS (20 mg/ml, 5 ml) was injected into three serially connected Hiload 26/60 Superdex 30 preparative grade columns with each a column volume of 300 ml (GE Healthcare). The temperature was set at 35°C and the flowrate at 2.6 ml H_2O/min. A refractive index (RI) detector (Shodex RI-72, Yokohama, Japan) was used to monitor the elution. Eluent containing GOS was collected in 5 ml fractions using a Frac-950 fraction collector (GE Healthcare). Subsequently, fractions were analysed using matrix-assisted laser desorption/ionisation time of flight mass spectrometry (MALDI-TOF-MS) as described previously [26] to determine the molecular weight of GOS present in the fractions. The fractions with a purity of at least 90% according to the signal intensity as measured by MALDI-TOF-MS were pooled. Fractions containing DP3 which eluted between 720 and 740 ml, of multiple runs were pooled and freeze-dried. Based on elution pattern and *m/z*, also DP1, 2, 4, 5, 6 and ≥7 were combined per DP and freeze-dried. Weights obtained per DP were used to determine the relative abundance of the different DPs in purified Vivinal GOS.

Reduction of purified GOS DP3

Prior to further fractionation, 100 mg of purified GOS DP3 was subjected to reduction conditions and subsequently purified by solid-phase extraction (SPE). Freshly prepared 0.5 M sodium borohydride ($NaBH_4$) was added to GOS DP3 (1.25 mg/ml) in a ratio 1:1 (v/v) and incubated overnight at room temperature. Cartridges (bed weight: 250 mg, column volume: 3 ml, Carbograph, Supelclean ENVI carb; Sigma Aldrich, St. Louis, MO, USA) were activated with 1.5 ml of 80:20 (v/v) acetonitrile (ACN)/H_2O, followed by 4x 1.5 ml H_2O. The reduced GOS DP3 including non-reducing isomers ((1-1)-linkage) (10 ml) were loaded on the cartridge, after which the cartridge was washed 2 times with 2 ml H_2O. Subsequently reduced (including non-reducing) GOS DP3 were eluted with 2x 1.5 ml of 40:60 (v/v) ACN/H_2O. Eluted reduced (including non-reducing) GOS were dried at 30°C under nitrogen gas, re-solubilized in H_2O and freeze-dried.

Fractionation of reduced (including non-reducing) DP3 using preparative UHPLC-PGC-MS

Fractionation was performed on a Waters preparative LC-MS system, equipped with a 2767 sample manager, 2545 quaternary gradient module, fluid organizer, 3100 mass detector and 2998 photodiode array detector (Waters, Milford, MA, USA). Reduced (including non-reducing) GOS DP3 (95 mg/ml, 0.5 ml) was centrifuged (5 min, 15 000g) and injected onto a porous graphitic carbon (pgc) column (150 mm x 21.2 mm, 5 µm particle size, Hypercarb; Thermo Scientific, San Jose, CA, USA). The flow rate was set at 18.34 ml/min. Mobile phase A consisted of: ULC-MS water + 0.1% (v/v) formic acid and B: acetonitrile (ACN) + 0.1% (v/v) formic acid. The gradient applied was as follows: 0-80.8 min, 3-11% B; 80.8-95.3 min, 11-100% B; 95.3-109.9 min, 100-3% B, followed by equilibration at 3% B. Fractions of 6.1 ml were collected and analysed using analytical UHPLC-PGC-MS (2.3.2). Fractions were pooled based on the retention time and MS^2 fragmentation of the isomer present. Only fractions with a purity of 90% according to the signal intensity as measured by analytical UHPLC-PGC-MS were pooled. Afterwards ACN was evaporated under a stream of nitrogen gas and the remaining water phase was freeze-dried.

Characterization of Vivinal GOS DP3

Determination monosaccharide composition Vivinal GOS DP3

The monosaccharide composition of reduced (including non-reducing) Vivinal GOS DP3 was determined using HPAEC-PAD. Prior to analysis reduced (including non-reducing) Vivinal GOS DP3 was completely hydrolysed using trifluoroacetic acid (TFA) and subsequently dissolved in 2M TFA (0.2 mg/ml). After an incubation of 1 h at 121°C, TFA was evaporated under a stream of air at 40°C. The dried sample was resolubilized in water (0.025 mg/ml) and centrifuged (5 min, 15 000g). Ten µl of sample was injected to an ICS5000 system (Dionex, Sunnyvale, CA, USA) with a CarboPac PA-1 column (250 mm x 2 mm ID), a CarboPac PA guard column (25 mm x 2 mm ID) and a ISC5000 ED detector (Dionex) in the PAD mode. The flow rate was set at 0.4 ml/min. Mobile phase A (0.1 M sodium hydroxide), B (1 M sodium acetate in 0.1 M sodium hydroxide) and C (H_2O) were used with the following elution profile: 0-35 min, 100% C; 35.1-50 min, 100% A – 40% B; 50.1-55 min, 100% B; 55.1-63 min, 100% A; 63.1-78 100% C. Post-column addition of 0.5M NaOH at 0.1 ml/min was performed between 0-35 min and 63.1-78 min. Galactose and glucose standards were included in the analysis. The data were analysed using Chromeleon 7.0 (Thermo Scientific).

Analytical UHPLC-PGC-MS

Reduced (including non-reducing) GOS DP3 isomers were analysed on an Accela UHPLC system (Thermo Scientific) coupled to a mass spectrometer (LTQ Velos Pro ion trap MS, Thermo Scientific) as described elsewhere with some minor modifications [27]. Samples (0.5 µl, 0.25 mg/ml) were injected on a Hypercarb PGC column (3 µm particle size, 2.1 mm x 150 mm) in combination with a Hypercarb guard column (3 µm particle size, 2 mm x 10 mm;

Thermo Scientific). As mobile phase A: ULC-MS water + 0.1% (v/v) formic acid was used. Mobile phase B consisted of ACN + 0.1% (v/v) formic acid. The flow rate was 300 µl/min. The solvents were eluted according to the following profile: 0-2 min, 3% B; 2-51.7 min, 3-11% B; 51.7-53.2 min, 11-100% B; 53.2-61 min, 100% B; 61-62.5 min, 100-3% B; 62.5-70.3 min, 3% B. The temperatures of the autosampler and column oven were controlled at 10 and 25°C respectively. ULC-MS water containing 3% ACN was used to wash the autosampler needle. DP3 standards β-3-Galactosyl-lactose, β-4-Galactosyl-lactose and β-6-Galactosyl-lactose were used for the identification of GOS isomers. Vivinal GOS was analysed to identify the DP3 isomers in the Vivinal GOS mixture. Prior to analysis both the standards and Vivinal GOS were reduced and purified using a small-scale SPE method as described elsewhere [27]. Data acquisition and processing were performed using Xcalibur (version 2.2, Thermo Scientific).

NMR

GOS DP3 isomer fractions (approximately 100 µg) were dissolved in 1 ml 99.8% deuterium oxide (D_2O) to exchange all protons of the sugar hydroxyl groups with deuterium. The samples were freeze-dried, dissolved in 0.7 ml 99.8% D_2O and transferred into a NMR-tube. A small droplet of acetone was added on the top of the inside of the tube as an internal standard. This droplet was evaporated for 10 s and then mixed in with the sample and set on δ=2.225 ppm for ^{1}H spectra and on δ =31.55 ppm for ^{13}C spectra.

Results

Vivinal GOS is highly complex

The complete Vivinal GOS preparation was analysed using UHPLC-PGC-MS after reduction of all reducing ends. Figure 1 shows the presence of a large number of oligosaccharides in Vivinal GOS. The structural complexity of Vivinal GOS becomes even more apparent when the *m/z* values are selected for each DP (Figure 1), which shows the large variety of isomers per DP.

The non-reducing isomers containing a (1-1)-linkage were easily distinguished based on a *m/z* difference of 2 as they could not be reduced by $NaBH_4$. Non-reducing DP3 isomers showed an overlap in retention time with reducing DP3 isomers (Figure 2). Taking into account their relatively low abundance, most non-reducing DP3 isomers would not have been detected without reduction prior to analysis. In total, UHPLC-PGC-MS of reduced Vivinal GOS enabled the identification of 15 non-reducing and 23 reducing DP3 isomers.

Theoretically, each DP3 isomer could be further elongated during GOS production by β-galactosidase via either a β(1-3)-, β(1-4)-, β(1-6)- or β(1-2)-linkage resulting in 4 distinct DP4 isomers for each distinct DP3 isomer, which number would be even higher when branching of the backbone is taken into consideration. However, Vivinal GOS DP4 is 'only' composed of 21 reducing and 13 non-reducing isomers (Figure 3) and DP5 of 24 reducing and 11 non-

reducing isomers (Figure 4). This finding confirms the presence of homologue series as reported in a previous study [10] with longer oligosaccharides (DP≥4) presented by β(1-4)-elongations of acceptor disaccharides and trisaccharides by β-D-Galp. Additionally, reducing isomers are most dominant in each DP as they contributed to 86, 87 and 84% of the peak area of DP3, DP4 and DP5 respectively. For further characterization the focus will be on DP3 as it will also give us insights in the structures of higher DPs.

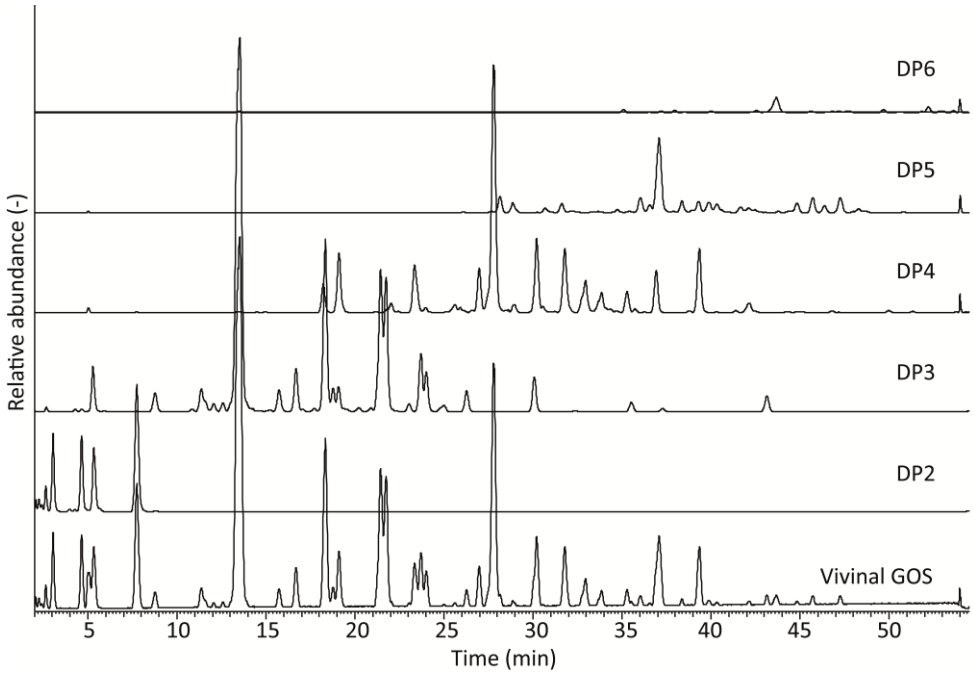

Figure 1 UHPLC-PGC-MS profile of reducing and non-reducing Vivinal GOS and of DP 2-6 after selection of the appropriate *m/z* for that DP. All elution profiles were normalised to the actual contribution of each DP to the total mixture.

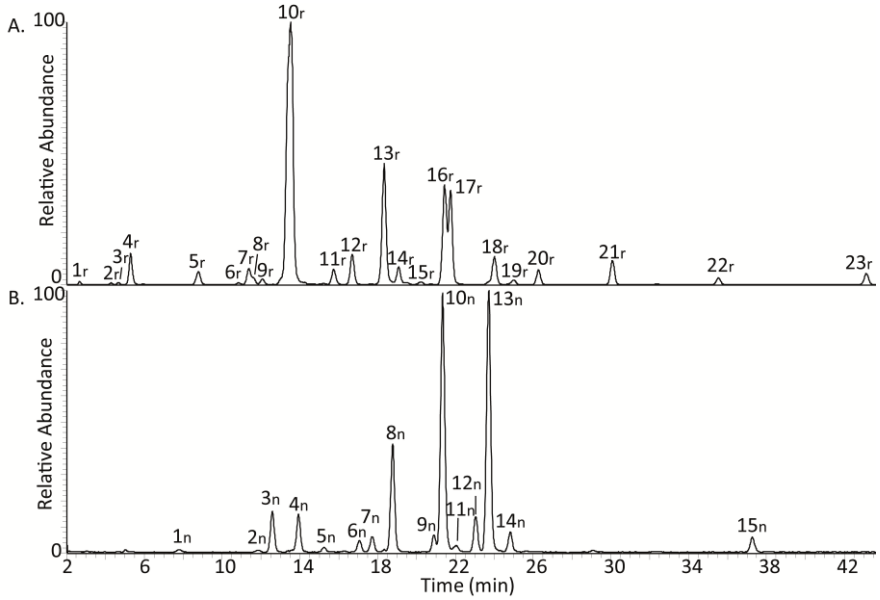

Figure 2 UHPLC-PGC-MS profile of Vivinal GOS DP3 with selection of A: reducing (*m/z* 505, 551 (M+FA)) and B: non-reducing (*m/z* 503, 549 (M+FA)) isomers. Most abundant peak in both chromatograms was set at 100%. Peak numbers correspond to characterized GOS isomers in Table 1 with r: reducing isomers and n: non-reducing isomers ((1-1)-linked).

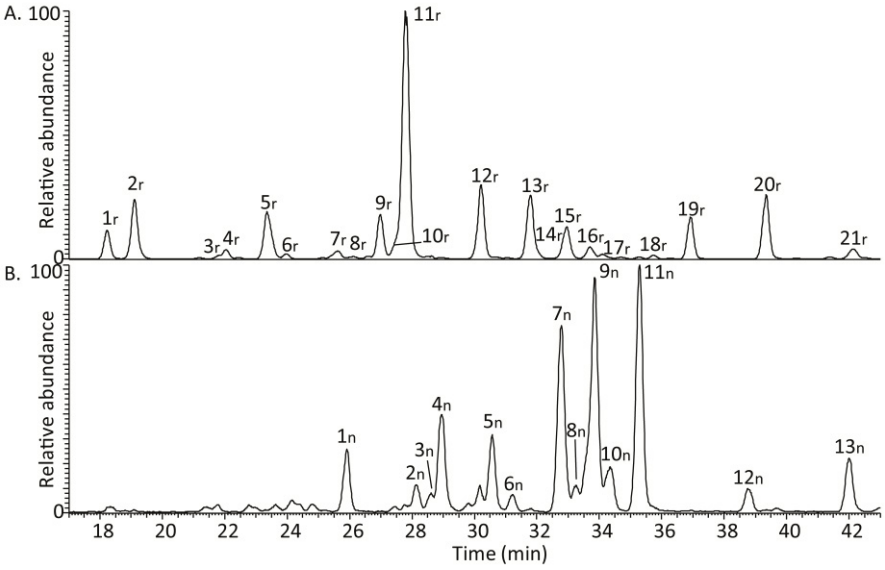

Figure 3 UHPLC-PGC-MS profile of Vivinal GOS DP4 with selection of A: reducing (m/z 667, 713 (M+FA)) and B: non-reducing (m/z 665, 711 (M+FA)) isomers. The most abundant peak in both chromatograms was set at 100%. Peak numbers of the reducing isomers (r) correspond to the different reducing GOS DP4 isomers in Table S3. Peak numbers of the non-reducing isomers (n) only present the different non-reducing GOS DP4 isomers.

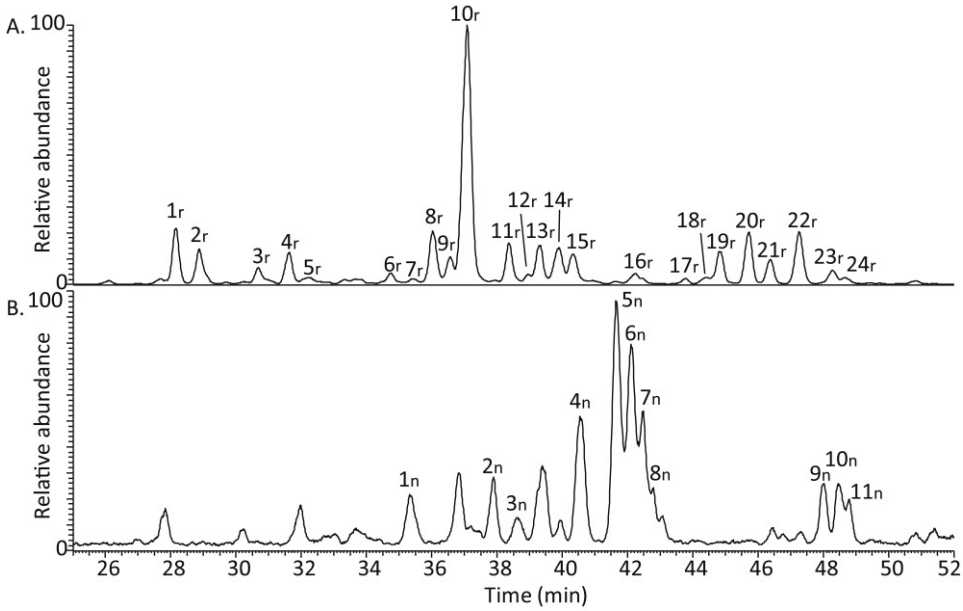

Figure 4 UHPLC-PGC-MS profile of Vivinal GOS DP5 with selection of A: reducing (*m/z* 829, 875 (M+FA)) and B: non-reducing (*m/z* 827, 873 (M+FA)) isomers. The most abundant peak in both chromatograms was set at 100%. Peak numbers present the different reducing (r) and non-reducing (n) GOS DP5 isomers.

Characterisation of Vivinal GOS DP3

Characterisation of GOS DP3 isomers was based on analytical UHPLC-PGC-MS covering all isomers. NMR analysis of pure isomers representing different isomer classes was performed to link the structures to the observed MS^2 fragmentation. This provides deeper insight into the fragmentation behaviour of GOS. Additionally, the constituent monomer composition was determined using hydrolysis prior to HPAEC analysis. In the following paragraphs the characterisation of various isomers will be further described.

Characterisation of purified GOS DP3 isomers using NMR

NMR is used for the characterization of GOS DP3 isomers representing different isomer classes. The purity of the isomers is of importance for NMR analysis. Due to substantial overlap of isomers with different DP (Figure 1), Vivinal GOS was first fractionated on size (DP) using SEC to facilitate further fractionation on isomer level. According to the weight obtained per DP, their relative abundance in Vivinal GOS was as follows: DP1, 2%; DP2, 11%; DP3, 46%; DP4, 25%; DP5, 10%; DP6, 4% and DP>7, 2%. The obtained GOS DP3 pool was reduced and further fractionated by preparative UHPLC-PGC-MS to obtain pure isomers. Preparative UHPLC-PGC-MS showed a similar peak resolution when compared to the analytical method (data not shown). In total 4 different GOS DP3 isomers representing different isomer classes (Figure 2; no. 4_r, 13_r, 21_r and 13_n) were obtained for further NMR analysis in sufficient amount and purity.

From the NMR data all ^{1}H and ^{13}C chemical shifts could be determined for the four isolated structures (Table S1). The chemical shift patterns of the two Gal residues B and C of structures 4_r and 13_r fit with data expected for non-reducing terminal β-D-Gal*p* residues. This suggests a structure with two terminal Gal residues, indicating a di-substituted glucitol residue A [10]. For structure 4_r the glucitol residue A showed H-2;C-2 and H-4;C-4 chemical shifts that significantly shifted from literature data for glucitol [28], indicating a di-substituted glucitol residue at positions O-2 and O-4. The heteronuclear multiple bond correlation (HMBC) spectrum showed correlations between C H-1:C-1 and A H-2:C-2 and between B H-1:C-1 and A H-4:C-4. These data fit the structure β-D-Gal*p*-(1→2)[β-D-Gal*p*-(1→4)]Glc-ol. For structure 13_r the H-2:C-2 and the H-6a/b:C-6 are significantly shifted, indicating substitution at these positions. The HMBC spectrum showed correlations between B H-1:C-1 and A H-6a/b:C-6 and between C H-1:C-1 and A H-2:C-2, confirming the disubstitution of glucitol residue A. These data lead to structure β-D-Gal*p*-(1→2)[β-D-Gal*p*-(1→6)]-Glc-ol. Structure 21_r showed only a shifted H-4;C-4 in the glucitol residue, fitting a monosubstituted glucitol residue. Residue B showed a chemical shift pattern matching a 4-substituted β-D-Gal*p* residue, while residue C matched with a terminal β-D-Gal*p* residue (Table S1). These data lead to a β-D-Gal*p*-(1→4)-β-D-Gal*p*-(1→4)-Glc-ol structure. The NMR spectra of structure 13_n matched exactly with data for the non-reducing GOS structure β-D-Gal*p*-(1→4)-α-D-Glc*p*-(1↔1)-β-D-Gal*p* reported previously [9].

Ratio of galactose and glucose monomers in Vivinal GOS DP3

Theoretically both glucose and galactose could be present at the reducing end of GOS, as lactose, galactose and glucose can serve as acceptor for the enzyme-galactose complex in the transgalactosylation reaction [29]. In contrast to NMR, UHPLC-PGC-MS analysis does not allow the conclusive differentiation between galactose and glucose monomers. Therefore, the monosaccharide composition of Vivinal GOS DP3 was determined using hydrolysis prior to HPAEC analysis. Galactose and glucose are present in 2.1:1 ratio in Vivinal GOS DP3. This means that only 3.4% of all GOS DP3 isomers is composed of three galactose monomers. The preference for glucose or lactose as acceptor in the transgalactosylation reaction was supported by previous in-depth characterization of Vivinal GOS, where the presence of isomers with a galactose at the reducing end was limited to DP2 [10]. For further characterization using UHPLC-PGC-MS it is thus assumed that glucose is present at the reducing end of the GOS DP3 isomers.

Characterization of DP3 isomers using UHPLC-PGC-MS

Analytical UHPLC-PGC-MS was used for the characterization of reduced and non-reducing GOS DP3 isomers present in Vivinal GOS. First of all, β-3'-Galactosyl-lactose (Figure 2; no. 20_r), β-4'-Galactosyl-lactose (no. 10_r) and β-6'-Galactosyl-lactose (no.18_r) were characterized based on comparison of retention time and MS^2 fragmentation to those of the corresponding commercial standards.

Linkage-specific cross-ring MS^2 fragmentation was investigated to determine β(1-4)- and β(1-6)-linkages, as described in previous studies of GOS [30,31]. The fragment ions are described according to the nomenclature of Domon and Costello [32] The presence of $^{0,2}A_2$(-H_2O) and the absence of $^{0,3}A_2$ cross-ring fragments indicate β(1-4)-linkages, whereas the presence of $^{0,3}A_2$ and the absence of $^{0,2}A_2$(-H_2O) cross-ring fragments indicate β(1-6)-linkages, with ions at *m/z* 263 for $^{0,2}A_2$(-H_2O) and at *m/z* 251 for $^{0,3}A_2$ cross-ring fragments in negative ionisation (NI) mode [30,31]. These MS fragmentation rules were confirmed by the MS fragmentation behaviour of known GOS DP3 structures present in pure form. Unfortunately, these rules are only applicable for linkage identification at the non-reducing end due to disappearance of the ring structure upon reduction. Nonetheless, these MS fragmentation rules resulted in the partial characterization of four reducing isomers; no. 3_r, no. 5_r, no. 7_r and no. 14_r (Figure 2) representing β-D-Gal*p*-(1→6)-β-D-Gal*p*-(1→X)-D-Glc, β-D-Gal*p*-(1→6)-β-D-Gal*p*-(1→X)-D-Glc, β-D-Gal*p*-(1→4)-β-D-Gal*p*-(1→3/6)-D-Glc and β-D-Gal*p*-(1→6)-β-D-Gal*p*-(1→X)-D-Glc respectively. MS^2 fragmentation of GOS DP3 isomers is summarized in Table S2.

Furthermore, comparison of the MS^2 fragmentation spectra of the selected isomers characterised by NMR no. 4_r, no. 21_r, no. 10_r and no. 13_r resulted in MS fragmentation rules to distinguish mono- and disubstitution of the glucitol (Figure 5). The dominance of an Z_2 fragment with *m/z* 325 indicates a disubstituted glucitol, whereas the dominance of Y_2 fragment with *m/z* 343 indicates a monosubstituted glucitol with 2 consecutive galactose units. In total 7 out of 23 reducing GOS DP3 isomers are composed of a disubstituted glucitol. The fragmentation rule can also be applied to higher DPs. For reducing GOS DP4 isomers clear differences in relative abundance were observed between Z_3 (*m/z* 487) and Y_3 (*m/z* 505) fragments in the mass spectra (Table S3). Interestingly, also for DP4 7 isomers with a disubstitution were detected. Additionally, PGC-elution patterns were comparable for DP3 and DP4 with on average lower retention times for disubstituted isomers. Taking into account the presence of homologous series, these findings suggest that also for DP4 disubstitution is located at the glucitol residue.

For the characterization of the non-reducing DP3 isomers, the same cross-ring MS fragmentation rules were applied. MS2 fragmentation did not provide conclusive information on the type of linkage or monomers present in each non-reducing isomer. Nonetheless, in total 6 non-reducing isomers with a β(1-4)-linkage and 2 non-reducing isomers with a β(1-6)-linkage were identified.

An overview of all conclusively- and tentatively characterized or unknown GOS isomers are shown in Table 1 and 2 for respectively reducing and non-reducing isomers. Peak numbers correspond to numbered peaks in Figure 2. In total 29 out of 38 reducing and non-reducing GOS DP3 isomers were partially or completely characterized. The developed characterization method based on UHPLC-PGC-MS thus showed us that Vivinal GOS DP3 is highly diverse.

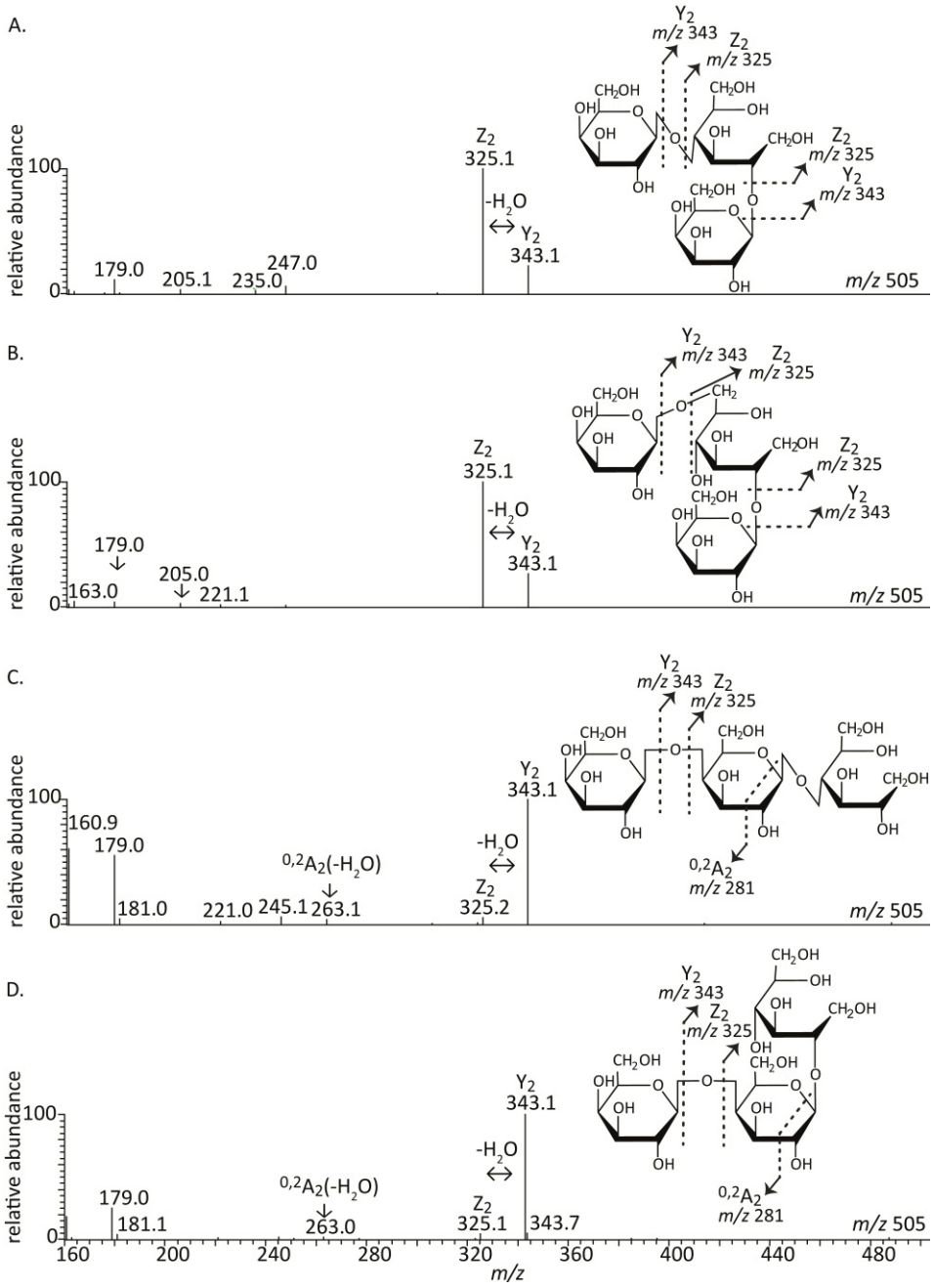

Figure 5 Fragmentation spectra (ESI MS^2) in negative mode of GOS DP3 isomers A: no. 4r, B: no. 21r, C: no. 10r, D: no. 13r. The proposed routes of formation of the fragment ions which are used to distinguish reducing isomers with a mono- and di-substituted glucitol, are indicated in the spectra. The fragment ions are described according to the nomenclature of Domon and Costello [32].The *m/z* of precursor ion was 505.

Table 1 Overview of conclusively and tentatively characterised or unknown reducing GOS DP3 isomers.

peak no.	graphical structure[a]	relative abundance (%)[b]	substitution glucitol	chemical structure[c]
1r	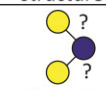	0.2	disubstituted	X
2r		0.1	disubstituted	X
3r		0.1	monosubstituted	(1→6)(1→X)
4r		2.3	disubstituted	β-D-Gal*p*-(1→2)-[β-D-Gal*p*-(1→4)-]D-Glc
5r		1.3	monosubstituted	(1→6)(1→X)
6r		0.2	disubstituted	X
7r	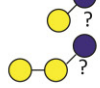	1.4	monosubstituted	(1→4)(1→3/6)
8r	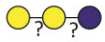	0.6	monosubstituted	X
9r		0.5	monosubstituted	X
10r	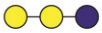	37.8	monosubstituted	β-D-Gal*p*-(1→4)-β-D-Gal*p*-(1→4)-D-Glc
11r	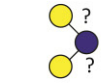	1.5	disubstituted	X
12r	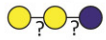	2.8	monosubstituted	X
13r		11.2	monosubstituted	β-D-Gal*p*-(1→4)-β-D-Gal*p*-(1→2)-D-Glc
14r		1.6	monosubstituted	(1→6)(1→X)
15r		0.3		X
16r	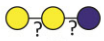	8.9	monosubstituted	X
17r		8.2	disubstituted	X
18r		2.9	monosubstituted	β-D-Gal*p*-(1→6)-β-D-Gal*p*-(1→4)-D-Glc
19r		0.6		X
20r		1.4	monosubstituted	β-D-Gal*p*-(1→3)-β-D-Gal*p*-(1→4)-D-Glc
21r		2.3	disubstituted	β-D-Gal*p*-(1→2)-[β-D-Gal*p*-(1→6)-]D-Glc
22r		0.7	monosubstituted	X
23r		1.1	monosubstituted	X

[a] included for conclusively and tentatively characterized isomers, yellow: galactose, blue: glucose and ?: unknown type of glycosidic linkage
[b] determined by integration of peak areas in UHPLC-PGC-MS with sum of both reduced and non-reducing DP3 isomers set at 100%
[c] X: unknown

Table 2 Overview of conclusively and tentatively characterised or unknown non-reducing GOS DP3 isomers.

peak no.	graphical structure[a]	relative abundance (%)[b]	chemical structure[c]
1n		0.1	X
2n		0.04	(1→4)(1↔1) / (1↔1)(4←1)
3n		0.6	X
4n		0.6	(1→4)(1↔1) / (1↔1)(4←1)
5n		0.1	(1→6)(1↔1) / (1↔1)(6←1)
6n		0.2	(1→4)(1↔1) / (1↔1)(4←1)
7n		0.2	X
8n		1.5	(1→4)(1↔1) / (1↔1)(4←1)
9n		0.2	X
10n		3.7	(1→4)(1↔1) / (1↔1)(4←1)
11n		0.2	X
12n		0.5	(1→6)(1↔1) / (1↔1)(6←1)
13n	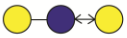	3.9	β-D-Gal*p*-(1→4)-α-D-Glc*p*-(1↔1)-β-D-Gal*p*
14n		0.3	X
15n		0.2	X

[a] included for conclusively characterized isomers, yellow: galactose, blue: glucose
[b] determined by integration of peak areas in UHPLC-PGC-MS with sum of both reduced and non-reducing DP3 isomers set at 100%
[c] X: unknown

Discussion

The glycosidic linkage and the degree of polymerization (DP) of galacto-oligosaccharides (GOS) affect their bioactivity as observed for fermentability and consequent health effects [14-18], but solid evidence for these structure-function relationships is still limited. This is partially due to the high complexity of GOS with several GOS isomers present per DP. In this study, a high-throughput characterization method based on UHPLC-PGC-MS was developed to enable efficient screening of structure-specific health effects of Vivinal GOS. The method focuses on GOS DP3 isomers, but will also provide insight into the structure of higher DPs as it was previously shown that higher DPs are mainly β(1-4)- elongations of DP3 isomers by β-D-Gal*p* [10]. Our study corroborates this finding as the number of isomers detected did not increase for DP4 and 5.

UHPLC-PGC was shown to be highly valuable for the recognition of the different isomers present in Vivinal GOS. The complex retention mechanism of PGC based on both the size

and planarity of neutral oligosaccharides [33] resulted in the excellent separation of 38 GOS DP3 isomers. A previous study using nano-PGC-LC only found 14 GOS DP3 isomers and unnoticed further characterisation [22]. Other chromatographic techniques such as HPAEC-PAD and HILIC-MS resulted in an inadequate separation as respectively 11 and 5 GOS DP3 isomers were detected [8,13]. Also for DP4 and DP5, UHPLC-PGC surpassed the chromatographic resolution of the aforementioned techniques. In total 34 and 35 GOS DP4 and DP5 isomers were separated using UHPLC-PGC, whereas less than 14 and 10 DP4 and DP5 isomers were detected using HPAEC-PAD and HILIC-MS [8,13].

NMR was used in order to characterize GOS DP3 isomers representing different isomer classes. The combination of SEC and preparative-PGC-MS resulted in 4 pure isomers which were successfully characterized by NMR; the reducing isomers β-D-Gal*p*-(1→2)-[β-D-Gal*p*-(1→4)-]D-Glc, β-D-Gal*p*-(1→4)-β-D-Gal*p*-(1→2)-D-Glc and β-D-Gal*p*-(1→2)-[β-D-Gal*p*-(1→6)-]D-Glc and the non-reducing isomer β-D-Gal*p*-(1→4)-α-D-Glc*p*-(1↔1)-β-D-Gal*p.* The characterized isomers confirmed structures reported in previous studies [9,10]. Consequently, they will serve as 'standards' to further develop the high-throughput characterization method based on UHPLC-PGC-MS. The laborious fractionation steps prior to analysis would be unnecessary once having such a LC-MS method.

Reflection of the fragmentation behaviour of the characterized isomers led to the discovery of a MS fragmentation rule to distinguish reducing isomers with a mono- and di-substituted glucitol. The type of linkage was determined using the linkage-specific cross-ring MS^2 fragments at the non-reducing end [30,31]. These two MS fragmentation rules resulted in the partial characterisation of 23 out of 38 GOS DP3 isomers. Interestingly, MS^2 fragmentation spectra of GOS DP4 illustrated that the fragmentation rules are also applicable to higher DPs for the determination of the substitution of the glucitol as well as for the type of glycosidic linkages.

The clear-cut distinction between reducing and non-reducing isomers on *m/z* value made it a straightforward approach to recognise the 15 GOS DP3 isomers with a (1-1)-linkage. A couple of non-reducing isomers have been reported in previous studies regarding the characterization of Vivinal GOS [8-10]. However, these studies required labour-intensive fractionation techniques prior to characterization of the non-reducing isomers by NMR analysis. In this study, MS^2 fragmentation analysis revealed 6 non-reducing DP3 isomers with a (1-4)-linkage. The β(1-4)-linked galactose can be connected to the (1-1)-linked glucose as observed for isomer 13_n: β-D-Gal*p*-(1→4)-α-D-Glc*p*-(1↔1)-β-D-Gal*p.* Next, it is hypothesized that the β(1-4)-linked galactose can also be connected to the (1-1)-linked galactose resulting in α-D-Glc*p*-(1↔1)-β-D-Gal*p*-(4←1)-β-D-Gal*p*. The study of Fransen et al [9] corroborates this hypothesis as they reported on the presence of non-reducing DP4 and DP5 GOS isomers consisting of β(1-4)-linked galactose connected to a (1-1)-linked galactose unit; β-D-Gal*p*-(1→4)-α-D-Glc*p*-(1↔1)-β-D-Gal*p*-(4←1)-β-D-Gal*p* and β-D-Gal*p*-(1→4)-α-D-Glc*p*-(1↔1)-β-D-Gal*p*-(4←1)-β-D-Gal*p*-(4←1)-β-D-Gal*p.* The large variety of non-reducing

DP3 isomers can be further explained by the presence of a structural motif containing solely β-linkages, like β-D-Glc*p*-(1↔1)-β-D-Gal*p,* as shown in previous research for GOS DP2 [8].
The complete characterisation of Vivinal GOS DP3 by solely UHPLC-PGC-MS is still impeded by the challenge to distinguish galactose/glucose and α/β-linkages based on MS^2 fragmentation. Furthermore, an optimal separation of the numerous GOS structures on PGC demands reduction of the reducing end prior to analysis which results in the lack of linkage-specific cross-ring fragments of the resulting terminal glucitol. More studies should be performed on alternative labelling techniques of GOS to obtain both optimal chromatographic separation and informative MS^2 fragmentation spectra.
Nevertheless, the established high-throughput characterization method based on UHPLC-PGC-MS will already have important implications for future structure-function studies on GOS as it provides a deeper insight in the complexity of the GOS mixtures. In particular, the fragmentation rule to distinguish the mono- and disubstituted glucitol turned out to be highly relevant as ongoing research revealed a difference in resistance to fermentation by infant faecal microbiota (results not shown).
The characterization method also shed light on the high diversity of non-reducing GOS isomers. The identification of non-reducing GOS isomers is hindered in currently used methods due to their co-elution with more abundant isomers. Hence, little is known about the fermentability and health effects of these specific structures. To our knowledge, only one study reported on the hydrolysis of non-reducing GOS DP2 by bacterial enzymes [34]. Nonetheless, with 12% the non-reducing isomers make up a considerable part of GOS DP3 and can therefore not be ignored. UHPLC-PGC-MS facilitates readily incorporation in future structure-function studies.
In summary, analytical UHPLC-PGC-MS has proven to be a powerful tool to touch upon the high complexity of Vivinal GOS. More than 100 different Vivinal GOS structures were separated in one single run by the separation mechanism of UHPLC-PGC-MS. In total, 23 reducing and 15 non-reducing DP3 isomers were identified, which shows us that Vivinal GOS is structurally much more diverse than previously noticed. The established characterization method facilitates the detection of non-reducing GOS and several structural features of GOS which could impact the fermentability by infant gut microbiota. Hence, this study will contribute to a deeper understanding of the structure-specific utilization of GOS by infant gut microbiota and consequent health effects.

Acknowledgements

We would like to thank Edwin Bakx (Laboratory of Food Chemistry, Wageningen University) for the fruitful discussions on the interpretation of the mass spectra.
This research was performed in the public-private partnership 'CarboKinetics' coordinated by the Carbohydrate Competence Center (CCC, www.cccresearch.nl). CarboKinetics is financed by participating industrial partners Agrifirm Innovation Center B.V., Cooperatie Avebe U.A., DSM Food Specialties B.V., FrieslandCampina Nederland B.V., Nutrition Sciences N.V., VanDrie Holding N.V. and Sensus B.V., and allowances of The Netherlands Organisation for Scientific Research (NWO).

References

1. Matamoros, S.; Gras-Leguen, C.; Le Vacon, F.; Potel, G.; de La Cochetiere, M.-F. Development of intestinal microbiota in infants and its impact on health. *Trends Microbiol.* **2013**, *21*, 167-173.
2. Marques, T.M.; Wall, R.; Ross, R.P.; Fitzgerald, G.F.; Ryan, C.A.; Stanton, C. Programming infant gut microbiota: influence of dietary and environmental factors. *Curr. Opin. Biotechnol.* **2010**, *21*, 149-156.
3. Smilowitz, J.T.; Lebrilla, C.B.; Mills, D.A.; German, J.B.; Freeman, S.L. Breast milk oligosaccharides: structure-function relationships in the neonate. *Annu. Rev. Nutr.* **2014**, *34*, 143-169.
4. Holscher, H.D.; Bode, L.; Tappenden, K.A. Human milk oligosaccharides influence intestinal epithelial cell maturation *in vitro*. *J. Pediatr. Gastroenterol. Nutr.* **2017**, *64*, 296-301.
5. Bych, K.; Mikš, M.H.; Johanson, T.; Hederos, M.J.; Vigsnæs, L.K.; Becker, P. Production of HMOs using microbial hosts — from cell engineering to large scale production. *Curr. Opin. Biotechnol.* **2019**, *56*, 130-137.
6. Verkhnyatskaya, S.; Ferrari, M.; de Vos, P.; Walvoort, M.T.C. Shaping the infant microbiome with non-digestible carbohydrates. *Front. Microbiol.* **2019**, *10*, 343-343.
7. Torres, D.P.M.; Gonçalves, M.d.P.F.; Teixeira, J.A.; Rodrigues, L.R. Galacto-oligosaccharides: Production, properties, applications, and significance as prebiotics. *Compr. Rev. Food Sci. Food Saf.* **2010**, *9*, 438-454.
8. Coulier, L.; Timmermans, J.; Bas, R.; Van Den Dool, R.; Haaksman, I.; Klarenbeek, B.; Slaghek, T.; Van Dongen, W. In-depth characterization of prebiotic galacto-oligosaccharides by a combination of analytical techniques. *J. Agric. Food Chem.* **2009**, *57*, 8488-8495.
9. Fransen, C.T.; Van Laere, K.M.; van Wijk, A.A.; Brull, L.P.; Dignum, M.; Thomas-Oates, J.E.; Haverkamp, J.; Schols, H.A.; Voragen, A.G.; Kamerling, J.P.; Vliegenthart, J.F. alpha-D-Glcp-(1-1)-beta-D-Galp-containing oligosaccharides, novel products from lactose by the action of beta-galactosidase. *Carbohydr. Res.* **1998**, *314*, 101-114.
10. van Leeuwen, S.S.; Kuipers, B.J.; Dijkhuizen, L.; Kamerling, J.P. (1)H NMR analysis of the lactose/beta-galactosidase-derived galacto-oligosaccharide components of Vivinal(R) GOS up to DP5. *Carbohydr. Res.* **2014**, *400*, 59-73.
11. Yin, H.; Bultema, J.B.; Dijkhuizen, L.; van Leeuwen, S.S. Reaction kinetics and galactooligosaccharide product profiles of the β-galactosidases from *Bacillus circulans*, *Kluyveromyces lactis* and *Aspergillus oryzae*. *Food Chem.* **2017**, *225*, 230-238.
12. van Leeuwen, S.S.; Kuipers, B.J.H.; Dijkhuizen, L.; Kamerling, J.P. Comparative structural characterization of 7 commercial galacto-oligosaccharide (GOS) products. *Carbohydr. Res.* **2016**, *425*, 48-58.
13. Hernández-Hernández, O.; Calvillo, I.; Lebrón-Aguilar, R.; Moreno, F.J.; Sanz, M.L. Hydrophilic interaction liquid chromatography coupled to mass spectrometry for the characterization of prebiotic galactooligosaccharides. *J. Chromatogr. A* **2012**, *1220*, 57-67.
14. Ladirat, S.; Schols, H.; Nauta, A.; Schoterman, M.; Schuren, F.; Gruppen, H. *In vitro* fermentation of galacto-oligosaccharides and its specific size-fractions using non-treated and amoxicillin-treated human inoculum. *Bioact. Carbohydr. Diet. Fibre* **2014**, *3*, 59-70.
15. Difilippo, E.; Pan, F.; Logtenberg, M.; Willems, R.; Braber, S.; Fink-Gremmels, J.; Schols, H.A.; Gruppen, H. *In vitro* fermentation of porcine milk oligosaccharides and galacto-oligosaccharides using piglet fecal inoculum. *J. Agric. Food Chem.* **2016**, *64*, 2127-2133.
16. Depeint, F.; Tzortzis, G.; Vulevic, J.; I'Anson, K.; Gibson, G.R. Prebiotic evaluation of a novel galactooligosaccharide mixture produced by the enzymatic activity of *Bifidobacterium bifidum* NCIMB 41171, in healthy humans: a randomized, double-blind, crossover, placebo-controlled intervention study. *Am. J. Clin. Nutr.* **2008**, *87*, 785-791.

17. Rodriguez-Colinas, B.; Kolida, S.; Baran, M.; Ballesteros, A.O.; Rastall, R.A.; Plou, F.J. Analysis of fermentation selectivity of purified galacto-oligosaccharides by *in vitro* human faecal fermentation. *Appl. Microbiol. Biotechnol.* **2013**, *97*, 5743-5752.
18. Akbari, P.; Fink-Gremmels, J.; Willems, R.H.A.M.; Difilippo, E.; Schols, H.A.; Schoterman, M.H.C.; Garssen, J.; Braber, S. Characterizing microbiota-independent effects of oligosaccharides on intestinal epithelial cells: insight into the role of structure and size : Structure-activity relationships of non-digestible oligosaccharides. *Eur. J. Nutr.* **2017**, *56*, 1919-1930.
19. Yin, H.; Pijning, T.; Meng, X.; Dijkhuizen, L.; van Leeuwen, S.S. Engineering of the *Bacillus circulan*s beta-galactosidase product specificity. *Biochemistry* **2017**, *56*, 704-711.
20. Ruhaak, L.R.; Deelder, A.M.; Wuhrer, M. Oligosaccharide analysis by graphitized carbon liquid chromatography–mass spectrometry. *Anal. Bioanal. Chem.* **2009**, *394*, 163-174.
21. Bao, Y.; Chen, C.; Newburg, D.S. Quantification of neutral human milk oligosaccharides by graphitic carbon high-performance liquid chromatography with tandem mass spectrometry. *Anal. Biochem.* **2013**, *433*, 28-35.
22. Peacock, K.S.; Ruhaak, L.R.; Tsui, M.K.; Mills, D.A.; Lebrilla, C.B. Isomer-specific consumption of galactooligosaccharides by bifidobacterial species. *J. Agric. Food Chem.* **2013**, *61*, 12612-12619.
23. Ni, W.; Bones, J.; Karger, B.L. In-depth characterization of N-linked oligosaccharides using fluoride-mediated negative ion microfluidic chip LC-MS. *Anal. Chem.* **2013**, *85*, 3127-3135.
24. Konda, C.; Londry, F.A.; Bendiak, B.; Xia, Y. Assignment of the stereochemistry and anomeric configuration of sugars within oligosaccharides via overlapping disaccharide ladders using MSn. *J. Am. Soc. Mass Spectrom.* **2014**, *25*, 1441-1450.
25. Duus, J.; Gotfredsen, C.H.; Bock, K. Carbohydrate structural determination by NMR spectroscopy: modern methods and limitations. *Chem. Rev.* **2000**, *100*, 4589-4614.
26. Jonathan, M.C.; van Brussel, M.; Scheffers, M.S.; Kabel, M.A. Characterisation of branched gluco-oligosaccharides to study the mode-of-action of a glucoamylase from *Hypocrea jecorina*. *Carbohydr. Polym.* **2015**, *132*, 59-66.
27. Logtenberg, M.J.; Vink, J.C.M.; Serierse, R.M.; An, R.; Hermes, G.D.A.; Smidt, H.; Schols, H.A. Pooled faecal inoculum can predict infant prebiotic fermentability despite high inter-individual variability of microbiota composition. **2020**, *Submitted*.
28. Wishart, D.S.; Feunang, Y.D.; Marcu, A.; Guo, A.C.; Liang, K.; Vazquez-Fresno, R.; Sajed, T.; Johnson, D.; Li, C.; Karu, N.; Sayeeda, Z.; Lo, E.; Assempour, N.; Berjanskii, M.; Singhal, S.; Arndt, D.; Liang, Y.; Badran, H.; Grant, J.; Serra-Cayuela, A.; Liu, Y.; Mandal, R.; Neveu, V.; Pon, A.; Knox, C.; Wilson, M.; Manach, C.; Scalbert, A. HMDB 4.0: the human metabolome database for 2018. *Nucleic Acids Res.* **2018**, *46*, D608-d617.
29. Warmerdam, A.; Zisopoulos, F.K.; Boom, R.M.; Janssen, A.E. Kinetic characterization of galacto-oligosaccharide (GOS) synthesis by three commercially important beta-galactosidases. *Biotechnol. Prog.* **2014**, *30*, 38-47.
30. Guan, B.; Cole, R.B. MALDI linear-field reflectron TOF post-source decay analysis of underivatized oligosaccharides: Determination of glycosidic linkages and anomeric configurations using anion attachment. *J. Am. Soc. Mass Spectrom.* **2008**, *19*, 1119-1131.
31. Black, B.A.; Lee, V.S.; Zhao, Y.Y.; Hu, Y.; Curtis, J.M.; Gänzle, M.G. Structural identification of novel oligosaccharides produced by *Lactobacillus bulgaricus* and *Lactobacillus plantarum*. *J. Agric. Food Chem.* **2012**, *60*, 4886-4894.
32. Domon, B.; Costello, C.E. A systematic nomenclature for carbohydrate fragmentations in FAB-MS/MS spectra of glycoconjugates. *Glycoconj. J.* **1988**, *5*, 397-409.
33. Bapiro, T.E.; Richards, F.M.; Jodrell, D.I. Understanding the complexity of Porous Graphitic Carbon (PGC) chromatography: Modulation of mobile-stationary phase interactions overcomes loss of retention and reduces variability. *Anal. Chem.* **2016**, *88*, 6190-6194.
34. Van Laere, K.M.; Abee, T.; Schols, H.A.; Beldman, G.; Voragen, A.G. Characterization of a novel beta-galactosidase from *Bifidobacterium adolescentis* DSM 20083 active towards transgalactooligosaccharides. *Appl. Environ. Microbiol.* **2000**, *66*, 1379-1384.

Supporting information

Table S1 Chemical shifts for GOS DP3 isomer 4r, 13r, 21r and 13n determined from 1D and 2D NMR spectra. Linkage positions are indicated in bold.

		4r		13r		21r		13n	
residue	substitution	H	C	H	C	H	C	H	C
A	1a	3.90	63.1	3.86	62.9	3.84	62.8		
	1b	3.77	63.1	3.77	62.9	3.77	62.8	**5.238**	**101.1**
	2	**4.136**	**83.5**	**3.96**	**84.5**	**3.95**	**84.4**	3.64	73.5
	3	4.02	70.7	4.04	70.2	4.04	70.3	3.90	72.7
	4	3.90	78.7	3.79	71.3	3.70	71.5	**3.68**	**79.4**
	5	3.96	72.4	3.92	70.9	3.77	72.2	4.101	72.5
	6a	3.90	63.1	**4.157**	**72.6**	3.84	64.0	3.89	61.0
	6b	3.77	63.1	**3.84**	**72.6**	3.66	64.0	3.83	61.0
B	1	4.432	104.0	4.435	104.6	4.603	105.2	4.585	104.6
	2	3.539	72.2	3.566	72.1	3.67	72.7	3.65	72.4
	3	3.65	73.7	3.67	73.9	3.77	74.3	3.69	73.8
	4	3.92	69.9	3.92	69.8	**4.185**	**78.3**	3.94	69.6
	5	3.66	76.1	3.71	76.5	3.74	75.5	3.72	76.7
	6a	3.80	62.2	3.80	62.2	3.84	61.9	3.77	62.2
	6b	3.77	62.2	3.74	62.2	3.77	61.9	3.73	62.2
C	1	4.590	105.3	4.568	104.9	4.601	105.2	4.452	104.0
	2	3.60	72.6	3.587	72.1	3.58	72.7	3.55	72.4
	3	3.68	73.7	3.67	73.6	3.66	74.1	3.67	73.8
	4	3.93	69.9	3.92	69.8	3.91	69.9	3.93	69.6
	5	3.72	76.3	3.71	76.5	3.68	76.2	3.72	76.7
	6a	3.80	62.2	3.80	62.2	3.84	61.9	3.77	62.2
	6b	3.77	62.2	3.74	62.2	3.77	61.9	3.73	62.2

Table S2 Overview of characterized reducing (*m/z* 505) and non-reducing (*m/z* 503) DP3 GOS isomers with the relative abundance of characteristic MS^2 fragments and used characterisation methods.

peak no.	Tr (min)[a]	relative abundance (%)[b]	tentative / conclusive identification	substitution glc-terminal	MS^2 (relative abundance)[c] *m/z* 251	263	325	343	characterisation method
1r	2.68	0.2	X	di-	ND	ND	61.5	9.3	MS^2
2r	4.29	0.1	X	di-	ND	ND	42.8	11.9	MS^2
3r	4.66	0.1	(1→6)(1→X)	mono-	1.0	ND	0.3	16.9	MS^2
4r	5.29	2.3	β-D-Gal*p*-(1→2)-[β-D-Gal*p*-(1→4)-]D-Glc	di-	ND	ND	61.8	13.9	NMR/MS^2
5r	8.77	1.3	(1→6)(1→X)	mono-	1.8	0.3	0.9	19.0	MS^2
6r	10.84	0.2	X	di-	0.1	0.3	61.7	5.8	MS^2
7r	11.38	1.4	(1→4)(1→3/6)	mono-	ND	2.0	1.5	18.3	MS^2
8r	11.60	0.6	X	mono-	0.1	0.1	1.1	66.4	MS^2
9r	12.07	0.5	X	mono-	0.2	2.3	1.4	19.3	MS^2
10r	13.54	37.8	β-D-Gal*p*-(1→4)-β-D-Gal*p*-(1→4)-D-Glc	mono-	0.1	1.2	1.5	34.9	standard/MS^2
11r	15.73	1.5	X	di-	ND	0.1	56.6	21.3	MS^2
12r	16.69	2.8	X	mono-	0.3	0.2	1.6	78.0	MS^2
13r	18.35	11.2	β-D-Gal*p*-(1→4)-β-D-Gal*p*-(1→2)-D-Glc	mono-	0.3	1.4	2.4	59.6	NMR/MS^2
14r	19.08	1.6	(1→6)(1→X)	mono-	1.0	0.7	3.6	40.1	MS^2
15r	20.24	0.3	X	X	1.5	0.3	1.0	9.3	-
16r	21.43	8.9	X	mono-	0.1	0.2	2.0	84.4	MS^2
17r	21.75	8.2	X	di-	ND	ND	72.3	9.4	MS^2
18r	24.01	2.9	β-D-Gal*p*-(1→6)-β-D-Gal*p*-(1→4)-D-Glc	mono-	1.2	0.2	1.2	28.0	standard/MS^2
19r	24.99	0.6	X	X	ND	0.2	9.4	13.2	-
20r	26.28	1.4	β-D-Gal*p*-(1→3)-β-D-Gal*p*-(1→4)-D-Glc	mono-	0.1	0.5	3.5	11.1	standard/MS^2
21r	30.08	2.3	β-D-Gal*p*-(1→2)-[β-D-Gal*p*-(1→6)-]D-Glc	di-	ND	ND	65.3	19.0	NMR/MS^2
22r	35.54	0.7	X	mono-	ND	ND	4.6	27.4	MS^2
23r	43.15	1.1	X	mono-	ND	ND	8.8	42.9	MS^2
1n	7.81	0.1	X	-	0.12	ND	-	-	-
2n	11.88	0.04	(1→4)(1↔1)	-	ND	1.28	-	-	MS^2
3n	12.59	0.6	X	-	ND	0.56	-	-	-
4n	13.92	0.6	(1→4)(1↔1)	-	ND	1.77	-	-	MS^2
5n	15.25	0.1	(1→6)(1↔1)	-	1.03	0.11	-	-	MS^2
6n	17.08	0.2	(1→4)(1↔1)	-	ND	3.13	-	-	MS^2
7n	17.73	0.2	X	-	ND	ND	-	-	-
8n	18.77	1.5	(1→4)(1↔1)	-	ND	2.26	-	-	MS^2
9n	20.89	0.2	X	-	0.59	0.37	-	-	-
10n	21.34	3.7	(1→4)(1↔1)	-	ND	2.81	-	-	MS^2
11n	22.07	0.2	X	-	ND	ND	-	-	-
12n	23.04	0.5	(1→6)(1↔1)	-	1.54	ND	-	-	MS^2
13n	23.73	3.9	β-D-Gal*p*-(1→4)-α-D-Glc*p*-(1↔1)-β-D-Gal*p*	-	ND	2.07	-	-	NMR/MS^2
14n	24.83	0.3	X	-	ND	0.09	-	-	-
15n	37.26	0.2	X	-	ND	0.97	-	-	-

[a] Tr: retention time

[b] determined by integration of peak areas in UHPLC-PGC-MS with sum of both reduced and non-reducing DP3 isomers set at 100%

[c] most abundant fragment set at 100%, ND: not detected
X: unknown, -: not applicable

Table S3 Fragmentation behaviour of reducing GOS DP4 isomers

peak no.	Tr (min)[a]	[M-H]⁻	relative abundance (%)[b]	substitution glc-terminal	MS² (relative abundance)[c] *m/z* 251	263	413	425	325	343	487	505
1r	18.22	667	2.9	di-	ND	0.3	0.1	0.1	7.9	2.3	50.6	32.6
2r	19.10	667	6.4	mono-	ND	0.1	ND	ND	8.3	5.0	17.7	62.3
3r	21.84	667	0.3	di-	0.2	0.4	0.3	0.2	5.9	1.7	33.0	21.3
4r	22.04	667	0.9	di-	2.5	0.8	ND	5.9	0.6	0.7	29.8	24.3
5r	23.35	667	5.9	mono-	0.7	0.2	2.9	2.6	0.5	9.7	3.0	27.7
6r	23.97	667	0.6	di-	0.1	0.1	ND	0.2	12.2	3.0	34.4	36.0
7r	25.62	667	1.1	mono-	0.4	0.1	0.8	11.0	1.4	11.4	5.6	45.1
8r	26.1	667	0.4	di-	ND	ND	0.1	0.3	9.5	2.3	60.2	13.2
9r	26.98	667	4.6	mono-	0.1	0.2	0.3	0.1	14.6	8.3	12.7	56.3
10r	27.5	667	1.6	mono-	0.2	0.2	2.5	1.2	4.0	15.6	9.2	36.6
11r	27.78	667	29.0	mono-	ND	0.7	0.5	8.5	0.4	18.8	2.3	57.8
12r	30.22	667	7.9	mono-	ND	0.1	0.1	ND	9.4	4.9	31.4	48.7
13r	31.79	667	6.8	mono-	ND	0.3	0.4	1.9	0.7	23.1	1.9	62.7
14r	32.00	667	0.7	di-	0.1	0.2	1.0	0.6	16.8	12.5	24.3	25.3
15r	32.97	667	3.9	mono-	ND	0.1	0.3	0.6	0.5	23.2	1.6	66.6
16r	33.7	667	1.5	mono-	0.3	0.4	0.4	0.9	0.5	4.9	1.2	46.2
17r	34.1	667	0.6	mono-	ND	0.1	0.6	0.3	1.0	12.1	3.7	58.3
18r	35.72	667	0.4	mono-	0.1	ND	ND	ND	12.8	4.5	14.2	56.6
19r	36.91	667	4.4	di-	ND	0.2	0.4	ND	16.6	7.7	32.6	28.9
20r	39.35	667	6.9	mono-	ND	0.1	0.1	ND	11.2	6.0	17.1	62.5
21r	42.15	667	1.4	mono-	0.1	0.2	ND	1.2	0.7	44.2	2.5	30.3

[a] Tr: retention time
[b] determined by integration of peak areas in UHPLC-PGC-MS with sum of both reduced and non-reducing DP4 isomers set at 100%
[b] most abundant fragment set at 100%, ND: not detected, X: unknown

Chapter 6

General discussion

Research aim and approach

Human milk is the gold standard for infant nutrition in early life. Especially, human milk oligosaccharides (HMOs) received quite some interest during the last decades. HMOs have shown to support the maturation of the gut barrier and the development of a balanced immune system, both directly and indirectly through their fermentation by gut bacteria [1-3]. For infants for which human milk is not an option, cow-milk based infant formula are supplemented with non-digestible carbohydrates (NDCs) to substitute for the immune benefits of HMOs.

Since previous research showed that the fermentability and immune effects of HMOs are highly dependent on their structure [4], several structurally different NDCs were investigated in the thesis research. The aim of the PhD thesis was firstly, to understand the structural complexity of these NDCs. Subsequently, we aimed to determine the structure-specific fermentability and microbiota-dependent immune effects of the NDCs in infants by applying an *in vitro* fermentation set-up using infant faecal material as inoculum. The changes in microbiota composition and production of short chain fatty acids (SCFAs) were followed in time, as well as the actual degradation of individual NDCs. This last point is often overlooked due to the high complexity of NDCs making their characterization challenging. Hence, in this study a high-throughput characterization method was developed to obtain more understanding on the preferential degradation of NDCs with specific size and type of linkages. Additionally, immune effects of NDC fermentation digesta were assessed by co-incubation with dendritic cells to determine changes in the production of both pro- and anti-inflammatory cytokines. The dendritic cells were derived from the umbilical vein to mimic the infant situation.

Selection of an ideal fermentation set-up

Nowadays several fermentation models exist to study the fate of NDCs in the gut. Continuous fermentation models such as TIM-2 and SHIME are preferred, because they are highly dynamic and closely resembling the gut [5,6]. Nutrients are continuously replenished and build-up of microbial metabolites is prevented by dialysis systems. Additionally, these models can be extended to incorporate host-gut microbiota interactions, such as the interaction between epithelial cells and the microbiota [7]. However, the drawbacks of these systems are the low-throughput and high workload. Additionally, these models require substantial amounts of substrate thereby hindering the study of highly tailored NDCs produced only at small scale. These models are therefore less suitable for a study in which many structurally different NDCs are included. For our research, a static batch fermentation model was chosen, which overcomes these limitations. Definitely, it should be taken into account that a static fermentation model does not resemble the intestinal environment as good as continuous models. In this case peristaltic movements in the gut are mimicked by

a simple incubator shaker and the presence of distinct bacterial niches in the mucus layer is ignored. Additionally, bacterial metabolites accumulate over time in the closed compartment, which limits the model to relatively short fermentation periods. Nonetheless, the static fermentation model has proven to be a suitable model for screening purposes related to fermentability of NDCs in the gut [8].

Inoculation of fermentation model

The type of faecal inoculum used in the fermentation model is crucial for the outcomes. Bacterial species all have their own set of enzymes with which they can degrade the substrates [9]. The presence of different bacteria at the start of the fermentation could thus result in different outcomes when we look at the degradation of the substrate and the resulting production of SCFAs and immune effects. This fact is especially important when studying the fate of NDCs in the infant gut as the infant microbiota composition changes rapidly upon aging [10]. To study the effects of the NDCs in this crucial timeframe of infant microbiota development, we included faecal inoculum of two different infant age groups, namely from 2- and 8-week-old infants. Previous research by Albrecht et al [11] found that infants of these ages exhibit large differences in HMO-degrading capacity. In the first 2 weeks of life most of the HMOs present in the corresponding human milk could still be traced back in the faeces of the infant (Figure 1, I), while two months postpartum only acidic HMOs and metabolization products were detected (Figure 1, II).

The exact timing of the development of HMO utilization by infant microbiota was found to be infant-dependent [11], which is consistent with the highly variable nature of infant gut microbiota [12]. Hence, *in vitro* studies should ideally include multiple fermentations with individual faecal inocula of different infants. This would mean a strong increase in workload and resources for this study including many NDCs and two age groups. The combination of faecal material of multiple infants in one pooled faecal inoculum proved highly valuable for the screening purposes of current study as the bacterial functionality of the pool largely resembled the functionality of the individual infant faecal inocula (Chapter 2). Nonetheless, the changes in microbiota composition upon fermentation of galacto-oligosaccharides (GOS) using pooled faecal inoculum did not fully represent the average changes in microbiota composition of the individual inocula. As expected, bacterial species more capable of degrading GOS in the different individual inocula, were more enriched during fermentation using pooled faecal inoculum. Consequently, in the case that research is focused on the exact fate of NDCs in a specific individual, obviously a pooled faecal inoculum should not be used.

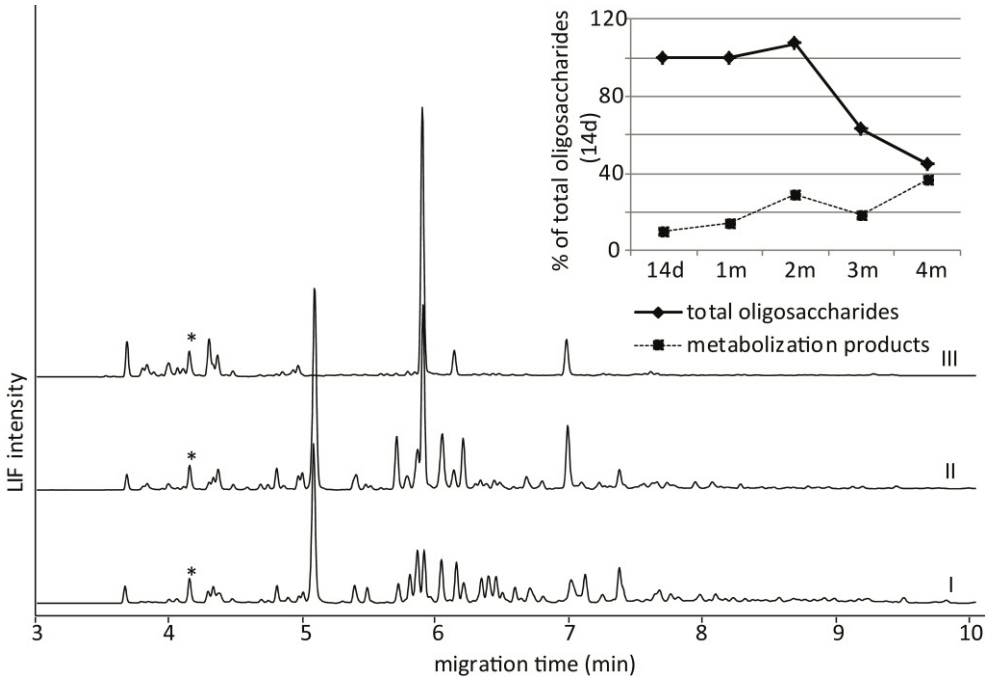

Figure 1 Human milk oligosaccharides and their metabolization products present in faeces of 2-week- (I), 2-month- (II) and 4-month- (III) old infants as analysed by capillary electrophoresis with laser induced fluorescence detection with *: internal standard xylose [11].

Furthermore, close attention was paid to the selection of the faecal donors. In this study we only included term, vaginally born and exclusively breast-fed infants. The human milk of all corresponding mothers had a Secretor positive/Lewis positive phenotype as determined by the presence of α(1-2) and α(1-4) fucosylated HMOs [13]. Faecal donor selection based on the most important determinants of infant microbial colonization minimizes the differences in microbiota composition between the individuals. In this way the accuracy of the prediction capability of the pooled faecal inoculum is maximized for a subgroup of infants.

Structural variability of NDCs

In our research seven different NDCs were studied, from which three of them are already applied in infant formula; chicory fructo-oligosaccharides (FOS) (Chapter 3), native inulin (Chapter 3) and GOS (Chapter 5). Also four potential NDCs were included namely, native and endo-1,3(4)-β-glucanase-treated oat ß-glucan (Chapter 4) as well as isomalto/malto-polysaccharides (IMMP) and isomalto-oligosaccharides (IMO).

The structural composition of the IMO preparation and IMMP have not been dealt with in the experimental chapters, but will be addressed in more detail in this section. The same applies to the fermentation of the IMO preparation, IMMP and GOS (vide infra). These three NDCS are studied at the same time as FOS, native inulin and the oat β-glucans, using identical inocula and fermentation set-up.

Galacto-oligosaccharides

GOS is probably one of the most studied NDCs and commonly applied in infant formula. GOS is produced from lactose by a hydrolysis and transgalactosylation reaction, which is catalysed by β-galactosidase. This process results in a highly complex mixture of galactose chains with a terminal galactose or glucose unit, varying in type and anomeric configuration of the glycosidic linkage as well as their degree of polymerization (DP) (2-8) [14]. The source of the enzyme influences the regioselectivity of the enzyme and the size of the produced oligosaccharides [15]. In this research Vivinal GOS is studied, which is a commercial GOS mixture produced by a *Bacillus circulans* β-galactosidase. GOS DP3 and DP4 oligomers are predominant with a relative abundance of respectively 48 and 29% (Figure 2A). The presence of both linear and branched chains with a disubstituted terminal reducing glucose or galactose unit further adds up to the complexity of GOS. In addition, next to reducing GOS with a free anomeric carbon at the terminal position, also non-reducing GOS containing a (1-1)-linkage are present in the GOS mixture [16,17] (Chapter 5).

Fructo-oligosaccharides and native inulin

FOS (synonym oligofructose) and native inulin are composed of linear chains of β(2-1)-linked fructose monomers with either a glucose (GF series) or fructose (F series) moiety at the reducing end. The main difference between these NDCs is their DP with the DP of FOS ranging between 2-10, while in native inulin mainly the GF series is present with a DP ranging between 2-60 (Figure 2A) [18]. This native inulin is extracted from chicory root and FOS was obtained by subsequent enzymatic hydrolysis of the inulin (Chapter 3).

Native and endo-1,3(4)-β-glucanase-treated oat ß-glucan

Oat β-glucans are polymers with an average molecular weight of 300 kDa, which consist of glucose moieties linked by primarily β(1-3)- or β(1-4)-linkages (Figure 2A) [19]. Upon endo-1,3(4)-β-glucanase-treatment oligomers are formed ranging between DP2-5 with glucosyl-(1-3)-β-D-cellotriose being most abundant (58%) (Figure 2A) (Chapter 4).

Isomalto/malto-polysaccharides and isomalto-oligosaccharide preparations

IMMP and IMO preparations are enzymatically produced from starch, the most abundant and renewable polysaccharide on earth. IMMP are polymers composed of mainly α(1-4)- and α(1-6)-linked glucose moieties. For the production of the IMMP included in this study the enzyme 4,6-α-glucanotransferase has been applied, which introduces consecutive α(1-6)-linkages onto linear α(1-4)-linked gluco-oligosaccharides [20]. The ratio between these two types of glycosidic linkages is dependent on the starch source and the process

conditions [21]. The resulting IMMP has a broad molecular weight distribution (1.4 – 52 kDa) (Figure 2A) and contains 91% α(1-6)-linkages, which prevents the polysaccharides from digestion in the upper gastrointestinal tract [20].
IMO preparations are also produced from starch, but require an additional hydrolysis step next to the application of transferase enzymes [22]. Production technologies used nowadays differ in the number and type of enzymes used, which results in the production of structurally distinct IMO preparations [23]. In this research the commercial IMO preparation Vitafiber (BioNeutra, Edmonton, Canada) is studied, which is a complex mixture of oligosaccharides varying in DP and type of linkages. The oligosaccharides present in Vitafiber have an average DP of 3.3, ranging between 2 and 6 (Figure 2A).

Fermentability and consequent immune effects of NDCs in infants

The fate of the seven NDCs in the infant gut was studied by *in vitro* batch fermentations using pooled faecal inoculum of 2- and 8-week-old infants. The fermentation digesta were analysed to determine the fermentability of the NDCs, their microbiota effects as well as the impact of the fermentation digesta on dendritic cell responses. The obtained results are summarized and discussed in coming sections.

Size- and age-dependent fermentability of NDCs by infant microbiota

Galacto-oligosaccharides

Our fermentation study confirmed that GOS is readily fermented by infant microbiota. Only 17 and 12% of GOS were remaining after 26 h of fermentation with faecal microbiota of respectively 2- and 8-week-old infants (Figure 2B/C). However, not all oligomers were degraded to the same extent. The fermentability was lower for oligomers with a higher DP. For instance, more than 40% of GOS DP6 was remaining after 26 h of fermentation with both inocula.

Fructo-oligosaccharides and native inulin

The fermentation of native inulin showed us that the fermentability is dependent on the age of the infants (Figure 2B/C and Chapter 3). Faecal microbiota of 2-week-old infants only utilized the DP3-8 portion of native inulin, whereas faecal microbiota of 8-week-old infants also degraded longer chains of native inulin up to DP16. Interestingly, the fermentation of FOS primarily resulted in the utilization of trisaccharides. Besides the age of the infants, the size and the relative abundance of the oligomers within the NDC class are thus also of importance.

Native and endo-1,3(4)-β-glucanase-treated oat ß-glucan

The enzyme treatment of native oat ß-glucan increased the fermentability by faecal microbiota of 2- and 8-week-old infants tremendously (Figure 2B/C and Chapter 4). The oligomers which were formed upon enzyme treatment prior to fermentation were utilized for around 40%, whereas the native oat ß-glucans were virtually intact after fermentation by faecal microbiota of 2- and 8-week-old infants.

Isomalto/malto-polysaccharides and isomalto-oligosaccharides

Fermentation of IMMP and the IMO preparation by infant faecal microbiota of 2- and 8-week-old infants was size-dependent. IMMPs were virtually resistant to fermentation by both inocula. In contrast to IMMPs, the IMO preparation was utilized for 80% and 50% after 26 h of fermentation with faecal microbiota of respectively 2- and 8-week-old infants. The relatively low molecular weight of the IMO preparation explains the high fermentability compared to IMMPs.

Correlating the structure of the NDCs to their fermentability

Overall, our findings indicate that the fermentation of NDCs by infant faecal microbiota is dependent on the size of the NDCs (Figure 2). Faecal microbiota of both 2- and 8-week-old infants were not able to degrade high molecular weight polysaccharides such as IMMP and native oat β-glucan. Interestingly, the fermentability increased tremendously upon decreasing the molecular weight of these polysaccharides. The same applies for the oligosaccharides, for which the fermentability was negatively correlated with the DP. However, it should be taken into account that the different DPs are not evenly distributed within each NDC class, which could impact the fermentability of the oligomers with a given DP. Highly abundant oligomers could steer the bacteria to the expression of enzymes specifically favouring the degradation of these oligomers [24]. In case of GOS, this could partly explain the preference by the bacteria for GOS DP3 and DP4 oligomers, which make up respectively 48% and 29% of GOS. However, GOS DP2 (10%) and DP5 (10%) oligomers significantly differed in fermentability, confirming the association between the size of the NDCs and the fermentability. This finding is in line with the intracellular utilization strategy of *Bifidobacterium* [25], a bacterial species which is highly abundant in the infant gut [26]. The intracellular utilization requires the uptake of the NDCs into the bacterial cell via specific transporter systems [27]. The size of the NDCs could limit this transport as exemplified for the degradation of long-chain inulin by individual bifidobacterial strains [28]. The preferred utilization of oligomers with a lower DP was also reported in a previous fermentation study concerning adult faecal microbiota in combination with GOS [29].

Our findings confirm the potential of tailored NDC preparations for infants of different age groups as the fermentability is dependent on the age of the infants (Figure 2). The IMO preparation and GOS displayed highest fermentability with faecal microbiota of 2-week-old infants, whereas native inulin and GOS were most preferred by faecal microbiota of 8-week-old infants. In line with our expectations, based on previous *in vitro* studies [4,29], the

structure of the NDCs also determined the fermentability. This was exemplified by significant differences in fermentability between DP4 oligomers present in the IMO preparation and enzyme-treated oat β-glucan, which structurally differ in the anomeric configuration and type of the glycosidic linkage. To obtain a deeper understanding of these structure-specific effects, it is of utmost importance to focus on the degradation of individual isomers by the infant faecal microbiota.

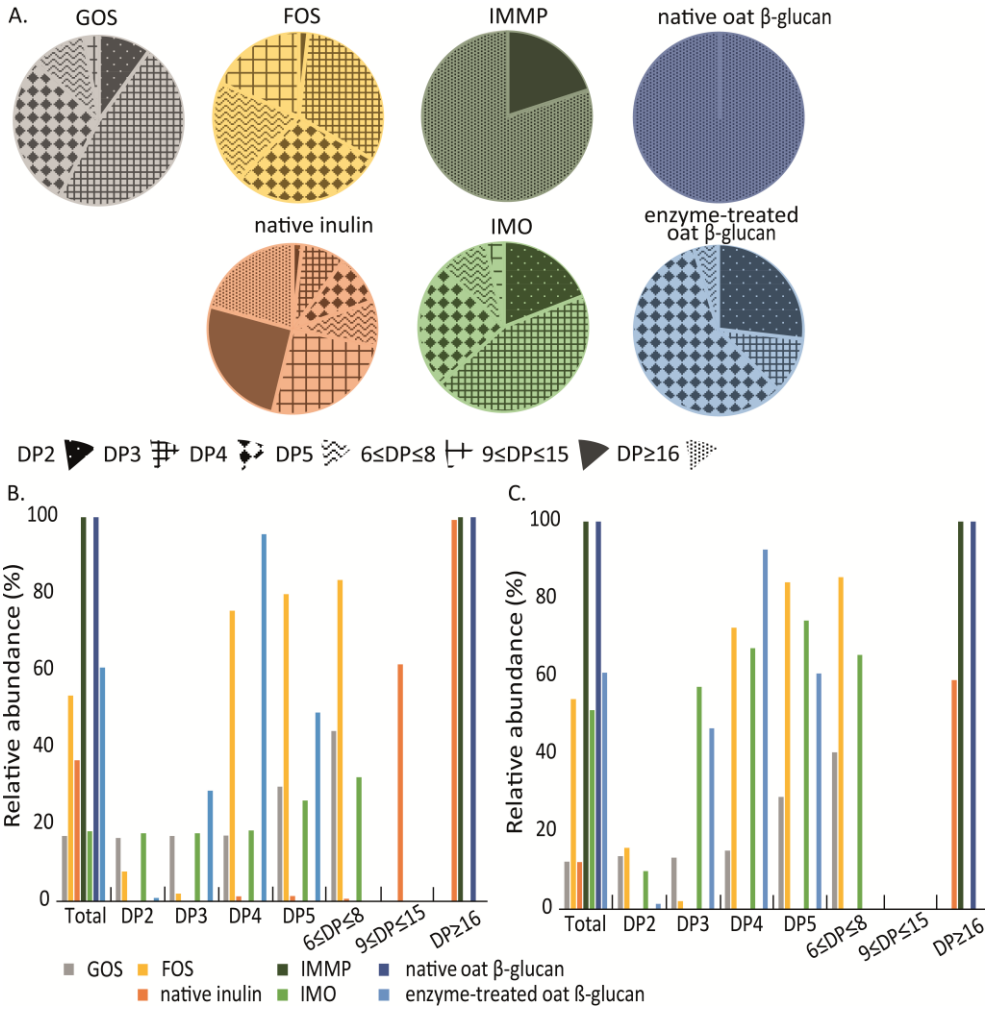

Figure 2 DP distribution of fructo-oligosaccharides (FOS), native inulin, galacto-oligosaccharides (GOS), the isomalto-oligosaccharide (IMO) preparation, isomalto/malto-polysaccharides (IMMP) and native and enzyme-treated oat ß-glucan (A) and the percentage of remaining oligomers per DP as well as the total mixture after 26 hours of *in vitro* fermentation of the NDCs with faecal inoculum of 2- (B) and 8-week-old (C) infants.

In-depth analysis of individual NDC isomers

Information on the fermentability of individual isomers present in NDCs is often lacking or highly limited in studies on health effects of NDCs due to the structural complexity of NDCs. Each NDC typically consists of a high number of isomers for each DP, varying in anomeric configuration and type of linkages. Characterisation of these almost identical components is highly challenging as coelution is inevitable with frequently used characterization methods based on high performance anion exchange chromatography (HPAEC) [30]. Additionally, once the oligosaccharides are chromatographically separated, the next challenge arises; the actual characterization. The coupling of HPAEC to mass spectrometry (MS), which is highly suitable for the characterization of oligosaccharides, is technically rather challenging due to high levels of salts present in the eluent [31]. Therefore, HPAEC relies mainly on reference components or nuclear magnetic resonance (NMR) analysis of purified fractions. Reference components are often limited and (semi) preparative fractionation of NDCs using techniques such as size-exclusion chromatography (SEC) are highly labour-intensive.

We developed a high-throughput characterization method to facilitate the analysis of the fermentability of individual GOS isomers by gut microbiota (Chapter 5). The method is based on analytical UHPLC-MS with porous graphitic carbon (PGC) as stationary phase. The retention mechanism of PGC, which is based on the size, type of linkage and the resulting 3D-structure [32], proved to be highly effective in the separation of the different isomers present in GOS. The oligosaccharides were characterized by the *m/z* and MS^2 fragmentation using validated fragmentation rules to distinguish oligosaccharides with (1-4)- and (1-6)-linked residues [33,34]. We recognized a fragmentation rule to distinguish oligosaccharides with a mono- or di-substituted reducing terminal residue. In addition, due to a reduction prior to analysis, UHPLC-PGC-MS enabled the recognition of non-reducing isomers containing a (1-1)-linkage, which remained relatively untouched in previous structure-function studies. Hence, one single run of UHPLC-PGC-MS enables the detection as well as the (partial) characterization of the different isomers present in the NDC preparations.

The characterization method as developed for GOS (Chapter 5), was also applied to characterize the IMO preparation and endo-1,3(4)-β-glucanase-treated oat ß-glucan (Chapter 4). These NDCs teach us most about the structural preferences of the infant faecal microbiota as they enable the comparison of isomers differing in only one structural variable. First, the composition of GOS and the IMO preparation are elucidated, after which the isomer-specific fermentability of GOS, the IMO preparation and enzyme-treated oat β-glucan are discussed. For now, we only focus on the DP3 isomers present in GOS and the IMO preparation, as these are most abundant and will also give us insights into the possible structure and fermentability of higher DPs.

Individual GOS DP3 isomers

UHPLC-MS showed us that Vivinal GOS is much more diverse than thought before. More than 100 different Vivinal GOS components were separated in one single run by UHPLC-PGC-MS, including a high number of non-reducing GOS isomers which have not been annotated from a chromatographic elution pattern before. In total 23 reducing and 15 non-reducing DP3 isomers were identified. The large variety of non-reducing isomers containing an (1-4)-linkage indicated the presence of a wide range of structural motifs within the non-reducing GOS DP3 isomers. The (1-1)-linkage could be located at two different positions providing structures like β-D-Gal*p*-(1→4)-β-D-Glc*p*-(1↔1)-β-D-Gal*p* and D-Glc*p*-(1↔1)-β-D-Gal*p*-(4←1)-β-D-Gal*p* [16]. Interestingly, non-reducing GOS DP3 isomers could also contain α-linkages with the structural motif α-D-Glc*p*-(1↔1)-β-D-Gal*p* [17]. More details about the composition of Vivinal GOS DP3 are presented in Chapter 5.

Individual IMO DP3 isomers

UHPLC-PGC-MS increased our understanding of the complexity of IMO preparations tremendously (Figure 3). For Vitafiber, in total 15 different DP3 isomers were detected, from which 9 reducing and 6 non-reducing isomers (Figure 4), whereas earlier HPAEC-PAD analysis of starch-derived IMO preparations only recognized 4 different reducing DP3 isomers [35]. The presence of non-reducing isomers in starch-derived IMO preparations has not been reported before. In total 13 out of 15 isomers were characterized with the use of our established MS-fragmentation rules and NMR analysis of pure isomers representing different isomers classes (Table 1). Interestingly, similar to GOS we identified non-reducing isomers with different location of the (1-1)-linkage e.g. β-D-Glc*p*-(1↔1)-α-D-Glc*p*-(6←1)-α-D-Glc*p* and α-D-Glc*p*-(1→6)-β-D-Glc*p*-(1↔1)-α-D-Glc*p*. Additionally, we also characterized oligosaccharides with a di-substituted reducing terminal glucose in the IMO preparation, which remained unnoticed in previous research.

Detailed isomer-specific fermentability of NDCs by infant microbiota

UHPLC-PGC-MS was used to determine the fate of individual isomers present in GOS, the IMO preparation and enzyme-treated oat β-glucan during fermentation by faecal inocula of 2- and 8-week-old infants.

Fermentability of reducing vs non-reducing isomers

The fermentability differed between reducing and non-reducing GOS isomers (Figure 5). GOS fermentation led to an enrichment of non-reducing DP3 isomers in the digesta with faecal microbiota of both 2- and 8-week-old infants. However, the resistance to fermentation was not only caused by the presence of the (1-1)-linkage. The non-reducing isomer β-D-Gal*p*-(1→4)-α-D-Glc*p*-(1↔1)-β-D-Gal*p* was for example completely utilized

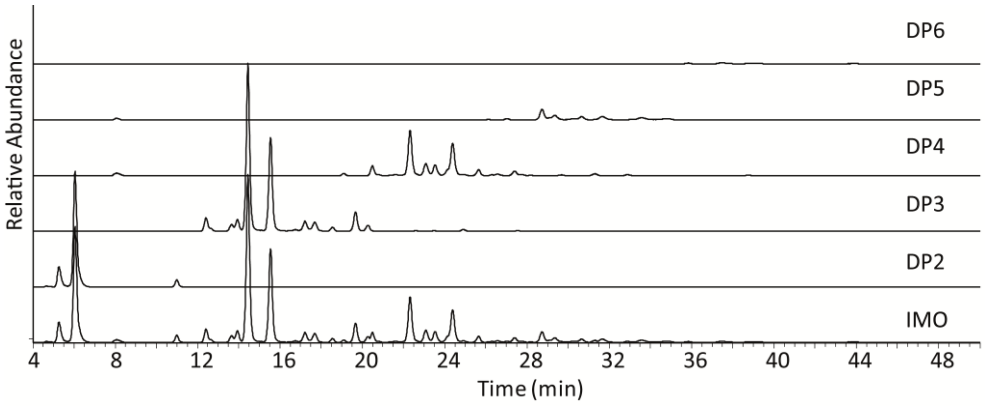

Figure 3 UHPLC-PGC-MS profile of reducing and non-reducing oligosaccharides present in the IMO preparation Vitafiber and of DP 2-6 after selection of the appropriate *m/z* for that DP. All elution profiles were normalised to the actual contribution of each DP to the total mixture.

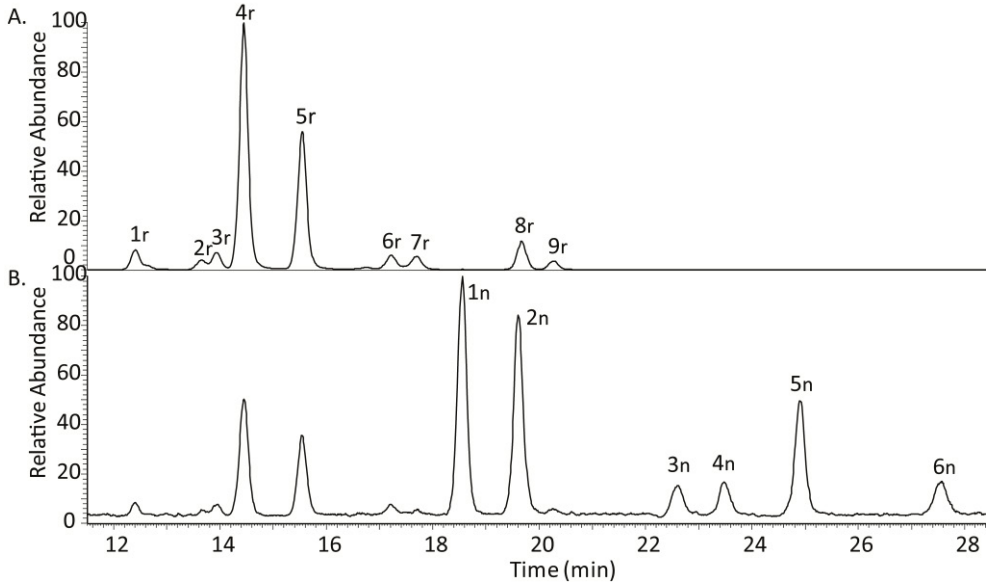

Figure 4 UHPLC-PGC-MS profile of oligosaccharides present in the IMO preparation Vitafiber with selection of A: reducing (*m/z* 505, 551 (M+FA)) and B: non-reducing (*m/z* 503, 549 (M+FA)) isomers. Most abundant peak in both chromatograms was set at 100%. Peak numbers correspond to characterized IMO isomers in Table 1 with r: reducing isomers and n: non-reducing isomers ((1-1)-linked). The contribution of DP3 to the total IMO mixture is displayed in Figure 3.

Table 1 Overview of conclusively and tentatively characterised or unknown reducing and non-reducing DP3 isomers present in the IMO preparation Vitafiber.

	peak no.	graphical structure[a]	relative abundance (%)[b]	substitution glucitol	chemical structure [c]
A.	1r		4.7	disubstituted	α-D-Glc*p*-(1→2)-[α-D-Glc*p*-(1→4)-]D-Glc
	2r		2.1	disubstituted	X
	3r		3.5	monosubstituted	α-D-Glc*p*-(1→6)-α-D-Glc*p*-(1→3)-D-Glc
	4r	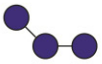	45.3	monosubstituted	α-D-Glc*p*-(1→6)-α-D-Glc*p*-(1→4)-D-Glc
	5r		26.8	monosubstituted	α-D-Glc*p*-(1→6)-α-D-Glc*p*-(1→6)-D-Glc
	6r		3.1	monosubstituted	α-D-Glc*p*-(1→4)-α-D-Glc*p*-(1→3/6)-D-Glc
	7r		3.0	monosubstituted	α-D-Glc*p*-(1→4)-α-D-Glc*p*-(1→4)-D-Glc
	8r	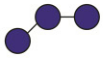	5.7	monosubstituted	α-D-Glc*p*-(1→3)-α-D-Glc*p*-(1→4)-D-Glc
	9r		1.9	monosubstituted	X
B.	1n	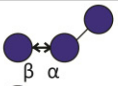	1.4	-	β-D-Glc*p*-(1↔1)-α-D-Glc*p*-(6←1)-α-D-Glc*p*
	2n	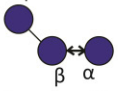	1.3	-	α-D-Glc*p*-(1→6)-β-D-Glc*p*-(1↔1)-α-D-Glc*p*
	3n	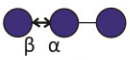	0.2	-	β-D-Glc*p*-(1↔1)-α-D-Glc*p*-(4←1)-α-D-Glc*p*
	4n	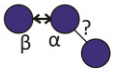	0.2	-	β-D-Glc*p*-(1↔1)-α-D-Glc*p*-(2/3←1)-α-D-Glc*p*
	5n	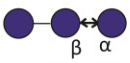	0.7	-	α-D-Glc*p*-(1→4)-β-D-Glc*p*-(1↔1)-α-D-Glc*p*
	6n	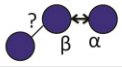	0.2	-	α-D-Glc*p*-(1→2/3)-β-D-Glc*p*-(1↔1)-α-D-Glc*p*

[a] included for conclusively and tentatively characterized isomers, blue: glucose, ?: type of glycosidic linkage unknown

[b] determined by integration of peak areas in UHPLC-PGC-MS with sum of both reduced and non-reducing DP3 isomers set at 100%

[c] X: unknown, /: both glycosidic linkages possible

- : not applicable

after 26 h of fermentation by both inocula, whereas another (1-1)-linked DP3 isomer containing a (1-4)-linkage remained virtually intact (data not shown). Hence, both the location and the anomeric configuration of the (1-1)-linkage could have affected its fermentability by infant faecal microbiota. More specifically, non-reducing GOS isomers with an elongation via the (1-1)-linked galactose unit (D-Glc*p*-(1↔1)-β-D-Gal*p*-(4←1)-β-D-Gal*p*) or non-reducing GOS isomers containing solely β-linkages were more resistant to fermentation. With respect to the IMO preparation, non-reducing IMOs with an elongation via the β(1-1)-linked glucose unit were more resistant to fermentation than non-reducing IMOs with an elongation via the α(1-1)-linked glucose unit (data not shown).

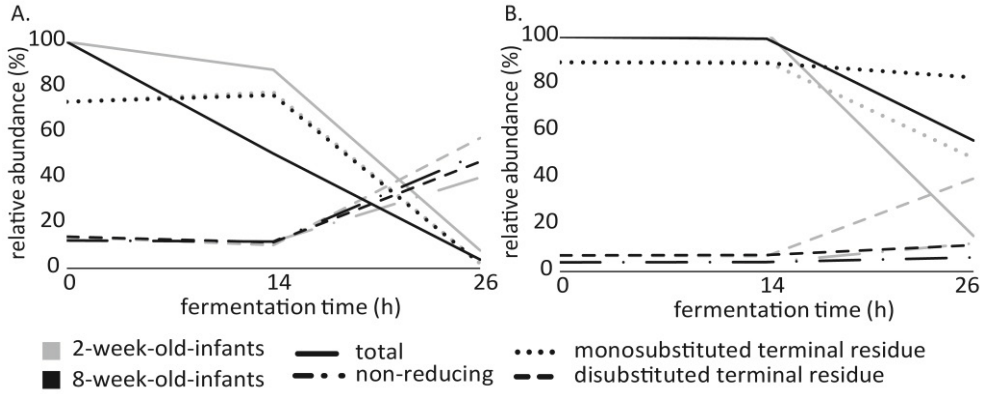

Figure 5 Percentage of total remaining DP3 isomers (solid line) after 14 and 26 h of *in vitro* fermentation of galacto-oligosaccharides (A) and the isomalto-oligosaccharide preparation (B) with faecal inoculum of 2- and 8-week-old infants together with the relative abundance of isomers with a mono- and di-substituted terminal residue as well as non-reducing isomers within the fermentation digesta at the different time points (sum of all DP3 isomers set at 100%)(dotted and dashed line).

Substitution of the terminal reducing residue impacts NDC fermentability

The substitution of the terminal reducing residue influenced the fermentability of the isomers present in GOS and the IMO preparation (Figure 5). Notably, DP3 isomers with a monosubstituted reducing glucose residue were preferably fermented by infant faecal microbiota. This structural preference was observed with faecal microbiota of both infant age groups, except for the fermentation of the IMO preparation by faecal microbiota of 8-week-old infants caused by limited fermentability.

Glycosidic linkage type influences NDC fermentability

The type of glycosidic linkage also affects the fermentability by infant faecal microbiota (Figure 6) with a similar fermentation behaviour for the faecal microbiota of 2- and 8-week-old infants. To enable the comparison of isomers only differing in the type of glycosidic linkage, solely reducing isomers with a monosubstituted terminal residue were taken into consideration. For GOS, (1-3)(1-4)-linked oligomers were most preferred, followed by DP3 oligomers with an (1-6)-linked galactose unit at the non-reducing end. Infant faecal

microbiota required most time for the degradation of GOS DP3 oligomers with an (1-4)-linked galactose unit at the non-reducing end. In line with the development of the gut microbial functionality upon aging [36], adult faecal microbiota showed different preferential utilization of GOS oligomers. Adult faecal microbiota preferred (1-4)-linked GOS DP3 oligomers over other DP3 oligomers [37]. In contrast to GOS, fermentation of the solely glucose-based oligomers (IMO preparation and enzyme-treated oat β-glucan) by infant faecal microbiota showed a clear preference for (1-4)-linked oligomers over (1-3)(1-4)-linked oligomers. Hence, the preference for specific type of glycosidic linkages by the infant faecal bacteria is dependent on the monomer composition.

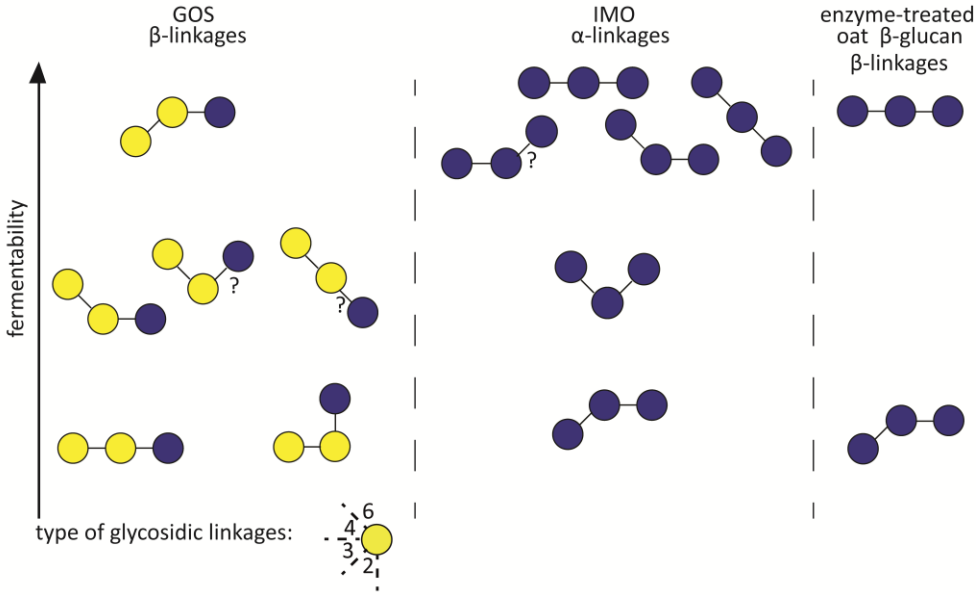

Figure 6 Schematic overview of fermentability of galacto-oligosaccharides (GOS), the isomalto-oligosaccharide (IMO) preparation and enzyme-treated oat β-glucans by infant faecal microbiota. For GOS and the IMO preparation only reducing DP3 isomers with a monosubstituted terminal residue are considered with yellow: galactose and blue: glucose.

Monomer composition and anomeric configuration influence NDC fermentability

Overall, GOS DP3 oligomers were fermented faster and to a higher extent than the solely glucose-based DP3 oligomers present in the IMO preparation and endo-1,3(4)-β-glucanase-treated oat β-glucan. With respect to the 2-week-old-infants, the faecal microbiota completely utilized the GOS DP3 oligomers within 26 h of fermentation, whereas DP3 oligomers present in the IMO preparation and enzyme-treated oat β-glucan were degraded only for 90 and 50% respectively. This finding is in line with the HMO-adapted metabolic activity of the gut microbiota of the exclusively breast-fed infants included in this study [38] as HMOs display significant structural overlap with GOS. The infant faecal microbiota have

not encountered α- and β-linked gluco-oligomers before due to their absence in the human milk. Nevertheless, the infant microbiota possessed and expressed the genes encoding the enzymes responsible for the degradation of the gluco-oligomers with a clear preference for α-linked over β-linked gluco-oligomers. The significant fermentability of the α-linked gluco-oligomers present in the IMO preparation is corroborated by previous metagenomic data analysis of infant faeces reporting a high abundance of genes encoding enzymes belonging to the glycoside hydrolase family 13, which showed to be highly relevant for the metabolism of IMOs [39].

The use of UHPLC-PGC-MS revealed that next to the size, subtle differences in the structure of oligosaccharides have a huge impact on the fermentability of NDCs by infant microbiota. The preferences for specific structural features of NDCs by the faecal bacteria are partly linked to the selectivity of ATP-binding cassette (ABC) transporter systems [40] and carbohydrate-active enzymes expressed by the bacteria. As such, the NDC degradation capability by bacteria even differs on species level, as exemplified by *Bifidobacterium* [41]. It is out of the scope of this research and practically impossible to relate all the structural preferences of the infant faecal microbiota to specific bacterial species. Nevertheless, the knowledge obtained on the substrate specificities of the infant faecal microbiota as a whole is highly valuable for the design of tailored NDC mixtures for infants of different age groups.

NDC-specific stimulation of *Bifidobacterium* and *Enterococcus*

Since the bacteria themselves as well as their fermentation metabolites have shown to impact immunity [42,43], we studied the changes in microbiota composition and the production of organic acids during fermentation of the NDCs by infant faecal microbiota of 2- and 8-week-old infants. Compared to the background fermentation of SIEM medium components, the fermentation of the NDCs mainly impacted the relative abundance of *Bifidobacterium*, *Enterococcus* and *Clostridium sensu stricto 1* (Figure 7). Based on their impact, the NDCs can be divided into two groups. Group I is characterized by the increase in relative abundance of *Bifidobacterium* species which are known to exhibit immunomodulatory properties [44], and consists of GOS, FOS and native inulin (Chapter 3) and the IMO preparation. The second group of NDCs consists of native as well as enzyme-treated oat β-glucan and can be characterized as *Enterococcus*-stimulating (Chapter 4). The unfermentable IMMP does not belong to these two groups as their effects on the microbiota composition were very minor.

The bifidogenic effect of GOS, FOS and native inulin is widely supported by previous *in vivo* studies concerning infants at different ages as reviewed by Vandenplas et al [45] and Firmansyah et al [46]. For the less studied IMO preparation, *in vitro* studies using pig faecal inoculum and bifidobacterial isolates supported the bifidogenic effect [47,48]. Interestingly, the bifidogenic effect of the IMO preparation was only observed with faecal microbiota of 2-week-old infants. The age-dependency of the bifidogenic effect also applies to native

inulin, corresponding to the differences in their fermentability between the faecal microbiota of 2- and 8-week-old infants (Figure 2). The bifidogenic effect of the NDCs in group I was largely reflected by the level of acetate and lactate after 26 h of fermentation (Figure 8). These organic acids are important end products of the bifid shunt, which is a unique hexose metabolism pathway of *Bifidobacterium* [49]. Overall, the bifidogenic effect was most pronounced for faecal microbiota of 2-week-old infants with GOS, whereas for 8-week-old infants native inulin resulted in the highest abundance of *Bifidobacterium*.

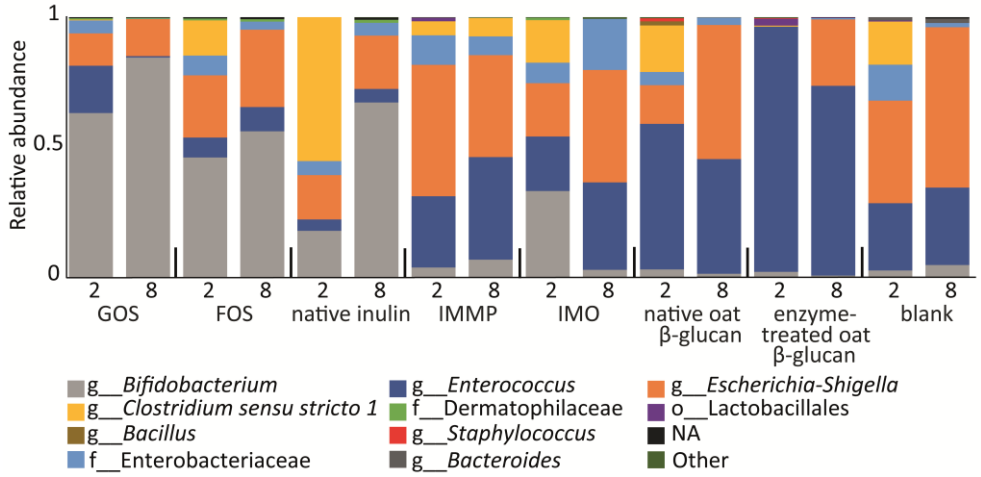

Figure 7 Changes in microbiota composition after 26 h of fermentation of galacto-oligosaccharides (GOS), fructo-oligosaccharides (FOS), native inulin, media supplemented with isomalto/malto-polysaccharides (IMMP), the isomalto-oligosaccharide (IMO) preparation, media supplemented with native oat β-glucan, enzyme-treated oat β-glucan and without added NDCs (blank) using pooled faecal inoculum of 2- and 8-week-old infants. Results are the average of duplicate fermentations.

The second group of NDCs resulted in an increase in relative abundance of *Enterococcus*. *Enterococcus* has received considerable negative attention in the past due to the pathogenicity of some *Enterococcus* strains [50]. In contrast, commensal enterococci are known to be one of the first colonizers of the infant gut [51] and are nowadays extensively studied for their potential probiotic activity [50]. The increase in relative abundance of *Enterococcus* upon fermentation of endo-1,3(4)-β-glucanase-treated oat β-glucan correlated with the production of lactate after 26 h of fermentation (Figure 7-8), which is the main end-product of the fermentation of hexoses by *Enterococcus* [52]. However, it is important to bear in mind the possible bias in these results introduced by the *in vitro* batch fermentation set-up. The build-up of lactate and the expected shift in pH in this one-compartment model could have inhibited the growth of lactate-utilizing bacteria commonly found in the infant gut [53,54]. These lactate-utilizing bacteria would otherwise have converted the lactate into acetate or butyrate [55]. The fermentation of media supplemented with native oat β-glucan did not result in the production of lactate. The

presence of native oat β-glucan further stimulated the growth of *Enterococcus* on SIEM medium components as observed in the background fermentation (Chapter 4).
Interestingly, the relative abundance of *Clostridium sensu stricto 1* increased exclusively during fermentation of native inulin by faecal microbiota of 2-week-old infants, alongside the production of their main metabolic end product butyrate (Figure 7-8 and Chapter 3). Taken together, our findings showed that the changes in microbiota composition and consequent organic acid production are dependent on the structure of the NDCs and the age of the infants, which could have implications for their immune effects (vide infra).

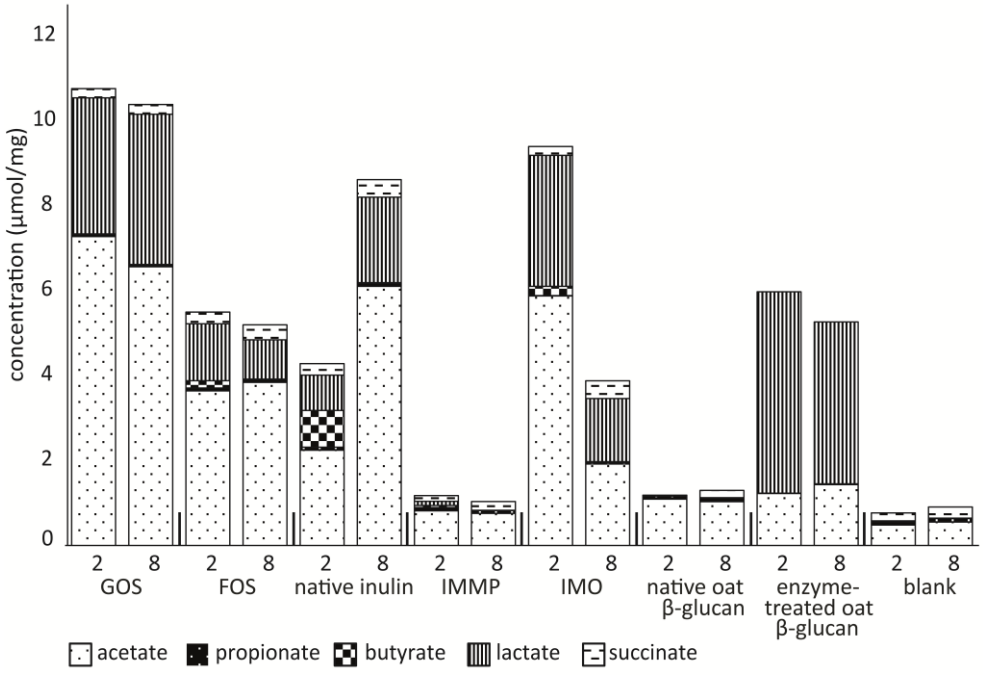

Figure 8 Production of SCFAs, lactate and succinate after 26 h of fermentation of galacto-oligosaccharides (GOS), fructo-oligosaccharides (FOS), native inulin, media supplemented with isomalto/malto-polysaccharides (IMMP), the isomalto-oligosaccharide (IMO) preparation, media supplemented with native oat β-glucan, enzyme-treated oat β-glucan and without added NDCs (blank) using pooled faecal inoculum of 2- and 8-week-old infants. Results are the average of duplicate fermentations.

Bacterial metabolites formed upon NDC fermentation cause immune attenuation

Several NDCs have been reported to influence immunity *in vitro* through their direct interaction with Toll-like receptors (TLR) present on epithelial and dendritic cells [56-58]. However, these studies generally do not consider the impact of the degradation of the NDCs by the gut bacteria and the consequent production of fermentation metabolites, on the immune effects. Since the gastrointestinal tract is aligned with numerous dendritic cells, we

studied the impact of the fermentation of NDCs on the cytokine responses by dendritic cells derived from the umbilical vein.

Interestingly, digesta from control fermentations without added NDCs resulted in substantial production of pro- and anti- inflammatory cytokines (Figure 9 and Chapter 3-4). This could have been caused by the presence of bacteria-derived metabolites other than SCFAs, such as histamines and exopolysaccharides [59]. In addition, the SIEM medium contained significant amount of protein to mimic the intestinal environment. As such, tryptophan was available, which can be metabolized by bacteria yielding immune-active indole derivatives [60]. Next to metabolites, potential immune-active bacteria-derived components such as DNA sequences and cell wall components [59], were present in the digesta due to cell lysis upon heat treatment.

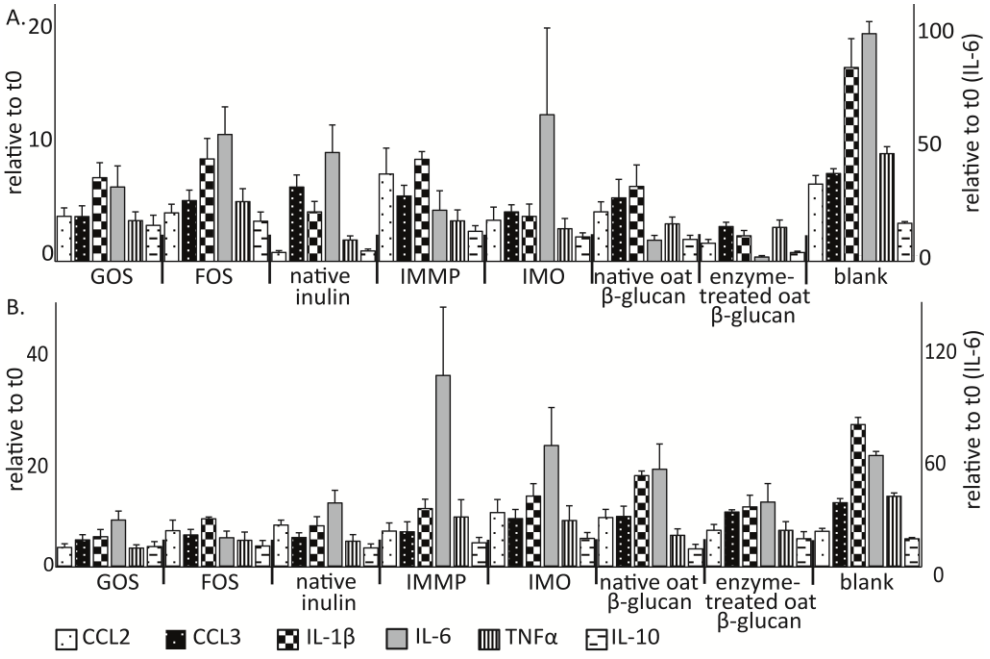

Figure 9 Induction of cytokines by dendritic cells (fold change compared to 0 h with the y-axis of IL-6 presented on the right side) after incubation with digesta collected after 26 h of fermentation of galacto-oligosaccharides (GOS), fructo-oligosaccharides (FOS), native inulin, media supplemented with isomalto/malto-polysaccharides (IMMP), the isomalto-oligosaccharide (IMO) preparation, media supplemented with native oat β-glucan, enzyme-treated oat β-glucan and without added NDCs (blank) using pooled faecal inoculum of 2- (A) and 8-week-old (B) infants. Data are shown as averages with n=6 and error bars represent standard error of the means.

In comparison to the control fermentation, fermentation of the NDCs principally attenuated the cytokine production by the dendritic cells (Figure 9 and Chapter 3, 4). The only increase in production was observed for IL-6 when the dendritic cells were incubated with the digesta of IMMP fermentation with faecal microbiota of 2-week-old infants. The extent of

attenuation varied depending on the NDC and the infant age. Overall, with faecal microbiota of 2-week-old infants the fermentation of endo-1,3(4)-β-glucanase-treated oat β-glucan was most effective in attenuating the cytokine production, whereas faecal microbiota of 8-week-old infants most effectively attenuated cytokine production through the fermentation of GOS.

The immune attenuation is partly assigned to specific organic acids produced upon fermentation of the NDCs (Figure 8). For example, the production of butyrate upon fermentation of native inulin was related to a strong attenuation of the CCL2 and IL-10 production (Chapter 3), which is in line with the immune-attenuating effects of butyrate demonstrated in previous *in vitro* studies [61]. The bacteria themselves could also play an important role in the immune attenuation as exemplified by native oat β-glucan (Chapter 4). The *Enterococcus*-stimulating effect of this unfermentable NDC contributed to the immune attenuation, presumably by carbohydrates on the cell surface of *Enterococcus* [62]. The previously reported stimulation of specific cytokine production through the direct interaction of NDCs with TLRs on dendritic cells or monocytes [58,63], has not been observed in this study. The digesta collected at t=0 as well as intact NDCs without fermentation medium did not result in significant production of cytokines (data not shown). This contradictory result may be due to the removal of lipopolysaccharide (LPS) using polymyxin-B from all the digesta which were incubated with the dendritic cells in our study. LPS is an ubiquitous immune-active contaminant specifically interacting with TLR4 [64]. Traces of LPS in NDCs are sufficient to generate misleading results when the cytokine production by dendritic cells is assessed as shown in previous study [65].

Potential direct attenuating effects of the intact NDCs cannot be excluded yet with the experimental set-up used in our study, since a certain amount of immune stimulation is needed to be able to observe the attenuation. In addition, it is unknown if the structural changes of the NDCs during fermentation influenced their interaction with immune receptors on the dendritic cells as reported previously for the glycosidic fermentation products of barley β-glucan and sugar beet pectin [66]. That study did not include microbiota-dependent immune effects of NDCs as the dendritic cells were derived from TLR2/4 knock out mice. Hence, it remains to be identified if the NDC glycosidic fermentation products contribute significantly to the observed immune effects of the NDCs.

Overall, the fermentability of the NDCs was positively correlated with the attenuation of the cytokine production by the dendritic cells. For example, the fermentability of the IMO preparation and enzyme-treated oat β-glucan (Figure 2) as well as the immune attenuation by their fermentation digesta were more pronounced with faecal microbiota of 2-week-old infants than with faecal microbiota of 8-week-old infants. Taken together, these findings imply a large contribution of the bacteria-derived components and metabolites to the immune effects of the NDCs, although the impact of the intact NDCs or glycosidic degradation products cannot be excluded.

Implications of results for tailoring NDC mixtures for infant formula

To our knowledge this is one of the first studies focusing on the impact of the fermentation of NDCs by infant faecal microbiota on the immune-modulating capacity of the NDCs. Fermentation digesta of the different NDCs included in this study attenuated the production of both pro- and anti-inflammatory cytokines by dendritic cells. The extent of attenuation depended on the age and consequent microbiota composition of the infants as well as the structure of the NDCs, which together determine the presence and abundance of the immune-active bacteria-derived components and metabolites in the digesta.

The attenuation of inflammatory responses is beneficial in infants with their immature intestinal immune system characterized by excessive inflammatory responses [67]. In accordance, inflammatory and infectious diseases such as necrotizing enterocolitis (NEC), are common in the first years of life [68]. HMOs have been reported to protect infants against these diseases through the attenuation of pro-inflammatory cytokines [69,70]. At this stage, it is impossible to predict if NDCs could resemble the immune-modulating effects of the HMOs as recent studies emphasized the complexity of the cytokine network present in the intestine, in which each cytokine can exhibit multiple functions [71,72]. As such, follow-up studies on tissue scale are necessary to more accurately predict the eventual health outcomes of the fermentation of the NDCs in infants.

Our research confirms the potential of tailored NDC mixtures for substitution of infant formula to meet the needs of infants of different ages as the NDC-degrading capacity of the infant microbiota changed upon aging. Interestingly, we even showed a negative correlation between the fermentability of IMOs and the infant age, impacting the eventual cytokine profiles of the dendritic cells. The results obtained in this study with pooled faecal inoculum of 2- and 8-week-old infants are applicable to a broader age range as the exact timing of the development of the NDC-degrading capacity was infant-dependent (Chapter 2). The fermentation behaviour of the pooled faecal inoculum more closely reflected the behaviour of the individual faecal inoculum with the highest NDC degrading capacity present in the pool.

Future perspectives

The aim of this thesis was to determine the fermentability of different NDCs and their microbiota-dependent immune effects in the infant gut. We especially paid close attention to the exact structure of the NDCs and how the structure affects the fermentability and consequent immune effects. The developed characterization method based on UHPLC-PGC-MS showed us that the fermentability of NDCs by infant microbiota is not only dependent on the size of the NDCs, but also on structural features such as the anomeric configuration and type of the glycosidic linkages. In addition, UHPLC-PGC-MS shed light on the high complexity of NDC mixtures. Commercial NDC mixtures often approached of containing one

structure with a straightforward bioactivity, even turned out to be structurally very different from each other. For example, commercial GOS preparations are produced with different β-galactosidases with specific stereochemistry, which results in mixtures enriched in either β(1-3)-, β(1-4)- or β(1-6)-linked galactose residues with different DP distribution [15,73]. This has significant implications for the type and level of bioactivity of the commercial GOS mixtures due to the structure-specific fermentability of NDCs by gut microbiota. Future studies concerning health-effects of NDCs should thus always include detailed information on the structure of the NDCs, which facilitates the comparison between results from different studies. In addition, fractionation of immune-active NDCs will contribute to the effective recognition of the structure-specific immune effects. In this way we will obtain a deeper understanding of the highly complex and fascinating interplay between NDCs, the microbiota and host immunity.

Our study provided potential NDCs which could be added to infant formula for specific infant age groups. These NDCs were selected based on the extent of attenuation of the cytokine production by dendritic cells through the fermentation digesta, which mainly depended on the bacteria-derived components and metabolites. However, the clinical relevance of the attenuation of specific cytokines by dendritic cells remains to be identified. In addition, next to the immune effects provoked by the dendritic cells there are undoubtedly many more pathways through which the NDCs can interact with host immunity [74]. Hence, the NDCs selected in this study should preferably be further investigated in an advanced model, which more closely mimics the intestinal environment by the presence of e.g. an epithelial layer, macrophages and lymphocytes. Organoid technologies which are currently rapidly advancing could prove highly suitable for this purpose [75]. These three-dimensional tissue cultures can be composed of different cell types commonly found in the gut, thereby reflecting both the phenotype and the physiology of the intestine. Several studies succeeded to co-culture intestinal organoids with bacteria to study their complex interactions [76,77].

Importantly, the model should consider the mucus layer that covers the intestinal epithelium and forms a solid barrier to prevent translocation of bacteria from the lumen into the systemic circulation. The microbiota composition of the mucus layer and the luminal intestinal contents significantly differ due to distinct availability of carbohydrates for bacterial growth in these intestinal regions [78]. The mucus-associated bacteria are closer located to the epithelial layer, which suggests that their interaction with immune cells either directly or via the production of metabolites, is more potent than for lumen-associated bacteria. Incorporation of the 'bacterial niche effect' in the model will demonstrate if the bacteria-derived components and metabolites present in the lumen can exert their immune-attenuating effects despite the presence of the mucus layer.

Finally, another important aspect to keep in mind is the regional immune specialization of the gut. The immune environment differs significantly throughout the gut with respect to

e.g. the thickness of the mucus layer and the distribution of T-cell subsets and dendritic cells [79]. The immune effects of a slowly and rapidly fermentable fibre resulting in similar bacteria-derived components and metabolites, might thus be completely different. Hence, NDC mixtures should preferably be designed in such a way that their structures tailor the microbiota composition and stimulate the desired region-specific immune response; a targeted approach. However, the production of such tailored NDC mixtures is practically impossible, due to high intra- and inter-individual variability as well as regional variation in microbiota composition throughout the infant gut [80]. This issue could be solved by the use of postbiotics, which refers to non-viable bacteria and their metabolites produced *ex vivo* [81]. In contrast to probiotics and synbiotics, postbiotics guarantee the release of the immune-active bacteria-derived components and metabolites in the infant gut. The targeted delivery of the postbiotics to the desired region of the intestine could be enabled by encapsulation techniques which are nowadays used for probiotics [82]. Taken together, the supplementation of cow-milk based infant formula with both postbiotics and NDCs could be of high value in the future to ensure a solid level of immunomodulation whilst at the same time supporting the colonization of the infant gut.

References

1. Comstock, S.S.; Wang, M.; Hester, S.N.; Li, M.; Donovan, S.M. Select human milk oligosaccharides directly modulate peripheral blood mononuclear cells isolated from 10-d-old pigs. *Br. J. Nutr.* **2014**, *111*, 819-828.
2. Engfer, M.B.; Stahl, B.; Finke, B.; Sawatzki, G.; Daniel, H. Human milk oligosaccharides are resistant to enzymatic hydrolysis in the upper gastrointestinal tract. *Am. J. Clin. Nutr.* **2000**, *71*, 1589-1596.
3. Vinolo, M.A.; Rodrigues, H.G.; Hatanaka, E.; Sato, F.T.; Sampaio, S.C.; Curi, R. Suppressive effect of short-chain fatty acids on production of proinflammatory mediators by neutrophils. *J. Nutr. Biochem.* **2011**, *22*, 849-855.
4. Bode, L.; Jantscher-Krenn, E. Structure-function relationships of human milk oligosaccharides. *Adv. Nutr.* **2012**, *3*, 383s-391s.
5. Van de Wiele, T.; Van den Abbeele, P.; Ossieur, W.; Possemiers, S.; Marzorati, M. The Simulator of the Human Intestinal Microbial Ecosystem (SHIME®). In *The Impact of Food Bioactives on Health: in vitro and ex vivo models*, Verhoeckx, K.; Cotter, P.; López-Expósito, I.; Kleiveland, C.; Lea, T.; Mackie, A.; Requena, T.; Swiatecka, D.; Wichers, H., Eds.; Springer International Publishing: Cham, Switzerland, **2015**, pp. 305-317.
6. Venema, K. The TNO *In Vitro* Model of the Colon (TIM-2). In *The Impact of Food Bioactives on Health: in vitro and ex vivo models*, Verhoeckx, K.; Cotter, P.; López-Expósito, I.; Kleiveland, C.; Lea, T.; Mackie, A.; Requena, T.; Swiatecka, D.; Wichers, H., Eds.; Springer International Publishing: Cham, Switzerland, **2015**, pp. 293-304.
7. Marzorati, M.; Vanhoecke, B.; De Ryck, T.; Sadaghian Sadabad, M.; Pinheiro, I.; Possemiers, S.; Van den Abbeele, P.; Derycke, L.; Bracke, M.; Pieters, J.; Hennebel, T.; Harmsen, H.J.; Verstraete, W.; Van de Wiele, T. The HMI module: a new tool to study the Host-Microbiota Interaction in the human gastrointestinal tract *in vitro*. *BMC Microbiol.* **2014**, *14*, 133.
8. Aura, A.-M.; Maukonen, J. One compartment fermentation model. In *The Impact of Food Bioactives on Health: in vitro and ex vivo models*, Verhoeckx, K.; Cotter, P.; López-Expósito, I.; Kleiveland, C.; Lea, T.; Mackie, A.; Requena, T.; Swiatecka, D.; Wichers, H., Eds.; Springer International Publishing: Cham, Switzerland, **2015**, pp. 281-292.
9. Flint, H.J.; Scott, K.P.; Duncan, S.H.; Louis, P.; Forano, E. Microbial degradation of complex carbohydrates in the gut. *Gut Microbes* **2012**, *3*, 289-306.
10. Rodríguez, J.M.; Murphy, K.; Stanton, C.; Ross, R.P.; Kober, O.I.; Juge, N.; Avershina, E.; Rudi, K.; Narbad, A.; Jenmalm, M.C. The composition of the gut microbiota throughout life, with an emphasis on early life. *Microb. Ecol. Health Dis.* **2015**, *26*, 26050.
11. Albrecht, S.; Schols, H.A.; van den Heuvel, E.G.; Voragen, A.G.; Gruppen, H. Occurrence of oligosaccharides in feces of breast-fed babies in their first six months of life and the corresponding breast milk. *Carbohydr. Res.* **2011**, *346*, 2540-2550.
12. Dogra, S.; Sakwinska, O.; Soh, S.-E.; Ngom-Bru, C.; Brück, W.M.; Berger, B.; Brüssow, H.; Lee, Y.S.; Yap, F.; Chong, Y.-S.; Godfrey, K.M.; Holbrook, J.D. Dynamics of infant gut microbiota are influenced by delivery mode and gestational duration and are associated with subsequent adiposity. *mBio* **2015**, *6*.
13. Thurl, S.; Munzert, M.; Henker, J.; Boehm, G.; Müller-Werner, B.; Jelinek, J.; Stahl, B. Variation of human milk oligosaccharides in relation to milk groups and lactational periods. *Br. J. Nutr.* **2010**, *104*, 1261-1271.
14. Torres, D.P.M.; Gonçalves, M.d.P.F.; Teixeira, J.A.; Rodrigues, L.R. Galacto-oligosaccharides: Production, properties, applications, and significance as prebiotics. *Compr. Rev. Food Sci. Food Saf.* **2010**, *9*, 438-454.
15. Yin, H.; Bultema, J.B.; Dijkhuizen, L.; van Leeuwen, S.S. Reaction kinetics and galactooligosaccharide product profiles of the β-galactosidases from *Bacillus circulans*, *Kluyveromyces lactis* and *Aspergillus oryzae*. *Food Chem.* **2017**, *225*, 230-238.
16. Fransen, C.T.; Van Laere, K.M.; van Wijk, A.A.; Brull, L.P.; Dignum, M.; Thomas-Oates, J.E.; Haverkamp, J.; Schols, H.A.; Voragen, A.G.; Kamerling, J.P.; Vliegenthart, J.F. alpha-D-Glcp-(1-1)-beta-D-Galp-containing oligosaccharides, novel products from lactose by the action of beta-galactosidase. *Carbohydr. Res.* **1998**, *314*, 101-114.
17. Coulier, L.; Timmermans, J.; Bas, R.; Van Den Dool, R.; Haaksman, I.; Klarenbeek, B.; Slaghek, T.; Van Dongen, W. In-depth characterization of prebiotic galacto-oligosaccharides by a combination of analytical techniques. *J. Agric. Food Chem.* **2009**, *57*, 8488-8495.
18. Kelly, G. Inulin-type prebiotics - a review: part 1. *Altern. Med. Rev.* **2008**, *13*, 315-329.
19. Daou, C.; Zhang, H. Oat beta-glucan: Its role in health promotion and prevention of diseases. *Compr. Rev. Food Sci. Food Saf.* **2012**, *11*, 355-365.
20. Leemhuis, H.; Dobruchowska, J.M.; Ebbelaar, M.; Faber, F.; Buwalda, P.L.; van der Maarel, M.J.E.C.; Kamerling, J.P.; Dijkhuizen, L. Isomalto/malto-polysaccharide, a novel soluble dietary fiber made via enzymatic conversion of starch. *J. Agric. Food Chem.* **2014**, *62*, 12034-12044.

21. van der Zaal, P.H.; Schols, H.A.; Bitter, J.H.; Buwalda, P.L. Isomalto/malto-polysaccharide structure in relation to the structural properties of starch substrates. *Carbohydr. Polym.* **2018**, *185*, 179-186.
22. Sorndech, W.; Nakorn, K.N.; Tongta, S.; Blennow, A. Isomalto-oligosaccharides: Recent insights in production technology and their use for food and medical applications. *LWT* **2018**, *95*, 135-142.
23. Niu, D.; Qiao, J.; Li, P.; Tian, K.; Liu, X.; Singh, S.; Lu, F. Highly efficient enzymatic preparation of isomalto-oligosaccharides from starch using an enzyme cocktail. *Electron. J. Biotechnol.* **2017**, *26*, 46-51.
24. Scott, K.P.; Martin, J.C.; Chassard, C.; Clerget, M.; Potrykus, J.; Campbell, G.; Mayer, C.-D.; Young, P.; Rucklidge, G.; Ramsay, A.G.; Flint, H.J. Substrate-driven gene expression in *Roseburia inulinivorans*: Importance of inducible enzymes in the utilization of inulin and starch. *Proc. Natl. Acad. Sci.* **2011**, *108*, 4672-4679.
25. van den Broek, L.A.; Hinz, S.W.; Beldman, G.; Vincken, J.P.; Voragen, A.G. *Bifidobacterium* carbohydrases-their role in breakdown and synthesis of (potential) prebiotics. *Mol. Nutr. Food Res.* **2008**, *52*, 146-163.
26. Milani, C.; Duranti, S.; Bottacini, F.; Casey, E.; Turroni, F.; Mahony, J.; Belzer, C.; Delgado Palacio, S.; Arboleya Montes, S.; Mancabelli, L.; Lugli, G.A.; Rodriguez, J.M.; Bode, L.; de Vos, W.; Gueimonde, M.; Margolles, A.; van Sinderen, D.; Ventura, M. The first microbial colonizers of the human gut: Composition, activities, and health implications of the infant gut microbiota. *Microbiol. Mol. Biol. Rev.* **2017**, *81*, e00036-00017.
27. Falony, G.; Lazidou, K.; Verschaeren, A.; Weckx, S.; Maes, D.; De Vuyst, L. *In vitro* kinetic analysis of fermentation of prebiotic inulin-type fructans by *Bifidobacterium* species reveals four different phenotypes. *Appl. Environ. Microbiol.* **2009**, *75*, 454-461.
28. Rossi, M.; Corradini, C.; Amaretti, A.; Nicolini, M.; Pompei, A.; Zanoni, S.; Matteuzzi, D. Fermentation of fructooligosaccharides and inulin by bifidobacteria: a comparative study of pure and fecal cultures. *Appl. Environ. Microbiol.* **2005**, *71*, 6150-6158.
29. Ladirat, S.; Schols, H.; Nauta, A.; Schoterman, M.; Schuren, F.; Gruppen, H. *In vitro* fermentation of galacto-oligosaccharides and its specific size-fractions using non-treated and amoxicillin-treated human inoculum. *Bioact. Carbohydr. Diet. Fibre* **2014**, *3*, 59-70.
30. van Leeuwen, S.S.; Kuipers, B.J.; Dijkhuizen, L.; Kamerling, J.P. (1)H NMR analysis of the lactose/beta-galactosidase-derived galacto-oligosaccharide components of Vivinal(R) GOS up to DP5. *Carbohydr. Res.* **2014**, *400*, 59-73.
31. Poinsot, V.; Carpéné, M.A.C., F. Coupled mass spectrometric strategies for the determination of carbohydrates at very low concentrations: The case of polysaccharides involved in the molecular dialogue between plants and rhizobia. In *The complex world of polysaccharides*; Karunaratne, D.N., Ed.; InTech: Rijeka, Croatia, **2012**.
32. Ruhaak, L.R.; Deelder, A.M.; Wuhrer, M. Oligosaccharide analysis by graphitized carbon liquid chromatography–mass spectrometry. *Anal. Bioanal. Chem.* **2009**, *394*, 163-174.
33. Black, B.A.; Lee, V.S.; Zhao, Y.Y.; Hu, Y.; Curtis, J.M.; Gänzle, M.G. Structural identification of novel oligosaccharides produced by *Lactobacillus bulgaricus* and *Lactobacillus plantarum*. *J. Agric. Food Chem.* **2012**, *60*, 4886-4894.
34. Guan, B.; Cole, R.B. MALDI linear-field reflectron TOF post-source decay analysis of underivatized oligosaccharides: Determination of glycosidic linkages and anomeric configurations using anion attachment. *J. Am. Soc. Mass Spectrom.* **2008**, *19*, 1119-1131.
35. Goffin, D.; Robert, C.; Wathelet, B.; Blecker, C.; Malmendier, Y.; Paquot, M. A step-forward method of quantitative analysis of enzymatically produced isomaltooligosaccharide preparations by AEC-PAD. *Chromatographia* **2008**, *69*, 287.
36. Bhattacharya, T.; Ghosh, T.S.; Mande, S.S. Global profiling of carbohydrate active enzymes in human gut microbiome. *PLoS One* **2015**, *10*, e0142038.
37. Ladirat, S.E.; Schuren, F.H.; Schoterman, M.H.; Nauta, A.; Gruppen, H.; Schols, H.A. Impact of galacto-oligosaccharides on the gut microbiota composition and metabolic activity upon antibiotic treatment during *in vitro* fermentation. *FEMS Microbiol. Ecol.* **2014**, *87*, 41-51.
38. Sakanaka, M.; Gotoh, A.; Yoshida, K.; Odamaki, T.; Koguchi, H.; Xiao, J.Z.; Kitaoka, M.; Katayama, T. Varied pathways of infant gut-associated *Bifidobacterium* to assimilate human milk oligosaccharides: prevalence of the gene set and its correlation with bifidobacteria-rich microbiota formation. *Nutrients* **2019**, *12*.
39. Abou Hachem, M.; S. Møller, M.; M. Andersen, J.; Fredslund, F.; Majumder, A.; Nakai, H.; Lo Leggio, L.; Goh, Y.-J.; Barrangou, R.; R. Klaenhammer, T.; Svensson, B. A snapshot into the metabolism of isomalto-oligosaccharides in probiotic bacteria. *J. Appl. Glycosci.* **2013**, *advpub*.
40. Ejby, M.; Fredslund, F.; Andersen, J.M.; Vujicic Zagar, A.; Henriksen, J.R.; Andersen, T.L.; Svensson, B.; Slotboom, D.J.; Abou Hachem, M. An ATP binding cassette transporter mediates the uptake of alpha-(1,6)-linked dietary oligosaccharides in *Bifidobacterium* and correlates with competitive growth on these substrates. *J. Biol. Chem.* **2016**, *291*, 20220-20231.
41. Viborg, A.H.; Katayama, T.; Abou Hachem, M.; Andersen, M.C.; Nishimoto, M.; Clausen, M.H.; Urashima, T.; Svensson, B.; Kitaoka, M. Distinct substrate specificities of three glycoside hydrolase family 42 β-galactosidases from *Bifidobacterium longum subsp. infantis* ATCC 15697. *Glycobiology* **2013**, *24*, 208-216.

42. Nastasi, C.; Candela, M.; Bonefeld, C.M.; Geisler, C.; Hansen, M.; Krejsgaard, T.; Biagi, E.; Andersen, M.H.; Brigidi, P.; Ødum, N.; Litman, T.; Woetmann, A. The effect of short-chain fatty acids on human monocyte-derived dendritic cells. *Sci. Rep.* **2015**, *5*, 16148.
43. Sánchez, B.; González-Rodríguez, I.; Arboleya, S.; López, P.; Suárez, A.; Ruas-Madiedo, P.; Margolles, A.; Gueimonde, M. The effects of *Bifidobacterium breve* on immune mediators and proteome of HT29 cells monolayers. *BioMed Res. Int.* **2015**, *2015*, 479140-479140.
44. Ruiz, L.; Delgado, S.; Ruas-Madiedo, P.; Sánchez, B.; Margolles, A. Bifidobacteria and their molecular communication with the immune system. *Front. Microbiol.* **2017**, *8*.
45. Vandenplas, Y.; Zakharova, I.; Dmitrieva, Y. Oligosaccharides in infant formula: more evidence to validate the role of prebiotics. *Br. J. Nutr.* **2015**, *113*, 1339-1344.
46. Firmansyah, A.; Chongviriyaphan, N.; Dillon, D.H.; Khan, N.C.; Morita, T.; Tontisirin, K.; Tuyen, L.D.; Wang, W.; Bindels, J.; Deurenberg, P.; Ong, S.; Hautvast, J.; Meyer, D.; Vaughan, E.E. Fructans in the first 1000 days of life and beyond, and for pregnancy. *Asia Pac. J. Clin. Nutr.* **2016**, *25*, 652-675.
47. Tran, T.H.T.; Boudry, C.; Everaert, N.; Bindelle, J. Prebiotic potential of novel carbohydrates in an *in vitro* co-inoculation fermentation model of the bacteria isolated from pig intestine and Salmonella. *J. Anim. Sci.* **2016**, *94*, 58-61.
48. Hu, Y.; Ketabi, A.; Buchko, A.; Gänzle, M.G. Metabolism of isomalto-oligosaccharides by *Lactobacillus reuteri* and bifidobacteria. *Lett. Appl. Microbiol.* **2013**, *57*, 108-114.
49. Palframan, R.J.; Gibson, G.R.; Rastall, R.A. Carbohydrate preferences of *Bifidobacterium* species isolated from the human gut. *Curr. Issues Intest. Microbiol.* **2003**, *4*, 71-75.
50. Hanchi, H.; Mottawea, W.; Sebei, K.; Hammami, R. The genus *Enterococcus*: between probiotic potential and safety concerns-an update. *Front. Microbiol.* **2018**, *9*, 1791-1791.
51. Fanaro, S.; Chierici, R.; Guerrini, P.; Vigi, V. Intestinal microflora in early infancy: composition and development. *Acta Paediatr. Suppl.* **2003**, *91*, 48-55.
52. Ramsey, M.; Hartke, A.; Huycke, M. The physiology and metabolism of Enterococci. In *Enterococci: From Commensals to Leading Causes of Drug Resistant Infection* Gilmore, M.S., Clewell, D.B., Ike Y., Eds.; Massachusetts Eye and Ear Infirmary: Boston, United States, **2014**.
53. Pham, V.T.; Lacroix, C.; Braegger, C.P.; Chassard, C. Early colonization of functional groups of microbes in the infant gut. *Environ. Microbiol.* **2016**, *18*, 2246-2258.
54. Pham, V.T.; Chassard, C.; Rifa, E.; Braegger, C.; Geirnaert, A.; Rocha Martin, V.N.; Lacroix, C. Lactate metabolism is strongly modulated by fecal inoculum, pH, and retention time in PolyFermS continuous colonic fermentation models mimicking young infant proximal colon. *mSystems* **2019**, *4*, e00264-00218.
55. Louis, P.; Flint, H.J. Formation of propionate and butyrate by the human colonic microbiota. *Environ. Microbiol.* **2017**, *19*, 29-41.
56. Vogt, L.M.; Meyer, D.; Pullens, G.; Faas, M.M.; Venema, K.; Ramasamy, U.; Schols, H.A.; de Vos, P. Toll-like receptor 2 activation by beta2-->1-fructans protects barrier function of T84 human intestinal epithelial cells in a chain length-dependent manner. *J. Nutr.* **2014**, *144*, 1002-1008.
57. Ortega-Gonzalez, M.; Ocon, B.; Romero-Calvo, I.; Anzola, A.; Guadix, E.; Zarzuelo, A.; Suarez, M.D.; Sanchez de Medina, F.; Martinez-Augustin, O. Nondigestible oligosaccharides exert nonprebiotic effects on intestinal epithelial cells enhancing the immune response via activation of TLR4-NFkappaB. *Mol. Nutr. Food Res.* **2014**, *58*, 384-393.
58. Lehmann, S.; Hiller, J.; van Bergenhenegouwen, J.; Knippels, L.M.; Garssen, J.; Traidl-Hoffmann, C. *In Vitro* Evidence for immune-modulatory properties of non-digestible oligosaccharides: Direct effect on human monocyte derived dendritic cells. *PLoS One* **2015**, *10*, e0132304.
59. Ruiz, L.; Hevia, A.; Bernardo, D.; Margolles, A.; Sanchez, B. Extracellular molecular effectors mediating probiotic attributes. *FEMS Microbiol. Lett.* **2014**, *359*, 1-11.
60. Zelante, T.; Iannitti, R.G.; Cunha, C.; De Luca, A.; Giovannini, G.; Pieraccini, G.; Zecchi, R.; D'Angelo, C.; Massi-Benedetti, C.; Fallarino, F.; Carvalho, A.; Puccetti, P.; Romani, L. Tryptophan catabolites from microbiota engage aryl hydrocarbon receptor and balance mucosal reactivity via interleukin-22. *Immunity* **2013**, *39*, 372-385.
61. Corrêa-Oliveira, R.; Fachi, J.L.; Vieira, A.; Sato, F.T.; Vinolo, M.A.R. Regulation of immune cell function by short-chain fatty acids. *Clin. Transl. Immunol.* **2016**, *5*, e73-e73.
62. Wang, S.; Ng, L.H.M.; Chow, W.L.; Lee, Y.K. Infant intestinal *Enterococcus faecalis* down-regulates inflammatory responses in human intestinal cell lines. *World J. Gastroenterol.* **2008**, *14*, 1067-1076.
63. Capitán-Cañadas, F.; Ortega-González, M.; Guadix, E.; Zarzuelo, A.; Suárez, M.D.; de Medina, F.S.; Martínez-Augustin, O. Prebiotic oligosaccharides directly modulate proinflammatory cytokine production in monocytes via activation of TLR4. *Mol. Nutr. Food Res.* **2014**, *58*, 1098-1110.
64. Govers, C.; Tomassen, M.M.M.; Rieder, A.; Ballance, S.; Knutsen, S.H.; Mes, J.J. Lipopolysaccharide quantification and alkali-based inactivation in polysaccharide preparations to enable *in vitro* immune modulatory studies. *Bioact. Carbohydr. Diet. Fibre* **2016**, *8*, 15-25.
65. Perdijk, O.; van Neerven, R.J.J.; van den Brink, E.; Savelkoul, H.F.J.; Brugman, S. The oligosaccharides 6'-sialyllactose, 2'-fucosyllactose or galactooligosaccharides do not directly modulate human dendritic cell differentiation or maturation. *PLoS One* **2018**, *13*, e0200356.
66. Rösch, C.; Taverne, N.; Venema, K.; Gruppen, H.; Wells, J.M.; Schols, H.A. Effects of *in vitro* fermentation of barley β-glucan and sugar beet pectin using human fecal inocula on cytokine expression by dendritic cells. *Mol. Nutr. Food Res.* **2017**, *61*, 1600243.

67. Nanthakumar, N.N.; Fusunyan, R.D.; Sanderson, I.; Walker, W.A. Inflammation in the developing human intestine: A possible pathophysiologic contribution to necrotizing enterocolitis. *Proc. Natl. Acad. Sci. U. S. A.* **2000**, *97*, 6043-6048.
68. Thai, J.D.; Gregory, K.E. Bioactive factors in human breast milk attenuate intestinal inflammation during early life. *Nutrients* **2020**, *12*, 581.
69. Cortez, J.; Makker, K.; Kraemer, D.F.; Neu, J.; Sharma, R.; Hudak, M.L. Maternal milk feedings reduce sepsis, necrotizing enterocolitis and improve outcomes of premature infants. *J. Perinatol.* **2018**, *38*, 71-74.
70. Newburg, D.S.; He, Y. Neonatal gut microbiota and human milk glycans cooperate to attenuate infection and inflammation. *Clin. Obstet. Gynecol.* **2015**, *58*, 814-826.
71. Andrews, C.; McLean, M.H.; Durum, S.K. Cytokine tuning of intestinal epithelial function. *Front. Immunol.* **2018**, *9*.
72. Neurath, M.F. Cytokines in inflammatory bowel disease. *Nat. Rev. Immunol.* **2014**, *14*, 329-342.
73. van Leeuwen, S.S.; Kuipers, B.J.H.; Dijkhuizen, L.; Kamerling, J.P. Comparative structural characterization of 7 commercial galacto-oligosaccharide (GOS) products. *Carbohydr. Res.* **2016**, *425*, 48-58.
74. Ma, N.; Guo, P.; Zhang, J.; He, T.; Kim, S.W.; Zhang, G.; Ma, X. Nutrients mediate intestinal bacteria-mucosal immune crosstalk. *Front. Immunol.* **2018**, *9*, 5-5.
75. Min, S.; Kim, S.; Cho, S.-W. Gastrointestinal tract modeling using organoids engineered with cellular and microbiota niches. *Exp. Mol. Med.* **2020**, *52*, 227-237.
76. Hill, D.R.; Huang, S.; Nagy, M.S.; Yadagiri, V.K.; Fields, C.; Mukherjee, D.; Bons, B.; Dedhia, P.H.; Chin, A.M.; Tsai, Y.H.; Thodla, S.; Schmidt, T.M.; Walk, S.; Young, V.B.; Spence, J.R. Bacterial colonization stimulates a complex physiological response in the immature human intestinal epithelium. *Elife* **2017**, *6*.
77. Hou, Q.; Ye, L.; Liu, H.; Huang, L.; Yang, Q.; Turner, J.R.; Yu, Q. *Lactobacillus* accelerates ISCs regeneration to protect the integrity of intestinal mucosa through activation of STAT3 signaling pathway induced by LPLs secretion of IL-22. *Cell Death Differ.* **2018**, *25*, 1657-1670.
78. Li, H.; Limenitakis, J.P.; Fuhrer, T.; Geuking, M.B.; Lawson, M.A.; Wyss, M.; Brugiroux, S.; Keller, I.; Macpherson, J.A.; Rupp, S.; Stolp, B.; Stein, J.V.; Stecher, B.; Sauer, U.; McCoy, K.D.; Macpherson, A.J. The outer mucus layer hosts a distinct intestinal microbial niche. *Nat. Commun.* **2015**, *6*, 8292.
79. Mowat, A.M.; Agace, W.W. Regional specialization within the intestinal immune system. *Nature Reviews Immunology* **2014**, *14*, 667.
80. Donaldson, G.P.; Lee, S.M.; Mazmanian, S.K. Gut biogeography of the bacterial microbiota. **2016**, *14*, 20-32.
81. Wegh, C.A.M.; Geerlings, S.Y.; Knol, J.; Roeselers, G.; Belzer, C. Postbiotics and their potential applications in early life nutrition and beyond. *Int. J. Mol. Sci.* **2019**, *20*, 4673.
82. Haffner, F.; Diab, R.; Pasc, A. Encapsulation of probiotics: insights into academic and industrial approaches. *AIMS Mater. Sci.* **2016**, *3*, 114-136.

Summary

Samenvatting

The bacterial colonization of the infant gut has been recognized to play a key role in the development and maturation of the infant intestinal immune system. Human milk oligosaccharides (HMOs) present in human milk have been considered the gold standard for guiding the bacterial colonization. The **first chapter** of this thesis describes the development of the intestinal immune system and the establishment of gut microbiota in early life, as well as the impact of HMOs on these processes. For those infants for which human milk is not a feasible option, cow-milk based infant formulas are supplemented with e.g. non-digestible carbohydrates (NDC) to replace HMOs and to resemble their functional properties. Some commonly used and novel, potential NDCs are discussed in more detail. Due to their complexity, little is known on the fate of NDCs in the infant gut and how the fermentation of the NDCs by infant gut bacteria affects the immunomodulating capacity of the NDCs.

Infants are known for their high inter-individual variability in gut microbiota composition in the first months of life. Numerous *in vitro* fermentations using individual faecal inocula of different infants would be required to study the fate of NDCs in the infant gut. An alternative high-throughput approach could be the use of pooled infant faecal inoculum as is evaluated in **Chapter 2**. An *in vitro* fermentation of galacto-oligosaccharides (GOS) using individual and pooled faecal inocula of 2-week-old infants showed that the bacterial functionality of the pool is largely equivalent to the functionality of the individual inocula. Hence, in the further research, pooled infant faecal inocula is used to study the structure-specific utilization of NDCs by infant gut bacteria.

In total, 7 structurally different NDCs were studied using an *in vitro* batch fermentation set-up. Faecal material of both 2- and 8-week-old infants were used as inoculum to determine the effects of NDCs in the crucial timeframe of infant microbiota development. Samples were collected at different time points. Subsequently, the degradation of the NDCs, the changes in microbiota composition and the production of organic acids were studied, as well as the effects of the fermentation digesta on the cytokine production by dendritic cells.

Chapter 3 describes the fermentability and consequent immune effects of FOS and native inulin. Both NDCs showed a bifidogenic effect, which correlated with the production of acetate and lactate. Faecal microbiota of both 2- and 8-week-old infants primarily fermented the trisaccharides present in FOS. In contrast, the effects of native inulin were dependent on the age of the infants. The bifidogenic effect and production of organic acids were higher with faecal microbiota of 8-week-old infants, which was assigned to a more pronounced degradation of native inulin. Whereas faecal microbiota of 2-week-old infants primarily utilized native inulin with degree of polymerization (DP) 3-8, faecal microbiota of 8-week-old infants degraded longer chains of native inulin up to DP 16. The fermentation of both FOS and native inulin attenuated the production of pro-inflammatory cytokines by dendritic cells. The extent of attenuation correlated with the type and abundance of organic acids formed during the fermentation.

The fermentation characteristics and immuno-modulating properties of native and endo-1,3(4)-β-glucanase-treated oat β-glucan are described in **Chapter 4.** The enzyme treatment of native oat β-glucan (≈300 kDa) resulted in the formation of gluco-oligomers with DP 2-5. While native oat β-glucan remained intact, the gluco-oligomers were fermented to a large extent by faecal microbiota of 2- and 8-week-old infants with a clear preference for β(1→4)-linked oligomers. The fermentation rate was highest with faecal microbiota of 2-week-old infants and correlated with the production of lactate. The fermentation digesta of native oat β-glucan attenuated the production of pro-inflammatory cytokines by dendritic cells, which was more pronounced after enzyme treatment of the glucan. Both the fermentation of native and enzyme-treated oat β-glucan increased the relative abundance of *Enterococcus*. The attenuation of the pro-inflammatory response might have resulted from the interaction between *Enterococcus* cell wall fragments and immune receptors on the dendritic cells.

Our study also includes some highly complex NDCs such as GOS and isomalto-oligosaccharides (IMO), which are composed of many oligosaccharides varying in size, type of linkage and monomer composition. The large number of isomers makes the characterization of these NDCs rather challenging. In this study, a high-throughput characterization method was developed based on UHPLC-MS with a porous graphitic carbon (PGC) stationary phase to facilitate the determination of structure-specific health effects of complex NDCs. **Chapter 5** describes the application of this method for the characterization of Vivinal GOS. The method provided deeper insight into the complexity of Vivinal GOS. The adequate retention mechanism of PGC resulted in the separation of more than 100 different GOS structures in one single run. Reduction of the reducing ends prior to analysis made it a straightforward approach to recognize the reducing and non-reducing isomers. In total, 23 reducing and 15 non-reducing GOS DP3 isomers with a (1-1)-linkage were identified. In addition, a fragmentation rule was discovered to distinguish reducing isomers with a mono- and di-substituted terminal glucose. In this way, UHPLC-PGC-MS facilitates effective recognition of structural features which could impact the fermentability of the NDCs by infant faecal microbiota.

In **Chapter 6**, the fermentation characteristics and immune effects of the NDCs included in Chapter 3 and 4 as well as GOS, IMO, and isomalto/malto-polysaccharides (IMMP) are discussed and compared in detail. The large number of NDCs included in this study together with the focus on the fate of individual oligomers present in the NDCs increased our understanding of their structure-specific fermentability by infant faecal microbiota and concomitant immune effects. The implications of the immune-attenuating effects of the NDCs are discussed taking into account the limitations of the *in vitro* set-up used in our study. Finally, we illustrate how the results obtained in this study contribute to the next generation of cow-milk based infant formula.

De kolonisatie van de babydarm met bacteriën speelt een sleutelrol bij de ontwikkeling en rijping van het immuunsysteem in het darmstelsel. Specifieke koolhydraten die aanwezig zijn in moedermelk (humane melk oligosachariden; HMOs) hebben een grote invloed op deze kolonisatie. HMOs worden niet verteerd in de dunne darm, waardoor ze onaangeroerd in de dikke darm terechtkomen. Hier vormen ze een bron van voeding voor de bacteriën in de darm, ofwel de darmmicrobiota. Het **eerste hoofdstuk** van dit proefschrift beschrijft de ontwikkeling van het immuunsysteem in het darmstelsel en de vestiging van de darmmicrobiota in baby's. Ook wordt de invloed van HMOs op deze processen besproken. Wanneer moedermelk geen optie is, wordt de baby gevoed met op koemelk gebaseerde flesvoeding aangevuld met bv. niet-digesteerbare carbohydraten (NDCs) om de HMOs met hun functionele eigenschappen te vervangen. Enkele veelgebruikte en potentiële NDCs worden in meer detail besproken. Door de complexiteit van de NDCs is er nog maar weinig bekend over hun afbraak door de darmmicrobiota van baby's. Ook is niet bekend of de fermentatie van de NDCs door deze darmbacteriën effect heeft op het immuunsysteem.

Baby's staan bekend om de hoge interindividuele variabiliteit in de samenstelling van de darmmicrobiota in de eerste levensmaanden. Hierdoor zouden talrijke *in vitro* fermentatie-experimenten met individuele fecale inocula van verschillende baby's nodig zijn om de afbraak van NDCs in de babydarm te bestuderen. Een alternatieve "high-throughput" benadering is het combineren van fecaal materiaal van verschillende baby's in een "gepoold fecaal inoculum", dat in **hoofdstuk 2** geëvalueerd wordt. Een *in vitro* fermentatie van galactose-oligosacharide (GOS) met zowel individuele als gepoolde fecale inocula van 2 weken oude baby's toonde aan dat de bacteriële functionaliteit van het gepoolde inoculum grotendeels gelijk is aan de functionaliteit van de individuele inocula. Daarom wordt in deze studie het gepoolde inoculum van babyfeces gebruikt om de structuur-specifieke afbraak van NDCs door de darmmicrobiota van baby's te bestuderen.

In totaal hebben we 7 verschillende NDCs onderzocht met behulp van een *in vitro* batch fermentatieopstelling. Fecaal materiaal van zowel 2 als 8 weken oude baby's werd gebruikt om de effecten van de NDCs te bepalen in het cruciale tijdsbestek van de ontwikkeling van de darmmicrobiota. Op verschillende tijdstippen werden monsters verzameld, die werden bestudeerd op de afbraak van de NDCs, de veranderingen in de samenstelling van de darmmicrobiota en hun productie van korte-keten vetzuren (KKVZ), evenals de effecten van de fermentatiedigesta op de productie van cytokines door dendritische cellen.

Hoofdstuk 3 beschrijft de fermenteerbaarheid en de daaruit voortvloeiende immuuneffecten van fructose-oligosacchariden (FOS) en inuline. FOS en inuline vertoonden een bifidogeen effect, dat correleerde met de productie van acetaat en lactaat. Fecale bacteriën van zowel 2 als 8 weken oude baby's fermenteerden voornamelijk de trisachariden die aanwezig zijn in FOS. In tegenstelling tot FOS waren de effecten van inuline afhankelijk van de leeftijd van de baby's. Het bifidogene effect en de productie van KKVZ waren hoger bij de 8 weken oude baby's, wat kan worden toegeschreven aan een hogere

afbraak van inuline. Terwijl de fecale bacteriën van 2 weken oude baby's voornamelijk gebruik maakten van inuline met polymerisatiegraad (DP) 3-8, braken de fecale bacteriën van 8 weken oude baby's ook de langere ketens van inuline tot DP16 af. De fermentatie van FOS en inuline verzwakte de productie van pro-inflammatoire cytokines door de dendritische cellen. De mate van verzwakking correleerde met het type en de hoeveelheid KKVZ die tijdens de fermentatie werden gevormd.

De fermentatiekarakteristieken en immuunmodulerende eigenschappen van natuurlijke en met endo-1,3(4)-β-glucanase behandelde haver-β-glucanen worden in meer detail besproken in **hoofdstuk 4**. De enzymbehandeling van natuurlijke haver-β-glucaan (≈ 300 kDa) resulteerde in de vorming van glucose-oligomeren met DP 2-5. Hoewel de natuurlijke β-glucanen onaangeroerd bleven, werden de glucose-oligomeren grotendeels afgebroken door fecale bacteriën van 2 en 8 weken oude baby's met een duidelijke voorkeur voor β(1→4) gekoppelde oligomeren. De fermentatiesnelheid was het hoogst met fecale bacteriën van 2 weken oude baby's en correleerde met de productie van lactaat. De fermentatiedigesta van de niet-fermenteerbare natuurlijke haver-β-glucaan verzwakte de productie van pro-inflammatoire cytokinen door dendritische cellen. De enzymbehandeling resulteerde in een nog verdere verzwakking van de pro-inflammatoire respons. De fermentatie van zowel de natuurlijke als de met enzym behandelde haver-ß-glucaan leidde tot een relatieve toename van *Enterococcus*. De verzwakking van de pro-inflammatoire respons kan het gevolg zijn van de interactie tussen celwandfragmenten van *Enterococcus* en immuunreceptoren op de dendritische cellen.

Deze studie omvat ook enkele zeer complexe NDCs zoals GOS en isomalto-oligosachariden (IMO). Deze NDCs bestaan uit een grote verscheidenheid aan oligosachariden die verschillen in grootte, de monomeersamenstelling en het type bindingen tussen de monomeren. Het grote aantal isomeren maakt de karakterisering van deze NDCs zeer uitdagend. In deze studie werd een "high-throughput" karakteriseringsmethode ontwikkeld op basis van UHPLC-MS met een stationaire fase van poreuze grafiet-koolstof (PGC) om de bepaling van structuur-specifieke gezondheidseffecten van complexe NDCs te vergemakkelijken. In **hoofdstuk 5** wordt de toepassing van deze methode voor de karakterisering van Vivinal GOS beschreven. De methode heeft ons inzicht gegeven in de complexiteit van Vivinal GOS. De hoge resolutie van PGC resulteerde in de scheiding van meer dan 100 verschillende GOS structuren in één enkele analyse. De reductie van de reducerende uiteinden voorafgaand aan de analyse maakte het mogelijk onderscheid te maken tussen de reducerende en niet-reducerende isomeren. In totaal werden er 23 reducerende en 15 niet-reducerende (1-1 binding) GOS DP3-isomeren geïdentificeerd met UHPLC-PGC-MS. Daarnaast werd er een fragmentatieregel ontdekt om reducerende isomeren met een mono- en di-gesubstitueerde terminale glucose te herkennen. Op deze manier faciliteert UHPLC-PGC-MS de detectie van structurele kenmerken die de fermenteerbaarheid van de NDCs door de darmmicrobiota kunnen beïnvloeden.

In **Hoofdstuk 6** worden de fermentatiekarakteristieken en immuuneffecten van zowel de NDCs van Hoofdstuk 3 en 4 als GOS, IMO en isomalto/malto-polysachariden (IMMP) in detail besproken en vergeleken. De grote verscheidenheid aan onderzochte NDCs in combinatie met de focus op de afbraak van individuele isomeren, heeft aanzienlijk bijgedragen tot de kennis van structuur-specifieke afbraak van NDCs door de darmmicrobiota van baby's en de daaruit voortvloeiende immuuneffecten. De implicaties van de immuunverzwakkende effecten van de NDCs worden besproken, rekening houdend met de beperkingen van de *in vitro* opstelling die in ons onderzoek werd gebruikt. Ten slotte wordt geïllustreerd hoe de resultaten van dit onderzoek bijdragen aan de volgende generatie flesvoeding op basis van koemelk.

Acknowledgements

Four years have passed, sometimes I was craving for a new chapter and months felt like ages, sometimes time flew by and the deadline was breathing down my neck. But here I am, looking back at my time at FCH. It all began around 7 years ago with a Bachelor thesis in the steamy Biotechnion, where we still had our coffee break in the lab. I enjoyed it that much that I continued with a Master thesis in the new Axis building, of course again accompanied by the other two Musketeers Gijs and Roelant. Milou and Elisabetta, thanks a lot for converting me to the FCH family!
I continued my journey with Henk. Henk, I feel very grateful to have had you as my supervisor. I am impressed by your knowledge and your critical view. Thank you for the many boks'en and high fives, that was often just what I needed to keep going. You regularly caught me on thinking in the same way as you would do yourself. Henkina Junior will now enter the world outside FCH! :) Thenks.
The research would not have been complete without the immune team in UMCG. Renate and Paul thank you very much for the nice collaboration (and the delicious venison). Talking about the CCC collaboration, I would like to thank all the other researchers and the industrial partners within CarboKinetics. Although I was sometimes complaining about feeling more like a PowerPoint expert than scientist, I really enjoyed being part of this consortium and to step out of my own bubble at FCH. Also special thanks to the microbiologists, Ran, Gerben, Erwin and Hauke, who gave me the opportunity to discover the magical world of the gut microbiota. Ran and Mara, thank you for being my microbiota buddies in Helix. Sharing the frustrations when repeating PCR for the umpteenth time or just having a chat during the many waiting times. Ran, you were always there when I faced some problems during the analysis, thank you for your time and patience!

I also would like to thank all the colleagues at FCH. Without you work would have been much less pleasant, which I have experienced clearly during the last Corona-months at home. I will definitely miss the WE-days! When I think about the wrecking ball, I still have to laugh :) I would like to thank my officemates Frederik, Matthias, Roelant, Zhibin and Weiwei for making the office feel like home. You were always there to just have a chat or to listen to my frustrations or achievements. Jan Willem, you were my hero every time the remote connection of my pc collapsed! Edwin, Eva, Gijs, Moheb, Christiane, Cynthia and Natalia, thank you for your company in the lab!
Special thanks to Peter, Edwin, Margaret, René, Mark and Wouter for their technical support and advice. Jolanda, thank you for having an answer on every non-research related question!
Eva, Sjors and Roelant, the PhD trip to Italy and Austria was a success and an unforgettable experience, not only because of the parking garage ;). I am glad I had the opportunity to organize the trip together with you.

I would like to thank Baris, Renske, Jolien, Charlotte, Lore, Anniek, Weijia, Rosan, Kristel and Edith for their contributions to my research! I enjoyed and learned a lot from supervising you.
Carolina and Eva, dear paranymphs, I am very grateful to have you sitting next to me on this special day. Thank you for the nice time we spent together!

Of course, it would have not been possible to complete all the work without any breaks. Theekransje, I am grateful we met each other during the first year of our studies and had so many nice dinners and cups of tea together :) Even though we have spread all over the Netherlands and next-generation Theekransje started evolving, we continued our tea sessions with hopefully many more years to come!
Mirjam, my travel partner in crime, thank you for sharing all the backpack adventures! Entering Valparaiso via the port in a truck, climbing mountains by scooter, stuffed on the local bus with Bollywood music through the speakers, I loved it. Cheers to many more trips together :)
Special thanks to my neighbour, Pleun. I am not sure if I would have survived the constant writing at home without a daily portion of chitchat on the balcony in the sun.

Moepsie & Harold, bedankt dat jullie er altijd voor me zijn. Zonder jullie was ik niet zover gekomen. De gezelligheid in Bilthoven zorgde ervoor dat ik het werk even helemaal los kon laten. Leonne & Marcel, Lisanne & Peter en Qtje, daar hebben jullie natuurlijk ook voor gezorgd! Het leek wel of jullie konden ruiken wanneer ik weer op 68 aangekomen was. Sophie, Stijn en Emma, ik ben blij dat ik jullie trotse tante mag zijn. Bedankt voor alle leuke uitjes samen!
Remco, ik ben dankbaar dat ik jou ben tegen gekomen! Ook in de laatste maanden lukte het je om me even niet aan het schrijven te laten denken. Het was bijzonder om tegelijkertijd onze PhD thesis af te ronden; elkaars frustraties aanhoren, het relativeren van de berg werk die nog op ons lag te wachten. De schrijfvakanties hebben zeker geholpen bij het halen van de deadline. Ik kijk uit naar onze toekomst samen, alle avonturen die we gaan beleven en de biggetjes in onze toekomstige tuin!

About the author

Curriculum vitae

Madelon Logtenberg was born on April 3rd, 1992 in Utrecht, The Netherlands. After graduating from secondary school (Het Nieuwe Lyceum, Bilthoven, The Netherlands) in 2010, she started her bachelor Food Technology at Wageningen University. Her bachelor study was completed with a thesis on stability and estrogenicity of pterocarpans, within the Laboratory of Food Chemistry. In 2013, she continued with the master Food technology at Wageningen University with the specialization Ingredient Functionality. She performed her master thesis at the Laboratory of Food Chemistry on the *in vitro* fermentation of lactose-based oligosaccharides using pig faecal inoculum. After her thesis, she moved to Santiago, Chile, for her internship within the International Centre of Excellence for Foods in Chile, where she created strategies for the development of the functional ingredient industry in Chile. In 2016, she obtained her MSc degree in Food Technology and started as PhD candidate at the Laboratory of Food Chemistry under supervision of Prof. Dr H.A. Schols. This research was performed in the public-private partnership 'CarboKinetics' coordinated by the Carbohydrate Competence Centre. The results of her PhD thesis are presented in this thesis.

Contact: madelonjoy@gmail.com

List of publications

Logtenberg, M.J.; Vink, J.C.M.; Serierse, R.M.; An, R.; Hermes, G.D.A.; Smidt, H.; Schols, H.A., Pooled infant faecal inoculum can predict infant prebiotic fermentability despite high inter-individual variability of microbiota composition. In press: *Bioactive Carbohydrates and Dietary Fibre*; 2020.

Logtenberg, M.J.*; Akkerman, R.*; An, R.; Hermes, G.D.A.; de Haan, B.J.; Faas, M.M.; Zoetendal, E.G.; Schols, H.A.; de Vos, P., Fermentation of chicory fructo-oligosaccharides and native inulin by infant faecal microbiota attenuates pro-inflammatory responses in immature dendritic cells in an infant-age dependent and fructan-specific way. *Molecular Nutrition and Food Research*; 2020; 64: 2000068.

Akkerman, R.*; **Logtenberg, M.J.***; An, R.; van den Berg, M.A.; de Haan, B.J.; Faas, M.M.; Zoetendal, E.G.; de Vos, P.; Schols, H.A., Endo-1,3(4)-β-glucanase-treatment of oat β-glucan enhances fermentability by infant faecal microbiota, stimulates Dectin-1 activation and attenuates inflammatory responses in immature dendritic cells. *Nutrients*; 2020; 12: 1660.

Logtenberg, M.J.; Donners, K.M.H.; Vink, J.C.M; van Leeuwen, S.S.; de Waard, P.; de Vos, P.; Schols, H.A., Touching the high complexity of prebiotic Vivinal galacto-oligosaccharides using porous graphitic carbon ultra-high-performance liquid chromatography coupled to mass spectrometry. *Journal of Agricultural and Food Chemistry*; 2020; 68: 7800-7808.

Van Trijp, M.P.H.; Rösch, C.; An, R.; Keshtkar, S.; **Logtenberg, M.J.**; Hermes, G.D.A.; Zoetendal, E.G.; Schols, H.A.; Hooiveld, G.J.E.J. Personalized responses of human small intestine microbiota to selected dietary fibers and their degradation patterns *in vitro*. *Submitted*.

Cheng, L.; Kiewiet, M.B.G.; **Logtenberg, M.J.**; Groeneveld, A.; Nauta, A.; Schols, H.A.; van Walvoort, M.T.C.; Harmsen, H.J.M.; de Vos, P. Human milk oligosaccharides (hMOs) modulate the growth and fermentation of *Bifidobacterium longum* subsp. *infantis* in a hMO specific fashion in both monoculture and co-culture with *Faecalibacterium prausnitzii*. *Submitted*.

Difilippo, E.; Pan, F.; **Logtenberg, M.**; Willems, R. H.; Braber, S.; Fink-Gremmels, J.; Schols, H. A.; Gruppen, H., Milk oligosaccharide variation in sow milk and milk oligosaccharide fermentation in piglet intestine. *Journal of Agricultural and Food Chemistry*; 2016; 64: 2087-93.

Difilippo, E.; Pan, F.; **Logtenberg, M.**; Willems, R.; Braber, S.; Fink-Gremmels, J.; Schols, H. A.; Gruppen, H., *In vitro* fermentation of porcine milk oligosaccharides and galacto-oligosaccharides using piglet fecal inoculum. *Journal of Agricultural and Food Chemistry*; 2016; 64; 2127-2133.

Nyffenegger, C.; Nordvang, R. T.; Zeuner, B.; Lezyk, M.; Difilippo, E.; **Logtenberg, M. J.**; Schols, H. A.; Meyer, A. S.; Mikkelsen, J. D., Backbone structures in human milk oligosaccharides: trans-glycosylation by metagenomic beta-N-acetylhexosaminidases. *Applied Microbiology and Biotechnology*; 2015; 99: 7997-8009.

van de Schans, M. G.; Vincken, J. P.; Bovee, T. F.; Cervantes, A. D.; **Logtenberg, M. J.**; Gruppen, H., Structural changes of 6a-hydroxy-pterocarpans upon heating modulate their estrogenicity. *Journal of Agricultural and Food Chemistry*; 2014; 62: 10475-84.

* authors contributed equally

Overview of completed training activities

Discipline specific activities

Courses

Summer course Glycosciences [a]	VLAG, Groningen, 2016
Advanced Food Analysis [a]	VLAG, Wageningen, 2017
Open & Reproducible Microbiome data analysis	MIB, Wageningen, 2018

Conferences and meetings

5th Beneficial Microbes Conference [a]	Bastiaanse Communication, Amsterdam, 2016
New Frontiers in Microbiome [a]	Radboud UMC, Nijmegen, 2017
CCC symposium [a,b]	CCC, Groningen, 2016-2020

General courses

The Essentials of Scientific Writing and Presenting	WGS, Wageningen, 2016
PhD Workshop Carousel	WGS, Wageningen, 2017
Effective Behaviour in Your Professional Surroundings	WGS, Wageningen, 2017
Competence Assessment	WGS, Wageningen, 2017
Traineeship for World Improvers [a,b]	Improve the World Foundation, Utrecht, 2017-2018
BioBusiness Summer School	Hyphen Projects, Amsterdam, 2019
Career Assessment	WGS, Wageningen, 2020

Optional courses and activities

Preparation research proposal	FCH, Wageningen, 2016
PhD study trip 2016 [a,b]	FCH, Japan, 2016
PhD study trip 2018 [a,b,c]	FCH, Austria – Italy, 2018
BSc/MSc thesis students supervision, presentations and colloquia	FCH, Wageningen, 2016-2020
PhD presentations	FCH, Wageningen, 2016-2020
Project meetings	CCC Consortium, 2016-2020

[a] Poster presentation. [b] Oral presentation. [c] Organizing committee
Abbreviations: VLAG, Graduate School for Advanced Studies in Food Technology, Agrobiotechnology, Nutrition and Health Science; MIB: Laboratory of Microbiology; UMC: University Medical Centre; CCC: Carbohydrate Competence Centre; WGS: Wageningen Graduate Schools; FCH: Laboratory of Food Chemistry

The research presented in this thesis was performed within the public-private partnership 'CarboKinetics' coordinated by the Carbohydrate Competence Center (CCC, www.cccresearch.nl). CarboKinetics is financed by participating industrial partners Agrifirm Innovation Center B.V., Cooperatie Avebe U.A., DSM Food Specialties B.V., FrieslandCampina Nederland B.V., Nutrition Sciences N.V., VanDrie Holding N.V. and Sensus B.V., and allowances of The Netherlands Organisation for Scientific Research (NWO).

Financial support from Wageningen University for printing this thesis is gratefully acknowledged.

Proudly printed on 100% recycled paper by DuurzameDissertatie.nl
Edition: 300 copies

A tree has been planted for every copy of this thesis.